Dynamic Behaviour of Microtubule Plus End Binding Proteins in Cultured Cells

Het dynamische gedrag van microtubuli plus einde bindende eiwitten in gekweekte cellen

Thesis

to obtain the degree of Doctor from the
Erasmus University Rotterdam
by command of the
Rector Magnificus

Prof.dr. S.W.J. Lamberts

and according to the decision of the Doctorate Board

The public defense shall be held on

Wednesday 29 September 2004 at 13.45 hrs
by

Tatiana Pavlovna Stepanova
born at Leningrad, Russia

Doctoral Committee

Promotor:	Prof. dr. F. G. Grosveld
Other members:	Prof. dr. C.I. de Zeeuw
	Dr. W. Vermeulen
	Dr. ir. D.N. Meijer
Copromotor:	Dr. ir. N. Galjart

Scope of the thesis

The aim of this thesis was to study the dynamic behaviour of microtubule (MT) plus end binding proteins in living, cultured cells, in order to understand more about MT organization and regulation of MT dynamics in different cell types. Because of major differences in MT organization in particular cell types, this investigation was performed in COS1 and 3T3 cells, hippocampal and Purkinje neurons and glia.

Chapter 1 reviews the current knowledge on the structure and function of the three cytoskeletal systems: actin filaments, intermediate filaments and microtubules. Attention is mainly focused on MTs and their roles in cellular processes. I describe MT behaviour in vitro and in vivo, cellular factors affecting MT dynamics, the role of centrosomes in MT growth, and MT minus end dynamics.

Chapter 2 gives a summary of MT associated proteins, including plus end tracking proteins, their functions and the mechanisms of association with the MT distal ends. This chapter describes also the GFP fusions of plus end-tracking proteins (TIPs) as tools to observe MT dynamic behaviour.

Chapter 3 is about the neuronal cytoskeleton and here I provide a detailed description of the role of MTs in key processes of neuronal development such as: neurite initiation, neurite outgrowth and differentiation into axons and dendrites, axonal pathfinding and neuronal migration.

The experimental work of this thesis is summarised in chapters 4-7.

Chapter 4 describes the isolation and characterization of CLASPs (CLIP-associating proteins), which bind to both CLIP-115 and CLIP-170. CLASP2 is asymmetrically distributed in motile fibroblasts and has a MT stabilizing effect. In contrast to CLIPs (cytoplasmic linker proteins), CLASP2 localises specifically to the leading edge of migrating fibroblasts. The distribution of CLASP2 is dependent on GSK3 β (glycogen synthase kinase) kinase activity.

Chapter 5 represents the study of MT dynamics in cultured neurons, using EB3-GFP fusion protein as a marker for growing MT ends. This research demonstrates events of MT growth in all neuronal compartments and at different stages of development. Remarkably, we found that velocities and number of MT growth events were very similar at different stage of differentiation. These data suggest that local MT polymerization contributes to the formation of the MT network in all neuronal compartments.

In **Chapter 6** it is speculated that CLIP-115 and CLIP-170 might play important and unique roles in neuronal functioning, implicating MT defects in the pathogenesis of Williams Syndrome. The documented increase of MT growth velocities in cultured neurons from CLIP-115 and CLIP-170 deficient mice, suggests that in CLIP knock out neurons, the absence of one of the CLIPs causes an enhanced, persistent MT depolymerization. This MT depolymerization leads to the enlargement of the cytoplasmic pool of free tubulin and the increase of polymerization speed of growing MTs.

Chapter 7 characterizes the generated, using tetracyclin-inducible system, stably expressing GFP-CLIP170 and GFP–CLASP2 cell lines and describes the behaviour of CLIP-170 and CLASP2 in living 3T3 cells.

Chapter 1

Filaments of cytoskeleton

1.1 Three types of cytoskeleton

A complex, highly dynamic network of protein filaments that extends throughout the cytoplasm is called the cytoskeleton. It reorganizes continuously, allowing eukaryotic cells to respond to the environment, adopt a variety of shapes, move, and divide. The cytoskeleton is responsible for such movements as the crawling of cells on a substratum, muscle contraction, and the many changes in shape of a developing vertebrate embryo; it also provides the machinery for intracellular movements, such as the transport of organelles from one place to another in the cytoplasm and the segregation of chromosomes at mitosis [1]. The cytoskeleton contains three types of filaments: actin filaments, microtubules (MTs), and intermediate filaments. All of them are connected to one another, and their functions are coordinated. Cytoskeletal filaments connect a large variety of accessory proteins, protein complexes and organelles to carry out distinct functions in different regions of a cell. Accessory proteins are essential for the controlled assembly of the protein filaments in particular locations, and they provide the motors that either move organelles along the filaments or move the filaments themselves.

1.2 Intermediate filaments

Intermediate filaments are protein fibres present in the cytoplasm and nuclei of most animal cells [2]. Their diameter is about 10 nm, which is intermediate between the diameters of the two other components of the cytoskeleton, actin filaments (about 7 nm) and MTs (about 25 nm) [3]. The important role of these filaments is to provide mechanical strength to cells and tissues. They are present in large numbers, for example, in epithelia, where they are linked from cell to cell at specialized junctions, or along the length of nerve cell axons, and in all types of muscle cells. Intermediate filaments also form the nuclear lamina. Intermediate filaments in vertebrate cells can be grouped into three classes: (1) keratin filaments, (2) vimentin and vimentin-related filaments, and (3) neurofilaments. These filaments are formed by polymerization of their corresponding subunit proteins.

The most diverse family of intermediate filaments is the keratin family (also called cytokeratins), which form filaments in epithelial cells [4]. Vimentin is the most widely distributed of the cytoplasmic intermediate filament proteins, being present in many cells of mesodermal origin, including fibroblasts, endothelial cells, and white blood cells [5]. Desmin is found mainly in muscle cells: it is distributed throughout the cytoplasm of smooth muscle cells, and links together adjacent myofibrils in skeletal and heart muscle cells. Glial fibrillary acidic protein forms glial filaments in astrocytes in the central nervous system and in some Schwann cells in peripheral nerves.

Nuclear lamins are the intermediate filament proteins, which are found in most eukaryotic cells [6]. Rather than being part of the cytoskeleton, the nuclear lamins are components of the nuclear envelope. They also differ from the other intermediate filament proteins in that they assemble to form an orthogonal meshwork underlying the nuclear membrane.

Despite considerable diversity in size and amino acid sequence, the various intermediate filament proteins share a common structural organization [7]. The protein monomers of intermediate filaments are highly elongated fibrous molecules that have an amino-terminal head, a carboxyl-terminal tail, and a central α-helical rod domain. The α-helical rod domain plays a central role in filament assembly, while the variable head and tail

domains presumably determine the specific functions of the different intermediate filament proteins.

The first stage of filament assembly is the formation of dimers in which the central rod domains of two polypeptide chains are wound around each other in a coiled-coil structure [7]. The dimers then associate in a staggered antiparallel fashion to form tetramers, which can assemble end to end to form protofilaments (Fig 1). The final intermediate filament contains approximately eight protofilaments wound around each other in a rope like structure. Because they are assembled from antiparallel tetramers, both ends of intermediate filaments are equivalent. Consequently, in contrast to actin filaments and MTs, intermediate filaments are not polarised; they do not have distinct plus and minus ends. Intermediate filaments are generally more stable than actin filaments or MTs and do not exhibit the dynamic behaviour associated with these other elements of the cytoskeleton. However, intermediate filament proteins are frequently modified by phosphorylation, which can regulate their assembly and disassembly within the cell [8].

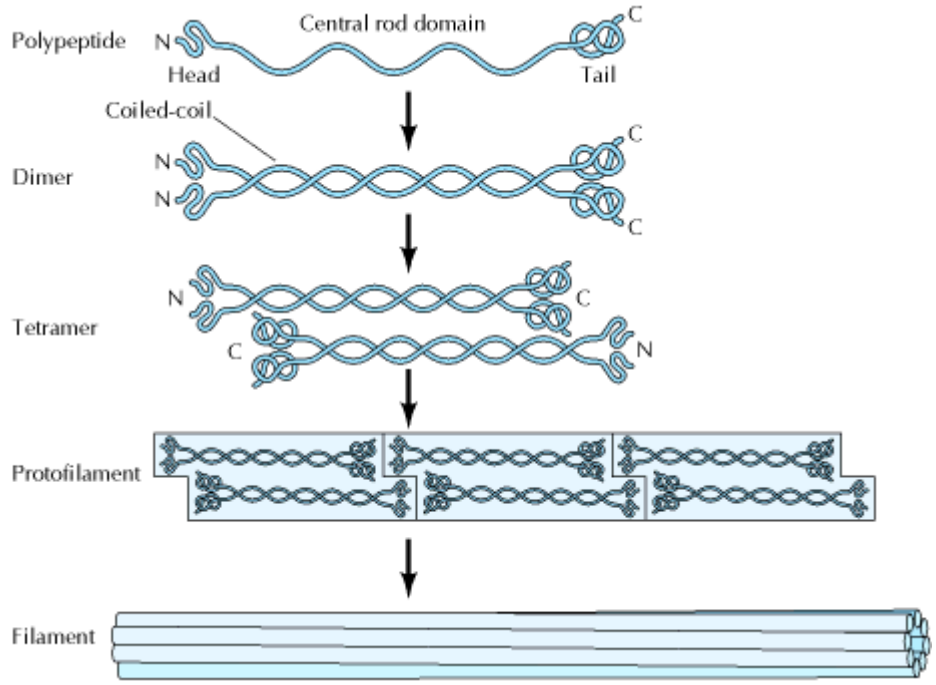

Figure 1. Assembly of intermediate filaments. The central rod domains of two polypeptides wind around each other in a coiled-coil structure to form dimers. Dimers then associate in a staggered antiparallel fashion to form tetramers. Tetramers associate end to end to form protofilaments and laterally to form filaments. Each filament contains approximately eight protofilaments wound around each other in a rope-like structure. (2000 by Geoffrey M. Cooper)

Intermediate filaments form an elaborate network in the cytoplasm of most cells, extending from a ring surrounding the nucleus to the plasma membrane. Both keratin and vimentin filaments attach to the nuclear envelope, apparently serving to position and anchor the nucleus within the cell. In addition, intermediate filaments can associate not only with the plasma membrane but also with the other elements of the cytoskeleton, actin filaments and MTs. Intermediate filaments thus provide a scaffold that integrates the components of the cytoskeleton and organizes the internal structure of the cell [9]. The keratin filaments of epithelial cells are tightly anchored to the plasma membrane at two areas of specialized cell

contacts, desmosomes and hemidesmosomes [10, 11]. Two types of intermediate filaments, desmin and neurofilaments play specialized roles in muscle and nerve cells, respectively. Desmin connects the individual actin-myosin assemblies of muscle cells both to one another and to the plasma membrane, thereby linking the actions of individual contractile elements.

1.2.1. Neurofilaments

Nerve cells contain a variety of unique intermediate filaments, which are expressed in different regions of the nervous system or at specific stages of development (Fig 2). The intermediate filaments include the three neurofilament (NF) proteins (designated NF-L, NF-M, and NF-H for light, medium, and heavy, respectively) [12]. These proteins form the major intermediate filaments of many types of mature neurons. They are particularly abundant in the axons of motor neurons and are thought to play a critical role in supporting these long, thin processes, which can extend more than a meter in length. Neurofilaments appear to be anchored to actin filaments and MTs by neuronal members of the plakin family. Another type of intermediate protein (α-internexin) is expressed at an earlier stage of neuron development, prior to expression of the neurofilament proteins. Yet another IF, nestin, is expressed even earlier during the development of neurons, in stem cells of the central nervous system.

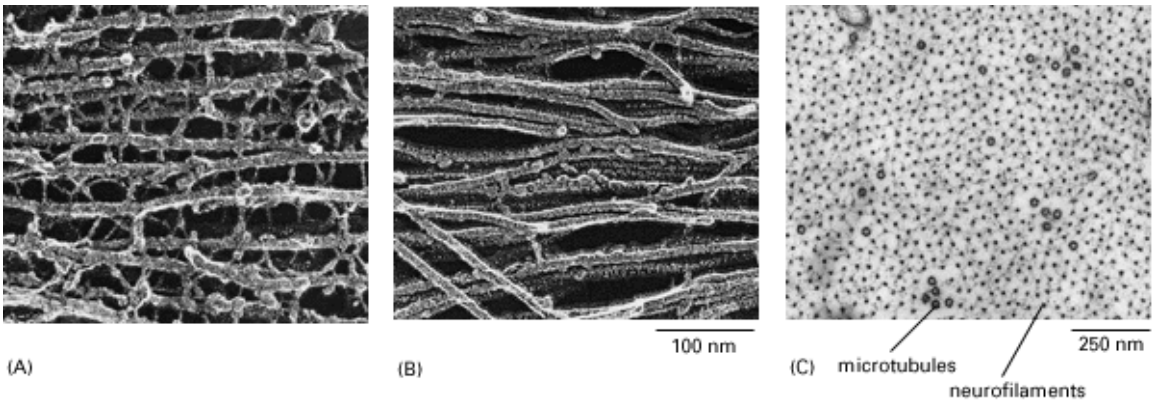

Figure 2. Electron micrographs of two types of intermediate filaments in cells of the nervous system. (A) Freeze-etch image of neurofilaments in a nerve cell axon, showing the extensive cross-linking through protein cross-bridges - an arrangement believed to provide great tensile strength in this long cell process. The cross-links are formed by the long, nonhelical extensions at the carboxyl terminus of the largest neurofilament protein. (B) Freeze-etch image of glial filaments in glial cells illustrating that these filaments are smooth and have few cross-bridges. (C) Conventional electron micrograph of a cross-section of an axon showing the regular side-to-side spacing of the neurofilaments, which greatly outnumber the MTs. (A and B, courtesy of Nobutaka Hirokawa; C, courtesy of John Hopkins.) (1994 by Bruce Alberts et al.).

The intermediate filaments have long been thought to provide structural support to the cell. Some cells in culture make no intermediate filament proteins, indicating that these proteins are not required for the growth of cells in vitro [13]. Similarly, injection of cultured cells with antibody against vimentin disrupts intermediate filament networks without affecting cell growth or movement. Therefore, it has been proposed that intermediate filaments are mostly needed to strengthen the cytoskeleton of cells in tissues of multicellular organisms, where they are subjected to a variety of mechanical stresses that do not affect cells in the isolated environment of a culture dish. Studies in transgenic mice have shown that abnormalities of neurofilaments are implicated in diseases of motor neurons, particularly amyotrophic lateral sclerosis (ALS) [14]. ALS, also known as Lou Gehrig's disease and the disease afflicting the renowned physicist Stephen Hawking, results from progressive loss of motor neurons, which in turn leads to muscle atrophy, paralysis, and death. The accumulation

and abnormal assembly of neurofilaments is one feature that characterises ALS and other types of motor neuron disease, suggesting that neurofilament abnormalities contribute to these pathologies. Consistent with this possibility, overexpression of NF-L or NF-H in transgenic mice has been found to result in the development of a condition similar to ALS. Although the mechanism involved remains to be understood, these experiments clearly suggest the involvement of neurofilaments in the pathogenesis of motor neuron disease.

1.3 Actin

Actin is the most abundant cytoskeletal protein in many eukaryotic cells and is highly conserved throughout evolution. Actin filaments are particularly enriched beneath the plasma membrane, where they form a network that provides mechanical support, determines cell shape, and allows movement of the cell surface, thereby enabling cells to migrate and engulf particles. Actin polymerizes to form actin filaments thin, flexible fibres approximately 7 nm in diameter and up to several micrometers in length (Fig. 3) [15]. Like a MT, an actin filament is a polar structure, with two structurally different ends: a slow-growing minus end (pointed end) and a faster-growing plus end (barbed end). This polarity of actin filaments is important both in their assembly and in establishing a unique direction of myosin movement relative to actin. Within the cell, actin filaments assemble and disassemble, form bundles or three-dimensional networks and associate with other cell structures (such as the plasma membrane). All these events are regulated by a variety of actin-binding proteins, which are critical components of the actin cytoskeleton [16]. A family of actin genes encodes several isoforms; at least six types of actin are present in mammalian tissues (α-actins are found in various types of muscle, whereas β- and g-actins are the principal constituents of nonmuscle cells).

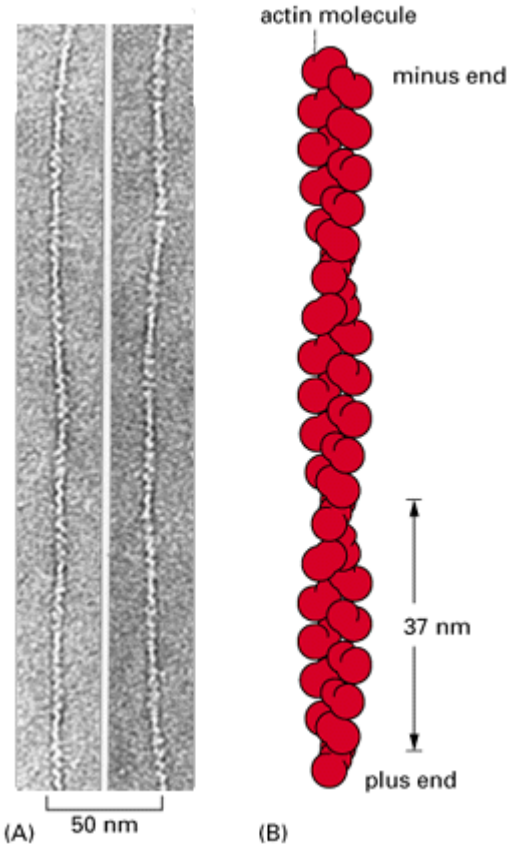

Figure 3. Actin filaments. (A) Electron micrographs of negatively stained actin filaments. (B) The helical arrangement of actin molecules in an actin filament. (A, courtesy of Roger Craig.) (1994 by Bruce Alberts et al.).

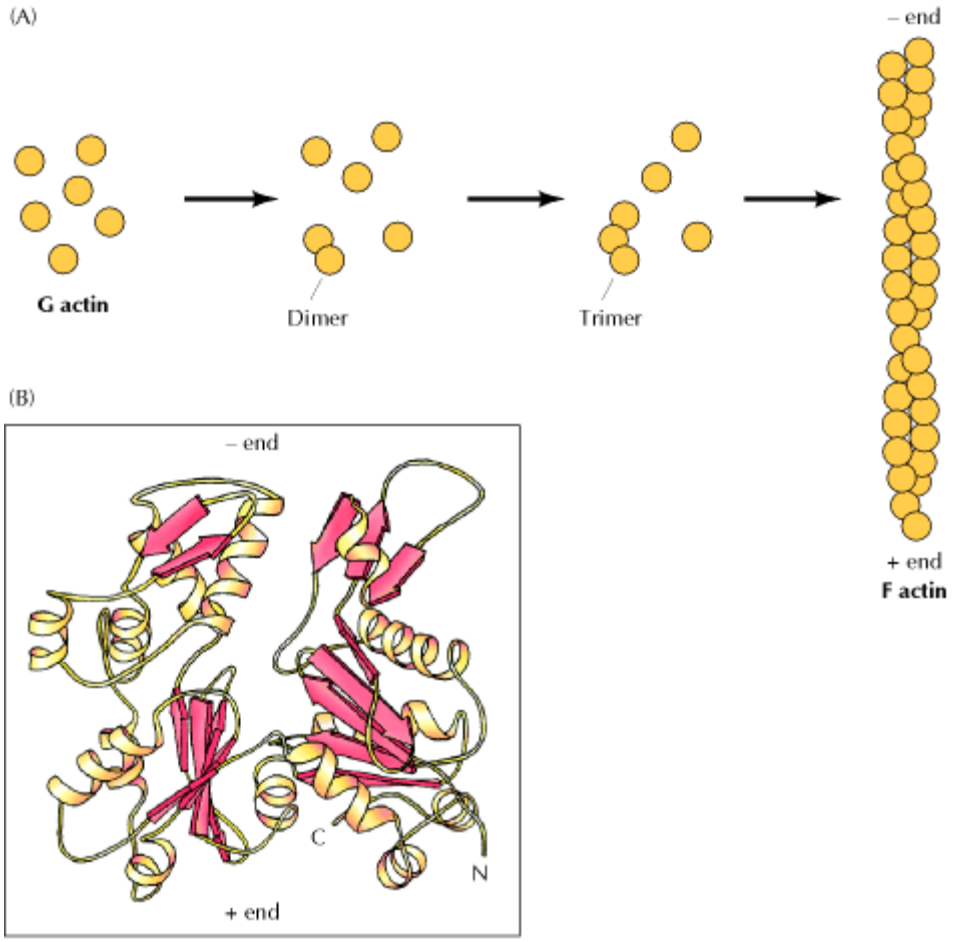

Figure 4. Assembly and structure of actin filaments (A) Actin monomers (G actin) polymerize to form actin filaments (F actin). The first step is the formation of dimers and trimers, which then grow by the addition of monomers to both ends. (B) Structure of an actin monomer. (2000 by Geoffrey M. Cooper)

Each actin monomer (globular G actin, 43 kd) has tight binding sites that mediate head-to-tail interactions with two other actin monomers, so actin monomers polymerize to form filaments (filamentous F actin) (Fig.4). The first step in actin polymerization (called nucleation) is the formation of a small aggregate consisting of three actin monomers. Actin filaments are then able to grow by the reversible addition of monomers to both ends, but one end (the plus end) elongates five to ten times faster than the minus end. The actin monomers also bind adenosine triphosphate (ATP), which is hydrolyzed to adenosine diphosphate (ADP) following filament assembly [17]. ATP binding and hydrolysis play a key role in regulating the assembly and dynamic behaviour of actin filaments, called treadmilling. Treadmilling requires ATP, with ATP-actin polymerizing at the plus end of filaments while ADP-actin dissociates from the minus end. Actin and tubulin have both evolved nucleoside tri-phosphate hydrolysis to provide dynamic instability, which is very important for their functions [18]. The critical concentration for actin polymerization (the concentration of free actin monomer at which the polymerization process stops) is around 8µg/ml [19]. Since the concentration of unpolymerized actin in a cell is much higher, the cell has developed special mechanisms to prevent most of its monomeric actin from assembling into filaments.

Within the cell, actin-binding proteins regulate both the assembly and disassembly of actin filaments. Thymosin is a protein that can bind to the actin-monomer molecule and inhibit its addition to the ends of actin filaments [20]. Two other examples of actin-monomer-binding proteins are profilin [21], which is thought to play a part in controlling actin polymerization in response to extracellular stimuli, stimulating the incorporation of actin

monomers into filaments, and the actin-depolymerising factor cofilin [22], which inhibits the assembly of actin into filaments. Cofilin is responsible for actin filament disassembly within the cell by binding to actin filaments and enhancing the rate of dissociation of actin monomers from the minus end. In addition, cofilin can sever actin filaments, generating more ends and further enhancing filament disassembly. Finally, Arp2/3 proteins can serve as nucleation sites to initiate the assembly of new filaments [23]. All actin-binding proteins act together to promote the rapid turnover of actin filaments and remodelling of the actin cytoskeleton, which is required for a variety of cell movements and changes in cell shape.

Individual actin filaments are assembled into two general types of structures, called actin bundles and actin networks, which play different roles in the cell [24]. In bundles, the actin filaments are crosslinked into closely packed parallel arrays. Stress fibres are an example of contractile bundles of actin filaments, crosslinked by α-actinin, that anchor the cell and exert tension against the substratum [25]. They are attached to the plasma membrane at focal adhesions via interactions with integrin. Several other proteins, including talin and vinculin mediate these associations. In networks, the actin filaments are loosely crosslinked in orthogonal arrays that form three-dimensional meshwork with the properties of semisolid gels. The formation of these structures is governed by other actin-binding proteins that crosslink actin filaments in distinct patterns [26]. Actin filaments are highly concentrated at the periphery of the cell, where they form a three-dimensional network beneath the plasma membrane, called the cell cortex. This determines cell shape and is involved in a variety of cell surface activities, including movement [27].

All of the actin filament motor proteins identified to date belong to the myosin family [28]. Muscle myosin (myosin-II subfamily) is responsible for muscle contraction, for driving membrane furrowing during cell division and for generation of the tension in stress fibres as well as of the cortical tension. Nonmuscle cells contain various smaller myosins, called myosin-I. The common feature of all myosins is a conserved motor domain (motor head); the other domains vary and determine the specific role of the molecule in the cell [29]. Depending on its tail, a myosin molecule can move a vesicle along an actin filament; attach an actin filament to the plasma membrane, or cause two actin filaments to align closely and then slide past each other. All known myosins hydrolyze ATP to move along actin filaments from the minus end toward the plus end [30]. Tropomyosin, for example, binds along the length of actin filaments, making them more rigid and altering their affinity for other proteins. Sets of actin-binding proteins are thought to act cooperatively in generating the movements of the cell surface, including cytokinesis, phagocytosis, and cell locomotion.

1.4 Microtubules (MTs)

MTs are the third important component of the cytoskeleton. They are long polymers, which are essential for cell shape, cell movements, intracellular transport of organelles, and the separation of chromosomes during mitosis. MTs have a cylindrical form with a diameter of about 25 nm (Fig. 5). MTs are formed from molecules of tubulin, each of which is a heterodimer consisting of two closely related and tightly linked globular polypeptides called α-tubulin and β-tubulin. In mammals, small families of related genes encode about six forms of both α- and β-tubulin. In addition, a third type of tubulin (γ-tubulin) is specifically localized to the centrosome, where it plays a critical role in initiating MT assembly. Tubulin dimers polymerize to form MTs, which generally consist of 13 linear protofilaments assembled around a hollow core (Fig. 5). Since the 13 protofilaments are aligned in parallel with the same polarity, the MT itself is a polar structure, and it is possible to distinguish a plus (fast-

growing) and a minus (slow-growing) end [31]. This polarity is an important consideration in determining the direction of movement along MTs.

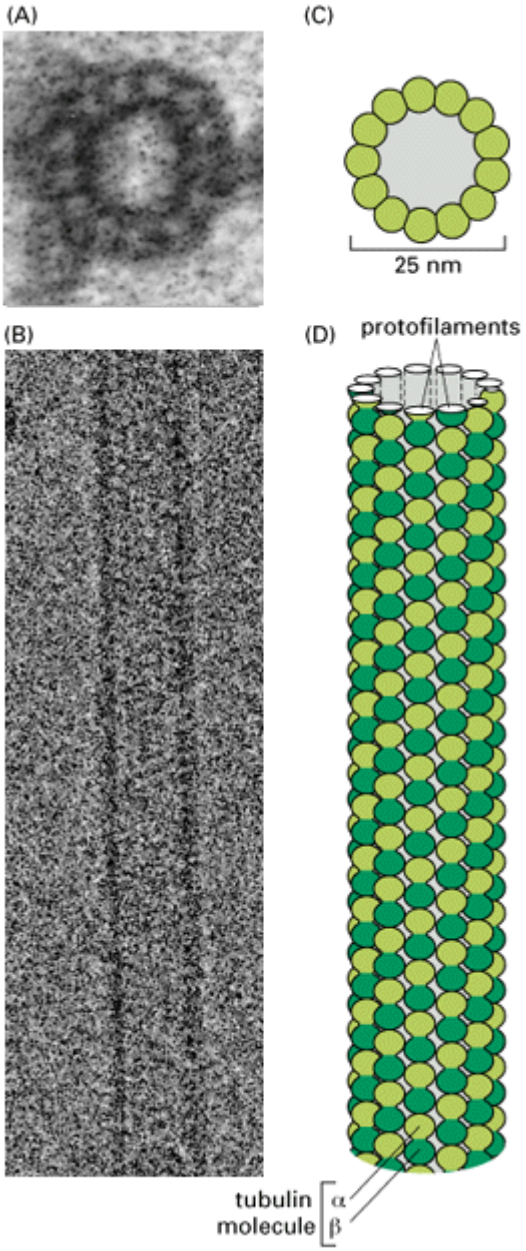

Figure 5. MTs. (A) Electron micrograph of a MT seen in cross-section, with its ring of 13 distinct subunits, each of which corresponds to a separate tubulin molecule (an a/b heterodimer). (B) Cryoelectron micrograph of a MT assembled in vitro. (C and D) Schematic diagrams of a MT, showing how the tubulin molecules pack together to form the cylindrical wall. (C) The 13 molecules in cross-section. (D) A side view of a short section of a MT, with the tubulin molecules aligned into long parallel rows, or protofilaments. Each of the 13 protofilaments is composed of a series of tubulin molecules, each an a/b heterodimer. Note that a MT is a polar structure, with a different end of the tubulin molecule (a or b) facing each end of the MT. (A, courtesy of Richard Linck; B, courtesy of Richard Wade; D, C by Bruce Alberts et al,1994).

1.4.1 Dynamic Instability of MTs

MTs can undergo rapid cycles of assembly and disassembly. Guanosine triphosphate (GTP), which is bound to β-tubulin when tubulin incorporates into MTs, is hydrolyzed to guanosine diphosphate (GDP) during, or shortly after assembly of tubulin. The role of GTP hydrolysis is apparently to allow MTs to depolymerise by weakening the bonds between tubulin subunits in the MT. MTs undergo treadmilling, a dynamic behaviour in which GDP-tubulin molecules are continuously lost from the minus end and replaced by the addition of GTP-tubulin molecules to the plus end of the same MT. In MTs in vivo, GTP hydrolysis inside the lattice results in a behaviour known as dynamic instability, in which the MT plus end alternates between cycles of growth and shrinkage [32] (Fig.6). Whether a MT grows or shrinks is determined by the rate of tubulin addition relative to the rate of GTP hydrolysis. As long as new GTP-bound tubulin molecules are added more rapidly than GTP is hydrolyzed,

the MT retains a GTP cap at its plus end and MT growth continues. However, once a MT has lost its GTP cap - for example, if the instantaneous rate of polymerization slows down – the GDP-cap renders the MT unstable and hence the MT will start to shrink.

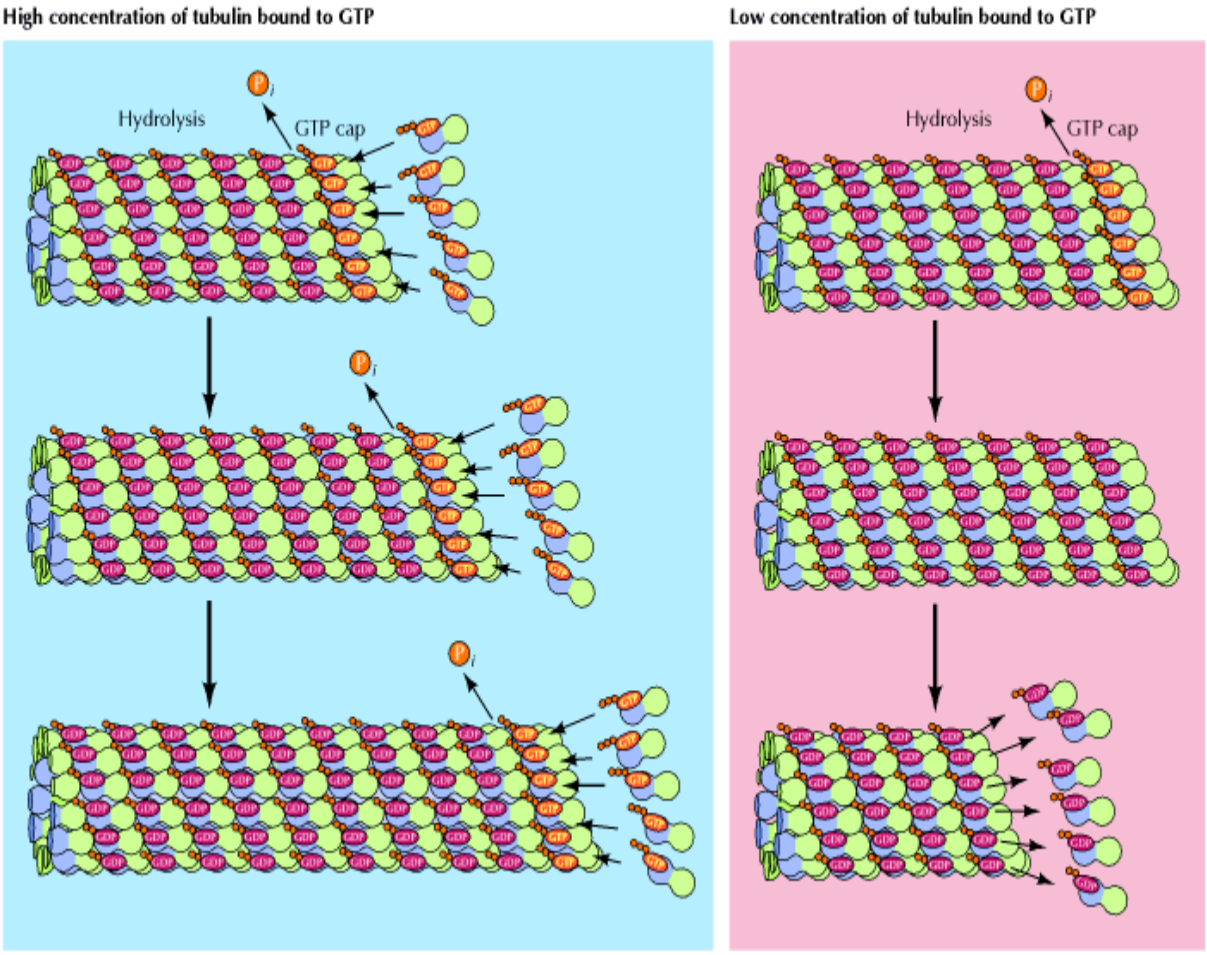

Figure 6. Dynamic instability of MTs. Dynamic instability results from the hydrolysis of GTP bound to β-tubulin during or shortly after polymerization, which reduces its binding affinity for adjacent molecules. Growth of MTs continues as long as there is a high concentration of tubulin bound to GTP. New GTP-bound tubulin molecules are then added more rapidly than GTP is hydrolyzed, so a GTP cap is retained at the growing end. However, if GTP is hydrolyzed more rapidly than new subunits are then added, the presence of GDP-bound tubulin at the end of the MT leads to disassembly and shrinkage. Only the plus ends of MTs are illustrated. (2000 by Geoffrey M. Cooper)

Dynamic instability [33, 34], results in the continuous and rapid turnover of most MTs, which have half-lives of only several minutes within the cell. This rapid turnover of MTs is particularly critical for the remodelling of the cytoskeleton that occurs during mitosis. In a fibroblast-like cell, the entire MT array is turning over rapidly. The half-life of an individual MT is about 10 minutes, while the average lifetime of a tubulin molecule, between its synthesis and proteolytic degradation, is more than 20 hours. This means that each tubulin molecule will participate in the formation and deformation of many MTs in its lifetime. Cells can modify the dynamic instability of their MTs for specific purposes [35]. Proteins that bind to the MTs and stabilize them against depolymerization often suppress the dynamic instability of MTs [36].

1.4.2 MT behaviour in vitro and in vivo

Association of free tubulin with minus end of MTs happens not often and goes very slowly. Thus, MT growth occurs only at the plus end. Most MTs of fibroblast-like cells are bound to the centrosome, or MT-organizing centre MTOC, by their minus ends, while the plus ends freely "explore" the cytoplasm and grow towards the cell periphery, or shrink from it [37-41]. The radial system of cytoplasmic MTs differs from the chaotic MT network, which is formed after spontaneous tubulin polymerization in vitro and which occurs at a concentration of 4-15 micromolars. Still, both in vitro and in vivo, the average velocity of MT growth critically depends on the tubulin concentration. When steady state is reached, MT ends continue to grow or shorten. For reasons outlined above, they mostly display dynamic instability in vivo [33], i.e. growth and shrinkage from the same end (the plus end), whereas in vitro treadmilling occurs, i.e. growth and shrinkage from different ends (plus and minus ends, respectively), unless centrosomes have been added to the polymerization reaction. In vitro, the duration of growth and shortening stages can differ from seconds to several minutes [33, 42-45]. The velocity of MT growth is about 3-4 micrometer/min [43, 44, 46-49], while the shortening rate is higher and varies from 15 to 100 micrometer/min [43, 45, 46, 48, 49]. The average length of MTs in tubulin solution may increase and during 30 minutes it can be enlarged by 10 fold (from 10 to 100 micrometers), but the number of MTs decreases correspondingly [42], once steady state is reached.

The microinjection of fluorescently labelled tubulin and the imaging of cells by using fluorescent microscopy [50-55] has allowed the observation of MTs in living cells, following MT dynamics for a long time without cell damaging [41, 53, 56]. This has revealed that growth and shortening velocities are different for MTs within each cell and can alter within one growth or shortening event [45]. Thus, MT behaviour in cells differs from the spontaneous tubulin polymerization in vitro. Cellular MTs grow quicker and shorten slower as compared with MTs in vitro, also the switching between the stages from growth to shrinkage (catastrophe) and vice versa (rescue) occurs more often in cellular cytoplasm than under vitro conditions [57, 58]. Besides growth and shrinking phases, cellular MTs also can remain static (pausing), which is a special characteristic of MT dynamics that never takes place in vitro. Below, we will describe what determines the differences of MT dynamics in vivo and in vitro.

1.4.3 Centrosomes

One of the important differences between most in vitro and in vivo tubulin polymerization experiments is the presence of centrosomes in cells. Centrosomes are major MT-organizing centres. The MTs in most cells extend from a MT-organizing centre, in which the minus ends of MTs are bound [59]. The number of MTs growing from the centrosomes reflects the amount of MT nucleation sites located at the MTOC [39]. In vitro experiments have shown that tubulin polymerisation on the centrosomes can occur at a lower concentration, than the critical concentration of spontaneous polymerisation [60]. Thus, the important features of MT dynamic instability in cellular systems are that MTs are bound at the centrosome by minus ends, which do not participate in the exchange of free cytoplasmic tubulin. All MTs start to grow from the centrosome; growth is at their plus ends. MT nucleation is very efficient at the MTOC, i.e. once a site for MT nucleation on the centrosome becomes available, a new MT will start to grow from it immediately.

In animal cells, the centrosome is located adjacent to the nucleus near the centre of interphase cells (Fig. 7). The centrosome duplicates and splits into two equal parts during interphase. When mitosis begins, two daughter centrosomes move to opposite sides of the nucleus and form the two poles of the mitotic spindle (Fig. 7). The centrosome serves as the

initiation site for the assembly of MTs, which grow outward from the centrosome toward the periphery of the cell [61]. Importantly, the initiation of MT growth at the centrosome establishes the polarity of MTs within the cell. The centrosomes of most animal cells contain a pair of centrioles, oriented perpendicular to each other, surrounded by amorphous pericentriolar material (Fig 7).

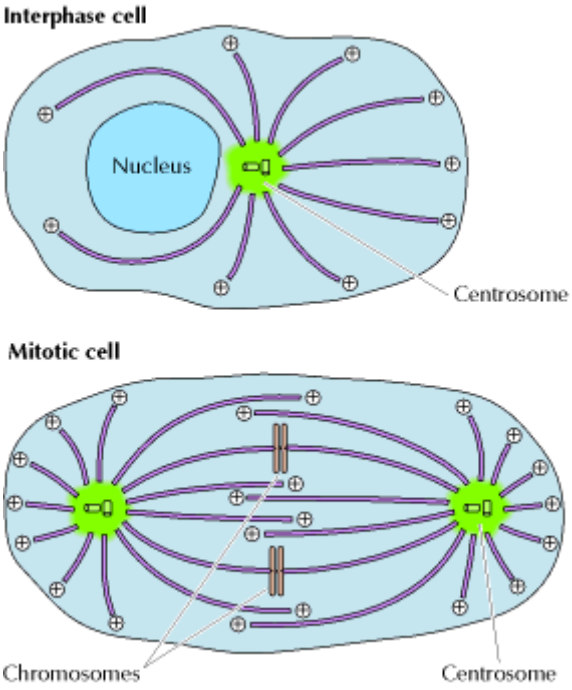

Figure 7. Intracellular organization of MTs The minus ends of MTs are anchored in the centrosome. In interphase cells, the centrosome is located near the nucleus and MTs extend outward to the cell periphery. During mitosis, duplicated centrosomes separate and MTs reorganize to form the mitotic spindle. (2000 by Geoffrey M. Cooper)

Centrioles are cylindrical structures consisting of nine triplets of MTs. Centrioles are surrounded by pericentriolar material, which is required for the nucleation, assembly and organization of MTs, while the cenrtioles themselves are not essential. The key protein in the centrosome that nucleates assembly of MTs is γ-tubulin, a minor species of tubulin. Complexes of γ-tubulin form ring structures that contain 10 to 13 γ-tubulin molecules and have diameters similar to those of MTs. These γ-tubulin rings serve as nucleation sites for the assembly of MTs and may remain bound to their minus ends [62].

1.4.4 MT minus end dynamics

Most cellular MTs are bound by minus ends to the MTOC, but some of the MTs are released from the MTOC. These free MTs can be spontaneously generated [53, 63-66], by the breaking of long MTs [53, 64, 66, 67], or by enzymatic separation of MTs from the centrosome [41, 68-71]. This latter event, also called MT severing, is regulated by katanin [58, 72] and is thought to be enhanced in neurons [73, 74]. In most cell types, it is, however, quite rare and occurs approximately 1 time per 100 MTs per minute [53, 69]. The behaviour of MT minus-end can be different in vivo, as compared to in vitro, in that minus ends can remain stable in vivo for a long time, even if not associated with the MTOC [53, 66]. In cells, where the MT minus ends can remain stable (neurons, epithelial cells), the MT system is not necessarily radial and “free” MTs may even represent the largest population of cytoplasmic MTs [53, 66]. The mechanisms which stabilize the minus ends of non-centrosome MTs are still largely mysterious, in epithelial cells cadherin signalling appears to be involved [75].

Cells with a radial MT organization also contain free minus ends, but these are unstable and undergo depolymerisation. The minus-end depolymerisation velocity is estimated from 7 to 15 micrometers/min [76-78]. The size of minus-end depolymerisation segment can be up to 30 micrometers [78]. The minus ends at the cell periphery depolymerise quickly and disappear within 1-2 minutes. Observations on keratinocytes demonstrated that in these cells free MTs exist about 4 minutes, spending about 90% of lifetime in pauses, and shortening with a velocity of 12 +/- 6.9 micrometers/min.

1.4.5 Barriers to MT growth

The growth velocity of individual MTs in cells strongly varies [51-54, 79-81]. The duration of MT growth phases in cells is much shorter than in vitro, for some cell types it takes just seconds. The elongation of the MT length during one growth phase in a typical cell is about 1-9 micrometer [51-55, 79-81], whereas in vitro it is estimated to be tens of micrometers [42, 45]. The shortness of growth phases in cells results from the increased frequency of catastrophe. This is mainly due to the fact that in cells MTs encounter the cell membrane, which acts as a barrier, thereby reducing the speed of MT growth and increasing the chances of catastrophe [82].

The limitation of MT growth by a mechanical barrier was theoretically proposed and analysed and later demonstrated in "in vitro" experiments [83-85]. These experiments have shown that MTs stop growing when they come into contact with a mechanical barrier [67]. Instead, MTs either bend, to grow laterally, or they pause, undergo catastrophe and start shrinking. In the cell, the membrane is the barrier and thus, cellular MTs grow radially from the cell centre and at the edge undergo pausing [77, 86], or oscillate between growth and shrinkage [78], or some MTs bend and continue to grow along the cellular membrane.

In keratinocytes, the length of 41% of MTs is greater than the cell radius, suggesting that they actually bend. What happens with MTs, which grow along the cellular membrane? In some cell types, the actin flow is very strong, directed to the cell centre and "pushes" the growing MTs there. In Xenopus pneumocytes, MTs which are growing parallel to the cell edge can bend, brake and depolymerise from their minus ends [69].

1.4.6 MT behaviour in different cell regions

The behaviour of MTs at the cell edge is described in more detail in literature than that of MTs deep in the cytoplasm, due to the fact that at the cell periphery individual MTs can be followed more easily [40, 51-55, 79-81]. Recently published papers have shown differences in MT behaviour, depending on the cell region analysed. MTs have been observed to persistently grow into the lamellipodia of newt lung cells [87] and to continuously elongate into newly formed protrusions of hepatocyte growth factor (HGF)-stimulated PtK_1 cells [88]. There are specific approaches for analysis of MT dynamics in regions near the centrosome and far from the cell edge. These model systems allow the following of individual MT ends or a reduced number of MTs. Fluorescent recovery after photobleaching (FRAP) allows to observe dynamics of a limited number of MTs in a bleached region, before total fluorescence recovery. Using this technique, it was shown in CHO cells that MTs grow persistently towards the cell edge, almost without catastrophes and pauses, with an average rate of growth of 17,8+/- 13,8 micrometers/min and oscillate only near the edge [86]. Thus, in CHO cells the balance between MT growth and shortening changes along the cell radius, i.e. in the cell centre MT growth is persistent, but at the cell edge growth is balanced by shrinkage [86]. The use of cytoplasts (enucleated cells, containing or lacking the centrosome) [89, 90] represents an interesting approach to study MT dynamics inside the cell cytoplasm, because cytoplasts contains less MTs compared to cells. The MT behaviour in cytoplasts is similar to that in cells, i.e. MTs grow persistently towards the cell edge where they oscillate, however the growth velocity is 25% slower than in normal cells. Together these observations suggest that in the cytoplasm MTs grow persistently, almost without catastrophes and pauses, so the duration of the growth phase is longer compared to the cell edge. To understand how the cell edge influences on MT behaviour, not only parameters of growth but also the pauses and shortenings stages should be analysed and compared in different regions of the cell.

1.4.7 Reorganization of MTs during Mitosis

During mitosis, MTs completely reorganize, demonstrating an example of the importance of their dynamic instability. The MT array, present in interphase cells, undergoes disassembly and the free tubulin subunits form the mitotic spindle, which is responsible for the separation of daughter chromosomes (Fig. 7). In interphase cells, the centrioles and other components of the centrosome are duplicated and remained together. During mitosis, two centrosomes separate and move to opposite sides of the nucleus, forming the two poles of the mitotic spindle [91]. The dynamic behaviour of MTs changes dramatically in mitosis. The number of MTs growing from the centrosome increases by five- to tenfold and the rate of MT disassembly increase about tenfold, resulting in overall depolymerization and shrinkage of MTs. These changes result in disassembly of the interphase MTs and the outgrowth of large numbers of short MTs from the centrosomes. The formation of the mitotic spindle involves the selective stabilization of some of these MTs [92]. The attachment to the kinetochore plays a critical role in separation of the mitotic chromosomes and stabilizes kinetochore MTs. Polar MTs are stabilized by overlapping with each other in the centre of the cell and are free from chromosomes. Astral MTs extend from the centrosomes to the cell periphery and have freely exposed plus ends. Both the polar and astral MTs contribute to chromosome movement by pushing and pulling the spindle poles apart. Motor proteins associated with the spindle MTs mediate chromosome movement. In the final stage of mitosis, nuclear envelopes re-form, the chromosomes decondense, and cytokinesis takes place. Each daughter cell then contains one centrosome, which nucleates the formation of a new network of interphase MTs.

Chapter 2

MT-associated proteins (MAPs)

2.1 Cellular factors affecting MT dynamics

The general concentration of tubulin in cells is 20-30 micromolar [93], the ratio between free cytoplasmic tubulin and polymerised tubulin is approximately 2:3 [50, 76]. This means that the concentration of free tubulin in the cell cytoplasm corresponds to what is used in vitro tubulin polymerization. However, in Xenopus extracts, that included centrosomes, MT growth velocity was higher (about 10 micrometers/min), than in purified tubulin solutions [68]. In many types of mammalian cells the average growth velocity is even higher and can reach 12-20 micrometers/min [51-55, 76, 79, 94, 95]. In Xenopus cells, which are cultured at a temperature of 23-28 ^{0}C, the MT growth velocity is usually lower (5-8 micrometers/min [77, 78, 80, 96]), but this is still higher than the tubulin polymerization speed at 37 ^{0}C in vitro. Thus, factors appear to exist that enhance MT polymerization rates in vivo.

Indeed, the most far-reaching and versatile modifications of MTs are those conferred by binding of other proteins [36]. These MT-associated proteins, or MAPs, serve both to stabilize MTs against disassembly and to mediate their interaction with other cell components [97]. There are many kinds of MAPs, some are found in most cells, whereas others are found only in specific cell types. Classically, two major classes of MAPs have been isolated from brain in association with MTs: high-molecular-weight proteins (HMW proteins), which have molecular weights of 200,000 to 300,000 or more and include MAP-1 and MAP-2; and tau proteins, which have molecular weights of 55,000 to 62,000 [98]. Recently cryoEM studies showed that MAP2 and tau stabilize MTs by binding along the outer ridges of protofilaments [99]. MAP1,MAP2 and tau are highly expressed in neurons before and during neurite outgrowth and, probably, promote MT bundle formation in the neurite shaft [100].

Members of the MAP2/tau family appear to be important regulators of neurite behaviour, including neurite initiation [101]. The STOP proteins are also known to stabilize MTs [102], but in contrast to MAP2/tau-stabilized MTs, which still display dynamic behaviour, STOP proteins arrest dynamic instability by blocking tubulin turnover and thereby confer cold stability and drug resistance.

In contrast to stabilizing MAPs, members of the Op18/stathmin family de-stabilize MTs. Op18/stathmin is well characterised [103], although the data about its interaction with MTs in vivo are still controversial [104]. It appears as if Op18/stathmin induces catastrophes by sequestering free tubulin, thereby effectively lowering the concentration of tubulin for polymerization. Similar to the encountering of a cell membrane (a barrier), lowering of the free tubulin concentration causes a reduced growth velocity, which in turn increases the chance of a catastrophe. Phosphorylation of stathmin lowers its affinity to free tubulin. In a recent, elegant fluorescent resonance energy transfer (FRET) (study it was shown that phosphorylation of stathmin regulates local tubulin concentrations via gradients of stathmin-tubulin interaction [105].

The average velocity of MT shortening in cells is about 12-30 micrometers/min, slightly lower than the similar parameter in vitro [51-55, 79-81]. Shrinkage velocities differ in cells similar to growth velocities, and a shortening event is about 1-9 micrometers [51-55, 79-81] making the average duration of the shortening phase in cells about 10-15 seconds. In cells, together with factors which initiate a catastrophe and increase MT growth rates, there appear to be factors, which are able to decrease the MT shortening velocity and factors, which provide MT rescue. Some of those factors were identified and cellular MT dynamics was partly reconstituted in vitro by addition of cellular proteins, which either stabilise MTs (e.g. Xenopus microtubule associated protein (XMAP215) or destabilise MTs (e.g. XKCM1) [106]. Used separately, these proteins have opposing effects on MT dynamics in vitro – XMAP215 stabilises MT ends and increases growth velocity [63, 107], but XKCM1 destabilises MT ends and increases catastrophe frequency [108, 109]. When added together,

these two proteins change the parameters of dynamic instability, making them more similar to parameters in vivo. This results in the increase of MT growth velocity and the number of shortenings events [106].

In vitro MTs all grow or shorten and pausing is very rarely observed; it occupies not more than 1% of total MT life time [43]. However cellular MTs may spend about 20-30% of their lifetime in a pausing state [51-55, 79-81]. Near the cell edge, MTs can even spend 90% of their lifetime in pausing [51, 110]; in effect rendering them stable. The analyses of the differences of MT behaviour in vivo and in vitro leads to the conclusion that in cells there are factors, which:

1) increase the efficiency of tubulin polymerization at MT ends;
2) decrease depolymerisation velocity;
3) increase the frequency of catastrophe as compared to in vitro tubulin polymerization;
4) increase the rescue frequency, i.e. the switching from catastrophe to growth;
5) induce pausing;

By making the localization of factors regional, a cell can modulate MT dynamics in a highly controlled manner in space and time.

2.2 MT motors and intracellular transport

A highly specific class of MAPs is formed by motor proteins, which can move along MTs. There are two classes of MT-dependent motor proteins, i.e. the kinesins and the cytoplasmic dyneins [111]. Both of these proteins move along MTs using energy, derived from ATP hydrolysis. Cytoplasmic dyneins are involved in organelle transport and mitosis [112]. Dynein is an extremely large molecule (up to 2000 kd), which consists of two or three heavy chains (each about 500 kd) and a variable number of light and intermediate polypeptides (from14 to 120 kd) (Fig. 8) [113]. The heavy chains form globular ATP-binding motor domains that are responsible for movement along MTs. The basal portion of the molecule, including the light and intermediate chains, is thought to bind to other subcellular structures, such as organelles and vesicles.

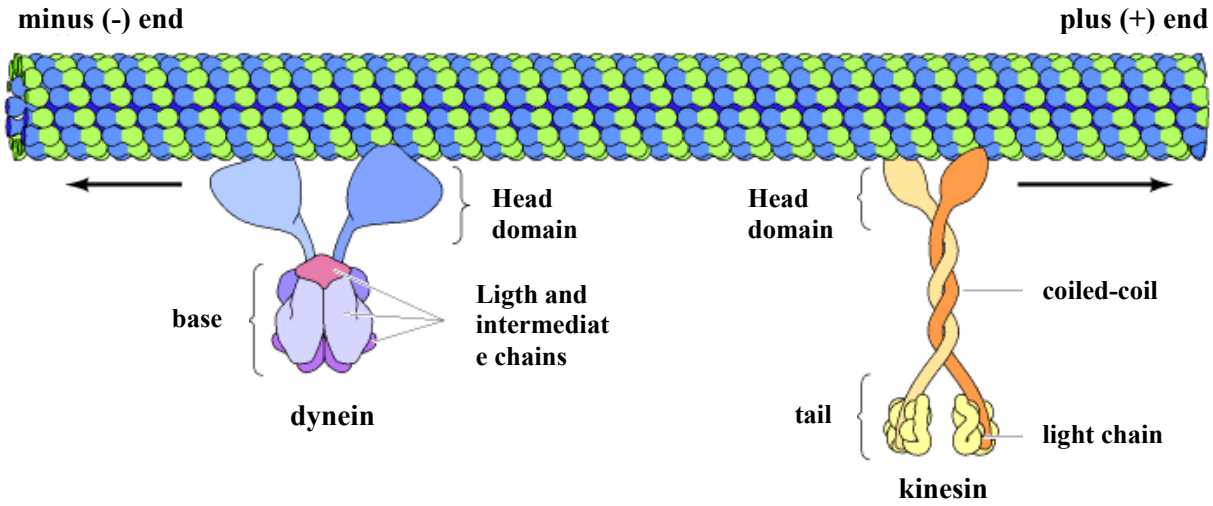

Figure 8. MT motor proteins Kinesin and dynein move in opposite directions along MTs, toward the plus and minus ends, respectively. Kinesin consists of two heavy chains, wound around each other in a coiled-coil structure, and two light chains. The globular head domains of the heavy chains bind MTs and are the motor domains of the molecule. Dynein consists of two or three heavy chains (two are shown here) in association with

multiple light and intermediate chains. The globular head domains of the heavy chains are the motor domains. (2000 by Geoffrey M. Cooper)

Kinesins [114] are more diverse than the dyneins, and different family members are involved in organelle transport, in mitosis, in meiosis, and in the transport of synaptic vesicles along axons. The neuronal axon, that can extend more than a meter in length, represents an obvious example of a compartment, in which cytoplasmic organelle transport is incredibly important.

Conventional kinesin [115] is a molecule of approximately 380 kd, consisting of two heavy chains (120 kd each) and two light chains (64 kd each) (Fig.8). The heavy chains have long α-helical regions that wind around each other in a coiled-coil structure. The amino-terminal globular head domains of the heavy chains are the motor domains of the molecule: they bind to both MTs and ATP, the hydrolysis of which provides the energy required for movement. The motor domain of kinesin is approximately 340 amino acids. The tail of the kinesin molecule is responsible for binding to other cell components (membrane vesicles and organelles) that are transported along MTs by the action of kinesin motors. It consists of the light chains and the carboxy-terminal domains of the heavy chains.

Most members of the kinesin family, move along MTs in the plus end direction, however this is not an absolute rule, since some members move in the opposite direction, toward the minus end. Some kinesins do not move at all, but are required for destabilization of MTs. Dynein moves toward the minus ends of MTs. MT-dependent motor proteins play an important role for transport of the membrane-bounded organelles (the endoplasmic reticulum, Golgi apparatus, lysosomes, and mitochondria) within a eukaryotic cell [116]. The positioning of the endoplasmic reticulum appears to involve the action of kinesins, which pull the endoplasmic reticulum along MTs in the plus end direction, toward the cell periphery. Kinesins play a key role in the movements of mitochondria and in the positioning of lysosomes away from the centre of the cell. Conversely, cytoplasmic dynein is thought to play a role in positioning the Golgi apparatus that locates in the centre of the cell, near the centrosome [117]. When cells are treated with a drug that depolymerises MTs, both of these organelles change their location: the ER collapses to the centre of the cell, while the Golgi apparatus fragments into small vesicles that distribute in the cytoplasm.

2.3 MT Plus End Binding Proteins

The proteins that were described above are localised, or move, along the MTs and are not limited to the MT ends. Dynamic instability, however, is regulated for a large part at the MT plus ends. The recent data have revealed a heterogeneous population of MT-binding proteins that accumulates mainly at the distal ends of polymerizing MTs**.** Such localization is ideally suited for regulation of MT dynamics. MT plus end binding proteins, also called "plus end-tracking proteins", or +TIPs [118], are able to "surf" the dynamic ends of MTs [119]. EB1[120]; EB3 [121], APC [122], CLASP2 [123], LIS1 [124, 125], CLIP-170 [86, 126] and CLIP 115 [86, 127] and dynactin complex [128] have recently emerged as MT binding proteins that have been observed to be present on the MT plus ends.

+TIPS associate with the plus-end of the MT during bouts of subunit addition. The association is transient, so these proteins rapidly lose their association as the MT continues to grow. Thus when +TIPs are expressed as GFP-fusions, fluorescence is brightest at the growing tip of the MT and trails off in intensity toward the minus-end of the MT, thus forming a "comet tail." This specific association of +TIPs with MT distal ends was initially explained by treadmilling [94]. Accumulation may also occur by "delivery (or deposition) of proteins", which is kinesin driven [119, 129]. Shrinking MTs should be, in principle, devoid

of +TIPs. This is in line with what was reported for GFP-CLIP-170, which is lost as soon as MTs depolymerise.

Visualization of GFP-TIP comets in living cells provides insight into the ongoing dynamic behaviour of MTs. The advantage of using GFP-TIPs instead of fluorescent tubulin is that only the ends of MTs are visualized instead of the whole MT. Thus, MT ends can be visualized throughout the cytoplasm of cells, also in areas where a dense MT network exists. The disadvantage of using GFP-TIPs in mammalian cells is that only growing MTs are described; other important parameters of MT behaviour can not be documented. In spite of this drawback, the study of MT behaviour using specific GFP-tagged MT plus end binding proteins as markers has become very popular. The first plus-end-binding protein described as fused to GFP, was CLIP-170 [126]. Later several other proteins were used in this manner [95, 123], 54). They mainly represent two families of proteins, i.e. the CLIPs and the EB1-related proteins [130]. Visualization of GFP-TIPs in cells by time-lapse fluorescence microscopy revealed that all fusion proteins move in a comet-like pattern and demonstrated that, at least in CHO cells, most MTs grow persistently from the cell centre towards the cell periphery. In line with studies using fluorescently injected tubulin, MT growth becomes less persistent upon reaching the cell edge [90]. As described in Chapters 5 and 6, we have used the GFP-TIP visualization technology to unveil the dynamic behaviour of MTs in cultured neurons.

2.3.1 Functions of +TIPs

Several categories of +TIPs have been identified thus far, including the EBs, the CLIPs, and the CLASPs [119, 131, 132] (see Table 1). +TIPs appear to have functions important for regulating MT behaviour. It was, for example, published recently that the CLIPs can play a role as rescue factors, or can recruit rescue factors, at the MT tip, which leads to a decrease of the duration of the shortening stage [86]. CLASPs are thought to interact with the CLIPs as well as cortical structures, and hence could be the elusive molecules that regulate the capture of MTs at the leading edge of migrating cells [123]. The EBs are proposed to modulate the dynamic instability of MTs, increasing a polymerization and decreasing MT depolymerization and pausing [118, 133].

+TIPs also appear to regulate key MT behaviour predicted by the "search and capture" model proposed by Kirschner and Mitchison (1986)[134] almost two decades ago. MTs are thought to explore the leading edge of a cell and then certain of the MTs are captured by molecules within the cortex, for example in the region of the edge destined to lead the direction of movement. Prior to the discovery of the +TIPs, the known MT stabilizers were generally not very attractive candidates for regulators of the behaviour of MTs exploring the leading edge.

There are suggestions that +TIPs can link the MT cytoskeleton to other structures within the cell [135-137]. For example, CLIP-associating proteins (CLASPs), cytoplasmic dynein/dynactin complex including p150 Glued (the biggest subunit of the dynactin complex; p150 Glued mediates interaction between dynein and dynactin), and APC are hypothesized to have such roles. The first +TIP found (CLIP-170) was also suggested to play a role as a linker between membranes and MTs. CLIP-170 targets dynein and dynactin to the MT ends and links dynein to MTs [126]. CLIP-170 family members in fibroblasts and in fission yeast play also a role in orientation of MTs towards a specific cortical region. The Tip1p in fission yeast promotes continuous MT polymerization until MTs reach the cell end. This process is essential for normal cell polarisation. CLASPs are particularly interesting because they stabilise MTs specifically at the leading edge of migrating cells. Data suggest that localized inhibition of glycogen synthase kinase-3β (GSK-3β) may be responsible for the remarkable asymmetric distribution of CLASPs [138].

Table 1. Characteristics of the vertebrate +TIPs and their homologs [a]

(TRENDS in Cell Biology Vol.13 No.5 May 2003)

		Potential mechanism for MT plus-end targeting	Effect on MT dynamics
APC homologs	APC	**Transport** (via KIF3A?); **Hitchhiking** (via EB1)	Promotes MT polymerization *in vitro*; stabilizes microtubules *in vitro* and *in vivo*
	Kar9[b] (*S. cerevisiae*)	**Transport** (via Kip2?); **Hitchhiking** (via Bim1)	N.D.
CLIP Homologs	CLIP-170	**Treadmilling**	Expression of D.N. decreases MT rescues
	CLIP-115	N.D.	Expression of D.N. decreases MT rescues
	Tip1 (*S. pombe*)	N.D.	Deletion increases MT catastrophes
	Bik1 (*S. cerevisiae*)	N.D.	Deletion induces very short or absence of cytoplasmic MTs
Dynein Homologs	Dynein heavy chain	N.D.	N.D.
	Dyn1 (*S. cerevisiae*)	**Hitchhiking** (via Bik1/Pac1)	Deletion has longer MTs; decreased shrinking rate
	NudA (*A. nidulans*)	**Hitchhiking** (via dynactin/NUDM) **Transport** (via KINA)	Loss-of-function mutant has decreased catastrophe and rescue frequencies; lower MT shrinkage rate
EB1 Homologs	EB1	**Treadmilling** (human recombinant EB1 in *Xenopus* egg extracts and mouse cDNA transfected in *Xenopus* A6 epithelial cells)	Addition of human recombinant protein to *Xenopus* egg extracts decreases MT pauses and catastrophes; increases rescues
	dEB1 (*D. melanogaster*)	N.D.	RNAi depletion decreases catastrophes and strongly induces MT pauses (S2 cell line)
	Bim1 (*S. cerevisiae*)	N.D.	Deletion shows slower shrinkage rate, fewer rescues and catastrophes and a dramatic increase in MT pauses
p150*Glued* Homologs	p150*Glued*	**Treadmilling**	Promotes MT nucleation *in vitro*
	NudM (*A. nidulans*)	N.D.	N.D.
LIS1 Homologs	LIS1	N.D.	Reduces MT catastrophes *in vitro*
	Pac1 (*S. cerevisiae*)	N.D.	N.D.
	NudF (*A. nidulans*)	N.D.	Loss-of-function mutant has decreased catastrophe and rescue frequencies; lower MT shrinkage rate
CLASP Homologs	CLASP	N.D.	Overexpression suggests a role in MT stabilization
	Mast/Orbit (*D. melanogaster*)	N.D.	N.D.

Abbreviations: MT, microtubule; N.D., not determined; D.N., dominant negative; RNAi, RNA-mediated interference.

[a] The yeast and Dictyostelium homologs of XMAP215 have been shown to be +TIPs; however, similar behaviour has not been observed for the vertebrate homologs

[b] Very limited degree of homology; however, they both bind to EB1 homologs and have been suggested to share generally similar functions

CLASPs are the mammalian orthologs of a Drosophila gene product Orbit [139] or Mast [140]. Orbit/MAST binds directly to MTs and is required for proper mitotic spindle function in Drosophila.

EB1 family members also play a role in tethering MT ends to special cortical sites. In budding yeast, binding to microtubules 1 protein (BIM1p), the yeast EB1homolog, interacts with Kar9p (yeast analogue of APC) at the tips and participates in spindle orientation [141, 142] and functions as an anti-pausing factor, providing dynamics of MT. EB1 itself plays a

similar role in animal cells, promoting MT elongation and preventing MTs from pausing [143]. Mammalian EB1 binds to the adenomatous polyposis coli (APC) protein, that associates with MTs and the attachment sites at the cell cortex [144-147]. It has been suggested that plus end directed KIP3A/B kinesin motor might target APC to the plus ends of MTs. Dynein has been observed at the plus ends in fungi and animal cells. Like APC, dynein associates with cell cortex and astral MTs and may act as astral MTs attachment sites. A major component of the dynactin complex, p150 Glued, has potential activity for MT nucleation [143].

MT–actin interactions in different cellular regions are very similar. These interactions between two major cytoskeletal systems can be basically explained by three "mechanochemical modules" [148]. In the first, termed the "plus end/cortex anchor" module, the plus ends of individual MTs become bound by stable attachments to special sites on the actin cortex. This is the most popular actin-MT interaction module. It is used to explain, for example, the polarisation of centrosomes or the mitotic spindle, the positioning of the centrosome in migrating cells, or defining the leading edge of a migrating cell. It is also used with respect to the "search and capture" model. A plus-end MT complex is located on the ends of MTs and seems to have the ability to recognize and bind to actin directly or via an actin binding proteins [149]. For example, it has been suggested that cortical astral MT capture in budding yeast depends on Kar9p, an actin binding protein, and that this is mediated by binding of Kar9p to the MT plus end binding protein Bim1p [150-152]. Adenomatous polyposis coli protein (APC) in mammals has some similarity to Kar9 and Bim1p is a member of the EB1/LRP family. APC, is concentrated in the neuronal growth cone and is highly expressed in the developing brain [153]. This protein is translocated along MTs toward the plus ends by kinesin motility and EB1 and accumulates at the plus end, regulating MT stability [95, 122, 154]. APC clusters at the MT distal ends directed to the leading edge and associates with basal plasma membranes where it anchors the MTs to the cell cortex [122]. CLASPs are CLIP associated proteins, which can influence MT dynamics too. A redistribution of CLASPs to the leading edge, in order to orient and stabilize MTs was observed, in a fibroblast wounding assay [123]. The overlap in function between CLASP and APC is currently under investigation.

The EB1**,** probably recruits APC to MT ends [155]. EB1 was observed on the MT distal ends in the P-domain of the growth cone in a chick dorsal root ganglion cells and in the neurites of growth cones in the NT2A neuroblastoma cell line [156]. Since, it is known, that APC connection with plasma membrane is actin dependent [157], the speculation that EB1-APC complex can mediate the interaction between filopodial actin and plus ends of dynamic MTs is reasonable.

It has been demonstrated, that the dynactin complex component, p62 [158], associates with the cortex actin cytoskeleton. Besides these data, several other reports suggested that dynein might play a crucial role in capturing of MTs at adherent junctions. Firstly B-catenin recruits dynein to cell-cell contacts [159] and secondarily dynein intermediate chain can bind directly to PLAC-24, one of the proteins that is specifically recruited to sites of cell-cell contact together with components of adherent junctions [160]. PLAC-24 is not a dynactin subunit, and the binding of PLAC-24 to the dynein intermediate chain is independent of the association between dynein and dynactin. Given the localization of PLAC-24 at intercellular attachment sites and its binding interaction with the MT motor dynein, it was proposed that PLAC-24 may be involved in the capture and localization of MT plus ends at sites of cell-cell contact [160].

The second "mechano-chemical module" is the "actin bundle/MT guidance" module [148]. This is a conserved MT-actin interaction module, where MTs bind to and then grow or move along actin filament bundles. It may be used in situations where single MTs must be

targeted to precise positions [148]. It is thought to be a static or dynamic (motor-mediated) connection between MT and actin filaments. This model is very suitable for neuronal pathfinding, where the distribution of filopodia guides the growth of MTs, which steers motility of the growth cone. This module may also be used for MT targeting to focal adhesions and their regulation in migrating cells.

The third "mechanochemical module" is the "polymerization /contraction treadmill" module. This comprises both structurally and regulatory MT-actin interactions, which resemble the leading edge of migrating cells and transition zone of the neuronal growth cone, and may be used in systems where gradients in polymerization and contractility must be perpetuated [148]. Thus, the "anchor" module may initiate a polarization of MTs towards the leading edge and this could activate the "treadmill" module, with the cycle of protrusion and retrograde flow in migrating cells or polar relaxation and contraction ring in dividing cells.

2.4 Stabilization of MTs and Cell Polarity

Cytoplasmic MTs in animal cells radiate out in all directions from the centrosome, where their minus ends are bound. Most animal cells are polarized and MTs tend to extend toward specific regions of the cell by the mechanisms depending on the dynamic instability. The inherent instability of MTs explains their growth in specific directions in a cell, for example toward the leading edge of a crawling cell. The array of MTs radiating from the centrosome is continually changing as new MTs grow and replace others that have depolymerised. This dynamic behaviour can, however, be modified by the interactions of MTs with other proteins. Some cellular proteins act to disassemble MTs, either by severing MTs or by increasing the rate of tubulin depolymerization from MT ends. Other proteins bind to MTs and increase their stability. MTs originating in the centrosome can be selectively stabilized at plus ends and/or at the particular region of the cell membrane. In many cells, the initial stabilization of MTs at their plus ends is consolidated to produce a more permanent polarization of the cell. Such interactions allow the cell to stabilize MTs in particular locations and provide an important mechanism for determining cell shape and polarity (Fig. 9).

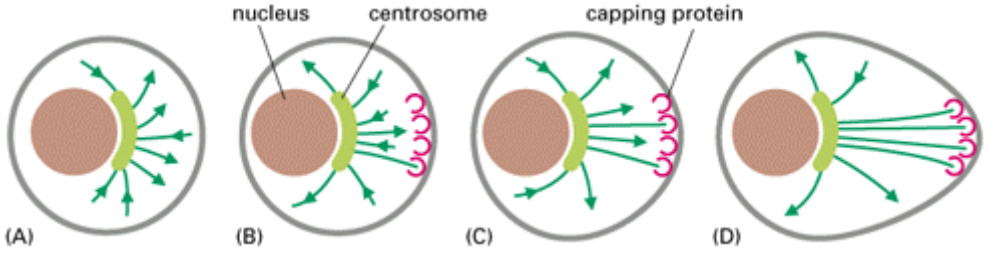

Figure 9. The selective stabilization of MTs can polarize a cell. A newly formed MT will persist only if both of its ends are protected from depolymerising. In cells, the minus ends of MTs are generally protected by the organizing centres, from which these filaments grow. The plus ends are initially free but can be stabilized by other proteins. Here, for example, a nonpolarized cell is depicted in (A) with new micro-tubules growing and shrinking from a centrosome in all directions randomly. The array of MTs then encounters hypothetical structures in a specific region of the cell cortex that can cap (stabilize) the free plus end of the MTs (B). The selective stabilization of those MTs that happen by chance to encounter these structures will lead to a rapid redistribution of the arrays and convert the cell to a polarized form (C and D). (1994 by Bruce Alberts et al,).

Adenomatous polyposis coli (APC) is transported by kinesin motor protein along selected MTs, clusters at the MT plus ends directed to the leading edge [145, 161], stabilizing them

and associating with basal plasma membranes to anchor the MTs to the cell cortex [122]. CLASP2 also stabilises the selected MTs, but attaches to the very distal ends of MTs growing into cortical capture sites on the plasma membrane. CLASPs colocalises with CLIP-170 and dynein/dynactin (p150 Glued) at the same MTs, but APC is not present there. These findings suggest that a molecular link between MTs and cell cortex might be provided by CLASPs or components of dynein/dynactin complex. It was demonstrated that p62 (component of the dynactin complex) associates with actin cytoskeleton in the cell cortex [162] and dynein can be recruited by β-catenin to the cell adhesion sites. Dynein intermediate chain also binds to PLAC-24 protein that locates in cell contacts and adherent junctions [163]. CLASPs bind to the plasma membrane through palmitoylated NH2 termini [123].

Chapter 3

The role of the cytoskeleton in neurons

3.1 Neurons

Neurons are probably the best example of a polarized cell type, in which polarization is intimately linked to a crucial function as signalling module. The polarized morphology of neurons allows them to carry out very specialized functions in organisms. Axons send information over long distances, while dendrites receive and integrate incoming information. Typical vertebrate neurons can extend a single thin axon over a very long distance, while dendrites remain comparatively short (Fig10). Many types of neurons have their own distinctive morphology. For example, monopolar sensory neurons from dorsal root ganglia extend a single axon that bifurcates and have no dendrites whatsoever [164]. In contrast, cerebellular Purkinje neurons have very thick and prominent dendrites. The functional difference between axons and dendrites are direct consequences of the distinct molecular compositions of both the cytoplasm and plasma membrane [165].

The correct formation and proper function of the nervous system requires several major morphological events, involving both neurons and glial cells, which occur during neuronal development. These changes involve many different processes, which include cell motility (e.g. neuronal migration), cell differentiation (e.g. neurite initiation, neurite outgrowth) and target site selection (e.g., pathfinding and growth cone turning). Neurons contain different types of cytoskeletal elements: MTs, actin filaments and neurofilaments. These polymers play key architectural roles and contribute significantly to the acquisition of asymmetrical cellular morphologies [164]. In order for a cell to move and change shape, its cytoskeleton must undergo rearrangements that involve breaking down and reforming these filaments.

The central aim of this thesis is the description of the dynamic behaviour of the MT cytoskeleton in neurons, using GFP-tagged proteins as a tool. In chapter 2, I have already explained the aspects of MT dynamic behaviour. Here, I will introduce some of the events that underlie neuronal differentiation and describe the specific features of the neuronal cytoskeleton.

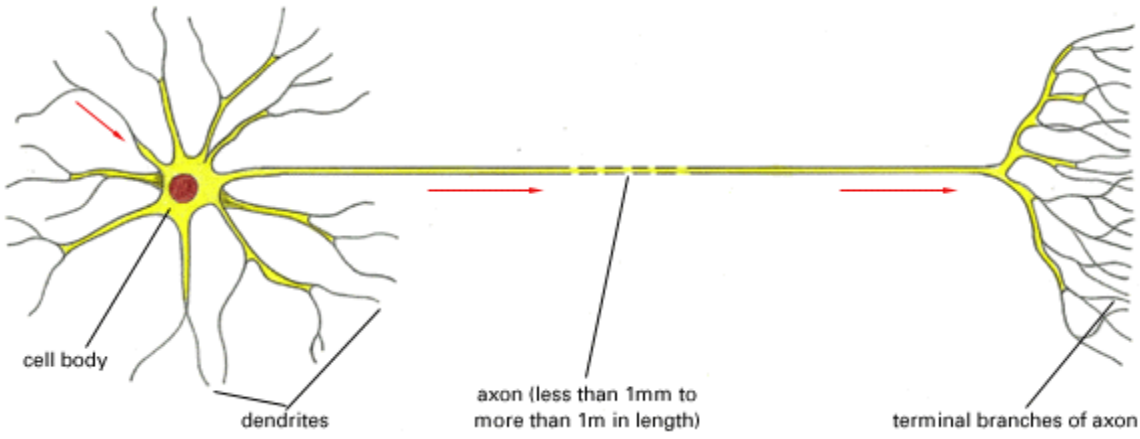

Fig 10. Schematic diagram of a typical vertebrate neuron. The arrows indicate the direction in which signals are conveyed. The single axon conducts signals away from the cell body, while the multiple dendrites receive signals from the axons of other neurons. The nerve terminals end on the dendrites or cell body of other neurons or on other cell types, such as muscle or gland cells. 1994 by Bruce Alberts

3.2 Neurite initiation

The question of "neuronal polarity ", i.e. how neurons know to extend a single axon and multiple dendrites and why only one particularly neurite becomes an axon, was first raised by Gary Banker in the 1980s [166, 167] (Fig 11) and is still unanswered.

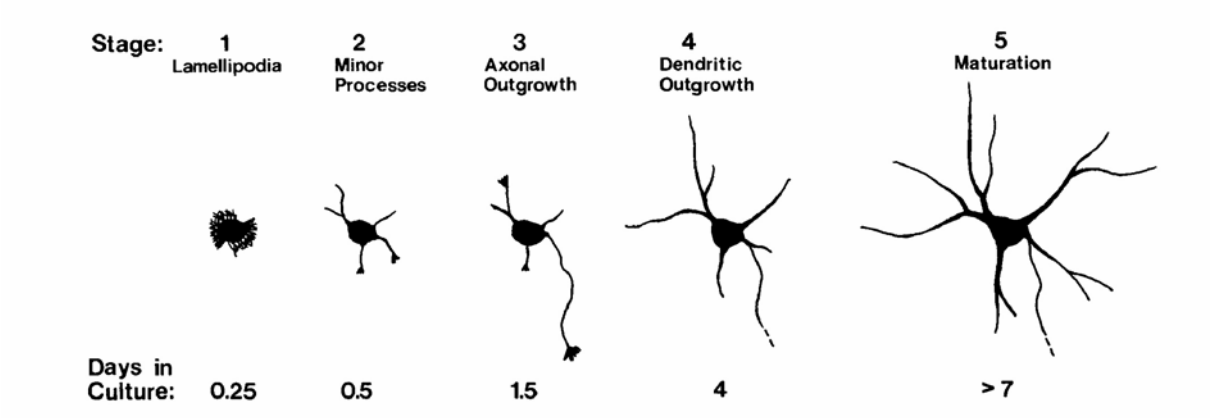

Fig 11. Stages of development of hippocampal neurons in culture. The approximate times at which cells enter each of the stages is indicated, by C.Dotti et al. 1988

The specification and regulation mechanisms of neuronal morphogenesis represent a field of intense research. What is emerging is that a major upstream signalling cascade for the establishment of neuronal polarity consists of Pi3-kinase and the mPar3/mPar6/aPKC complex [168]. In fact, the polarized distribution of mPar3 and mPar6 proteins, which have evolutionary conserved functions in determining cell polarity in worms and flies [169-171], is essential for neuronal polarity as well. Pi3-kinase acting upstream of mPar3/mPar6 complex is likely to be activated by growth factors and/or receptor tyrosine kinases. This causes the polarized localization of mPar3. Previous studies suggested that also actin and MTs play an important role in generating the asymmetry of Par proteins [172, 173]. It was found that Pi 3-kinase activates aPKC and Rho family GTPases, which leads to differential regulation of cytoskeleton dynamics in the growth cone of the future axon [168].

The formation of dendrites and axons starts out by the growth of "inert" neurites, which are thin, elongated and dynamic cell protrusions, formed by active outgrowth from the cell body. An actin-rich growth cone is located at the end of each neurite. Observations on hippocampal neuronal cultures [174] demonstrated that neurite initiation starts by lamellipodia formation, which acts as a precursor of the neurite. Later the initially broad lamellipodium undergoes segmentation, accumulates MTs in an ordered array [174, 175] and gradually migrates away from the cell body, tethered by the newly formed neurite shaft. The lamellipodia transform into the growth cone as the neurite elongates and becomes thinner, because of MT compression in the shaft.

The cytoskeletal components of a neurite are actin, MTs and associated with them the specific proteins that coordinate cytoskeletal rearrangements and other processes. It is certain that MTs play an important role in neuronal outgrowth; but are they also essential for neurite initiation? It was shown that incubation of cells with nanomolar concentrations of taxol [176] or nocodazole, the drugs which interfere with MT dynamics in opposing manners [177], reversibly inhibits spontaneous neurite initiation in cultured primary neurons. Observations on chick cortical neurons [178] suggested that MTs might be dispensable for the formation of the thick protrusion after cell-cell contact. However, in the absence of MT polymerisation,

processes fail to form growth cones and generate a thin neurite shaft. This suggests that the presence of MTs and their dynamic properties are very important for neurite initiation.

As mentioned above, an actin–rich lamellipodum around the neuroblast is observed in early stages of neurite initiation. This lamellipodum undergoes segmentation, accumulates mitochondria and transforms into a growth cone [174]. Interestingly, experimental evidence suggests that actin filaments can play both an inhibitory and stimulatory role in neurite initiation and axon outgrowth [179]. The clutch hypothesis of Mitchison and Kirschner, proposed that actin-mediated retrograde flow is a major driving force for neurite outgrowth, suggesting that actin based mechanisms facilitate neurite formation. However, in the presence of cytochalasin B, an actin destabilising drug, chick embryo dorsal root ganglion cells produce neurites without filopodia and lamellipodia [174, 180-182], suggesting that actin is dispensable for neurite initiation.

The actin cytoskeleton is more stable in the growth cones of immature neurites compared with the growth cone of the future axon [183]. This corresponds to current models of axonal path finding, in which increased dynamics of the actin cytoskeleton in the axonal growth cone results in rapid elongation [184]. Some years ago it was found that MTs in the potential axon are more stable than in the other neurites [185] and that suppression of tau, a major axonal MT associated protein, stops the process of transformation of an immature neurite into an axon [186]. These data suggested that increased MT stabilization in certain neuronal compartments might be an important event for axonal marking, which is contrary to the increased actin dynamics in the growth cone. Studies with electron-micrograph serial reconstruction of MTs, showed an increase of the amount of MT and their length in the neurite that becomes the axon, as compared to the other neurites [187]. Experiments with the actin destabilising drugs, demonstrated that all of the immature neurites grow longer and, remarkably, one of them (potential axon) consistently grew longer than the others in the presence of the drug [188]. These data strongly support an important role of MTs in neurite growth.

Both cytoskeletal systems, MTs and actin filaments, are highly integrated, to provide different morphological changes during the initial stages of neuronal development. The main suggestion is that actin acts as a “brake” to prevent neurite initiation, while MTs provide forward growth (either via polymerization or via motor-based transport of material). MTs try to “invade” the cell periphery in order to induce and stabilize newly formed protrusions.

3.3 The neuronal growth cone

During neuronal development, axons and dendrites undergo different morphological changes, induced by extensive growth, branching, but also retraction. All of these processes are guided by activities of the growth cone, such as turning, collapse, and consolidation. The axonal growth cone is a neuronal navigation structure, which is highly responsive to environmental cues [164]. During neuronal polarization, the growth cone of the potential axon becomes very large with a highly dynamic and very labile actin cytoskeleton[183].The cytoskeleton of the neuronal growth cone is composed of central, transition and peripheral domains [189] (Fig.12).

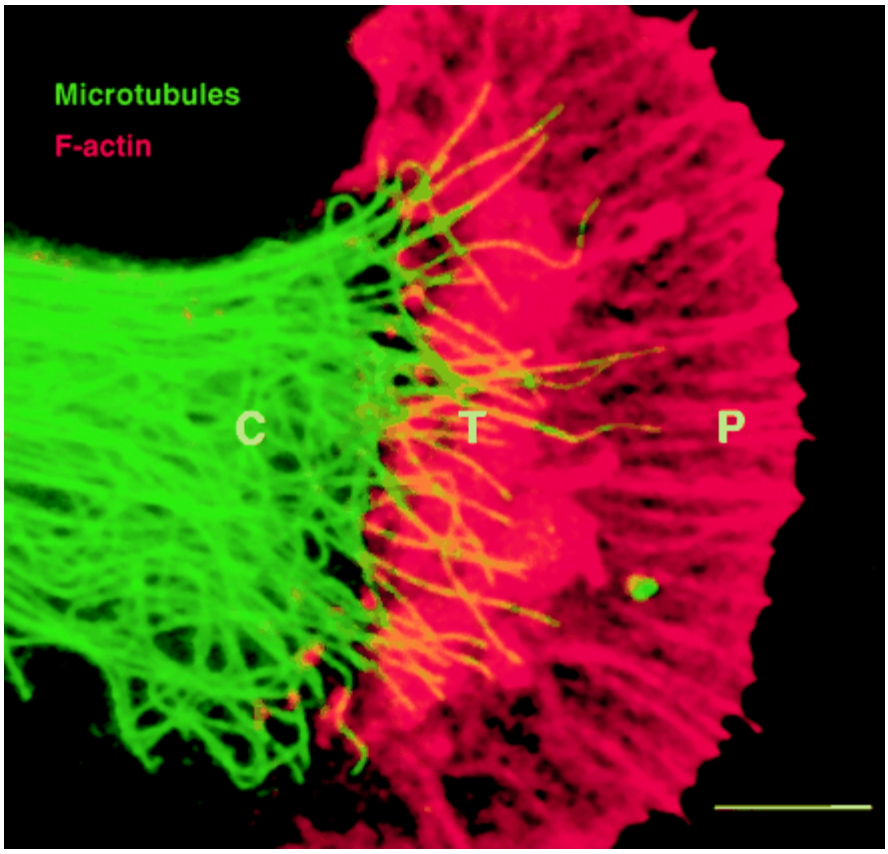

Fig. 12. F-actin and MT distribution in Aplysia bag cell neuron growth cone. The growth cones of Aplysia bag cells are characterized by a P-domain rich in F-actin and a C-domain rich in MTs. The T zone is characterized by ruffles containing both F-actin and MTs. Note that although under control conditions some MTs invade the P-domain F-actin, almost none reach near the leading edge (75% threshold). Scale bar, 5 µm. by Kabir N., 2001.

The majority of MTs in the neurite shaft are bundled, but upon entering the central C-domain of the growth cone they tend to be separated from each other and unbundled in order to enter the C-domain as single MTs [190-200]. After traversing the central domain MTs have a straight or slightly crooked shape [201, 202], but some of them are looped or form hairpin bends that cause the MT to re-enter the neurite shaft [203]. The main population of MTs is located in the central domain, but some of them can extend into the peripheral zone, into the actin filament network of filopodia [184, 191, 204-207]. MTs may also penetrate filopodia, which did not retract along the neurite shaft [190]. The growth cone MTs are pointed with their plus ends to the actin filament network in the peripheral P-domain of the growth cone [208-210]. Electron microscopy has shown that MTs that penetrate filopodia can be closely apposed to a bundle of actin filaments that constitute the core of the filopodium [204]. Basically the actin bundles within filopodia function as guides, along which MTs grow towards the leading edge in the direction of growth cone extension [184, 211, 212]. The simultaneous imaging of actin and MT systems demonstrated that retrograde flow in filopodial actin bundles moves MT rearwards [211], indicating that MTs may be structurally linked to actin.

Within neurons, actin is present throughout the cell, but is particularly abundant in the growth cone. As described above, the axonal growth cone contains a P-domain with highly dynamic actin filaments and only a few MTs, and a C-domain, consisting of organelles and terminating MTs [213]. The bulk of the actin filaments is turned over in the transition zone between C- and P- domains [214]. Neuronal growth cones contain at their periphery

lamellipodia and filopodia. Lamellipodia are flattened sheets containing a highly branched network of actin filaments. Protrusive and adhesive properties of lamellipodia are very important for cell motility. Filopodia consist of packed, parallel bundles of actin filaments. Both structures undergo rapid retrograde flow from the leading edge toward the growth cone centre. This phenomenon is thought to influence the advance of the growth cone [211, 215]. Filopodia act as environmental sensors and distribute membrane receptors to evaluate the environment that will dictate a path of growth [216]. The fast-growing barbed ends of actin filaments are orientated toward the periphery, so that actin polymerisation takes place at the leading edge of lamellipodia and at the tips of filopodia. Maintaining outgrowth requires a continuous supply of monomers to the leading edge, which comes from an increased rate of pointed end depolymerization [217] and by keeping the number of free barbed ends low [218]. Actin can be pulled, through association with myosin motor proteins, towards the centre of growth cone, where it depolymerises again [219]. Actin arcs found at the border between the peripheral and central domains of the growth cones [211], where they are thought to be involved in MT organization. Finally, intrapodia are actin and alpha1-integrin rich protrusive structures in growth cones [220]. The interpretation of intrapodia and its function is still in debate however, similar structures were observed early by Dent and Kalil [221]. The observation that polymerising MTs can initiate the intrapodia, points to links between MTs and actin cytoskeleton in this structure [220].

The relationship between MTs and actin in the peripheral and central domains of neuronal growth cones has been the subject of several recent studies. Experiments with acute inhibition of actin assembly resulted in rapid MT advance into the peripheral domain, demonstrating that the MT cytoskeleton can be affected by F-actin assembly dynamics [222]. Interestingly, when no actin assembly is taking place unguided axonal growth can occur [180]. In the case of affecting MT dynamics, growth cones became highly motile and were unable to recognize substratum components. All these data strongly suggest that MT-actin interactions are essential for organizing directed motility and related signal transduction in the neuronal growth cone [223].

Experiments with actin assembly inhibitors result in invasion of MTs in the peripheral domain of the growth cone [222]. These data lead to the idea that actin-based retrograde flow or other forces establish a ”barrier” for advance of MTs, organelles and cytoplasm toward the growth cone periphery. The time-lapsing imaging of non-neuronal cells [224] and growth cones [211] demonstrate that MTs in the peripheral domain are often swept backward at the same rate as the retrograde flow. However, there is growing evidence that certain configurations of actin filaments (especially actin bundles) can actually facilitate the MT forward progress [211].

3.4 Neurite outgrowth and differentiation into axons and dendrites

Actin is thought to play the leading role in elongation of the neurite: coupling of the peripheral actin network of the growth cone to the substrate is thought to facilitate the advance of MTs and other cytoplasmic constituents [225, 226]. Recent studies demonstrate the possibility of MT-dependent accumulation of F-actin at the front of the growth cone. Actin-rich intrapodia are stimulated by MTs to grow from the dorsal surface of growth cone [220] and interdependence of actin filaments and MTs at axon branch points has been described [227, 228]. These different experiments indicate that extracellular cues might affect actin in the growth cone via MTs, as well as affect MTs via actin.

There is no doubt that MTs are also essential for neurite outgrowth. For example, MT-based membrane transport is a very important factor for neurite elongation. Several studies have demonstrated that most membrane insertion takes place at the growth cone of axons

[229, 230]. In contrast, in Xenopus axons, most membrane insertion actually occurs along the length of the axon and in the cell body of Xenopus neurons [231]. Compared with mammalian neurons, Xenopus neurites are much larger and have been characterized as fast-growing [232]. This specifity probably explains the insertion of new membrane at the cell body and along the neurite in growing Xenopus neurites.

MTs have a stabilizing role in neurites. The growing axon contains a dense array of MTs that are individually short relative to the length of the axon but are tightly coalesced into a continuous bundle. MTs are essential for architectural support and also act as railways for the transport of various materials along the length of the axon. During growth and navigation of the axon, the MT array within the growth cone reorganizes and reorients toward the future direction of axon outgrowth [233-239]. The role that MTs play in axon growth is not limited to their continuous rearrangement at the terminal growth cone. In many neural systems directed axon growth is also accomplished by the formation of collateral branches, which extend interstitially from the axon shaft [240-243]. Studies on cultured hippocampal neurons suggest that MTs fragment within the region of the axon where interstitial branches are formed [187]. However, little is known about how the MT array reorganizes during the formation of such branches.

In the axon, MTs are oriented with their plus-ends distal to the cell body [244]**.** Remarkably, the orientation of the MT cytoskeleton in differentiated dendrites is different compared to axons [245-250], in that the plus ends of MTs can point both towards the cell body (plus ends proximal) as well as away from it (plus ends distal). This makes the question of the reorganization of the MT cytoskeleton in neurons highly interesting and suggests that different mechanisms are at work in dendrites and axons, perhaps to maintain identity of the two subcellular compartments. Moreover, as shown in (Fig 13), virtually none of the MTs in neurons is linked to the centrosome with their minus ends (see chapter 2); razing the question of which mechanism stabilizes the minus ends of the highly stable MT tracks.

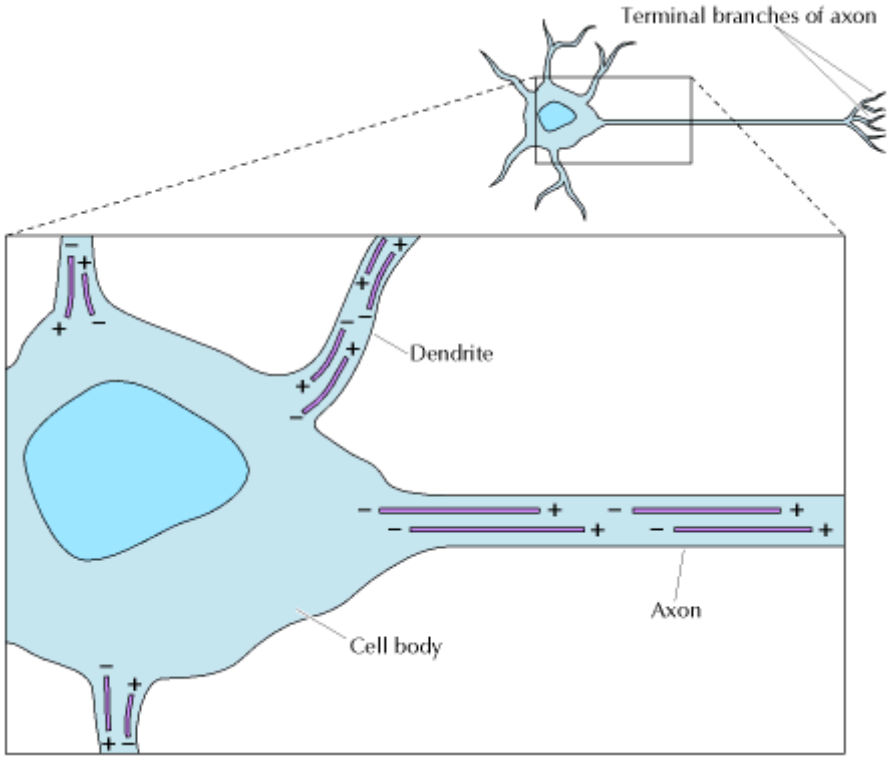

Figure 13. Organization of MTs in nerve cells Two distinct types of processes extend from the cell body of nerve cells (neurons). Dendrites are short processes that receive stimuli from other nerve cells. The single long

axon then carries impulses from the cell body to other cells, which may be either other neurons or an effecter cell, such as a muscle. Stable MTs in both axons and dendrites terminate in the cytoplasm rather than being anchored in the centrosome. In dendrites, MTs are oriented in both directions, with their plus ends pointing both toward and away from the cell body. In contrast, all of the axonal MTs are oriented with their plus ends pointing toward the tip of the axon. (2000 by Geoffrey M. Cooper)

3.5 Axonal pathfinding

As discussed above, the MT and actin cytoskeletons are essential for axonal and dendritic development. The same holds true for neuronal pathfinding. During neuronal navigation, one of the manoeuvres performed by the axon is growth cone turning. Experimental observations demonstrate that dynamic instability (see chapter 2) allows MTs to invade the actin network in the P-domain, and after that, MTs become stabilised against catastrophe, specifically in the direction of growth cone turn [200, 251]. All these modifications of the MT cytoskeleton result from guidance cues. Different experiments with MT stabilizing or depolymerising drugs, such as nocodazole and taxol [206, 252, 253], have shown a blockade of growth cone turning in response to guidance cues [254], indicating the importance of MT dynamics in this process. It is remarkable that the growth cone always turns towards the side with stabilized MTs [254]. MT dynamics can actually be directly regulated by signalling pathways, which are activated by guidance cues [254, 255]. Moreover MT dynamics can influence actin filaments dynamics, regulating the extension and retraction of lamellipodia and filopodia in the growth cone [200, 205, 220, 254]. Thus, if one wants to identify the mechanisms that control axonal pathfinding, it is essential to find out what factors are involved in the local regulation of MT dynamics.

The axonal pathfinding process means finding appropriate targets under the influence of guidance cues. Removal of filopodia or lamellipodia from axonal growth cones decreases axon growth rates and leads to a complete loss of guidance although neurite extension continues [256]. Repulsive cues cause the retraction of filopodia and collapse of lamellipodia. Conversely, the extension of these structures occurs upon exposure to attractive cues [257]. Actin dynamics in growth cones is influenced by interaction with soluble extracellular signals, matrix proteins and with other cells [258]. Each one of the different guidance molecules utilizes different receptor systems to elicit their effects on the growth cone [259-264]. Common features of most these receptors systems are the activation of the small non-heterotrimeric G-proteins, Rho/Rac/Cdc42, PI3-kinase and changes in calcium levels [258, 265, 266]. Signalling molecules can act through actin by modulating actin-kinases or phosphatases. Other regulators of actin filament formation, such as profilin [267], capping proteins [268], gelsolin [269] and Ena/Vasp proteins [270], may be involved in mediating signals from guidance cues as well. Because of the complexity of actin and MT regulation, the connection between receptor activation, the signalling cascade and cytoskeletal changes is still very difficult to establish.

3.6 Neuronal migration

During development of the central and peripheral nervous systems, there is a great deal of cellular movement. Precursor cells that will become neurons are born in particular locations within the embryo and then migrate, often over substantial distances, to reach their ultimate destinations. The classic example of this kind of migration is the neural crest cell, which originates from the dorsal margins of the neural tube and then migrates away from it in order to form the various ganglia that comprise the peripheral nervous system. The other major mode of migration is observed within the developing central nervous system, in which

neurons that have already completed their last mitotic division still undergo significant journeys before reaching their final locations. This kind of migration is critical, for example, for the lamination of many brain regions. In both cases, the cell body ultimately becomes stationary, after which motility mainly occurs at the growth cones at the tips of developing neurites. Variations on these forms of migration exist during development, but in general, these two modes, fibroblastic movement of crest cells and process-guided migration of central nervous systems (CNS) neurons, are representative of the cellular movements that result in the placement of neuronal cell bodies within the nervous system.

Recently, a great deal of attention has focused on the extracellular molecules that direct migrating neurons and their precursors to their proper location [271-275]. Less is known about changes in the cytoskeleton that must underlie cell movements. Complex systems of actin filaments and MTs must respond to intrinsic and extrinsic cues for cells to migrate and for this migration to occur with appropriate directionality. In addition, these cytoskeletal systems must undergo modifications in order for the cell to cease migration once it has reached its destination. The forces necessary for movement result from contractility of the actinomyosin system, which is highly sensitive to biochemical pathways responsive to growth factors [276, 277]. MTs are thought to consolidate the morphological alterations induced by the actinomyosin-based forces, and appear to be key to determining the direction of movement of growth cones [149] and migrating cells [276]. The earlier view was that MTs, while necessary for migration, passively follow the actin filaments, which are the principle targets of signalling molecules including small G-proteins and kinases. However, recent studies indicate that MT-related proteins may respond directly to signalling pathways [149, 276], suggesting that MTs play a far more active role in regulating cellular migration than once believed. In support of this view, it is now known that certain human disorders resulting from abnormalities of neuronal migration are caused by mutations in MT-related proteins such as Lis1 and doublecortin [278, 279].

For migrating neural crest cells, both microfilaments and MTs are required for normal movement [280]. In these cells, the leading edge of the cell presumably extends forward via the actinomyosin system, the centrosome relocates to a position between the nucleus and the leading edge, and the cell is dragged along in response to the movement of the leading edge [148, 281]. A dense array of MTs emanates from the centrosome to the leading edge, thus determining the direction of movement by polarizing the cell and providing mechanical struts that transduce the actinomyosin-based forces back to the nucleus and the rest of the cell. The centrosome usually precedes the nucleus in the direction of migration [282].

Migrating neurons such as cerebellar granule cells move along processes of glia or other neurons and consist of a spherical cell body that extends a leading process that is axon-like in appearance [283, 284]. The leading process contains a paraxial array of MTs that presumably transduces forces back to the cell body [285, 286]. In this case, however, the MTs within the leading process are not attached to the centrosome, but instead cooperate with a “cage” of MTs around the nucleus [286]. It is unknown whether the MTs that comprise the cage are attached or unattached to the centrosome, but they are cross-linked with one another, and presumably linked with MTs in the leading process, such that forces can be transduced from one type of MT to the other.

The importance of MTs to neuronal migration has been highlighted by work from several laboratories on the MT-related proteins known as Lis1 and doublecortin [278]. Mutations in the genes for these proteins are responsible for different forms of lissencephaly, which is a disorder resulting in profound mental retardation and neurological abnormalities. These disorders have been shown to result from a failure of neurons to migrate properly during embryogenesis. At the cellular level, LIS1 exhibits a punctate staining along MTs and accumulates in the area of the centrosome [78, 79]. Lis1 interacts with the dynein/dynactin

system [287-290] which transports membranous elements retrogradely and which transports MTs anterogradely within neurons. Lis1 can also affect the assembly dynamics of MTs [291], possibly through an interaction with one of the +TIPs [287, 292] discussed in chapter 2. Doublecortin, which is highly expressed in migrating neurons [293, 294], bundles MTs and also stabilizes them against disassembly, but via a mechanism distinct from that of Lis1 [278]. Doublecortin is concentrated at the tips of processes of neurons during migration and axon outgrowth [278, 295, 296], while Lis1 assists in the distribution of actin filaments in the leading process of migrating neurons via a mechanism involving Rho GTPase signalling [297]. Thus, Lis1 and perhaps doublecortin may serve to integrate the MT and actin systems during neuronal migration.

The actin cytoskeleton plays an important role in initiation of neuronal migration and process outgrowth. A number of genes that emphasize the essential role of actin regulation in cortical migration were identified. Flamin1 is an actin–binding protein, which cross-links actin filaments to the membrane and to each other [298]. At the deficiency of this protein neuronal migration does not occur [299, 300]. The other example is Ena/Vasp protein family that represents regulators of cell motility through the effect on the actin cytoskeleton [301]. The experiments suggest that the Ena/Vasp family of proteins can modulate the rate of cortical neuronal migration [302, 303].

3.7 Cytoskeletal rearrangements within neurons

During a long time, the question of how the neuronal cytoskeleton, and in particular the MT network, reorganizes itself, was one of the main challenges for neuroscientists. There are several crucial points to be made. First, MT assembly requires free tubulin. In contrast to other cell types, diffusion can not account for the presence of free tubulin in all compartments of a neuron, since it would take far too long to fill, for example, the growth cone by diffusion. Thus, for local MT polymerization to occur, tubulin must have been transported to a subcellular compartment first. Alternatively, it can be argued that there is no local MT polymerization; MTs are synthesized in the cell body only and subsequently transported outward by motors. Following these views, some authors have argued that the reorganization of the MT array in neurons is based solely on the assembly and disassembly of MTs and not on their movement through the cytoplasm [304]. Using fluorescence correlation spectroscopy it was shown that tubulin is transported through axons as oligomeric complexes [305]. Others were convinced that individual MTs can interact with motor proteins that actively transport them to new locations [306-308]. To date, this issue remains controversial, in large part because of results based on relatively low resolution fluorescence analyses.

One of the first MT imaging experiments was performed on large growth cones of *Aplysia* neurons with video-enhanced, differential interference contrast optics [222]. This study has demonstrated MT growth behaviour at the distal plus ends of individual MTs towards the actin cytoskeleton of the growth cone P-zone, suggesting that local MT polymerization indeed does take place. Experiments with microinjection of fluorescently labelled, rhodamine-conjugated tubulin fully confirmed this observation of MT behaviour [198-200, 309]. The application of fluorescent speckle microscopy (FSM) to neuronal growth cone MTs has also indicated dynamic instability [310], but MT translocation was not excluded and as was shown later also to occur [184, 211, 311]. In yet other studies, a mass of MTs was marked by photobleaching or photoactivation, but no movement of the mass was observed [312-317]. Nevertheless there is quite good evidence from indirect studies that individual MTs are capable of movement [318-320]. Thus, both systems local polymerization and MT transport may actually exist.

Because of MT bundling in the axonal shaft, it has always been a problem to resolve MTs optically and distinguish between the population of MTs, which are growing due to plus end assembly and that which is moving due to the MT translocation. Relatively short MTs were visualized in the growth cone, which, surprisingly underwent anterograde and retrograde movements [227, 311]. The inhibition of actin retrograde flow in the growth cone [184], as well as an activation of protein kinase C, increases the MT polymerization lifetimes and reduces catastrophe rates, resulting in a striking MT invasion in P-domain in growth cones [212].

The balance between plus end polymerization and retrograde movement probably determines the distal positions of MT plus ends in P-domain of growth cone. When MTs are retrogradly moved they may buckle, form loops and even brake in two that creates a new elongated plus ends and depolymerising minus ends [69, 211]. Whether actin retrograde flow and MT retrograde transport is coupled directly or through a molecular link remains to be established.

References

1. Janmey, P.A., *Mechanical properties of cytoskeletal polymers*, in *Curr Opin Cell Biol*. 1991. p. 4-11.
2. Steinert, P.M. and D.R. Roop, *Molecular and cellular biology of intermediate filaments*, in *Annu Rev Biochem*. 1988. p. 593-625.
3. Albers, K. and E. Fuchs, *The molecular biology of intermediate filament proteins*, in *Int Rev Cytol*. 1992. p. 243-79.
4. Coulombe, P.A., *The cellular and molecular biology of keratins: beginning a new era*, in *Curr Opin Cell Biol*. 1993. p. 17-29.
5. Gyoeva, F.K. and V.I. Gelfand, *Coalignment of vimentin intermediate filaments with microtubules depends on kinesin*, in *Nature*. 1991. p. 445-8.
6. Nigg, E.A., *Assembly and cell cycle dynamics of the nuclear lamina*, in *Semin Cell Biol*. 1992. p. 245-53.
7. Stewart, M., *Intermediate filament structure and assembly*, in *Curr Opin Cell Biol*. 1993. p. 3-11.
8. Chou, Y.H., et al., *Intermediate filament reorganization during mitosis is mediated by p34cdc2 phosphorylation of vimentin*, in *Cell*. 1990. p. 1063-71.
9. Fuchs, E. and Y. Yang, *Crossroads on cytoskeletal highways*, in *Cell*. 1999. p. 547-50.
10. Schwarz, M.A., et al., *Desmosomes and hemidesmosomes: constitutive molecular components*, in *Annu Rev Cell Biol*. 1990. p. 461-91.
11. Garrod, D.R., *Desmosomes and hemidesmosomes*, in *Curr Opin Cell Biol*. 1993. p. 30-40.
12. Okabe, S., H. Miyasaka, and N. Hirokawa, *Dynamics of the neuronal intermediate filaments*, in *J Cell Biol*. 1993. p. 375-86.
13. Fuchs, E. and D.W. Cleveland, *A structural scaffolding of intermediate filaments in health and disease*, in *Science*. 1998. p. 514-9.
14. Brown, R.H., Jr., *Amyotrophic lateral sclerosis: recent insights from genetics and transgenic mice*, in *Cell*. 1995. p. 687-92.
15. Kabsch, W. and J. Vandekerckhove, *Structure and function of actin*, in *Annu Rev Biophys Biomol Struct*. 1992. p. 49-76.
16. Hartwig, J.H. and D.J. Kwiatkowski, *Actin-binding proteins*, in *Curr Opin Cell Biol*. 1991. p. 87-97.
17. Carlier, M.F., *Role of nucleotide hydrolysis in the dynamics of actin filaments and microtubules.* Int Rev Cytol, 1989. **115**: p. 139-70.
18. Carlier, M.F., *Role of nucleotide hydrolysis in the dynamics of actin filaments and microtubules*, in *Int Rev Cytol*. 1989. p. 139-70.
19. Bonder, E.M., D.J. Fishkind, and M.S. Mooseker, *Direct measurement of critical concentrations and assembly rate constants at the two ends of an actin filament*, in *Cell*. 1983. p. 491-501.
20. Goldschmidt-Clermont, P.J., et al., *The control of actin nucleotide exchange by thymosin beta 4 and profilin. A potential regulatory mechanism for actin polymerization in cells*, in *Mol Biol Cell*. 1992. p. 1015-24.
21. Theriot, J.A. and T.J. Mitchison, *The three faces of profilin*, in *Cell*. 1993. p. 835-8.

22. Bamburg, J.R., A. McGough, and S. Ono, *Putting a new twist on actin: ADF/cofilins modulate actin dynamics*, in *Trends Cell Biol*. 1999. p. 364-70.
23. Welch, M.D., *The world according to Arp: regulation of actin nucleation by the Arp2/3 complex*, in *Trends Cell Biol*. 1999. p. 423-7.
24. Janmey, P.A., *Mechanical properties of cytoskeletal polymers.* Curr Opin Cell Biol, 1991. **3**(1): p. 4-11.
25. Burridge, K., et al., *Focal adhesions: transmembrane junctions between the extracellular matrix and the cytoskeleton*, in *Annu Rev Cell Biol*. 1988. p. 487-525.
26. Matsudaira, P., *Modular organization of actin crosslinking proteins*, in *Trends Biochem Sci*. 1991. p. 87-92.
27. Luna, E.J. and A.L. Hitt, *Cytoskeleton--plasma membrane interactions*, in *Science*. 1992. p. 955-64.
28. Titus, M.A., *Myosins*, in *Curr Opin Cell Biol*. 1993. p. 77-81.
29. Spudich, J.A., *How molecular motors work.* Nature, 1994. **372**(6506): p. 515-8.
30. Tan, J.L., S. Ravid, and J.A. Spudich, *Control of nonmuscle myosins by phosphorylation*, in *Annu Rev Biochem*. 1992. p. 721-59.
31. Sammak, P.J. and G.G. Borisy, *Direct observation of microtubule dynamics in living cells*, in *Nature*. 1988. p. 724-6.
32. Erickson, H.P. and E.T. O'Brien, *Microtubule dynamic instability and GTP hydrolysis*, in *Annu Rev Biophys Biomol Struct*. 1992. p. 145-66.
33. Mitchison, T. and M. Kirschner, *Dynamic instability of microtubule growth*. Nature. Vol. 312. 1984. 237-42.
34. Gelfand, V.I. and A.D. Bershadsky, *Microtubule dynamics: mechanism, regulation, and function*, in *Annu Rev Cell Biol*. 1991. p. 93-116.
35. Drechsel, D.N., et al., *Modulation of the dynamic instability of tubulin assembly by the microtubule-associated protein tau*, in *Mol Biol Cell*. 1992. p. 1141-54.
36. Lee, G., *Non-motor microtubule-associated proteins*, in *Curr Opin Cell Biol*. 1993. p. 88-94.
37. Brinkley, B.R., E.M. Fuller, and D.P. Highfield, *Cytoplasmic microtubules in normal and transformed cells in culture: analysis by tubulin antibody immunofluorescence*, in *Proc Natl Acad Sci U S A*. 1975. p. 4981-5.
38. Osborn, M. and K. Weber. *Cytoplasmic microtubules in tissue culture cells appear to grow from an organizing structure towards the plasma membrane*. in *Proc Natl Acad Sci U S A*. 1976.
39. Kuriyama, R. and G.G. Borisy, *Microtubule-nucleating activity of centrosomes in Chinese hamster ovary cells is independent of the centriole cycle but coupled to the mitotic cycle*, in *J Cell Biol*. 1981. p. 822-6.
40. Desai, A. and T.J. Mitchison, *Microtubule polymerization dynamics*, in *Annu Rev Cell Dev Biol*. 1997. p. 83-117.
41. Keating, T.J., et al., *Microtubule release from the centrosome*, in *Proc Natl Acad Sci U S A*. 1997. p. 5078-83.
42. Kristofferson, D., T. Mitchison, and M. Kirschner, *Direct observation of steady-state microtubule dynamics*, in *J Cell Biol*. 1986. p. 1007-19.
43. Walker, R.A., et al., *Dynamic instability of individual microtubules analyzed by video light microscopy: rate constants and transition frequencies*, in *J Cell Biol*. 1988. p. 1437-48.
44. Walker, R.A., S. Inoue, and E.D. Salmon, *Asymmetric behavior of severed microtubule ends after ultraviolet-microbeam irradiation of individual microtubules in vitro*, in *J Cell Biol*. 1989. p. 931-7.
45. Gildersleeve, R.F., et al., *Microtubules grow and shorten at intrinsically variable rates*, in *J Biol Chem*. 1992. p. 7995-8006.
46. Pryer, N.K., et al., *Brain microtubule-associated proteins modulate microtubule dynamic instability in vitro. Real-time observations using video microscopy*, in *J Cell Sci*. 1992. p. 965-76.
47. Odde, D.J., L. Cassimeris, and H.M. Buettner, *Kinetics of microtubule catastrophe assessed by probabilistic analysis*, in *Biophys J*. 1995. p. 796-802.
48. Tran, P.T., R.A. Walker, and E.D. Salmon, *A metastable intermediate state of microtubule dynamic instability that differs significantly between plus and minus ends*, in *J Cell Biol*. 1997. p. 105-17.
49. Panda, D., H.P. Miller, and L. Wilson, *Determination of the size and chemical nature of the stabilizing "cap" at microtubule ends using modulators of polymerization dynamics*, in *Biochemistry*. 2002. p. 1609-17.
50. Zhai, Y. and G.G. Borisy, *Quantitative determination of the proportion of microtubule polymer present during the mitosis-interphase transition*, in *J Cell Sci*. 1994. p. 881-90.
51. Dhamodharan, R. and P. Wadsworth, *Modulation of microtubule dynamic instability in vivo by brain microtubule associated proteins*, in *J Cell Sci*. 1995. p. 1679-89.

52. Danowski, B.A., ed. *Microtubule dynamics in serum-starved and serum-stimulated Swiss 3T3 mouse fibroblasts: implications for the relationship between serum-induced contractility and microtubules*. Cell Motil Cytoskeleton. Vol. 40. 1998. 1-12.
53. Vorobjev, I.A., T.M. Svitkina, and G.G. Borisy, *Cytoplasmic assembly of microtubules in cultured cells*, in *J Cell Sci*. 1997. p. 2635-45.
54. Yvon, A.M., P. Wadsworth, and M.A. Jordan, *Taxol suppresses dynamics of individual microtubules in living human tumor cells*, in *Mol Biol Cell*. 1999. p. 947-59.
55. Rusan, N.M., et al., *Cell cycle-dependent changes in microtubule dynamics in living cells expressing green fluorescent protein-alpha tubulin*, in *Mol Biol Cell*. 2001. p. 971-80.
56. Mikhailov, A.V. and G.G. Gundersen, *Centripetal transport of microtubules in motile cells*, in *Cell Motil Cytoskeleton*. 1995. p. 173-86.
57. Cassimeris, L., *Regulation of microtubule dynamic instability*, in *Cell Motil Cytoskeleton*. 1993. p. 275-81.
58. McNally, F.J., *Modulation of microtubule dynamics during the cell cycle*, in *Curr Opin Cell Biol*. 1996. p. 23-9.
59. Brinkley, B.R., *Microtubule organizing centers*, in *Annu Rev Cell Biol*. 1985. p. 145-72.
60. Hyman, A. and E. Karsenti, *The role of nucleation in patterning microtubule networks*, in *J Cell Sci*. 1998. p. 2077-83.
61. Glover, D.M., C. Gonzalez, and J.W. Raff, *The centrosome*, in *Sci Am*. 1993. p. 62-8.
62. Zheng, Y., et al., *Nucleation of microtubule assembly by a gamma-tubulin-containing ring complex*, in *Nature*. 1995. p. 578-83.
63. Gard, D.L. and M.W. Kirschner, *Microtubule assembly in cytoplasmic extracts of Xenopus oocytes and eggs*, in *J Cell Biol*. 1987. p. 2191-201.
64. Dye, R.B., et al., *End-stabilized microtubules observed in vitro: stability, subunit, interchange, and breakage*, in *Cell Motil Cytoskeleton*. 1992. p. 171-86.
65. Maniotis, A. and M. Schliwa, *Microsurgical removal of centrosomes blocks cell reproduction and centriole generation in BSC-1 cells*, in *Cell*. 1991. p. 495-504.
66. Yvon, A.M. and P. Wadsworth, *Non-centrosomal microtubule formation and measurement of minus end microtubule dynamics in A498 cells*, in *J Cell Sci*. 1997. p. 2391-401.
67. Dogterom, M. and B. Yurke, *Measurement of the force-velocity relation for growing microtubules*, in *Science*. 1997. p. 856-60.
68. Belmont, L.D., et al., *Real-time visualization of cell cycle-dependent changes in microtubule dynamics in cytoplasmic extracts*, in *Cell*. 1990. p. 579-89.
69. Waterman-Storer, C.M. and E.D. Salmon, *Actomyosin-based retrograde flow of microtubules in the lamella of migrating epithelial cells influences microtubule dynamic instability and turnover and is associated with microtubule breakage and treadmilling*, in *J Cell Biol*. 1997. p. 417-34.
70. Henderson, C.G., et al., *Reorganization of the centrosome and associated microtubules during the morphogenesis of a mouse cochlear epithelial cell*, in *J Cell Sci*. 1994. p. 589-600.
71. Ahmad, F.J. and P.W. Baas, *Microtubules released from the neuronal centrosome are transported into the axon*, in *J Cell Sci*. 1995. p. 2761-9.
72. Ahmad, F.J., et al., *An essential role for katanin in severing microtubules in the neuron*, in *J Cell Biol*. 1999. p. 305-15.
73. Ahmad, F.J., et al., *An essential role for katanin in severing microtubules in the neuron.* J Cell Biol, 1999. **145**(2): p. 305-15.
74. Quarmby, L., *Cellular Samurai: katanin and the severing of microtubules*, in *J Cell Sci*. 2000. p. 2821-7.
75. Chausovsky, A., A.D. Bershadsky, and G.G. Borisy, *Cadherin-mediated regulation of microtubule dynamics*, in *Nat Cell Biol*. 2000. p. 797-804.
76. Rodionov, V., E. Nadezhdina, and G. Borisy, *Centrosomal control of microtubule dynamics*, in *Proc Natl Acad Sci U S A*. 1999. p. 115-20.
77. Rodionov, V.I. and G.G. Borisy, *Self-centring activity of cytoplasm*, in *Nature*. 1997. p. 170-3.
78. Vorobjev, I.A., et al., *Contribution of plus and minus end pathways to microtubule turnover*, in *J Cell Sci*. 1999. p. 2277-89.
79. Shelden, E. and P. Wadsworth, *Observation and quantification of individual microtubule behavior in vivo: microtubule dynamics are cell-type specific*, in *J Cell Biol*. 1993. p. 935-45.
80. Cassimeris, L., N.K. Pryer, and E.D. Salmon, *Real-time observations of microtubule dynamic instability in living cells*, in *J Cell Biol*. 1988. p. 2223-31.
81. Sammak, P.J., G.J. Gorbsky, and G.G. Borisy, *Microtubule dynamics in vivo: a test of mechanisms of turnover*, in *J Cell Biol*. 1987. p. 395-405.

82. Janson, M.E., M.E. de Dood, and M. Dogterom, *Dynamic instability of microtubules is regulated by force*, in *J Cell Biol*. 2003. p. 1029-34.
83. Dogterom, M. and S. Leibler, *Physical aspects of the growth and regulation of microtubule structures*, in *Physical Review Letters*. 1993. p. 1347-1350.
84. Dogterom, M., A.C. Maggs, and S. Leibler, *Diffusion and formation of microtubule asters: physical processes versus biochemical regulation*, in *Proc Natl Acad Sci U S A*. 1995. p. 6683-8.
85. Holy, T.E., et al., *Assembly and positioning of microtubule asters in microfabricated chambers*, in *Proc Natl Acad Sci U S A*. 1997. p. 6228-31.
86. Komarova, Y.A., I.A. Vorobjev, and G.G. Borisy, *Life cycle of MTs: persistent growth in the cell interior, asymmetric transition frequencies and effects of the cell boundary*, in *J Cell Sci*. 2002. p. 3527-39.
87. Waterman-Storer, C.M. and E.D. Salmon, *Actomyosin-based retrograde flow of microtubules in the lamella of migrating epithelial cells influences microtubule dynamic instability and turnover and is associated with microtubule breakage and treadmilling.* J Cell Biol, 1997. **139**(2): p. 417-34.
88. Wadsworth, P., *Regional regulation of microtubule dynamics in polarized, motile cells.* Cell Motil Cytoskeleton, 1999. **42**(1): p. 48-59.
89. Rodionov, V., E. Nadezhdina, and G. Borisy, *Centrosomal control of microtubule dynamics.* Proc Natl Acad Sci U S A, 1999. **96**(1): p. 115-20.
90. Komarova, Y.A., I.A. Vorobjev, and G.G. Borisy, *Life cycle of MTs: persistent growth in the cell interior, asymmetric transition frequencies and effects of the cell boundary.* J Cell Sci, 2002. **115**(Pt 17): p. 3527-39.
91. Inoue, S., *Cell division and the mitotic spindle*, in *J Cell Biol*. 1981. p. 131s-147s.
92. Kirschner, M.W. and T. Mitchison, *Microtubule dynamics*, in *Nature*. 1986. p. 621.
93. Gliksman, N.R., R.V. Skibbens, and E.D. Salmon, *How the transition frequencies of microtubule dynamic instability (nucleation, catastrophe, and rescue) regulate microtubule dynamics in interphase and mitosis: analysis using a Monte Carlo computer simulation*, in *Mol Biol Cell*. 1993. p. 1035-50.
94. Perez, F., et al., *CLIP-170 highlights growing microtubule ends in vivo.* Cell, 1999. **96**(4): p. 517-27.
95. Mimori-Kiyosue, Y., N. Shiina, and S. Tsukita, *The dynamic behavior of the APC-binding protein EB1 on the distal ends of microtubules*, in *Curr Biol*. 2000. p. 865-8.
96. Howell, B., D.J. Odde, and L. Cassimeris, *Kinase and phosphatase inhibitors cause rapid alterations in microtubule dynamic instability in living cells*, in *Cell Motil Cytoskeleton*. 1997. p. 201-14.
97. Drewes, G., A. Ebneth, and E.M. Mandelkow, *MAPs, MARKs and microtubule dynamics*, in *Trends Biochem Sci*. 1998. p. 307-11.
98. Olmsted, J.B., *Microtubule-associated proteins*, in *Annu Rev Cell Biol*. 1986. p. 421-57.
99. Al-Bassam, J., et al., *MAP2 and tau bind longitudinally along the outer ridges of microtubule protofilaments*, in *J Cell Biol*. 2002. p. 1187-96.
100. Takemura, R., et al., *Polarity orientation and assembly process of microtubule bundles in nocodazole-treated, MAP2c-transfected COS cells*, in *Mol Biol Cell*. 1995. p. 981-96.
101. Gonzalez-Billault, C., et al., *Participation of structural microtubule-associated proteins (MAPs) in the development of neuronal polarity*, in *J Neurosci Res*. 2002. p. 713-9.
102. Job, D., et al., *Recycling of cold-stable microtubules: evidence that cold stability is due to substoichiometric polymer blocks*, in *Biochemistry*. 1982. p. 509-15.
103. Belmont, L.D. and T.J. Mitchison, *Identification of a protein that interacts with tubulin dimers and increases the catastrophe rate of microtubules*, in *Cell*. 1996. p. 623-31.
104. Cassimeris, L., *The oncoprotein 18/stathmin family of microtubule destabilizers*, in *Curr Opin Cell Biol*. 2002. p. 18-24.
105. Niethammer, P., P. Bastiaens, and E. Karsenti, *Stathmin-tubulin interaction gradients in motile and mitotic cells*, in *Science*. 2004. p. 1862-6.
106. Kinoshita, K., et al., *Reconstitution of physiological microtubule dynamics using purified components*, in *Science*. 2001. p. 1340-3.
107. Vasquez, R.J., D.L. Gard, and L. Cassimeris, *XMAP from Xenopus eggs promotes rapid plus end assembly of microtubules and rapid microtubule polymer turnover*, in *J Cell Biol*. 1994. p. 985-93.
108. Walczak, C.E., T.J. Mitchison, and A. Desai, *XKCM1: a Xenopus kinesin-related protein that regulates microtubule dynamics during mitotic spindle assembly*, in *Cell*. 1996. p. 37-47.
109. Desai, A.P., A.A. Pandit, and P.D. Gupte, *Cutaneous blastomycosis. Report of a case with diagnosis by fine needle aspiration cytology*, in *Acta Cytol*. 1997. p. 1317-9.
110. Wadsworth, P., *Regional regulation of microtubule dynamics in polarized, motile cells*, in *Cell Motil Cytoskeleton*. 1999. p. 48-59.
111. Hirokawa, N., *Kinesin and dynein superfamily proteins and the mechanism of organelle transport*, in *Science*. 1998. p. 519-26.

112. Porter, M.E. and K.A. Johnson, *Dynein structure and function*, in *Annu Rev Cell Biol*. 1989. p. 119-51.
113. Holzbaur, E.L. and R.B. Vallee, *DYNEINS: molecular structure and cellular function*, in *Annu Rev Cell Biol*. 1994. p. 339-72.
114. Vale, R.D., T.S. Reese, and M.P. Sheetz, *Identification of a novel force-generating protein, kinesin, involved in microtubule-based motility*, in *Cell*. 1985. p. 39-50.
115. Mandelkow, E. and K.A. Johnson, *The structural and mechanochemical cycle of kinesin*, in *Trends Biochem Sci*. 1998. p. 429-33.
116. Terasaki, M., *Recent progress on structural interactions of the endoplasmic reticulum*, in *Cell Motil Cytoskeleton*. 1990. p. 71-5.
117. Corthesy-Theulaz, I., A. Pauloin, and S.R. Rfeffer, *Cytoplasmic dynein participates in the centrosomal localization of the Golgi complex*, in *J Cell Biol*. 1992. p. 1333-45.
118. Schuyler, S.C. and D. Pellman, *Microtubule "plus-end-tracking proteins": The end is just the beginning.* Cell, 2001. **105**(4): p. 421-4.
119. Carvalho, P., J.S. Tirnauer, and D. Pellman, *Surfing on microtubule ends.* Trends Cell Biol, 2003. **13**(5): p. 229-37.
120. Mimori-Kiyosue, Y., N. Shiina, and S. Tsukita, *The dynamic behavior of the APC-binding protein EB1 on the distal ends of microtubules.* Curr Biol, 2000. **10**(14): p. 865-8.
121. Stepanova, T., et al., *Visualization of microtubule growth in cultured neurons via the use of EB3-GFP (end-binding protein 3-green fluorescent protein).* J Neurosci, 2003. **23**(7): p. 2655-64.
122. Mimori-Kiyosue, Y., N. Shiina, and S. Tsukita, *Adenomatous polyposis coli (APC) protein moves along microtubules and concentrates at their growing ends in epithelial cells.* J Cell Biol, 2000. **148**(3): p. 505-18.
123. Akhmanova, A., et al., *Clasps are CLIP-115 and -170 associating proteins involved in the regional regulation of microtubule dynamics in motile fibroblasts.* Cell, 2001. **104**(6): p. 923-35.
124. Coquelle, F.M., et al., *LIS1, CLIP-170's key to the dynein/dynactin pathway*, in *Mol Cell Biol*. 2002. p. 3089-102.
125. Sapir, T., M. Elbaum, and O. Reiner, *Reduction of microtubule catastrophe events by LIS1, platelet-activating factor acetylhydrolase subunit*, in *Embo J*. 1997. p. 6977-84.
126. Perez, F., et al., *CLIP-170 highlights growing microtubule ends in vivo*, in *Cell*. 1999. p. 517-27.
127. Hoogenraad, C.C., et al., *Functional analysis of CLIP-115 and its binding to microtubules*, in *J Cell Sci*. 2000. p. 2285-97.
128. Vaughan, K.T., et al., *Colocalization of cytoplasmic dynein with dynactin and CLIP-170 at microtubule distal ends.* J Cell Sci, 1999. **112**(Pt 10): p. 1437-47.
129. Galjart, N. and F. Perez, *A plus-end raft to control microtubule dynamics and function.* Curr Opin Cell Biol, 2003. **15**(1): p. 48-53.
130. McNally, F.J., *Cytoskeleton: CLASPing the end to the edge*, in *Curr Biol*. 2001. p. R477-80.
131. Stepanova, T., et al., *Visualization of microtubule growth in cultured neurons via the use of EB3-GFP (end-binding protein 3-green fluorescent protein)*, in *J Neurosci*. 2003. p. 2655-64.
132. Mimori-Kiyosue, Y. and S. Tsukita, *"Search-and-capture" of microtubules through plus-end-binding proteins (+TIPs).* J Biochem, 2003. **134**(3): p. 321-6.
133. Tirnauer, J.S. and B.E. Bierer, *EB1 proteins regulate microtubule dynamics, cell polarity, and chromosome stability.* J Cell Biol, 2000. **149**(4): p. 761-6.
134. Kirschner, M.W. and T. Mitchison, *Microtubule dynamics.* Nature, 1986. **324**(6098): p. 621.
135. Sawin, K.E., *Microtubule dynamics: the view from the tip*, in *Curr Biol*. 2000. p. R860-2.
136. Schroer, T.A., *Motors, clutches and brakes for membrane traffic: a commemorative review in honor of Thomas Kreis*, in *Traffic*. 2000. p. 3-10.
137. Schuyler, S.C. and D. Pellman, *Microtubule "plus-end-tracking proteins": The end is just the beginning*, in *Cell*. 2001. p. 421-4.
138. Akhmanova, A., et al., *Clasps are CLIP-115 and -170 associating proteins involved in the regional regulation of microtubule dynamics in motile fibroblasts*, in *Cell*. 2001. p. 923-35.
139. Inoue, Y.H., et al., *Orbit, a novel microtubule-associated protein essential for mitosis in Drosophila melanogaster*, in *J Cell Biol*. 2000. p. 153-66.
140. Lemos, C.L., et al., *Mast, a conserved microtubule-associated protein required for bipolar mitotic spindle organization*, in *Embo J*. 2000. p. 3668-82.
141. Schwartz, K., K. Richards, and D. Botstein, *BIM1 encodes a microtubule-binding protein in yeast*, in *Mol Biol Cell*. 1997. p. 2677-91.
142. Miller, R.K. and M.D. Rose, *Kar9p is a novel cortical protein required for cytoplasmic microtubule orientation in yeast*, in *J Cell Biol*. 1998. p. 377-90.
143. Ligon, L.A., et al., *The microtubule plus-end proteins EB1 and dynactin have differential effects on microtubule polymerization*, in *Mol Biol Cell*. 2003. p. 1405-17.

144. Munemitsu, S., et al., *The APC gene product associates with microtubules in vivo and promotes their assembly in vitro*, in *Cancer Res*. 1994. p. 3676-81.
145. Nathke, I.S., et al., *The adenomatous polyposis coli tumor suppressor protein localizes to plasma membrane sites involved in active cell migration*, in *J Cell Biol*. 1996. p. 165-79.
146. Mimori-Kiyosue, Y., N. Shiina, and S. Tsukita, *Adenomatous polyposis coli (APC) protein moves along microtubules and concentrates at their growing ends in epithelial cells*, in *J Cell Biol*. 2000. p. 505-18.
147. Jimbo, T., et al., *Identification of a link between the tumour suppressor APC and the kinesin superfamily*, in *Nat Cell Biol*. 2002. p. 323-7.
148. Rodriguez, O.C., et al., *Conserved microtubule-actin interactions in cell movement and morphogenesis.* Nat Cell Biol, 2003. **5**(7): p. 599-609.
149. Gordon-Weeks, P.R., *Microtubules and growth cone function.* J Neurobiol, 2004. **58**(1): p. 70-83.
150. Korinek, W.S., et al., *Molecular linkage underlying microtubule orientation toward cortical sites in yeast.* Science, 2000. **287**(5461): p. 2257-9.
151. Lee, L., et al., *Positioning of the mitotic spindle by a cortical-microtubule capture mechanism.* Science, 2000. **287**(5461): p. 2260-2.
152. Miller, R.K., S.C. Cheng, and M.D. Rose, *Bim1p/Yeb1p mediates the Kar9p-dependent cortical attachment of cytoplasmic microtubules.* Mol Biol Cell, 2000. **11**(9): p. 2949-59.
153. Morrison, E.E., et al., *The cellular distribution of the adenomatous polyposis coli tumour suppressor protein in neuroblastoma cells is regulated by microtubule dynamics.* Neuroscience, 1997. **81**(2): p. 553-63.
154. Zumbrunn, J., et al., *Binding of the adenomatous polyposis coli protein to microtubules increases microtubule stability and is regulated by GSK3 beta phosphorylation.* Curr Biol, 2001. **11**(1): p. 44-9.
155. Askham, J.M., et al., *Regulation and function of the interaction between the APC tumour suppressor protein and EB1.* Oncogene, 2000. **19**(15): p. 1950-8.
156. Morrison, E.E., P.M. Moncur, and J.M. Askham, *EB1 identifies sites of microtubule polymerisation during neurite development.* Brain Res Mol Brain Res, 2002. **98**(1-2): p. 145-52.
157. Rosin-Arbesfeld, R., G. Ihrke, and M. Bienz, *Actin-dependent membrane association of the APC tumour suppressor in polarized mammalian epithelial cells*, in *Embo J*. 2001. p. 5929-39.
158. Garces, J.A., et al., *Interaction of the p62 subunit of dynactin with Arp1 and the cortical actin cytoskeleton.* Curr Biol, 1999. **9**(24): p. 1497-500.
159. Ligon, L.A., et al., *Dynein binds to beta-catenin and may tether microtubules at adherens junctions.* Nat Cell Biol, 2001. **3**(10): p. 913-7.
160. Karki, S., et al., *PLAC-24 is a cytoplasmic dynein-binding protein that is recruited to sites of cell-cell contact.* Mol Biol Cell, 2002. **13**(5): p. 1722-34.
161. Jimbo, T., et al., *Identification of a link between the tumour suppressor APC and the kinesin superfamily.* Nat Cell Biol, 2002. **4**(4): p. 323-7.
162. Garces, J.A., et al., *Interaction of the p62 subunit of dynactin with Arp1 and the cortical actin cytoskeleton*, in *Curr Biol*. 1999. p. 1497-500.
163. Karki, S., et al., *PLAC-24 is a cytoplasmic dynein-binding protein that is recruited to sites of cell-cell contact*, in *Mol Biol Cell*. 2002. p. 1722-34.
164. Baas, P.W. and D.W. Buster, *Slow axonal transport and the genesis of neuronal morphology.* J Neurobiol, 2004. **58**(1): p. 3-17.
165. Craig, A.M. and G. Banker, *Neuronal polarity.* Annu Rev Neurosci, 1994. **17**: p. 267-310.
166. Dotti, C.G. and G.A. Banker, *Experimentally induced alteration in the polarity of developing neurons.* Nature, 1987. **330**(6145): p. 254-6.
167. Dotti, C.G., C.A. Sullivan, and G.A. Banker, *The establishment of polarity by hippocampal neurons in culture.* J Neurosci, 1988. **8**(4): p. 1454-68.
168. Shi, S.H., L.Y. Jan, and Y.N. Jan, *Hippocampal neuronal polarity specified by spatially localized mPar3/mPar6 and PI 3-kinase activity.* Cell, 2003. **112**(1): p. 63-75.
169. Kemphues, K., *PARsing embryonic polarity.* Cell, 2000. **101**(4): p. 345-8.
170. Jan, Y.N. and L.Y. Jan, *Asymmetric cell division in the Drosophila nervous system.* Nat Rev Neurosci, 2001. **2**(11): p. 772-9.
171. Ohno, S., *Intercellular junctions and cellular polarity: the PAR-aPKC complex, a conserved core cassette playing fundamental roles in cell polarity.* Curr Opin Cell Biol, 2001. **13**(5): p. 641-8.
172. Rappleye, C.A., et al., *The coronin-like protein POD-1 is required for anterior-posterior axis formation and cellular architecture in the nematode caenorhabditis elegans.* Genes Dev, 1999. **13**(21): p. 2838-51.
173. Wallenfang, M.R. and G. Seydoux, *Polarization of the anterior-posterior axis of C. elegans is a microtubule-directed process.* Nature, 2000. **408**(6808): p. 89-92.

174. Dehmelt, L., et al., *The role of microtubule-associated protein 2c in the reorganization of microtubules and lamellipodia during neurite initiation.* J Neurosci, 2003. **23**(29): p. 9479-90.
175. Tang, D. and D.J. Goldberg, *Bundling of microtubules in the growth cone induced by laminin.* Mol Cell Neurosci, 2000. **15**(3): p. 303-13.
176. Letourneau, P.C. and A.H. Ressler, *Inhibition of neurite initiation and growth by taxol.* J Cell Biol, 1984. **98**(4): p. 1355-62.
177. Downing, K.H., *Structural basis for the interaction of tubulin with proteins and drugs that affect microtubule dynamics.* Annu Rev Cell Dev Biol, 2000. **16**: p. 89-111.
178. Smith, C.L., *The initiation of neurite outgrowth by sympathetic neurons grown in vitro does not depend on assembly of microtubules.* J Cell Biol, 1994. **127**(5): p. 1407-18.
179. Mitchison, T. and M. Kirschner, *Cytoskeletal dynamics and nerve growth.* Neuron, 1988. **1**(9): p. 761-72.
180. Marsh, L. and P.C. Letourneau, *Growth of neurites without filopodial or lamellipodial activity in the presence of cytochalasin B.* J Cell Biol, 1984. **99**(6): p. 2041-7.
181. Edson, K., B. Weisshaar, and A. Matus, *Actin depolymerisation induces process formation on MAP2-transfected non-neuronal cells.* Development, 1993. **117**(2): p. 689-700.
182. Knowles, R., N. LeClerc, and K.S. Kosik, *Organization of actin and microtubules during process formation in tau-expressing Sf9 cells.* Cell Motil Cytoskeleton, 1994. **28**(3): p. 256-64.
183. Bradke, F. and C.G. Dotti, *The role of local actin instability in axon formation.* Science, 1999. **283**(5409): p. 1931-4.
184. Zhou, F.Q., C.M. Waterman-Storer, and C.S. Cohan, *Focal loss of actin bundles causes microtubule redistribution and growth cone turning.* J Cell Biol, 2002. **157**(5): p. 839-49.
185. Ferreira, A., J. Busciglio, and A. Caceres, *Microtubule formation and neurite growth in cerebellar macroneurons which develop in vitro: evidence for the involvement of the microtubule-associated proteins, MAP-1a, HMW-MAP2 and Tau.* Brain Res Dev Brain Res, 1989. **49**(2): p. 215-28.
186. Caceres, A. and K.S. Kosik, *Inhibition of neurite polarity by tau antisense oligonucleotides in primary cerebellar neurons.* Nature, 1990. **343**(6257): p. 461-3.
187. Yu, W., F.J. Ahmad, and P.W. Baas, *Microtubule fragmentation and partitioning in the axon during collateral branch formation.* J Neurosci, 1994. **14**(10): p. 5872-84.
188. Ruthel, G. and P.J. Hollenbeck, *Growth cones are not required for initial establishment of polarity or differential axon branch growth in cultured hippocampal neurons.* J Neurosci, 2000. **20**(6): p. 2266-74.
189. Suter, D.M. and P. Forscher, *An emerging link between cytoskeletal dynamics and cell adhesion molecules in growth cone guidance*, in *Curr Opin Neurobiol*. 1998. p. 106-16.
190. Yamada, K.M., B.S. Spooner, and N.K. Wessells, *Ultrastructure and function of growth cones and axons of cultured nerve cells*, in *J Cell Biol*. 1971. p. 614-35.
191. Letourneau, P.C., *Differences in the organization of actin in the growth cones compared with the neurites of cultured neurons from chick embryos*, in *J Cell Biol*. 1983. p. 963-73.
192. Bunge, M.B., *Fine structure of nerve fibers and growth cones of isolated sympathetic neurons in culture*, in *J Cell Biol*. 1973. p. 713-35.
193. Tsui, H.T., et al., *Novel organization of microtubules in cultured central nervous system neurons: formation of hairpin loops at ends of maturing neurites*, in *J Neurosci*. 1984. p. 3002-13.
194. Cheng, T.P. and T.S. Reese, *Polarized compartmentalization of organelles in growth cones from developing optic tectum*, in *J Cell Biol*. 1985. p. 1473-80.
195. Cheng, T.P. and T.S. Reese, *Compartmentalization of anterogradely and retrogradely transported organelles in axons and growth cones from chick optic tectum*, in *J Neurosci*. 1988. p. 3190-9.
196. Bridgman, P.C. and M.E. Dailey, *The organization of myosin and actin in rapid frozen nerve growth cones*, in *J Cell Biol*. 1989. p. 95-109.
197. Dailey, M.E. and P.C. Bridgman, *Structure and organization of membrane organelles along distal microtubule segments in growth cones*, in *J Neurosci Res*. 1991. p. 242-58.
198. Sabry, J.H., et al., *Microtubule behavior during guidance of pioneer neuron growth cones in situ*, in *J Cell Biol*. 1991. p. 381-95.
199. Tanaka, E.M. and M.W. Kirschner, *Microtubule behavior in the growth cones of living neurons during axon elongation*, in *J Cell Biol*. 1991. p. 345-63.
200. Tanaka, E. and J. Sabry, *Making the connection: cytoskeletal rearrangements during growth cone guidance*, in *Cell*. 1995. p. 171-6.
201. Cheng, T.P. and T.S. Reese, *Polarized compartmentalization of organelles in growth cones from developing optic tectum.* J Cell Biol, 1985. **101**(4): p. 1473-80.
202. Cheng, T.P. and T.S. Reese, *Compartmentalization of anterogradely and retrogradely transported organelles in axons and growth cones from chick optic tectum.* J Neurosci, 1988. **8**(9): p. 3190-9.

203. Tsui, H.T., et al., *Novel organization of microtubules in cultured central nervous system neurons: formation of hairpin loops at ends of maturing neurites.* J Neurosci, 1984. **4**(12): p. 3002-13.
204. Bush, M.S., et al., *An analysis of an axonal gradient of phosphorylated MAP 1B in cultured rat sensory neurons*, in *Eur J Neurosci*. 1996. p. 235-48.
205. Gallo, G., *Involvement of microtubules in the regulation of neuronal growth cone morphologic remodeling*, in *J Neurobiol*. 1998. p. 121-40.
206. Williamson, T., et al., *Microtubule reorganization is obligatory for growth cone turning*, in *Proc Natl Acad Sci U S A*. 1996. p. 15221-6.
207. DiTella, M.C., et al., *MAP-1B/TAU functional redundancy during laminin-enhanced axonal growth*, in *J Cell Sci*. 1996. p. 467-77.
208. Heidemann, S.R., J.M. Landers, and M.A. Hamborg, *Polarity orientation of axonal microtubules*, in *J Cell Biol*. 1981. p. 661-5.
209. Baas, P.W., et al., *Polarity orientation of microtubules in hippocampal neurons: uniformity in the axon and nonuniformity in the dendrite*, in *Proc Natl Acad Sci U S A*. 1988. p. 8335-9.
210. Baas, P.W., L.A. White, and S.R. Heidemann, *Microtubule polarity reversal accompanies regrowth of amputated neurites*, in *Proc Natl Acad Sci U S A*. 1987. p. 5272-6.
211. Schaefer, A.W., N. Kabir, and P. Forscher, *Filopodia and actin arcs guide the assembly and transport of two populations of microtubules with unique dynamic parameters in neuronal growth cones.* J Cell Biol, 2002. **158**(1): p. 139-52.
212. Kabir, N., et al., *Protein kinase C activation promotes microtubule advance in neuronal growth cones by increasing average microtubule growth lifetimes.* J Cell Biol, 2001. **152**(5): p. 1033-44.
213. Bridgman, P.C. and M.E. Dailey, *The organization of myosin and actin in rapid frozen nerve growth cones.* J Cell Biol, 1989. **108**(1): p. 95-109.
214. Suter, D.M. and P. Forscher, *Substrate-cytoskeletal coupling as a mechanism for the regulation of growth cone motility and guidance*, in *J Neurobiol*. 2000. p. 97-113.
215. Bray, D. and K. Chapman, *Analysis of microspike movements on the neuronal growth cone*, in *J Neurosci*. 1985. p. 3204-13.
216. Kater, S.B. and V. Rehder, *The sensory-motor role of growth cone filopodia*, in *Curr Opin Neurobiol*. 1995. p. 68-74.
217. Pollard, T.D. and G.G. Borisy, *Cellular motility driven by assembly and disassembly of actin filaments*, in *Cell*. 2003. p. 453-65.
218. Gremm, D. and A. Wegner, *Gelsolin as a calcium-regulated actin filament-capping protein*, in *Eur J Biochem*. 2000. p. 4339-45.
219. Lin, C.H., et al., *Myosin drives retrograde F-actin flow in neuronal growth cones*, in *Neuron*. 1996. p. 769-82.
220. Rochlin, M.W., M.E. Dailey, and P.C. Bridgman, *Polymerizing microtubules activate site-directed F-actin assembly in nerve growth cones.* Mol Biol Cell, 1999. **10**(7): p. 2309-27.
221. Dent, E.W. and K. Kalil, *Axon branching requires interactions between dynamic microtubules and actin filaments*, in *J Neurosci*. 2001. p. 9757-69.
222. Forscher, P. and S.J. Smith, *Actions of cytochalasins on the organization of actin filaments and microtubules in a neuronal growth cone.* J Cell Biol, 1988. **107**(4): p. 1505-16.
223. Tanaka, E., T. Ho, and M.W. Kirschner, *The role of microtubule dynamics in growth cone motility and axonal growth*, in *J Cell Biol*. 1995. p. 139-55.
224. Salmon, W.C., M.C. Adams, and C.M. Waterman-Storer, *Dual-wavelength fluorescent speckle microscopy reveals coupling of microtubule and actin movements in migrating cells.* J Cell Biol, 2002. **158**(1): p. 31-7.
225. Lin, C.H. and P. Forscher, *Growth cone advance is inversely proportional to retrograde F-actin flow.* Neuron, 1995. **14**(4): p. 763-71.
226. Heidemann, S.R., *Cytoplasmic mechanisms of axonal and dendritic growth in neurons.* Int Rev Cytol, 1996. **165**: p. 235-96.
227. Dent, E.W. and K. Kalil, *Axon branching requires interactions between dynamic microtubules and actin filaments.* J Neurosci, 2001. **21**(24): p. 9757-69.
228. Gibney, J. and J.Q. Zheng, *Cytoskeletal dynamics underlying collateral membrane protrusions induced by neurotrophins in cultured Xenopus embryonic neurons.* J Neurobiol, 2003. **54**(2): p. 393-405.
229. Craig, A.M., R.J. Wyborski, and G. Banker, *Preferential addition of newly synthesized membrane protein at axonal growth cones*, in *Nature*. 1995. p. 592-4.
230. Dai, J. and M.P. Sheetz, *Axon membrane flows from the growth cone to the cell body*, in *Cell*. 1995. p. 693-701.
231. Popov, S., A. Brown, and M.M. Poo, *Forward plasma membrane flow in growing nerve processes*, in *Science*. 1993. p. 244-6.

232. Popov, S., A. Brown, and M.M. Poo, *Forward plasma membrane flow in growing nerve processes.* Science, 1993. **259**(5092): p. 244-6.
233. Sabry, J.H., et al., *Microtubule behavior during guidance of pioneer neuron growth cones in situ.* J Cell Biol, 1991. **115**(2): p. 381-95.
234. Tanaka, E.M. and M.W. Kirschner, *Microtubule behavior in the growth cones of living neurons during axon elongation.* J Cell Biol, 1991. **115**(2): p. 345-63.
235. Lin, C.H. and P. Forscher, *Cytoskeletal remodeling during growth cone-target interactions.* J Cell Biol, 1993. **121**(6): p. 1369-83.
236. Tanaka, E. and J. Sabry, *Making the connection: cytoskeletal rearrangements during growth cone guidance.* Cell, 1995. **83**(2): p. 171-6.
237. Tanaka, E., T. Ho, and M.W. Kirschner, *The role of microtubule dynamics in growth cone motility and axonal growth.* J Cell Biol, 1995. **128**(1-2): p. 139-55.
238. Letourneau, P.C., *The cytoskeleton in nerve growth cone motility and axonal pathfinding.* Perspect Dev Neurobiol, 1996. **4**(2-3): p. 111-23.
239. Suter, D.M. and P. Forscher, *An emerging link between cytoskeletal dynamics and cell adhesion molecules in growth cone guidance.* Curr Opin Neurobiol, 1998. **8**(1): p. 106-16.
240. O'Leary, D.D. and T. Terashima, *Cortical axons branch to multiple subcortical targets by interstitial axon budding: implications for target recognition and "waiting periods".* Neuron, 1988. **1**(10): p. 901-10.
241. Halloran, M.C. and K. Kalil, *Dynamic behaviors of growth cones extending in the corpus callosum of living cortical brain slices observed with video microscopy.* J Neurosci, 1994. **14**(4): p. 2161-77.
242. Kuang, R.Z. and K. Kalil, *Development of specificity in corticospinal connections by axon collaterals branching selectively into appropriate spinal targets.* J Comp Neurol, 1994. **344**(2): p. 270-82.
243. Bastmeyer, M. and D.D. O'Leary, *Dynamics of target recognition by interstitial axon branching along developing cortical axons.* J Neurosci, 1996. **16**(4): p. 1450-9.
244. Heidemann, S.R., J.M. Landers, and M.A. Hamborg, *Polarity orientation of axonal microtubules.* J Cell Biol, 1981. **91**(3 Pt 1): p. 661-5.
245. Sharp, D.J., W. Yu, and P.W. Baas, *Transport of dendritic microtubules establishes their nonuniform polarity orientation.* J Cell Biol, 1995. **130**(1): p. 93-103.
246. Yu, W., et al., *Depletion of a microtubule-associated motor protein induces the loss of dendritic identity.* J Neurosci, 2000. **20**(15): p. 5782-91.
247. Wang, J., et al., *Microtubule assembly in growing dendrites.* J Neurosci, 1996. **16**(19): p. 6065-78.
248. Baas, P.W. and F.J. Ahmad, *The transport properties of axonal microtubules establish their polarity orientation*, in *J Cell Biol*. 1993. p. 1427-37.
249. Baas, P.W., M.M. Black, and G.A. Banker, *Changes in microtubule polarity orientation during the development of hippocampal neurons in culture.* J Cell Biol, 1989. **109**(6 Pt 1): p. 3085-94.
250. Baas, P.W., et al., *Polarity orientation of microtubules in hippocampal neurons: uniformity in the axon and nonuniformity in the dendrite.* Proc Natl Acad Sci U S A, 1988. **85**(21): p. 8335-9.
251. Challacombe, J.F., D.M. Snow, and P.C. Letourneau, *Actin filament bundles are required for microtubule reorientation during growth cone turning to avoid an inhibitory guidance cue*, in *J Cell Sci*. 1996. p. 2031-40.
252. Challacombe, J.F., D.M. Snow, and P.C. Letourneau, *Dynamic microtubule ends are required for growth cone turning to avoid an inhibitory guidance cue.* J Neurosci, 1997. **17**(9): p. 3085-95.
253. Mack, T.G., M.P. Koester, and G.E. Pollerberg, *The microtubule-associated protein MAP1B is involved in local stabilization of turning growth cones*, in *Mol Cell Neurosci*. 2000. p. 51-65.
254. Buck, K.B. and J.Q. Zheng, *Growth cone turning induced by direct local modification of microtubule dynamics*, in *J Neurosci*. 2002. p. 9358-67.
255. Krendel, M., F.T. Zenke, and G.M. Bokoch, *Nucleotide exchange factor GEF-H1 mediates cross-talk between microtubules and the actin cytoskeleton*, in *Nat Cell Biol*. 2002. p. 294-301.
256. Bentley, D. and A. Toroian-Raymond, *Disoriented pathfinding by pioneer neurone growth cones deprived of filopodia by cytochalasin treatment*, in *Nature*. 1986. p. 712-5.
257. Song, H.J. and M.M. Poo, *Signal transduction underlying growth cone guidance by diffusible factors*, in *Curr Opin Neurobiol*. 1999. p. 355-63.
258. Song, H. and M. Poo, *The cell biology of neuronal navigation*, in *Nat Cell Biol*. 2001. p. E81-8.
259. Gallo, G., F.B. Lefcort, and P.C. Letourneau, *The trkA receptor mediates growth cone turning toward a localized source of nerve growth factor*, in *J Neurosci*. 1997. p. 5445-54.
260. Kuhn, T.B., et al., *Myelin and collapsin-1 induce motor neuron growth cone collapse through different pathways: inhibition of collapse by opposing mutants of rac1*, in *J Neurosci*. 1999. p. 1965-75.
261. Shekarabi, M. and T.E. Kennedy, *The netrin-1 receptor DCC promotes filopodia formation and cell spreading by activating Cdc42 and Rac1*, in *Mol Cell Neurosci*. 2002. p. 1-17.

262. Luo, Y., D. Raible, and J.A. Raper, *Collapsin: a protein in brain that induces the collapse and paralysis of neuronal growth cones*, in *Cell*. 1993. p. 217-27.
263. Challacombe, J.F., D.M. Snow, and P.C. Letourneau, *Actin filament bundles are required for microtubule reorientation during growth cone turning to avoid an inhibitory guidance cue.* J Cell Sci, 1996. **109**(Pt 8): p. 2031-40.
264. Kuhn, T.B., M.F. Schmidt, and S.B. Kater, *Laminin and fibronectin guideposts signal sustained but opposite effects to passing growth cones*, in *Neuron*. 1995. p. 275-85.
265. Dickson, B.J., *Molecular mechanisms of axon guidance*, in *Science*. 2002. p. 1959-64.
266. Meyer, G. and E.L. Feldman, *Signaling mechanisms that regulate actin-based motility processes in the nervous system*, in *J Neurochem*. 2002. p. 490-503.
267. Kim, Y.S., et al., *Calmodulin and profilin coregulate axon outgrowth in Drosophila*, in *J Neurobiol*. 2001. p. 26-38.
268. Cooper, J.A. and D.A. Schafer, *Control of actin assembly and disassembly at filament ends*, in *Curr Opin Cell Biol*. 2000. p. 97-103.
269. McGough, A. and M. Way, *Molecular model of an actin filament capped by a severing protein*, in *J Struct Biol*. 1995. p. 144-50.
270. Bear, J.E., et al., *Antagonism between Ena/VASP proteins and actin filament capping regulates fibroblast motility*, in *Cell*. 2002. p. 509-21.
271. Wu, W., et al., *Directional guidance of neuronal migration in the olfactory system by the protein Slit.* Nature, 1999. **400**(6742): p. 331-6.
272. Yee, K.T., et al., *Extension of long leading processes and neuronal migration in the mammalian brain directed by the chemoattractant netrin-1.* Neuron, 1999. **24**(3): p. 607-22.
273. Alcantara, S., et al., *Netrin 1 acts as an attractive or as a repulsive cue for distinct migrating neurons during the development of the cerebellar system.* Development, 2000. **127**(7): p. 1359-72.
274. Santiago, A. and C.A. Erickson, *Ephrin-B ligands play a dual role in the control of neural crest cell migration.* Development, 2002. **129**(15): p. 3621-32.
275. Marin, O., et al., *Sorting of striatal and cortical interneurons regulated by semaphorin-neuropilin interactions.* Science, 2001. **293**(5531): p. 872-5.
276. Ridley, A.J., et al., *Cell migration: integrating signals from front to back.* Science, 2003. **302**(5651): p. 1704-9.
277. Dehmelt, L. and S. Halpain, *Actin and microtubules in neurite initiation: are MAPs the missing link?* J Neurobiol, 2004. **58**(1): p. 18-33.
278. Feng, Y. and C.A. Walsh, *Protein-protein interactions, cytoskeletal regulation and neuronal migration.* Nat Rev Neurosci, 2001. **2**(6): p. 408-16.
279. Lambert de Rouvroit, C. and A.M. Goffinet, *Neuronal migration.* Mech Dev, 2001. **105**(1-2): p. 47-56.
280. Haendel, M.A., K.E. Bollinger, and P.W. Baas, *Cytoskeletal changes during neurogenesis in cultures of avain neural crest cells.* J Neurocytol, 1996. **25**(4): p. 289-301.
281. Pollard, T.D. and G.G. Borisy, *Cellular motility driven by assembly and disassembly of actin filaments.* Cell, 2003. **112**(4): p. 453-65.
282. Gregory, W.A., et al., *Cytology and neuron-glial apposition of migrating cerebellar granule cells in vitro.* J Neurosci, 1988. **8**(5): p. 1728-38.
283. Rakic, P., *Principles of neural cell migration.* Experientia. 1990 Sep 15;46(9):882-91., 1990. **46**: p. 882-91.
284. Hatten, M.E., *Central nervous system neuronal migration.* Annu Rev Neurosci, 1999. **22**: p. 511-39.
285. Rakic, P., E. Knyihar-Csillik, and B. Csillik, *Polarity of microtubule assemblies during neuronal cell migration.* Proc Natl Acad Sci U S A, 1996. **93**(17): p. 9218-22.
286. Rivas, R.J. and M.E. Hatten, *Motility and cytoskeletal organization of migrating cerebellar granule neurons.* J Neurosci, 1995. **15**(2): p. 981-9.
287. Tai, C.Y., et al., *Role of dynein, dynactin, and CLIP-170 interactions in LIS1 kinetochore function.* J Cell Biol, 2002. **156**(6): p. 959-68.
288. Smith, D.S., et al., *Regulation of cytoplasmic dynein behaviour and microtubule organization by mammalian Lis1*, in *Nat Cell Biol*. 2000. p. 767-75.
289. Faulkner, N.E., et al., *A role for the lissencephaly gene LIS1 in mitosis and cytoplasmic dynein function.* Nat Cell Biol, 2000. **2**(11): p. 784-91.
290. Aumais, J.P., et al., *NudC associates with Lis1 and the dynein motor at the leading pole of neurons*, in *J Neurosci*. 2001.
291. Sapir, T., M. Elbaum, and O. Reiner, *Reduction of microtubule catastrophe events by LIS1, platelet-activating factor acetylhydrolase subunit.* Embo J, 1997. **16**(23): p. 6977-84.
292. Coquelle, F.M., et al., *LIS1, CLIP-170's key to the dynein/dynactin pathway.* Mol Cell Biol, 2002. **22**(9): p. 3089-102.

293. Gleeson, J.G., et al., *Doublecortin is a microtubule-associated protein and is expressed widely by migrating neurons.* Neuron, 1999. **23**(2): p. 257-71.
294. Francis, F., et al., *Doublecortin is a developmentally regulated, microtubule-associated protein expressed in migrating and differentiating neurons.* Neuron, 1999. **23**(2): p. 247-56.
295. Burgess, H.A. and O. Reiner, *Doublecortin-like kinase is associated with microtubules in neuronal growth cones.* Mol Cell Neurosci, 2000. **16**(5): p. 529-41.
296. Friocourt, G., et al., *Doublecortin functions at the extremities of growing neuronal processes.* Cereb Cortex, 2003. **13**(6): p. 620-6.
297. Kholmanskikh, S.S., et al., *Disregulated RhoGTPases and actin cytoskeleton contribute to the migration defect in Lis1-deficient neurons.* J Neurosci, 2003. **23**(25): p. 8673-81.
298. Stossel, T.P., et al., *Filamins as integrators of cell mechanics and signalling.* Nat Rev Mol Cell Biol, 2001. **2**(2): p. 138-45.
299. Fox, J.W., et al., *Mutations in filamin 1 prevent migration of cerebral cortical neurons in human periventricular heterotopia.* Neuron, 1998. **21**(6): p. 1315-25.
300. Nagano, T., et al., *Filamin A-interacting protein (FILIP) regulates cortical cell migration out of the ventricular zone.* Nat Cell Biol, 2002. **4**(7): p. 495-501.
301. Lanier, L.M., et al., *Mena is required for neurulation and commissure formation.* Neuron, 1999. **22**(2): p. 313-25.
302. Bear, J.E., et al., *Negative regulation of fibroblast motility by Ena/VASP proteins.* Cell, 2000. **101**(7): p. 717-28.
303. Goh, K.L., et al., *Ena/VASP proteins regulate cortical neuronal positioning.* Curr Biol, 2002. **12**(7): p. 565-9.
304. Hirokawa, N., Terada, S., Funakoshi, T., and Takeda, S., *Slow axonal transport: the subunit transport model.* Trends Cell Biol., 1997. **7**: p. 384-388.
305. Terada, S., M. Kinjo, and N. Hirokawa, *Oligomeric tubulin in large transporting complex is transported via kinesin in squid giant axons.* Cell, 2000. **103**(1): p. 141-55.
306. Baas, P.W.a.B., A. Trends Cell Biol. 7, 380-384. [Medline], *Slow axonal transport: the polymer transport model.* Trends Cell Biol., 1997. **7**: p. 380-384.
307. Baas, P.W., *Microtubules and neuronal polarity: lessons from mitosis.* Neuron, 1999. **22**(1): p. 23-31.
308. Baas, P.W., *Microtubules and axonal growth.* Curr Opin Cell Biol, 1997. **9**(1): p. 29-36.
309. Tanaka, E. and M.W. Kirschner, *The role of microtubules in growth cone turning at substrate boundaries*, in *J Cell Biol*. 1995. p. 127-37.
310. Chang, S., et al., *Speckle microscopic evaluation of microtubule transport in growing nerve processes*, in *Nat Cell Biol*. 1999. p. 399-403.
311. Dent, E.W., et al., *Reorganization and movement of microtubules in axonal growth cones and developing interstitial branches*, in *J Neurosci*. 1999. p. 8894-908.
312. Okabe, S. and N. Hirokawa, *Do photobleached fluorescent microtubules move?: re-evaluation of fluorescence laser photobleaching both in vitro and in growing Xenopus axon.* J Cell Biol, 1993. **120**(5): p. 1177-86.
313. Okabe, S. and N. Hirokawa, *Differential behavior of photoactivated microtubules in growing axons of mouse and frog neurons.* J Cell Biol, 1992. **117**(1): p. 105-20.
314. Sabry, J., T.P. O'Connor, and M.W. Kirschner, *Axonal transport of tubulin in Ti1 pioneer neurons in situ.* Neuron, 1995. **14**(6): p. 1247-56.
315. Funakoshi, T., S. Takeda, and N. Hirokawa, *Active transport of photoactivated tubulin molecules in growing axons revealed by a new electron microscopic analysis.* J Cell Biol, 1996. **133**(6): p. 1347-53.
316. Takeda, S., T. Funakoshi, and N. Hirokawa, *Tubulin dynamics in neuronal axons of living zebrafish embryos.* Neuron, 1995. **14**(6): p. 1257-64.
317. Chang, S., et al., *Transport and turnover of microtubules in frog neurons depend on the pattern of axonal growth.* J Neurosci, 1998. **18**(3): p. 821-9.
318. Yu, W., M.J. Schwei, and P.W. Baas, *Microtubule transport and assembly during axon growth.* J Cell Biol, 1996. **133**(1): p. 151-7.
319. Slaughter, T., J. Wang, and M.M. Black, *Microtubule transport from the cell body into the axons of growing neurons.* J Neurosci, 1997. **17**(15): p. 5807-19.
320. Gallo, G. and P.C. Letourneau, *Different contributions of microtubule dynamics and transport to the growth of axons and collateral sprouts.* J Neurosci, 1999. **19**(10): p. 3860-73.

Chapter 4

Clasps are CLIP-115 and –170 associating proteins involved in the regional regulation of microtubule dynamics in motile fibroblasts

Anna Akhmanova, Casper C. Hoogenraad, Ksenija Drabek, Tatiana Stepanova,
Bjorn Dortland, Ton Verkerk, Wim Vermeulen, Boudewijn M. Burgering, Chris I. De Zeeuw,
Frank Grosveld, and Niels Galjart

Cell, Vol. 104, 923–935, March 23, 2001, Copyright ©2001 by Cell Press

CLASPs Are CLIP-115 and -170 Associating Proteins Involved in the Regional Regulation of Microtubule Dynamics in Motile Fibroblasts

Anna Akhmanova,*‖ Casper C. Hoogenraad,*†‖ Ksenija Drabek,* Tatiana Stepanova,* Bjorn Dortland,* Ton Verkerk,* Wim Vermeulen,* Boudewijn M. Burgering,‡ Chris I. De Zeeuw,† Frank Grosveld,* and Niels Galjart*§

*MGC Department of Cell Biology and Genetics and
†MGC Department of Anatomy
Erasmus University
P.O. Box 1738
3000 DR Rotterdam
The Netherlands
‡Laboratory for Physiological Chemistry and Centre for Biomedical Genetics
University of Utrecht
Universiteitsweg 100
3584 CG Utrecht
The Netherlands

Summary

CLIP-170 and CLIP-115 are cytoplasmic linker proteins that associate specifically with the ends of growing microtubules and may act as anti-catastrophe factors. Here, we have isolated two *CL*IP-*as*sociated *p*roteins (CLASPs), which are homologous to the *Drosophila* Orbit/Mast microtubule-associated protein. CLASPs bind CLIPs and microtubules, colocalize with the CLIPs at microtubule distal ends, and have microtubule-stabilizing effects in transfected cells. After serum induction, CLASPs relocalize to distal segments of microtubules at the leading edge of motile fibroblasts. We provide evidence that this asymmetric CLASP distribution is mediated by PI3-kinase and GSK-3β. Antibody injections suggest that CLASP2 is required for the orientation of stabilized microtubules toward the leading edge. We propose that CLASPs are involved in the local regulation of microtubule dynamics in response to positional cues.

Introduction

Microtubules (MTs) constitute an important part of the cellular cytoskeleton. They are essential for chromosome segregation in mitosis and for organelle movement and positioning in interphase cells. MTs are inherently polarized structures, with a fast-growing end (the plus end) and a slow growing end (the minus end). In fibroblasts, the majority of MTs is attached with the minus end to the MT organizing center (MTOC), while the plus ends are directed to the cell periphery. Both in vitro and in vivo, the MT plus ends alternate between phases of elongation and shrinkage. This phenomenon is called dynamic instability (reviewed by Desai and Mitchison, 1997).

MT dynamics in living cells is regulated by a variety of protein factors. These include MT destabilizing proteins, such as stathmin/Op18 and XKCM1, as well as factors that promote MT elongation, such as XMAP215/TOG1 (for review, see Wittmann et al., 2001). Some of the proteins involved in regulating MT growth, depolymerization, and/or MT interaction with the cellular cortex are localized specifically at the MT plus end. For example, the yeast protein BIM1p, which increases MT dynamicity, localizes to dots at the distal ends of cytoplasmic MTs (Tirnauer et al., 1999), as does its mammalian homolog EB1 (Mimori-Kiyosue et al., 2000). Another protein demonstrated to be present at the plus ends is mammalian CLIP-170. Using a fusion of CLIP-170 to the green fluorescent protein (GFP), it was shown that CLIP-170 moves together with the tips of growing MTs in living cells (Perez et al., 1999). However, CLIP-170 was previously also implicated in the attachment of endosomes to MTs (Pierre et al., 1992) and, in addition, it was found at the kinetochores of the prometaphase chromosomes (Dujardin et al., 1998). In fibroblasts, CLIP-170 colocalizes with cytoplasmic dynein and dynactin at the distal ends of MTs (Valetti et al., 1999; Vaughan et al., 1999). It was suggested, therefore, that these regions represent the cargo-loading sites for the minus end directed organelle movement by dynein, and that CLIP-170 might be involved in this process. However, no association of CLIP-170 with dynein and dynactin has been demonstrated. To resolve CLIP-170 function at MT plus ends, it is essential to define with what proteins it interacts directly.

The closest homolog of CLIP-170 in mammals is CLIP-115 (De Zeeuw et al., 1997). Both CLIP-170 and CLIP-115 contain two MT binding (MTB) domains at their N termini, surrounded by positively charged, serine rich regions. One such MTB motif, together with one serine rich region, is sufficient for MT binding (Hoogenraad et al., 2000). The middle part of both proteins contains a long region of heptad repeats, which form a coiled-coil and mediate homodimerization of these proteins (Scheel et al., 1999; Hoogenraad et al., 2000). While CLIP-170 is expressed in many different cell lines and tissues, CLIP-115 appears to be predominantly present in neurons, where it is localized in dendrites (De Zeeuw et al., 1997). When expressed in fibroblasts at low levels, CLIP-115 localizes at the MT plus ends, similar to CLIP-170 (Hoogenraad et al., 2000). This suggests that in neurons, the function of CLIP-115 might be related to some aspect of MT dynamics.

Given the common properties of the two CLIPs, we hypothesized that they might have overlapping functions and, therefore, common protein partners. We searched for such partners (*CL*IP-*as*sociating *p*roteins, or CLASPs) with the aid of a yeast two-hybrid system, using a conserved part of the coiled-coil region of CLIP-115 as bait. We identified two mammalian proteins, CLASP1 and CLASP2, with similarity to regulators of MT dynamics. CLASPs bind both to CLIPs and to MTs and

§To whom correspondence should be addressed (e-mail: galjart@ch1.fgg.eur.nl).
‖These authors contributed equally to the results described in this paper.

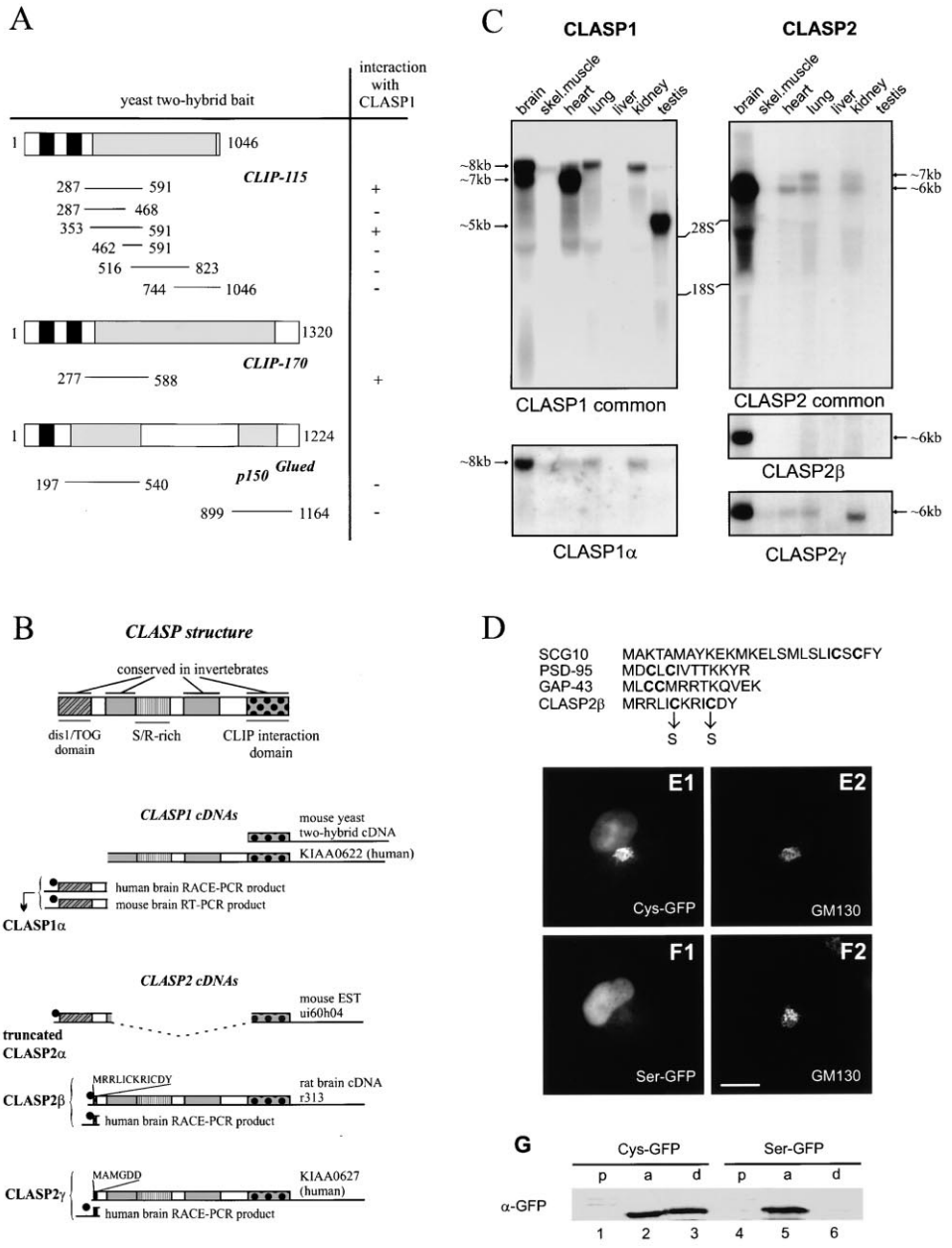

Figure 1. CLASP Isolation and Structure

(A) The region spanning amino acids 287–591 of CLIP-115 was used in a yeast two-hybrid screen of an E14.5 day mouse cDNA library. Mouse *CLASP1* cDNA, isolated in this screen, was next tested in yeast two-hybrid assays with protein fragments from CLIP-115, CLIP-170, and p150^{Glued}. The domain structure of these three proteins, with MT binding motifs (black bars) and coiled-coil regions (gray bars), is represented. The amino acids covered by each fragment are indicated; their interaction with mCLASP1 is shown to the right (+: positive interaction, −: no interaction).

(B) Schematic representation of CLASP structure and the CLASP-encoding cDNAs. Protein-coding regions are represented by bars and untranslated regions by lines. The top bar represents the largest CLASP ORF, encoded by CLASP1/2α cDNAs. Above the CLASP2β and -γ cDNAs, the sequence of the alternatively spliced, N-terminal domain is shown. A vertical line with a filled circle on top indicates a stop codon upstream and in-frame with the translational start codon, suggesting the presence of a full-length ORF. The stippled line in the mouse EST clone ui60h04 indicates the position of a deletion, which is probably an artifact, because it could not be confirmed by Northern blotting or RT-PCR.

(C) *CLASP* expression profile. Northern blots with total RNA from different mouse tissues (~20 μg per lane) were hybridized with probes, encompassing the CLIP binding domain of CLASP1 and -2 ("common" probes), or with 5′ probes, specific for particular CLASP variants. Approximate sizes of the different CLASP transcripts and positions of the 18S and 28S rRNAs are indicated.

(D) Comparison of the N terminus of CLASP2β with known palmitoylation motifs. Fatty acylated cysteine residues are in bold. Amino acid substitutions are indicated.

(E and F) Intracellular distribution of GFP, fused either to the first 40 amino acids of wild-type CLASP2β (Cys-GFP) or to the sequence with two serine substitutions (Ser-GFP). Transfected COS-1 cells were fixed and stained with antibodies to the *cis*-Golgi marker GM130. GFP

have a MT stabilizing effect in transfected cells. Using motile fibroblasts as a model system, we find that CLASPs specifically mark the distal ends of MTs at the leading edge of the cell and are involved in organizing stabilized MTs. Thus, CLASPs may play a role in local MT stabilization in response to positional cues.

Results

Characterization of CLIP-Associating Proteins (CLASPs)

Within the coiled-coil region of CLIP-115 and -170, the N-terminal portion is best conserved. This part of CLIP-115 (amino acids 287–591; Figure 1A) was therefore used as bait in a yeast two-hybrid screen to identify common *CL*IP-*as*sociating *p*roteins (CLASPs). We found one clone, which interacted both with CLIP-115 and with the corresponding region of CLIP-170 and which was therefore named CLASP1. This clone did not interact with vector alone, with other portions of CLIP-115, or with the coiled-coil domains of $p150^{Glued}$, a dynactin subunit that structurally resembles CLIP-170 (Pierre et al., 1992). Deletion analysis demonstrated that the whole coiled-coil part of the CLIP-115 bait construct is necessary and sufficient for binding to CLASP1 (Figure 1A).

Mouse *CLASP1* cDNA (*mCLASP1*) contains a 5′ truncated open reading frame (ORF) with very high similarity to the C termini of the proteins encoded by the incomplete human brain cDNAs KIAA0622 (98% identity, hCLASP1) and KIAA0627 (75% identity, hCLASP2). We searched for complete ORFs of CLASP1 and -2 by cDNA library screening, RACE-PCR, and EST database analysis. This yielded several cDNAs, named *CLASP1/2*α, *-2*β, and *-2*γ, which encode different protein isoforms (Figure 1B). Northern blot analysis with probes to the common C-terminal domains of *CLASP1* and *-2* shows that differently sized *CLASP* mRNAs are present in various tissues (Figure 1C), indicating that *CLASP* transcripts undergo alternative splicing. *CLASP1* shows highest expression in brain, heart, and testis, while *CLASP2* mRNAs are enriched in the brain. Interestingly, the *CLASP2*β transcript appears to be brain specific (Figure 1C). Using probes, specific for *CLASP1*α (Figure 1C) or *CLASP2*α (data not shown), we only detect hybridization to the longest transcript of each *CLASP* (∼8 kb for *CLASP1*α and ∼7 kb for *CLASP2*α, respectively). The presence of 5 and 7 kb *CLASP1* transcripts indicates that there are additional N-terminal variants of CLASP1, similar to CLASP2.

The different *CLASP1* and *-2* cDNAs encode proteins with a predicted molecular mass of ∼170 kDa (α isoforms) and ∼140 kDa (β/γ isoforms). A database search revealed a striking similarity of the CLASPs to a protein called either Orbit or Mast, which is an essential MT-associated protein (MAP) from *D. melanogaster*, involved in the regulation of MT behavior during mitosis (Inoue et al., 2000; Lemos et al., 2000). Three putative CLASPs are also present in *C. elegans* (ZC84.3, R107.6, and C07h6.3). The domains of CLASP that are conserved in invertebrates are schematically indicated in Figure 1B. Interestingly, our 5′ RACE analysis demonstrates that an N-terminal ∼200 amino acid domain in Mast, which is similar to a repeated motif in the dis1/TOG family of vertebrate MT stabilizing proteins (Lemos et al., 2000), is also present in CLASP1α and -2α. These observations indicate that CLASPs might bind MTs.

CLASP2β is represented by the rat hippocampus cDNA clone r313 (Figure 1B). Instead of the dis1/TOG-homologous domain, this isoform contains a short N-terminal motif, which is conserved in humans (Figure 1B). It is characterized by two cysteines, surrounded by positively charged and hydrophobic residues (Figures 1B and 1D). Similar motifs in other proteins were shown to cause membrane anchoring, due to palmitoylation of the cysteine residues (Resh, 1999). Fusion of the N terminus of CLASP2β to GFP gives rise to a protein that accumulates in the region of the Golgi complex in transfected COS-1 cells (Figure 1E1, compare to the Golgi marker GM130 in Figure 1E2). Substitution of cysteine residues for serines (Figure 1F) or alanines (not shown) abolishes targeting to the Golgi, supporting the idea that fatty acylation of the cysteines within the N-terminal peptide stretch of CLASP2β causes membrane targeting. Triton-X114 partitioning experiments (Hancock et al., 1989), in which the cysteine-containing, but not the serine-containing, GFP fusion is partially retained in the detergent enriched (i.e., the membranous) phase (Figure 1G, compare lanes 1–3 and 4–6, respectively), further support this notion. Subsequent shortening of the CLASP2β N terminus within the fusion construct demonstrated that the first 14 amino acids of this CLASP isoform are sufficient for membrane association (data not shown).

In contrast to the α- and β-isoforms, CLASP2γ, represented by KIAA0627 cDNA, contains an inconspicuous peptide (MAMGDD) at its N terminus (Figure 1B). In conclusion, CLASPs appear to be the mammalian counterparts of the *D. melanogaster* protein Orbit/Mast. They exist as a family of widely distributed isoforms, each with a CLIP interaction domain but with variable N termini, and are likely to have MT binding properties.

CLASPs Colocalize with CLIPs at MT Distal Ends

We raised antibodies against the conserved C-terminal domain of hCLASP2 (antiserum #2358) in order to investigate the intracellular distribution of different CLASP isoforms. These studies were carried out both in COS-1 cells and in 3T3 fibroblasts, to compare results in different systems and to take advantage of the fact that COS-1 cells are easily transfected, whereas in 3T3 cells MT dynamics have been extensively studied. Interestingly, COS-1 cells express only CLIP-170, while in 3T3 fibroblasts, both CLIP-115 and CLIP-170 are present at MT distal ends. The specificity of antiserum #2358 was

fluorescence is shown in (E1) and (F1), and the antibody labeling of the same cells in (E2) and (F2). Bar, 10 μm.

(G) COS-1 cells, transfected with Cys-GFP or Ser-GFP, were lysed using Triton X-114. After pelleting of the insoluble fraction (lanes marked "p"), the lysate was partitioned into an aqueous phase ("a") and a detergent-enriched phase ("d"). The volumes of the three fractions were equalized before loading on gel and proteins were analyzed by Western blotting with anti-GFP serum.

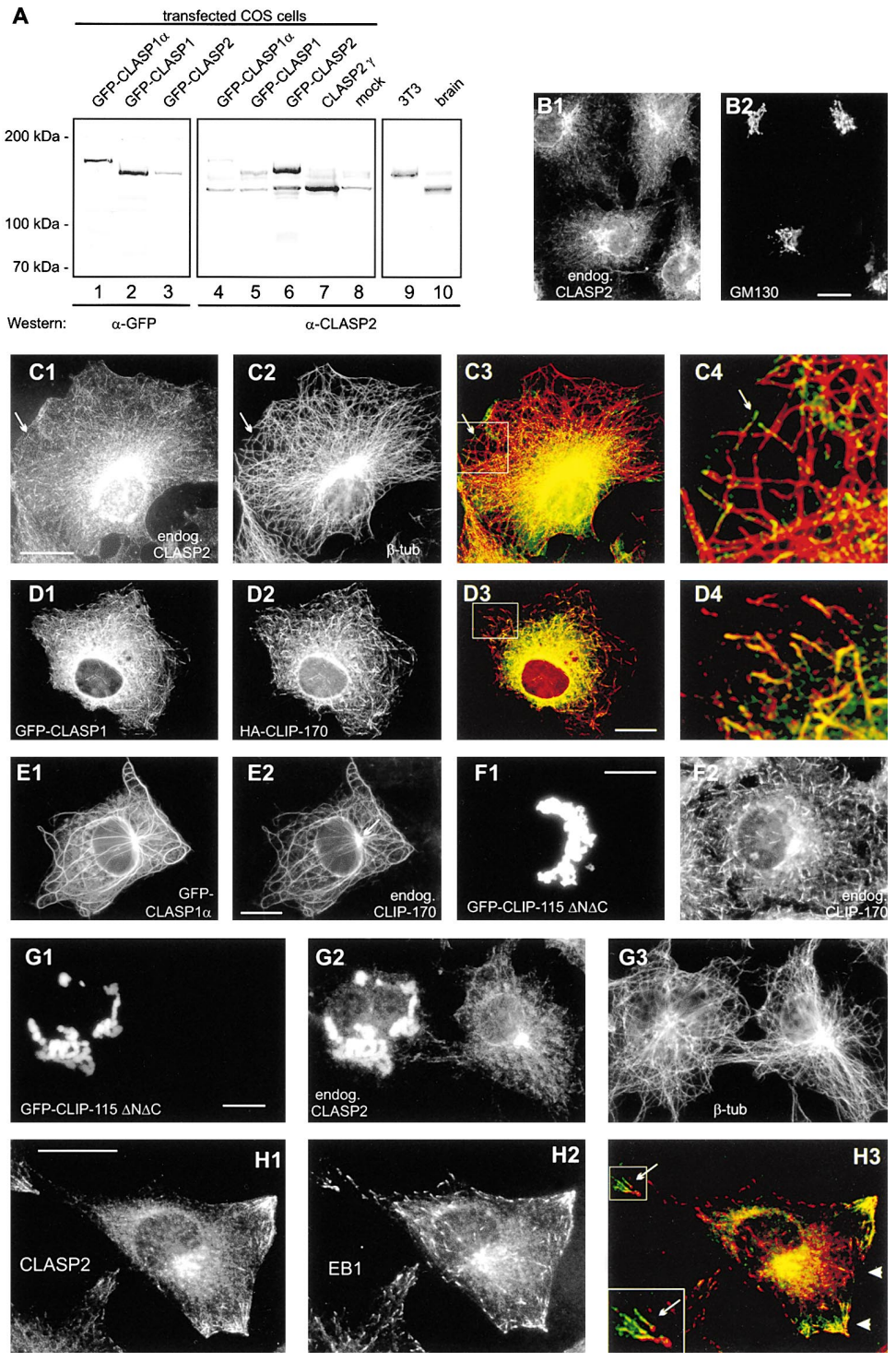

Figure 2. Localization of CLASPs in Cultured Cells

(A) Specificity of #2358 antibodies. Protein extracts from COS-1 cells, transiently transfected with the indicated CLASP expression constructs (lanes 1–7) or mock transfected (lane 8), and from 3T3 cells (lane 9) or mouse brain (lane 10) were analyzed by Western blotting, using antibodies against GFP (lanes1–3, α-GFP) or with the #2358 antiserum (lanes 4–10, α-CLASP2). Notice that GFP-CLASP1 fusions are more abundantly expressed than GFP-CLASP2 (lanes 1–3), but less well recognized by #2358 antibodies (lanes 4–6).

(B and C) Untransfected COS-1 cells, immunostained with #2358 antiserum and anti-GM130 (B) or anti-β-tubulin (C). In (C3) and (C4), signals of (C1) (green) and (C2) (red) are merged. (C4) is an enlargement of the indicated area in (C3) to demonstrate the MT plus end labeling of CLASP2 (indicated by an arrow). Bar, 10 μm.

(D–G) COS-1 cells, transfected with different cDNA constructs, fixed 24 hr after transfection and immunostained using specific antisera. Bar, 10 μm.

first analyzed by Western blotting in transfected COS-1 cells using different GFP-CLASP1 and -2 fusion proteins or untagged CLASP2γ (Figure 2A). In these cells, the #2358 antibodies react strongly with GFP-CLASP2 and with untagged CLASP2γ (Figure 2A, lanes 6 and 7, respectively). Weak cross-reactivity with GFP-CLASP1 proteins is also observed (Figure 2A, lanes 4 and 5). In agreement with these Western blot data, immunofluorescence experiments in transfected COS-1 cells with #2358 antibodies show very strong reaction with GFP-CLASP2 proteins and a weak reaction with GFP-CLASP1 fusions (data not shown). Based on these observations, we conclude that antiserum #2358 recognizes CLASPs specifically, but that use of these antibodies predominantly reflects the distribution of CLASP2 isoforms. Thus, the #2358 antiserum is also named anti-CLASP2 antiserum.

In mock transfected COS-1 cells, #2358 antibodies detect proteins of ~170 and ~140 kDa (Figure 2A, lane 8), which are the expected lengths for CLASP2α and -β/γ, respectively. Surprisingly, Western blot analysis of 3T3 cell lysates with antiserum #2358 reveals only a protein of ~170 kDa (Figure 2A, lane 9), whereas in mouse brain, the tissue with highest expression of CLASP2, proteins of ~140 and ~170 kDa are detected (Figure 2A, lane 10). These Western blots results with antiserum #2358 were verified by Northern blot analysis (data not shown). Together, the data demonstrate that CLASP2β and -γ are not highly expressed in 3T3 cells, whereas in brain they are more abundant than CLASP2α.

CLASP2 distribution was next examined using immunofluorescence microscopy. In COS-1 cells, prominent labeling is detected in the perinuclear region, corresponding to the Golgi apparatus (Figure 2B). In addition, anti-CLASP2 antibodies stain MT plus ends (Figure 2C) in a pattern similar to that described previously for CLIP-170 (Pierre et al., 1992; Perez et al., 1999). Both types of CLASP staining are completely inhibited by preincubation of the antibodies with the antigen used for their generation, while affinity-purified antibodies produce the same signal as the crude serum (data not shown). Thus, CLASP2 distribution in COS-1 cells overlaps with that of CLIP-170 at the distal ends of MTs.

Using GFP-CLASP1 (containing the 5′ truncated ORF from KIAA0622), GFP-CLASP1α, and GFP-CLASP2 (derived from KIAA0627), we next investigated the distribution of individual, overexpressed CLASP1 and -2 isoforms and the effect of coexpression with the CLIPs. At low expression levels, all three GFP-CLASP fusions colocalize with CLIP-170 or CLIP-115 at MT plus ends (Figure 2D and data not shown). When GFP-CLASPs are highly overexpressed, they accumulate along the whole length of MTs, causing MT rearrangement and bundling and CLIP-170 relocalization to these MT bundles (Figure 2E). At low expression levels in live transfected cells, GFP-CLASP2 behaves very similar to GFP-CLIP-170 (see Supplemental Information for live GFP-CLASP2 and GFP-CLIP-170 behavior in COS-1 cells at http://www.cell.com/cgi/content/full/104/6/923/DC1), which was shown to move with the growing ends of MTs (Perez et al., 1999). Taken together, these data verify the distribution of endogenous CLASP2, as detected with #2358 antibodies and establish CLASPs as a novel family of proteins that bind to the distal ends of interphase MTs.

A GFP fusion protein, containing the CLASP-interacting region of CLIP-115 (GFP-CLIP-115ΔNΔC, including amino acids 353–756 of CLIP-115), is unable to bind MTs, since it lacks the MTB domains. Instead, it forms cytoplasmic aggregates, which contain no significant amount of tubulin (Figures 2G1 and 2G3). Strikingly, in cells overexpressing this mutant protein, endogenous CLASP is titrated away from the Golgi complex as well as from MT distal ends and is detected in the aggregates (Figure 2G2). In contrast, both CLIP-170 (Figure 2F) and EB1 (data not shown) remain bound to MT distal ends. These results validate the yeast two-hybrid interaction between CLIPs and CLASPs. In addition, they indicate that CLIP-170 and EB1 are able to associate with MT distal ends in the absence of CLASP.

In 3T3 cells, CLASP2 distribution is similar to that in COS-1 cells. However, we noted that in cells with a shape characteristic of motile fibroblasts, intense labeling of MT distal segments is detected at the leading edge, but not in the cell body (Figures 2H1 and 2H3). This asymmetric distribution is particularly apparent when CLASP2 localization is compared to that of EB1, which marks MT tips throughout 3T3 cells (Figures 2H2 and 2H3). When a distal segment of an MT appears positive for both CLASP2 and EB1, the highest concentration of EB1 is often observed at the tip, while a more proximal portion of the MT is strongly stained with anti-CLASP2 antibodies (see insets in Figure 2H3). Thus, the MT labeling by CLASP2 at the periphery of subconfluent 3T3 cells is often nonuniform.

CLASPs Bind to CLIPs and MTs

To verify the CLIP–CLASP interactions, we tested their association in vitro. Radioactively labeled hCLASP1 and hCLASP2, generated by in vitro transcription-translation, bind to bacterially produced GST fusions of full-length CLIP-115 and the yeast two-hybrid fragment (CLIP-115-TH), but not to control GST fusion proteins (Figure 3C). Alternatively, in vitro translated CLIP-115 specifically binds to the GST fusion of the mCLASP1 C terminus (GST-CLASP1-C; Figure 3D). A GST pulldown assay with mouse brain extracts shows that both CLIP-115 and CLIP-170 are retained by GST-CLASP1-C, but not by GST alone (Figure 3E). Since all GST fusion pro-

(D) Cotransfection of GFP-CLASP1 (low level of expression) and HA-tagged CLIP-170, staining with antibody against the HA tag. (D4) is an enlargement of the indicated area in (D3).

(E) Transfection with GFP-CLASP1α, staining with antibodies against CLIP-170. The MTOC is indicated by an arrow.

(F and G) Transfections with GFP-CLIP-115ΔNΔC, staining with antibodies against CLASP2 (G2) and tubulin (G3), or with antibodies against CLIP-170 (F2).

(H) Intracellular distribution of CLASP2 in Swiss 3T3 fibroblasts. Cells were stained with anti-CLASP2 (H1) and anti-EB1 (H2) antisera. The overlay is shown in (H3) (CLASP2 is green, EB1 red). The arrow in (H3) indicates an example of MT distal ends with a high concentration of EB1 at the tip and CLASP2 at a more proximal segment. Arrowheads indicate the leading edge.

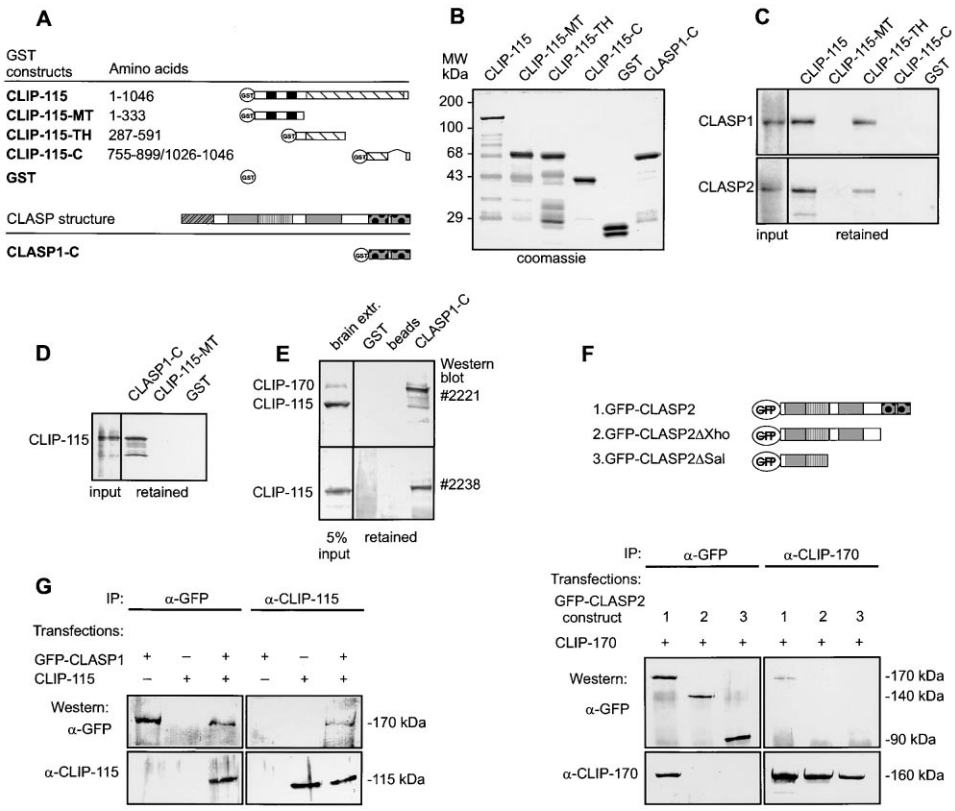

Figure 3. Analysis of CLIP–CLASP Interactions

(A) Schematic representation of bacterial GST fusion proteins of CLIP-115 and mCLASP1.

(B) SDS-PAGE analysis of purified GST fusions. All proteins are soluble and have the expected size. Molecular weight markers are indicated on the left.

(C) In vitro binding of ^{35}S-methionine-labeled CLASP1 and CLASP2 (see lanes, marked "input") to the GST fusion proteins, depicted in (A) and (B). Radioactive proteins were visualized by X-ray film exposure of dried gels.

(D) In vitro binding of ^{35}S-methionine-labeled CLIP-115 to GST fusion proteins. The experiment was performed as in (C).

(E) GST pulldown assay using mouse brain extract. Proteins, retained by glutathione-sepharose beads alone, beads decorated with GST, or with GST-mCLASP1-C, were analyzed by Western blotting, using antibody #2221, which recognizes both CLIP-115 and CLIP-170, or antibody #2238, which is specific for CLIP-115.

(F) Immunoprecipitations (IP) from COS-1 cells, transiently expressing rat brain CLIP-170, together with GFP-CLASP2, or C-terminal deletion mutants of CLASP2 (see scheme above the Western). Precipitated proteins were analyzed by Western blotting with antibodies against GFP or CLIP-170.

(G) Immunoprecipitations (IP) from COS-1 cells, transiently expressing GFP-CLASP1, CLIP-115, or both proteins. Precipitated proteins were analyzed by Western blotting with antibodies against GFP or CLIP-115.

teins (Figure 3A) are soluble and produced in comparable quantities (Figure 3B), these data suggest that the retention of CLASP1 and -2 by GST-CLIP-115 and GST-CLIP-115-TH and that of CLIP-115 and -170 by GST-CLASP1-C is specific.

We next immunoprecipitated different transfected GFP-CLASP fusion proteins from COS-1 cells, cotransfected with the CLIPs. Both full-length GFP-CLASP1 and -2 coprecipitate with CLIP-115 and -170 (Figures 3F and 3G and data not shown). These immunoprecipitates of CLIPs and CLASPs contain neither tubulin nor EB1 or dynactin (data not shown), indicating that these proteins do not mediate the CLIP–CLASP interaction. In addition, truncated GFP-CLASP2 proteins, where the C-terminal CLIP binding domain (GFP-CLASP2ΔXho) or the whole C-terminal half of the protein (GFP-CLASP2ΔSal) is deleted (Figure 3F), do not coprecipitate with CLIP-170 (Figure 3F) or CLIP-115 (data not shown) while being present in similar quantities as full-length GFP-CLASP2 (Figure 3F). Since these mutants still bind MTs (see below) but fail to bind CLIPs, these data strongly suggest that the CLIP–CLASP interaction is not mediated via tubulin, but occurs directly through the C-terminal CLIP-interacting domain of the CLASPs.

A sedimentation assay, whereby in vitro translated CLASPs were tested for their ability to cosediment with purified, taxol-stabilized MTs, reveals that only a small proportion of the CLASPs comes down with MTs (Figure 4A, left panels). This could be partially due to phosphorylation of CLASPs in the translation mix since this has been shown to inhibit MT binding of CLIP-115 and CLIP-170 (Pierre et al., 1992; Hoogenraad et al., 2000). To reduce the extent of phosphorylation of the CLASPs, after translation the system was depleted of ATP with apyrase. This caused a considerable increase in the proportion of CLASPs pelleted with MTs (Figure 4A,

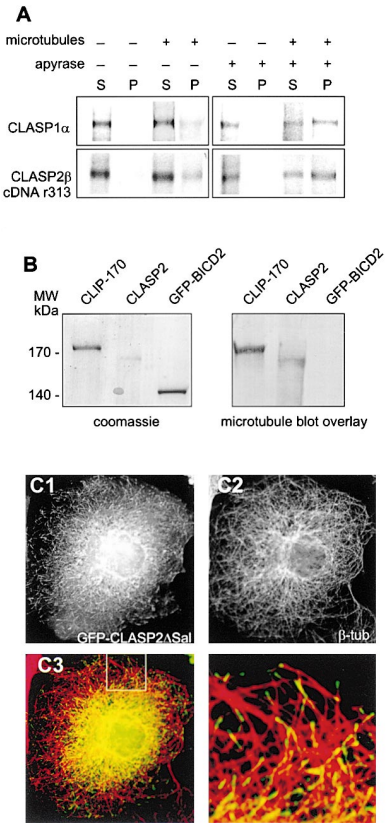

Figure 4. CLASPs Bind MTs Directly and Independently of CLIPs

(A) In vitro binding of CLASPs to MTs. ^{35}S-methionine-labeled CLASP1 and -2 were pelleted in the absence or in the presence of MTs, and the supernatants (lanes marked "S") and pellets (lanes marked "P") were analyzed by SDS-PAGE and autoradiography. In some cases, translation products were incubated with apyrase prior to the addition of MTs.

(B) MT blot overlay. CLIP-170, immunoprecipitated with antibodies #2221 from HeLa cells (500 ng), CLASP2, immunoprecipitated with antibodies #2358 from 3T3 cells (100 ng), and GFP-BICD2, immunoprecipitated from transfected COS-1 cells with GFP-specific antibodies (500 ng) were analyzed by SDS-PAGE or transferred to a Western blot, which was incubated with taxol-stabilized MTs (50 mg/ml). MTs, retained on the blot, were detected with anti-tubulin antibodies.

(C) COS-1 cells, transfected with GFP-CLASP2ΔSal (GFP signal shown in [C1]) were stained with anti-tubulin antibodies (C2). In (C3) and (C4), signals of (C1) (green) and (C2) (red) are merged. In (C4), an enlargement of the area indicated in (C3) is shown to demonstrate MT plus end labeling. Bar, 10 μm.

right panels). In MT blot overlays, immunoprecipitated CLASP2 and CLIP-170 bind MTs, whereas a Golgi-associated GFP fusion protein of similar size and quantity (GFP-BICD2; C. Hoogenraad et al., submitted) does not (Figure 4B). Thus, these results suggest that CLASPs bind MTs directly and this binding may be influenced by phosphorylation.

The GFP-CLASP2ΔSal mutant binds neither CLIP-115 nor CLIP-170 (Figure 3F) due to the absence of the C-terminal CLIP interaction domain. However, this protein does contain a presumptive MT binding domain (Inoue et al., 2000; Lemos et al., 2000). At low expression levels in transfected cells, this fusion protein localizes to the distal ends of MTs (Figure 4C) and colocalizes with CLIP-170 and EB1, while at high expression levels, GFP-CLASP2ΔSal is detected along the MTs (data not shown). These results suggest that CLASPs can accumulate on distal ends of MTs independently of their binding to CLIPs.

CLASP2 Localization in 3T3 Fibroblasts Correlates with the Orientation of Stabilized MTs

Since we observed that CLASP2 distribution in 3T3 cells with a representative motile shape is asymmetric, we investigated CLASP2 function further using the in vitro wound healing model (Liao et al., 1999). Swiss 3T3 fibroblasts were grown to confluence and a stripe of cells was scraped off, creating a "wound" in the monolayer. Cells at the edge of the wound polarize in such a way that their leading edges face the cell-free area. A subset of MTs, oriented in the direction of the wound along the polarization axis, becomes stabilized (Liao et al., 1999) and accumulates posttranslationally modified forms of tubulin, such as detyrosinated (Glu) tubulin and acetylated (Ac) tubulin, which can be visualized using specific antibodies (Bulinski and Gundersen, 1991).

Selective stabilization of MTs, oriented toward the leading edge, does not occur in serum-starved 3T3 cells, but can be quickly induced by the addition of serum (Cook et al., 1998). In agreement with these data, we find that after 24–48 hr of serum starvation, fibroblasts contain very few detyrosinated and acetylated MTs, which are concentrated in the region occupied by the Golgi complex (Figure 5A). Under these conditions, CLASP2 is mainly detected in the region of the Golgi complex, although weak staining with anti-CLASP2 antibodies is observed at the MT tips, which are also positive for EB1 (Figure 5B). Addition of serum induces formation of detyrosinated and acetylated MTs directed toward the edge of the wound (Figure 5C). The distribution of the two different posttranslationally modified forms of tubulin shows a strong correlation (but not a complete colocalization). MT tips at the leading edge and in the cell body are still stained with anti-EB1 antiserum as well as with anti-CLIP antibodies, which produce a highly similar staining pattern (Figure 5D).

In contrast to the MT distribution of EB1 and CLIP, anti-CLASP2 antibodies mainly stain the distal segments of MTs at the leading edge of the cell (Figure 5E). Very little MT bound CLASP2 is observed in the cell body and at the lateral edges of the cells, in areas of intercellular contacts (compare Figure 5E5 to 5E4). When CLASP2 localization is compared to that of acetylated tubulin, it becomes clear that many stabilized, acetylated MT bundles display a high accumulation of CLASP2 at their distal ends (Figure 5F).

MT stabilization at the leading edge of fibroblasts is induced rapidly (~5 min) in response to serum factors, although it takes about 30 min before posttranslationally modified tubulin isoforms have accumulated (Cook et al., 1998). Redistribution of CLASP2 in response to serum addition can be observed already after 5 min (data not shown), although all cells at the edge of the monolayer acquire a highly polarized CLASP2 staining pattern only after 15–20 min. Taken together, these data suggest that serum addition to wounded monolayers of 3T3 cells causes the rapid and asymmetric redistribution of CLASP2 to a subset of MT distal ends.

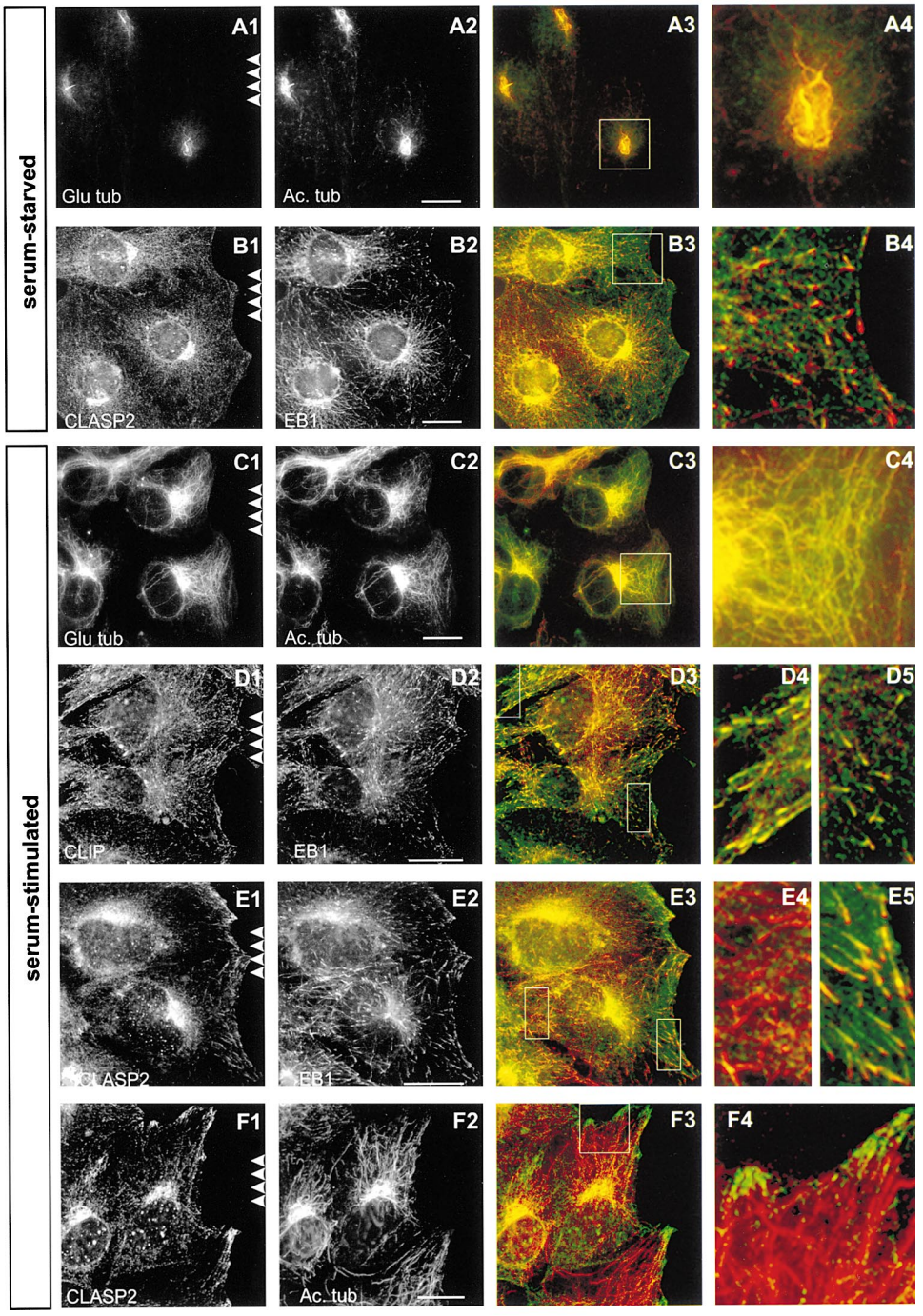

Figure 5. Localization of CLASP2 at the Leading Edge of Serum-Stimulated 3T3 Cells

3T3 cells were grown to 95% confluence in serum-containing medium and then incubated with serum-free medium for 30 hr. Narrow stripes of cells were removed by scraping, and after incubating for 2 more hr without serum, cells were fed either serum-free (A and B) or serum-containing medium (C–F) for an additional 30 min. Cells were fixed and costained with antibodies against Glu tubulin and acetylated tubulin (A and C), CLASP2 and EB1 (B and E), CLIP-115/CLIP-170 (#2221) and EB1 (D), and CLASP2 and acetylated tubulin (F). Images (A3)–(F3) represent overlays of images (A1)–(F1) (green) with images (A2)–(F2) (red). Panels on the right show an enlargement of part of the overlays (indicated by white rectangles). MT tips from the trailing part of the cell are shown in (D4) and (E4), MT tips from the leading edge in (D5) and (E5). The position of the wound is indicated (arrowheads; in [F], the leading edge also extends towards the top). Bar, 10 μm.

CLASPs Stabilize MTs

The similarity of CLASPs to Orbit/Mast and their asymmetric distribution in motile fibroblasts suggests that these proteins might be involved in the regulation of MT dynamics. We examined the MT-stabilizing effect of CLASPs first in COS-1 cells, which normally have few stabilized MTs, as determined by Glu tubulin antibody staining (Figure 6B). Overexpression of GFP-CLASP fu-

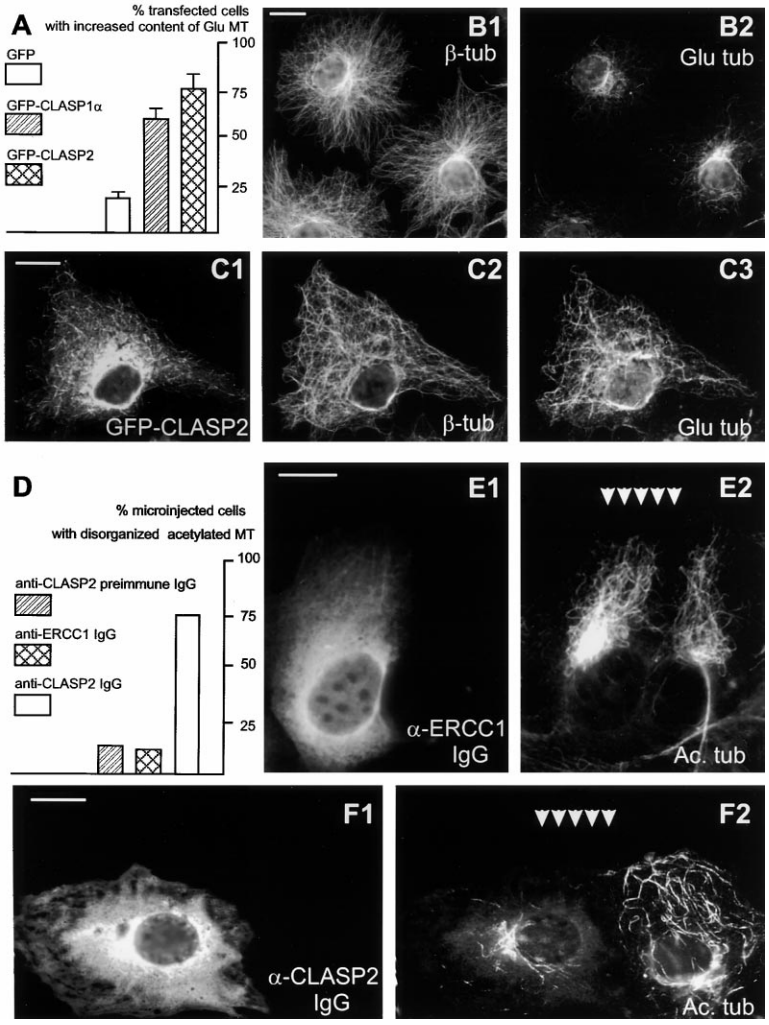

Figure 6. CLASPs Have an MT-Stabilizing Effect

(A) COS-1 cells were transfected with constructs, expressing GFP, GFP-CLASP1α, or GFP-CLASP2, and stained with Glu tubulin antibodies to detect stabilized MTs. The percentage of transfected cells, displaying a significant amount of Glu tubulin at the cell periphery, is shown in (A) (three experiments performed per construct, 100 cells counted per experiment, standard deviation indicated). Cells with very low GFP levels (not visible at data collection times below 600 ms, see Experimental Procedures) or high expression levels (visible at data collection times of 150 ms) were excluded from the analysis.

(B and C) Examples of tubulin (β-tub) and Glu tubulin (Glu tub) staining in untransfected COS-1 cells (B), or in cells expressing moderate levels of GFP-CLASP2 (C). The data collection time was 600 ms in (C1). Bar, 10 μm.

(D–F) Serum-starved 3T3 fibroblasts were injected with anti-CLASP2 or control antibodies, induced with serum for 2 hr, and stained for rabbit IgG (E1 and F1) and acetylated tubulin (E2 and F2). Position of the wound is indicated (arrowheads).

(D) The percentage of injected cells, displaying few or disorganized acetylated MTs, was determined for cells injected with control (#2358 preimmune and anti-ERCC1) antibodies or with anti-CLASP2 antibodies.

(E) 3T3 fibroblast injected with control antibodies.

(F) 3T3 fibroblast injected with anti-CLASP2 antibodies. Bar, 10 μm.

sions induces highly increased levels of detyrosinated MTs (Figures 6A and 6C). In the GFP-CLASP transfected cells, almost all cells contain many stabilized MTs outside the Golgi region, while in a control transfection, GFP alone does not have this effect. Importantly, MT stabilization occurs already at moderate levels of CLASP overexpression, when the distal segments of MTs are decorated by CLASPs (Figure 6C).

In the MT stabilizing assay, GFP-CLASP1α and GFP-CLASP2 fusions show comparable induction of detyrosinated MTs (Figure 6A), indicating that both CLASP1 and -2 have MT-stabilizing properties. In cells displaying an increased number of detyrosinated MTs, also the level of acetylated MTs is increased (data not shown). Such accumulation of two independent posttranslationally modified forms of tubulin argues in favor of an effect of GFP-CLASP overexpression on MT longevity rather than on the tubulin modification machinery itself. In agreement with a stabilizing function of CLASPs, the whole MT cytoskeleton becomes much more dense and entangled in GFP-CLASP-expressing cells (compare Figure 6B1 to Figure 6C2).

In a second experiment, we examined the effect of injected anti-CLASP2 antibodies on the orientation of stabilized MTs at the leading edge. A very high proportion of cells, injected with purified anti-CLASP2 antibodies, show reduced and disorganized stabilized MTs (Figures 6D and 6F) as compared to cells injected with control antibodies (Figures 6D and 6E). The fact that not all cells are affected by anti-CLASP2 injection might be due to variations in the amount of antibody injected, to variations in the state of polarization of motile fibroblasts that were injected, and/or to differences in the expression levels of CLASP1 and -2 within individual cells. Taken together, both the overexpression and antibody inhibition analyses point to a crucial role for CLASPs in the regulation of MT dynamics, in particular in the stabilization of MTs in polarized fibroblasts.

Regulation of CLASP-MT Association by Phosphorylation

The relocalization of CLASP2 upon serum stimulation suggests that CLASPs associate with MTs in a spatially regulated manner. Recently, it was documented that spatial sensing in fibroblasts is mediated by 3′ phosphoinositides (Haugh et al., 2000), implying the involvement of phosphoinositide (PI)-3 kinase at the leading edge. We therefore tested whether inhibition of PI-3 kinase activity affects polarized localization of CLASP2. Serum stimulation in the presence of the PI-3 kinase inhibitors

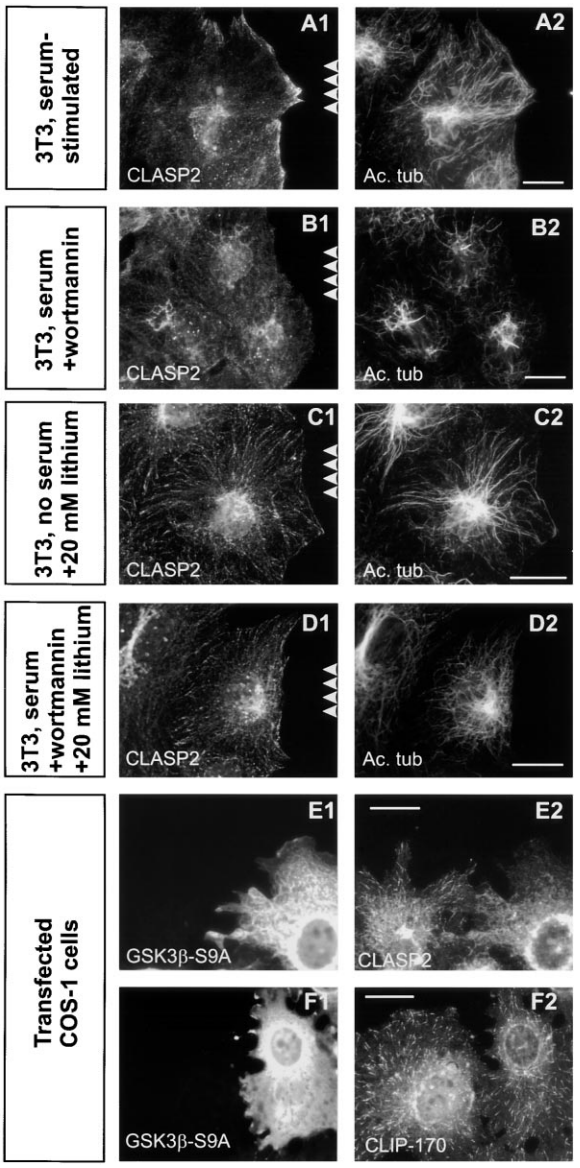

Figure 7. Regulation of Asymmetric CLASP2 Distribution

(A–D) A wounded monolayer of 3T3 cells (see Figure 5) was serum stimulated (A, B, and D) or kept on serum-free medium (C). To inhibit PI-3 kinase or GSK3β, either wortmannin (B and D) or LiCl (C and D) were added, respectively. Cells were fixed and costained with antibodies against CLASP2 and acetylated tubulin. White arrowheads mark the position of the wound in the monolayer.

(E and F) COS-1 cells, transfected with constitutively active, HA-tagged GSK3β-S9A, were fixed and costained with anti-HA antibodies (E1 and F1) and antibodies against CLASP2 (E2) or CLIP-170 (F2). Bar, 10 μm.

wortmannin or LY294002 indeed reduces the normal serum-induced accumulation of CLASP2 at the leading edge (compare Figure 7B to Figure 7A, or 5E). Absence of CLASP accumulation correlates with lack of polarized arrays of acetylated MTs (Figure 7B2). We next tested if glycogen synthase kinase (GSK)-3β, one of the downstream targets of PI-3 kinase, plays a role in regulating CLASP-MT distal end association. Treatment of serum-starved 3T3 cells (which normally do not contain much MT bound CLASP, Figure 5B) with lithium chloride, a direct inhibitor of GSK-3β, results in a significant increase in CLASP2 signal at distal MT ends (Figure 7C1) and in the appearance of extended acetylated MTs (Figure 7C2), which, like CLASP2, are localized throughout the cell. A similar result is observed in lithium-treated cells, which are serum stimulated in the presence of wortmannin (Figure 7D), indicating that GSK-3β inhibition is critical in regulating CLASP–MT interactions. This idea is supported by the observation that overexpression of a constutively active form (GSK-3β-S9A, where serine 9 is replaced by alanine) significantly inhibits CLASP2 localization to MT plus ends in transfected COS-1 cells (Figure 7E), but not that of CLIP-170 (Figure 7F).

Discussion

CLASPs Induce Local Stabilization of MTs

The MT network is a highly dynamic structure that is capable of quick rearrangements in response to environmental cues (Kirschner and Mitchison, 1986). Proteins, which bind to MT tips are of particular interest, since they are likely to be involved in regulation of MT dynamics and/or the interaction of MTs with the cellular cortex. CLIP-170 and CLIP-115 are such plus end binding proteins (Perez et al., 1999; Hoogenraad et al., 2000). Recently, a CLIP-170-like protein from fission yeast, tip1p, was shown to function as an anti-catastrophe factor (Brunner and Nurse, 2000), indicating that CLIP-115 and -170 might have a similar role in mammals. In this study, we identified CLASP1 and -2 as common protein partners of CLIP-115 and -170, which, similar to CLIPs, localize to MT tips. CLASPs are homologous along their entire length to the *Drosophila* MAP Orbit/Mast (Inoue et al., 2000; Lemos et al., 2000). Like Orbit/Mast, CLASPs directly bind MTs. Overexpression of CLASPs in COS-1 cells induces MT stabilization, while inhibition of CLASP2 function by antibody injections prevents the formation of aligned and stabilized MTs in motile fibroblasts. CLASP2 is predominantly bound to MTs at the leading edge of 3T3 cells, where they tend to grow or become stabilized, and not in the cell body, where MTs are unstable and often depolymerize. Taken together, this evidence strongly suggests that CLASPs are MAPs that regulate MT dynamics in polarized cells.

Potential Role of CLASP Isoform Variability

CLASPs exist as a family of isoforms, distinguished by their N-terminal sequences. The domain present in the long CLASP1/2α isoforms (and in Orbit/Mast) is similar to protein sequences in the MT stabilizing proteins of the dis1/TOG family. Although this suggests a function for the dis1/TOG domain of CLASPα in MT stabilization, deletion of the domain did not make a difference in the MT stabilization assay in transfected COS-1 cells. Interestingly, the dis1/TOG members ZYG-9 and Mini Spindles associated with spindle poles and centrosomes (Matthews et al., 1998; Cullen et al., 1999) and transfected GFP-CLASP1α preferentially accumulated in centrosomally originating MT bundles, while the other isoforms did not. It is therefore possible that the N-terminal domain of CLASPα plays a role in centrosomal MT nucleation.

The N terminus of CLASP2β is a membrane-targeting domain, similar to the dual palmitoylation module identified in several other proteins (Resh, 1999). Palmitoylation plays an essential role in protein sorting; for example, it is required to target the membrane-associated guanylate kinase PSD-95 to the postsynaptic density (El-Husseini et al., 2000). The existence of a brain-specific CLASP isoform with a membrane-targeting signal, together with more widely expressed isoforms lacking such a signal, is reminiscent of a situation described for the stathmin protein family. Stathmin is a small cytosolic phosphoprotein, which destabilizes MTs and which is the prototype member of a family, that includes the nervous system proteins SCG10, SCLIP, and RB3 (Gavet et al., 1998). These proteins can associate with membranes through their dually palmitoylated N termini and at least one of them, SCG10, is specifically localized to neuronal growth cones (Di Paolo et al., 1997). The existence of both stabilizing (CLASP) and destabilizing (stathmin) factors with similar targeting properties could provide a mechanism for the fine regulation of MT dynamics in particular neuronal compartments.

Regulation of CLASP–MT Interactions at Distal Ends

Different from other MT-stabilizing factors, such as XMAP215, which bind along the whole length of MTs, CLASPs can induce MT stabilization when present only at the distal ends of MTs. Both in CLASP-overexpressing COS-1 cells and at the leading edge of 3T3 fibroblasts, this stabilization is associated with the presence of a "coat" of CLASP at distal segments. Our findings indicate that PI-3 kinase signaling through GSK3β is an important mediator of the asymmetric CLASP2–MT interactions in 3T3 fibroblasts. These results are consistent with the observation that PI-3 kinase plays an essential role in the polarization of fibroblasts (Haugh et al., 2000) and that one of the biological responses of PI-3 kinase activation is the inactivation of GSK3β (van Weeren et al., 1998). The latter actually fulfills all the requirements for being a negative regulator of CLASP2–MT interactions. First, our in vitro studies suggest that MT binding by CLASPs is negatively influenced by phosphorylation. Second, unlike many other kinases, GSK3β is constitutively active in resting cells (such as serum-starved cells) and is inhibited when cells are stimulated by a number of growth factors. These results are in line with the fact that CLASP binding to distal ends is reduced in serum-starved cells (or in cells overexpressing a constitutively active form of GSK3β) and stimulated by serum (or by inactivation of GSK3β with lithium chloride). Thus, the polarized accumulation of CLASPs is subject to regulation by positional cues and by serum, which distinguishes CLASPs from other MT plus end binding proteins, such as CLIPs and EB1.

Functional Significance of the CLIP–CLASP Interaction

We have shown that the C-terminal domain of CLASPs specifically binds to a portion of the coiled-coil domain of CLIP-115 and -170. In vivo, this CLIP–CLASP interaction might be transient since the distribution of CLIPs and CLASPs shows only partial overlap in interphase fibroblasts. There is a substantial Golgi-associated pool of CLASPs, while CLIP-170 and CLIP-115 do not accumulate significantly in the Golgi. Also, in serum-stimulated 3T3 cells, only a subset of EB1/CLIP-positive MT tips are labeled strongly with anti-CLASP2 antibodies. In serum-grown 3T3 cells, CLIPs and EB1 are most concentrated at the very tip of an MT, while longer and more proximal MT segments are stained by anti-CLASP2 antibodies. A transient CLIP–CLASP interaction would account for previous failures to copurify CLASPs (or any other protein) with CLIP-170 (Scheel et al., 1999). Also, in our hands, no significant amounts of CLIP-170 could be coprecipitated with CLASP from untransfected COS-1 cells.

The affinity of CLASPs for MT tips is not solely dependent on interaction with CLIPs since a CLASP2 mutant, lacking the CLIP binding domain, is still targeted to MT plus ends. In spite of this fact and the putative transient nature of the CLIP–CLASP interaction, these proteins are highly likely to influence the affinity of each other for MTs and thereby affect the fate of MTs. For example, CLIPs could stimulate the loading of (membrane bound) CLASPs onto the MT plus ends. Conversely, accumulation of CLASPs on distal segments of a subset of MTs might serve to attract CLIP-170 (or CLIP-115) to the tips of MTs, even under conditions of MT shrinkage and/or pausing, conditions that normally cause dissociation of CLIP-170 from the distal ends (Perez et al., 1999). Attraction of the CLIPs by a CLASP-positive segment may rescue pausing/retracting MTs and revert them to a state of growth and may be one of the mechanisms by which CLASPs stabilize MTs. This model is both in line with the proposed anti-catastrophe role of tip1p (Brunner and Nurse, 2000) and with the observation that CLIP-170 treadmills on the growing ends of MTs by copolymerization with tubulin and could thus be an inherent part of the MT polymerization machinery (Diamantopoulos et al., 1999; Perez et al., 1999). It also would explain the increased longevity of a subset of MTs at the leading edge (Cook et al., 1998) and why these MTs still have their tips decorated with EB1/CLIP. In conclusion, we propose that CLIP–CLASP interactions constitute part of a regulatory device on the distal ends of MTs that is needed to target or modulate MT dynamics in polarized cells. The partnership between CLIPs and CLASPs bears a striking resemblance to that of APC and EB1, two proteins which bind to each other, accumulate at MT plus ends, and regulate MT dynamics in polarized cells (for review, see Tirnauer and Bierer, 2000). It will be interesting to investigate to what extent CLIP-CLASP and APC-EB1 pathways interact.

Experimental Procedures

Yeast Two-Hybrid Screen

A mouse E14.5 day embryonic cDNA library (Chevray and Nathans, 1992) was screened by the yeast two-hybrid assay (Wolthuis et al., 1996). Fragments of rat CLIP-115, rat brain CLIP-170, and chicken $p150^{Glued}$ were cloned into the pPC97 yeast two-hybrid vector (see Figure 1A). Production of yeast proteins was verified by Western blotting using monoclonal antibodies against GAL4 DNA binding and activation domains (Clontech). Mouse CLASP1 cDNA, derived from the yeast two-hybrid screen, corresponds to the 3′ portion of KIAA0622, starting from position 3010 (see Figure 1B). Interaction of mCLASP1 with CLIP-115 was verified by exchanging the inserts of bait and fish vectors.

cDNA Isolation and Northern Blotting

The CLIP-170 clone used here is a rat brain cDNA encoding a CLIP-170 isoform with a 115 amino acid deletion in the C-terminal portion of the coiled-coil region (accession number AJ237670). Human KIAA0622 (CLASP1) and KIAA0627 (CLASP2) cDNAs (Ishikawa et al., 1998) were obtained from the Kazuza DNA Research Institute. To complete the 5′ ends of these cDNAs, we used RACE-PCR with human adult brain poly(A)$^+$ RNA (Clontech) or mouse brain RNA as a template. Mouse EST ui60h04 (truncated CLASP2α) is an IMAGE clone. Rat cDNA clone r313 (CLASP2β) was isolated by screening of a rat hippocampus cDNA library (De Zeeuw et al., 1997). Accession numbers are: AJ288057 (human brain 5′ end CLASP1α), AJ288058, and AJ288059 (human brain 5′ end CLASP2γ and -β, respectively); AJ288060 (clone r313); AJ288061 (mouse yeast two-hybrid CLASP1); AJ276961 (ui60h04), and AJ276962 (mouse brain 5′ end CLASP1α). Northern blots were prepared and hybridized using standard protocols (Sambrook et al., 1989).

GST Fusion Constructs and Generation of CLASP Antisera

Glutathione S-transferase (GST) fusions were generated using plasmids pGEX-2T and pGEX-3X (Pharmacia). GST-mCLASP1-C contains the whole coding part of the mouse yeast two-hybrid CLASP1 cDNA. GST-hCLASP2 contains the corresponding C terminus of human CLASP2 (nucleotide positions 3074–3976 of the KIAA0627 cDNA). The GST-CLIP fusion proteins are explained in Figure 3A. Purification of GST fusion proteins and immunization of rabbits were performed as described (Hoogenraad et al., 2000). Antiserum #2358 is against GST-hCLASP2.

Western Blot Analysis and Immunoprecipitations

Protein extract preparation, Western blotting, and CLIP antisera have been described (Hoogenraad et al., 2000). Proteins were detected using rabbit polyclonal anti-GFP (1:2500; Clontech) or anti-CLIP and CLASP antibodies (all used at 1:2500). The Triton-X114 partitioning assay was performed as published (Hancock et al., 1989).

In the immunoprecipitation experiments, transfected COS-1 cells were lysed in buffer containing 30 mM HEPES (pH 7.4), 100 mM KCl, 1% NP-40, supplemented with protease inhibitors (Boehringer Mannheim), and incubated at 4°C for 30 min to depolymerize MTs. All subsequent steps were carried out as described (Hoogenraad et al., 2000).

GST Pulldown and MT Binding Assays

KIAA0622, KIAA0627, and CLIP-115 cDNAs were transcribed and translated in vitro using the TnT-coupled transcription-translation system (Promega) and ^{35}S-methionine (Trans35S label, ICN). Aliquots of radiolabeled proteins were incubated with different GST fusion proteins in NETT buffer (100 mM NaCl, 50 mM Tris (pH 7.5), 5 mM EDTA, 0.5% Triton X-100) for 2 hr at room temperature. Afterwards, samples were washed five times in NETT buffer. Proteins were eluted by boiling in sample buffer and analyzed by SDS-PAGE. Dried gels were exposed to film.

Mouse brains were homogenized in NETT buffer containing protease inhibitors. After removing insoluble material by centrifugation for 10 min at 10,000 $\times$ g, protein extract was used for the GST pulldown assay, as described above. Bound proteins were detected by Western blotting.

For the MT binding assays (Hoogenraad et al., 2000), CLASP1α and r313 plasmids were transcribed and translated. Some samples were treated for 15 min at 30°C with apyrase (1 U, Sigma) immediately after translation. The MT blot overlay was performed as described (Brunner and Nurse, 2000).

Expression Constructs

GFP-CLASP1 contains the whole open reading frame of KIAA0622, subcloned in-frame into pEGFP-C1 (Clontech). CLASP1α was constructed from KIAA0622 and an overlapping human brain RACE product, encoding the XMAP215-homologous domain, by using a unique AvrII site at position 580 in KIAA0622. Fusing the CLASP1α insert into pEGFP-C1 produced GFP-CLASP1α. Untagged CLASP2γ consists of the whole insert of KIAA0627, cloned into pCI-neo (Promega). GFP-CLASP2 was made by inserting KIAA0627 cDNA from the BspEI site at position 184 into pEGFP-C1; it therefore lacks the first 29 amino acids encoded by KIAA0627. In the GFP-CLASP2 C-terminal deletion constructs, the CLASP2 coding sequence was abrogated at nucleotide positions 1830 (GFP-CLASP2ΔSal) and 3138 (GFP-CLASP2ΔXho) of the KIAA0627 sequence. The GSK-3β (S9A) construct has been described (van Weeren et al., 1998).

Cell Culture Manipulations and Immunofluorescence

COS-1 cells were cultured and transfected as described (Hoogenraad et al., 2000). Swiss 3T3 fibroblasts were cultured in DMEM medium with 8% fetal calf serum. Serum starvation and monolayer wounding were as reported (Gundersen et al., 1994). For PI3-kinase inhibition, 100 nM wortmannin or 300 μM LY294002 (Sigma) was used. For GSK-3β inhibition, 10–20 mM LiCl was added to the culture medium. Antibody injections into fibroblasts on the edge of the stripes were performed as published previously (van Vuuren et al., 1994). Injections were done 2 hr prior to serum induction using IgG-purified antibodies at 5 mg/ml. Injected cells were detected using fluorescently labeled rabbit secondary antibodies. The percentage of cells with reduced or disorganized stabilized MTs was determined by staining with antibodies against acetylated tubulin. Stabilized MTs were scored as disorganized if their amount was highly reduced (see example in Figure 6F) and/or if they displayed random orientation with respect to the leading edge. Percentages were determined by counting 79 cells injected with control #2358 preimmune IgG (16% disorganized), 86 cells injected with control anti-ERCC1 antibodies (van Vuuren et al., 1994; 14% disorganized), and 233 cells injected with anti-CLASP2 antibodies (results from the two independent experiments with the different control antibodies; 76% disorganized).

Immunofluorescence experiments (Hoogenraad et al., 2000) were performed using rabbit anti-CLASP2 antiserum, antiserum #2221, which recognizes both CLIP-115 and CLIP-170 and antiserum #2238, which is specific for CLIP-115 (Hoogenraad et al., 2000), in a dilution of 1:300. Rabbit antibodies against Glu tubulin (a gift from Dr. J. C. Bulinski) were diluted at 1:500. Mouse monoclonal antibodies against the HA tag (BAbCO), β-tubulin, acetylated tubulin and vinculin (Sigma), EB1, and GM130 (Transduction Laboratories) were diluted 1:100. Secondary antibodies used were rhodamine-conjugated sheep anti-mouse (1:25, Boehringer Mannheim), Alexa 594-conjugated goat anti-rabbit (1:500, Molecular Probes), FITC-conjugated goat anti-rabbit (1:100, Nordic Laboratories), and Alexa 350-conjugated sheep anti-mouse (1:250, Molecular Probes).

Signals were captured with a Leica DMRBE fluorescence microscope equipped with a Hamamatsu C4880 DCC camera. To quantify the GFP fluorescence, cells were imaged using fixed data collection times: 150 ms for highly expressing cells, 600 ms for moderately expressing cells, and 1200 ms for cells expressing low levels of GFP fusion protein.

Acknowledgments

We are grateful to Dr. T. A. Schroer for sending the chicken p150^{Glued} cDNA, to Dr. J. C. Bulinski for sending anti-Glu tubulin antiserum, and to Dr. T. Nagase for providing KIAA0622 and KIAA0627 cDNAs. This research was supported by grants from the Netherlands Organization for Scientific Research (NWO; GB-MW 903-68-361), the Life Sciences Foundation (SLW; 805.33.310; 803.33.311), and the Royal Dutch Academy of Sciences (KNAW).

Received June 23, 2000; revised January 25, 2001.

References

Brunner, D., and Nurse, P. (2000). CLIP170-like tip1p spatially organizes microtubular dynamics in fission yeast. Cell *102*, 695–704.

Bulinski, J.C., and Gundersen, G.G. (1991). Stabilization of post-translational modification of microtubules during cellular morphogenesis. Bioessays *13*, 285–293.

Chevray, P.M., and Nathans, D. (1992). Protein interaction cloning in yeast: identification of mammalian proteins that react with the leucine zipper of Jun. Proc. Natl. Acad. Sci. USA *89*, 5789–5793.

Cook, T.A., Nagasaki, T., and Gundersen, G.G. (1998). Rho guano-

sine triphosphatase mediates the selective stabilization of microtubules induced by lysophosphatidic acid. J. Cell Biol. *141*, 175–185.

Cullen, C.F., Deak, P., Glover, D.M., and Ohkura, H. (1999). Mini spindles: a gene encoding a conserved microtubule-associated protein required for the integrity of the mitotic spindle in Drosophila. J. Cell Biol. *146*, 1005–1018.

Desai, A., and Mitchison, T.J. (1997). Microtubule polymerization dynamics. Annu. Rev. Cell Dev. Biol. *13*, 83–117.

De Zeeuw, C.I., Hoogenraad, C.C., Goedknegt, E., Hertzberg, E., Neubauer, A., Grosveld, F., and Galjart, N. (1997). CLIP-115, a novel brain-specific cytoplasmic linker protein, mediates the localization of dendritic lamellar bodies. Neuron *19*, 1187–1199.

Di Paolo, G., Lutjens, R., Pellier, V., Stimpson, S.A., Beuchat, M.H., Catsicas, S., and Grenningloh, G. (1997). Targeting of SCG10 to the area of the Golgi complex is mediated by its NH2-terminal region. J. Biol. Chem. *272*, 5175–5182.

Diamantopoulos, G.S., Perez, F., Goodson, H.V., Batelier, G., Melki, R., Kreis, T.E., and Rickard, J.E. (1999). Dynamic localization of CLIP-170 to microtubule plus ends is coupled to microtubule assembly. J. Cell Biol. *144*, 99–112.

Dujardin, D., Wacker, U.I., Moreau, A., Schroer, T.A., Rickard, J.E., and De Mey, J.R. (1998). Evidence for a role of CLIP-170 in the establishment of metaphase chromosome alignment. J. Cell Biol. *141*, 849–862.

El-Husseini, A.E., Craven, S.E., Chetkovich, D.M., Firestein, B.L., Schnell, E., Aoki, C., and Bredt, D.S. (2000). Dual palmitoylation of PSD-95 mediates its vesiculotubular sorting, postsynaptic targeting, and ion channel clustering. J. Cell Biol. *148*, 159–172.

Gavet, O., Ozon, S., Manceau, V., Lawler, S., Curmi, P., and Sobel, A. (1998). The stathmin phosphoprotein family: intracellular localization and effects on the microtubule network. J. Cell Sci. *111*, 3333–3346.

Gundersen, G.G., Kim, I., and Chapin, C.J. (1994). Induction of stable microtubules in 3T3 fibroblasts by TGF-beta and serum. J. Cell Sci. *107*, 645–659.

Hancock, J.F., Magee, A.I., Childs, J.E., and Marshall, C.J. (1989). All ras proteins are polyisoprenylated but only some are palmitoylated. Cell *57*, 1167–1177.

Haugh, J.M., Codazzi, F., Teruel, M., and Meyer, T. (2000). Spatial sensing in fibroblasts mediated by 3′ phosphoinositides. J. Cell Biol. *151*, 1269–1280.

Hoogenraad, C.C., Akhmanova, A., Grosveld, F., De Zeeuw, C.I., and Galjart, N. (2000). Functional analysis of CLIP-115 and its binding to microtubules. J. Cell Sci. *113*, 2285–2297.

Inoue, Y.H., do Carmo Avides, M., Shiraki, M., Deak, P., Yamaguchi, M., Nishimoto, Y., Matsukage, A., and Glover, D.M. (2000). Orbit, a novel microtubule-associated protein essential for mitosis in Drosophila melanogaster. J. Cell Biol. *149*, 153–166.

Ishikawa, K., Nagase, T., Suyama, M., Miyajima, N., Tanaka, A., Kotani, H., Nomura, N., and Ohara, O. (1998). Prediction of the coding sequences of unidentified human genes. X. The complete sequences of 100 new cDNA clones from brain which can code for large proteins in vitro. DNA Res. *5*, 169–176.

Kirschner, M., and Mitchison, T. (1986). Beyond self-assembly: from microtubules to morphogenesis. Cell *45*, 329–342.

Lemos, C.L., Sampaio, P., Maiato, H., Costa, M., Omel'yanchuk, L.V., Liberal, V., and Sunkel, C.E. (2000). Mast, a conserved microtubule-associated protein required for bipolar mitotic spindle organization. EMBO J. *19*, 3668–3682.

Liao, G., Kreitzer, G., Cook, T.A., and Gundersen, G.G. (1999). A signal transduction pathway involved in microtubule-mediated cell polarization. Faseb. J. *13*, S257–S260.

Matthews, L.R., Carter, P., Thierry-Mieg, D., and Kemphues, K. (1998). ZYG-9, a Caenorhabditis elegans protein required for microtubule organization and function, is a component of meiotic and mitotic spindle poles. J. Cell Biol. *141*, 1159–1168.

Mimori-Kiyosue, Y., Shiina, N., and Tsukita, S. (2000). The dynamic behavior of the APC-binding protein EB1 on the distal ends of microtubules. Curr. Biol. *10*, 865–868.

Perez, F., Diamantopoulos, G.S., Stalder, R., and Kreis, T.E. (1999). CLIP-170 highlights growing microtubule ends in vivo. Cell *96*, 517–527.

Pierre, P., Scheel, J., Rickard, J.E., and Kreis, T.E. (1992). CLIP-170 links endocytic vesicles to microtubules. Cell *70*, 887–900.

Resh, M.D. (1999). Fatty acylation of proteins: new insights into membrane targeting of myristoylated and palmitoylated proteins. Biochim. Biophys. Acta *1451*, 1–16.

Sambrook, J., Fritsch, E.F., and Maniatis, T. (1989). Molecular Cloning: A Laboratory Manual, 2nd Edition (New York: Cold Spring Harbor Laboratory Press).

Scheel, J., Pierre, P., Rickard, J.E., Diamantopoulos, G.S., Valetti, C., van der Goot, F.G., Haner, M., Aebi, U., and Kreis, T.E. (1999). Purification and analysis of authentic CLIP-170 and recombinant fragments. J. Biol. Chem. *274*, 25883–25891.

Tirnauer, J.S., and Bierer, B.E. (2000). EB1 proteins regulate microtubule dynamics, cell polarity, and chromosome stability. J. Cell Biol. *149*, 761–766.

Tirnauer, J.S., O'Toole, E., Berrueta, L., Bierer, B.E., and Pellman, D. (1999). Yeast Bim1p promotes the G1-specific dynamics of microtubules. J. Cell Biol. *145*, 993–1007.

Valetti, C., Wetzel, D.M., Schrader, M., Hasbani, M.J., Gill, S.R., Kreis, T.E., and Schroer, T.A. (1999). Role of dynactin in endocytic traffic: effects of dynamitin overexpression and colocalization with CLIP-170. Mol. Biol. Cell *10*, 4107–4120.

van Vuuren, A.J., Vermeulen, W., Ma, L., Weeda, G., Appeldoorn, E., Jaspers, N.G., van der Eb, A.J., Bootsma, D., Hoeijmakers, J.H., Humbert, S., et al. (1994). Correction of xeroderma pigmentosum repair defect by basal transcription factor BTF2 (TFIIH). EMBO J. *13*, 1645–1653.

van Weeren, P.C., de Bruyn, K.M., de Vries-Smits, A.M., van Lint, J., and Burgering, B.M. (1998). Essential role for protein kinase B (PKB) in insulin-induced glycogen synthase kinase 3 inactivation. Characterization of dominant-negative mutant of PKB. J. Biol. Chem. *273*, 13150–13156.

Vaughan, K.T., Tynan, S.H., Faulkner, N.E., Echeverri, C.J., and Vallee, R.B. (1999). Colocalization of cytoplasmic dynein with dynactin and CLIP-170 at microtubule distal ends. J. Cell Sci. *112*, 1437–1447.

Wittmann, T., Hyman, A., and Desai, A. (2001). The spindle: a dynamic assembly of microtubules and motors. Nat. Cell Biol. *3*, E28–E34.

Wolthuis, R.M., Bauer, B., van't Veer, L.J., de Vries-Smits, A.M., Cool, R.H., Spaargaren, M., Wittinghofer, A., Burgering, B.M., and Bos, J.L. (1996). RalGDS-like factor (Rlf) is a novel Ras and Rap 1A-associating protein. Oncogene *13*, 353–362.

GenBank Accession Numbers

The GenBank accession numbers for the eight sequences reported in this paper are: AJ237670 (rat brain CLIP-170); AJ288057 (human brain 5′ end CLASP1α); AJ288058 and AJ288059 (human brain 5′ end CLASP2γ and -β, respectively); AJ288060 (clone r313); AJ288061 (mouse yeast two-hybrid CLASP1); AJ276961 (ui60h04) and AJ276962 (mouse brain 5′ end CLASP1α).

Chapter 5

Visualization of microtubule growth in cultured neurons via the use of EB3-GFP (end-binding protein 3-green fluorescent protein)

Tatiana Stepanova, Jenny Slemmer, Casper C. Hoogenraad, Gideon Lansbergen, Bjorn Dortland, Chris I. De Zeeuw, Frank Grosveld, Gert van Cappellen, Anna Akhmanova and Niels Galjart

Visualization of Microtubule Growth in Cultured Neurons via the Use of EB3-GFP (End-Binding Protein 3-Green Fluorescent Protein)

Tatiana Stepanova,[1] Jenny Slemmer,[2] Casper C. Hoogenraad,[1,2] Gideon Lansbergen,[1] Bjorn Dortland,[1] Chris I. De Zeeuw,[2] Frank Grosveld,[1] Gert van Cappellen,[3] Anna Akhmanova,[1] and Niels Galjart[1]

Medical Genetics Center Departments of [1]Cell Biology and Genetics and [2]Neuroscience, and [3]Department of Reproduction and Development, Erasmus University, 3000 DR Rotterdam, The Netherlands

Several microtubule binding proteins, including CLIP-170 (cytoplasmic linker protein-170), CLIP-115, and EB1 (end-binding protein 1), have been shown to associate specifically with the ends of growing microtubules in non-neuronal cells, thereby regulating microtubule dynamics and the binding of microtubules to protein complexes, organelles, and membranes. When fused to GFP (green fluorescent protein), these proteins, which collectively are called +TIPs (plus end tracking proteins), also serve as powerful markers for visualizing microtubule growth events. Here we demonstrate that endogenous +TIPs are present at distal ends of microtubules in fixed neurons. Using EB3-GFP as a marker of microtubule growth in live cells, we subsequently analyze microtubule dynamics in neurons. Our results indicate that microtubules grow slower in neurons than in glia and COS-1 cells. The average speed and length of EB3-GFP movements are comparable in cell bodies, dendrites, axons, and growth cones. In the proximal region of differentiated dendrites ~65% of EB3-GFP movements are directed toward the distal end, whereas 35% are directed toward the cell body. In more distal dendritic regions and in axons most EB3-GFP dots move toward the growth cone. This difference in directionality of EB3-GFP movements in dendrites and axons reflects the highly specific microtubule organization in neurons. Together, these results suggest that local microtubule polymerization contributes to the formation of the microtubule network in all neuronal compartments. We propose that similar mechanisms underlie the specific association of CLIPs and EB1-related proteins with the ends of growing microtubules in non-neuronal and neuronal cells.

Key words: **microtubules; microtubule dynamics; microtubule plus end tracking proteins; cytoskeleton; neurons; neuronal differentiation**

Introduction

Neurons are signaling cells with a unique polarized composition, which is paralleled by a highly specific microtubule (MT) network organization. For example, MTs are organized nonuniformly in differentiated dendrites, with dynamic (plus) ends pointing both distally and toward the cell body (Baas et al., 1988). In axons, on the other hand, MTs are organized unidirectionally, with all plus ends pointing toward the growth cone. This organization is different from that of other cell types in which minus ends of MTs often are, for example, embedded in the MT organizing center (MTOC), whereas plus ends explore the cytoplasm. In view of these differences and the fact that the distance between cell body and neuronal periphery can be quite extensive, it is logical to assume that the localization and transport of membrane-bound organelles over MT tracks, the formation and maintenance of the neuronal MT cytoskeleton itself as well as the transport of cytoskeletal elements might be organized in a unique manner.

The dynamic properties of MTs are regulated by a large number of cellular factors, including MT-associated proteins (MAPs) and MT motors. Recently, a novel type of microtubule binding has attracted considerable interest, both with respect to the regulation of MT dynamics and intracellular membrane transport over MTs. Live imaging studies have shown that an increasing number of MT regulatory proteins from various organisms specifically associates with the distal ends of growing MTs. This characteristic behavior was documented first for CLIP-170 (cytoplasmic linker protein-170) (Perez et al., 1999); it was explained by a mechanism called "treadmilling" or "plus end tracking," and MT plus end-binding proteins that show this behavior have since been called "plus end-tracking proteins" or +TIPs (Schuyler and Pellman, 2001). Treadmilling involves the incorporation of +TIPs into growing MT ends either by copolymerization with tubulin or by recognition of a specific feature of the MT distal end and subsequent release from an older, more proximal part of the MT. The kinetics of association and release may be regulated by post-translational modifications of the +TIP, for example, phosphorylation (Rickard and Kreis, 1991; Hoogenraad et al., 2000; Tirnauer et al., 2002; Vaughan et al., 2002). In addition to CLIP-170, CLIP-115, and CLIP-associated proteins or CLASPs (Akhmanova et al., 2001), LIS1 (Han et al., 2001; Coquelle et al., 2002), EB1 (end-binding protein 1) and its associated protein APC (Mimori-Kiyosue et al., 2000a,b) as well as components of the dynein/dynactin motor complex (Han et al., 2001; Vaughan et al., 2002) appear to undergo treadmilling behavior. Besides their role in the regulation of MT dynamic events, some of these +TIPs also may exert an influence on intracellular transport of vesicular

Received Dec. 9, 2002; revised Jan. 23, 2003; accepted Jan. 24, 2003.

This research was supported by the Netherlands Organization for Scientific Research (NWO; Grants NWO-MW 903.47.067, NWO-ALW 810.67.012, and NWO-SLW 805–33.311-P), The Dutch Royal Academy of Sciences, and Erasmus University. We thank Dr. Carlos Dotti for his help with setting up the neuronal hippocampal cultures and Michael van der Reijden and Dr. Gerard Borst for their assistance with the generation of the EB3-GFP virus.

Correspondence should be addressed to Dr. Niels Galjart, MGC Department of Cell Biology and Genetics, Erasmus University, P.O. Box 1738, 3000 DR Rotterdam, The Netherlands. E-mail: galjart@ch1.fgg.eur.nl.

 0270-6474/03/232655-10$15.00/0

cargo via their control over MT tip association of the dynein/dynactin complex (Valetti et al., 1999; Vaughan et al., 1999).

All live imaging studies so far have documented the behavior of +TIPs, fused to GFP (green fluorescent protein) (GFP+TIPs), in non-neuronal cells. Because the growth rates of MTs as measured with various GFP+TIPs are similar to values obtained after the injection of fluorescently labeled tubulin (see Komarova et al., 2002a), the dynamic behavior of MTs is not altered significantly by low expression levels of the +TIPs. Thus GFP+TIPs appear to be excellent tools for studying MT growth dynamics in living cells. Using these markers in neurons, we have addressed the important question of whether changes in the MT network during neuronal differentiation are reflected by changes in MT polymerization dynamics in different neuronal compartments. We first show that endogenous CLIPs and EB1-related proteins are present at the distal ends of neuronal MTs. Using EB3-GFP as a marker, we subsequently highlight polymerizing MTs in two different types of cultured neurons. Our results support the conclusion that local MT polymerization events occur throughout neuronal differentiation. We propose that similar mechanisms control the association of +TIPs with MT distal ends in neurons and non-neuronal cells.

Materials and Methods

Antibodies and immunocytochemistry. For immunocytochemistry the cultured neurons were washed in PBS and fixed first in freshly prepared −20°C methanol/1 mM EGTA, followed by a 2% paraformaldehyde fixation at room temperature (20 min for each step). Subsequent antibody incubation and washing steps have been described, as have the CLIP-115- and CLIP-170-specific antisera (numbers 2221, 2238, and 2360) (Hoogenraad et al., 2000; Coquelle et al., 2002). A combination of these sera was used, each in a 1:1000 dilution. For EB3 the novel polyclonal antibodies (number 02-1005-07) were raised in rabbit, as described previously (Hoogenraad et al., 2000), using glutathione *S*-transferase-EB3 (GST-EB3) as an antigen. Monoclonal antibodies against EB1 (Transduction Laboratories, Lexington, KY), actin (Chemicon, Temecula, CA), acetylated α-tubulin, tyrosine α-tubulin, and β-tubulin (Sigma, St. Louis, MO) were used in a dilution of 1:100. FITC-conjugated goat anti-rabbit (1:100; Nordic Laboratories, Tilburg, The Netherlands) and Alexa 594-conjugated goat anti-mouse (1:500; Molecular Probes, Eugene, OR) were used as secondary antibodies. Signals were captured as described previously (Hoogenraad et al., 2000; Akhmanova et al., 2001), using either a Leica DMRBE microscope with a 100× oil immersion lens (numerical aperture, 1.3) and a Hamamatsu C4880 camera or a Zeiss (Jena, Germany) LSM510 confocal microscope with a 63× oil immersion lens (numerical aperture, 1.4). EB3 and EB1 fluorescent intensities at plus ends were analyzed with Image-Pro Plus, version 4.5 (Media Cybernetics, Silver Spring, MD). After subtraction of the background a threshold was put in the red fluorescent channel to select the plus ends. Then the red and green intensities were measured at the same spot. Small spots (≤0.1 μm^2) and large spots (>1 μm^2) were discarded from the analysis. The confocal images representing EB3-tubulin costaining (see Fig. 2*H,I*) were reconstructed with a Quick Maximum Likelihood Estimation (Huygens2 pro, Scientific Volume Imaging, Hilversum, The Netherlands) that is based on a theoretical point spread function. Different color channels were analyzed with different point spread functions. After analysis the channels were merged again.

GFP–fusion constructs. The *GFP-CLIP-115* and *GFP-CLIP-170* constructs have been described (Perez et al., 1999; Hoogenraad et al., 2000; Akhmanova et al., 2001). Mutant GFP-CLIP-170 (called GFP-CLIP-170ΔHind), lacking the C-terminal domain and part of the coiled-coil region of rat CLIP-170, was generated by *Hin*dIII/*Bam*HI digestion of GFP-CLIP-170 in the pEGFP vector, removal of the insert containing the 3′ CLIP-170 sequence, and religation of blunted ends. For cloning of *EB1*, *EB2*, and *EB3* cDNAs gene-specific primers were designed, with restriction sites for in-frame cloning after PCR amplification into *pEGFP-N1* (Clontech, Palo Alto, CA). Primer sequences were based on the following accession numbers: AW106491 (Image clone 2225780, mouse *EB1*); AW231083 (Image clone 2644901, mouse *EB2* or *RP1*); AA2892 (Image clone 714028; human *EB3* cDNA). Western blot analysis of COS-1 cells transfected with the different cDNAs (Hoogenraad et al., 2000) shows that all EB-GFP fusions are produced with an expected molecular weight (see Fig. 1).

Cell culture and protein expression. COS 1 cells were cultured and transfected as described previously (Akhmanova et al., 2001). Mouse hippocampal neurons were isolated from embryonic day 17 (E17) embryos and cultured on the basis of published procedures (Dotti et al., 1988; de Hoop et al., 1998). Neurons were electroporated immediately after isolation, using highly purified DNA (EndoFree Maxi Prep, Qiagen, Hilden, Germany). Thus hippocampi were dissected from fetal brains, treated with 0.25% trypsin for 15 min at 37°C, washed in Ca/Mg-free HBSS, and dissociated by repeated passage through a constricted Pasteur pipette. Directly after isolation 25 μg of plasmid DNA was added to the suspension of neurons in HBSS (0.4 ml), and neurons were electroporated in a Bio-Rad (Hercules, CA) Gene Pulser at 850 V, 25 mF, and 200 Ω (time constant, 0.8 sec). Subsequently, neurons were plated on 22 mm poly-L-lysine-coated coverslips. Plating medium contained 2 mM sodium butyrate for 17–24 hr to enhance the expression of cytomegalovirus CMV promoter-driven genes. After this time the coverslips with the neuronal cultures were placed upside down in 3.5 cm dishes containing N2 medium (de Hoop et al., 1998) conditioned by a confluent monolayer of astroglial cells. Small paraffin droplets on the coverslips prevented the neurons from making contact with the glia.

Mouse Purkinje cell (PC) neurons were isolated from E18 FVB/N embryos. Cerebella were washed twice in HBSS and then treated with 0.5% Trypsin-EDTA for 13–15 min at 37°C. After centrifugation the cerebella were washed with growth medium, i.e., basal modified Eagle's (Invitrogen, San Diego, CA), containing 10% horse serum (Invitrogen), 10 μg/ml gentamycin, 0.5% glucose (Sigma), 1 mM sodium pyruvate (Sigma), and 1% N2 supplements (Invitrogen). Cells were triturated with fresh growth medium, filtered through a 70 μm nylon cell strainer, and plated in 1 ml aliquots (1×10^6 cells/ml) onto four-well LabTek II chambered cover glasses (Nalge Nunc, Rochester, NY) coated overnight with poly-L-ornithine (500 μg/ml; Sigma). Neuronally enhanced cultures were obtained by replacing one-half of the medium at 2 d *in vitro* (2 DIV) and then twice per week with serum-free culture medium containing 2% B27 supplement (Invitrogen).

To express foreign proteins in PC neurons, we used Semliki Forest virus (SFV)-mediated gene delivery (Ehrengruber et al., 1999; Lundstrom et al., 2001a,b). The EB3-GFP construct was cloned into the pSFV2 vector according to the manufacturer's instructions (Invitrogen). Constructs were packaged into SFV replicons, using coelectroporation of helper and vector RNA into baby hamster kidney-21 cells. Cultured PCs (or hippocampal neurons) were infected between 10 and 17 DIV by the addition of 1 and 5 μl of SFV infectious replicons to the cultures.

Live cell imaging and analysis of GFP movements. Cells were analyzed at 37°C on a Zeiss LSM510 confocal laser-scanning microscope as described previously (Akhmanova et al., 2001). In most experiments the optical slice (*z*-dimension) was set to 1 μm. Other settings that were used (e.g., laser intensity and gain value) differed slightly in the various experiments and were adapted to obtain optimal signal-to-noise ratios. Nocodazole (Sigma) and taxol (Molecular Probes) were added at 0.1 or 10 μM final concentrations. Images of GFP+TIP movements in transfected cells were acquired every 1–3.5 sec. Image capture time was typically <1 sec in COS-1 cells. In contrast, capture times for neuronal imaging were in the range of 1–3.5 sec because of the lower signals that were present at MT tips in these cells. Images were recorded and movies were assembled by using LSM510 software.

Distances traveled by GFP+TIP dashes were measured in different neuronal areas. The velocity of the different +TIP dashes was calculated by dividing the distances traveled by time spent traveling. We included only dashes that could be followed for at least three consecutive frames. To measure the percentage of forward or anterograde EB3-GFP movements (i.e., movements toward the distal end of neurons) and backward or retrograde movements (i.e., toward cell body of neurons), we mea-

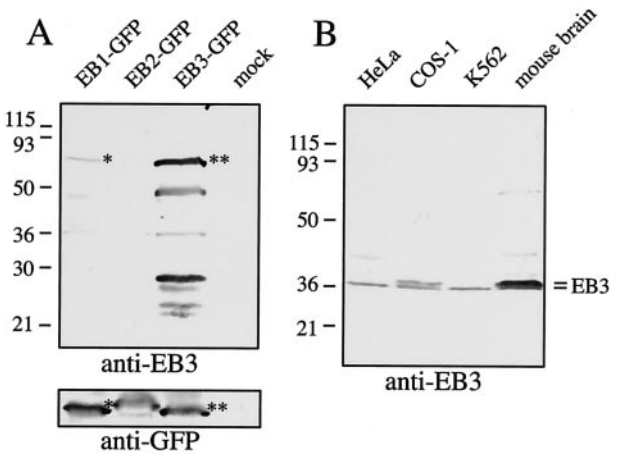

Figure 1. Characterization of anti-EB3 antiserum. Novel anti-EB3 antibodies were raised in rabbit against GST-EB3 and characterized on Western blot. *A*, COS-1 cells were mock transfected or transfected with EB1, EB2, and EB3 fused to GFP. The *bottom panel* (Western blot with anti-GFP antiserum) demonstrates that each fusion protein is expressed at a similar level. The *top panel* (Western blot with the novel anti-EB3 antiserum) shows that anti-EB3 antibodies recognize full-length EB3-GFP (marked by a *double asterisk*). EB1-GFP (marked by a *single asterisk*) also is weakly recognized, whereas EB2-GFP is not. *B*, Equal amounts of whole-cell protein extract from HeLa, COS-1, and K562 cells and from mouse brain are analyzed. Two isoforms of EB3, which are expressed more abundantly in brain extracts, are recognized by the novel anti-EB3 antiserum.

sured fluorescent displacements occurring within one complete time-lapse movie within selected areas of the neuron (i.e., in different neuronal compartments). In this analysis all movements were included irrespective of how many consecutive frames they lasted. Also, each fluorescent movement within the selected area was traced to determine the average number of consecutive frames that we could follow the displacements. Percentages of forward and backward movement are expressed either relative to the total number of fluorescent movements observed or relative to the number of fluorescent MT distal ends (see Table 2). Because the values that were obtained do not differ considerably, this analysis suggests that the average duration of forward and backward displacements is similar.

Results

+TIP localization in cultured neurons

Several +TIPs have been shown to localize to the ends of a subset of MTs in fixed cultured cells in line with their plus end tracking behavior in live cells. We wanted to analyze whether a similar MT distal end localization is present in neurons, because this has not yet been described. We focused our analysis on CLIP-115 and CLIP-170, EB1 and EB3. Both CLIP-115 (De Zeeuw et al., 1997) and EB3 (Nakagawa et al., 2000) mRNAs are enriched in the CNS, making the analysis of the distribution pattern of these proteins particularly interesting. Antibodies against CLIP-115 and CLIP-170 have been described previously (Hoogenraad et al., 2000), and a commercial monoclonal antiserum against EB1 is available. To obtain EB3 localization data, we raised a novel polyclonal antiserum in rabbit. When tested on Western blot, this anti-EB3 antiserum specifically recognizes EB3-GFP in transfected COS-1 cells (Fig. 1*A, lane 3*). Transfected EB1-GFP (Fig. 1*A, lane 1*) also is recognized weakly, whereas EB2-GFP (Fig. 1*A, lane 2*) is not detected. In extracts from different cell lines and from mouse brain the novel anti-EB3 antiserum mainly recognizes two closely migrating EB3 isoforms of ~36 kDa (Fig. 1*B*), which are enriched in the brain extract as compared with the cell line lysates and likely represent the two splice forms of EB3 that have been described previously (Su and Qi, 2001). Together, these results indicate that the novel antiserum is specific for EB3.

To determine whether endogenous CLIPs associate with the ends of MTs in neurons, we incubated fixed mouse hippocampal cell cultures with antibodies against CLIP-115 or CLIP-170. However, labeling with the individual CLIP antibodies failed to demonstrate a clear plus end staining pattern in neurons, in contrast to the bright staining observed in neighboring glial cells (data not shown). We therefore attempted the staining of neurons with a mixture of the different antibodies. This labeling procedure revealed cytoplasmic labeling, most intense in cell bodies, in addition to a clear staining of comet-like dashes in cell bodies, dendrites, axons, and growth cones (Fig. 2; *arrows* highlight examples of this staining). Double labeling with anti-tubulin antibodies identified these dashes as MT distal ends (data not shown). These data indicate that endogenous CLIPs associate with MT plus ends in cultured hippocampal neurons. However, the labeling is substantially weaker than in non-neuronal cell types, suggesting that less protein is present per MT tip in neurons. This may be the main reason why plus end staining of CLIP-115 in cultured neurons was not observed previously (De Zeeuw et al., 1997).

To analyze whether EB-related proteins also associate with MT distal ends in neuronal cultures, we incubated fixed cells with a mixture of monoclonal antibodies against EB1 and the new polyclonal anti-EB3 antiserum (Fig. 2*E–G*). In these experiments colocalization is observed of EB1 (Fig. 2*E*) and EB3 (Fig. 2*F*) on comet-like dashes in glia and in neurons (merge in Fig. 2*G*). Because EB1 is a verified marker of growing MT ends in non-neuronal cells (Mimori-Kiyosue et al., 2000b), these data suggest that the same holds true for EB3. Quantification of EB1 and EB3 fluorescent intensity on comets reveals that EB1 signal intensity (expressed in arbitrary units per comet) is similar in glia and neurons (i.e., ~0.95 AU/comet), whereas EB3 signal increases from ~0.5 AU in glia to 1 AU in neurons (>1000 comets measured in three glia and four neurons). Although this quantification does not reveal the absolute levels of EB1 or EB3 in neurons and glia, the data suggest that in neurons more EB3 is associated per MT distal end than in glia.

Costaining of EB3 antiserum with monoclonal anti-β-tubulin antibodies reveals that, in those cases in which individual MTs can be distinguished within the dense MT network, the EB3-positive dashes are always located at the ends of MTs, both in neurons (Fig. 2*H*) and glia (Fig. 2*I*). In the latter example some of the MTs, which are visible, are not embedded in the MTOC. On those MTs EB3 staining is observed only at one of the two ends, which presumably represents the growing end.

Nocodazole and taxol are drugs that interfere with MT dynamics in opposing manners (for review, see Downing, 2000). Nocodazole acts by sequestering tubulin dimers, eventually causing a collapse of the MT network, whereas taxol stabilizes the MT network by specifically binding to MTs. Application of low amounts of both drugs completely abolishes the binding of +TIPs to the ends of growing MTs (Perez et al., 1999; Mimori-Kiyosue et al., 2000b; Akhmanova et al., 2001) despite the fact that MTs are still present and MT-based motors are active. The addition of low concentrations of these drugs to hippocampal cultures leaves the MT network intact, yet both EB1- and EB3-positive comets disappear (Fig. 2*J,K*; data not shown). Taken together, our results suggest that in neurons, like in non-neuronal cells, CLIPs and EB-related proteins specifically associate with the ends of growing MTs.

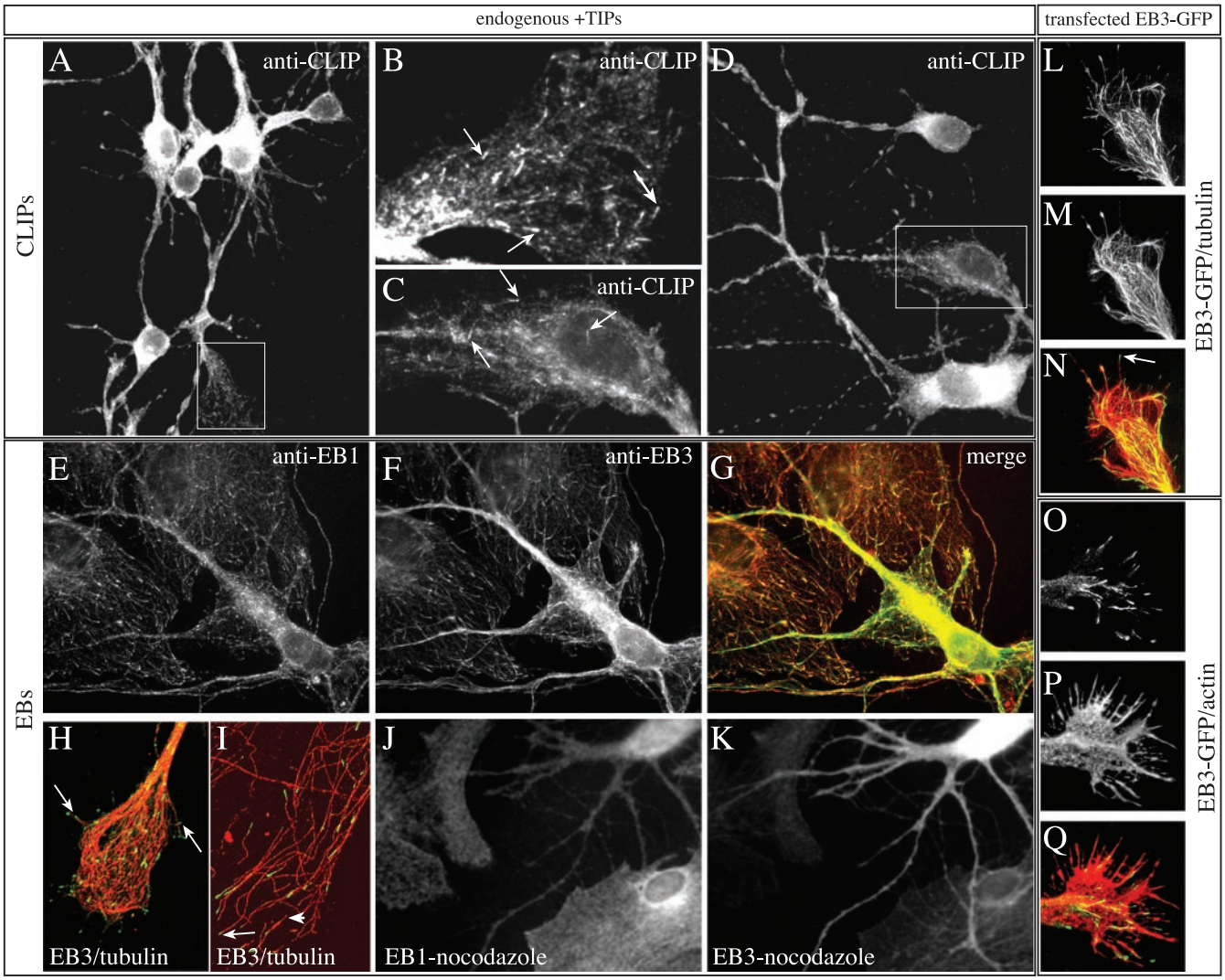

Figure 2. +TIPs in hippocampal neurons. *A–K*, Hippocampal neurons of 2–6 d in culture were fixed and incubated with a mixture of antibodies recognizing both CLIP-115 and CLIP-170 (*A–D*), with an antibody mixture recognizing EB1 and EB3 (*E–G*), with a mixture recognizing EB3 and β-tubulin (*H, I*), or with the single EB1 (*J*) and EB3 (*K*) antibodies. *B* (growth cone) and *C* (neurites) are magnifications of the *rectangles* in *A* and *D*, respectively. Examples of comet-like CLIP dashes are indicated by *arrows*. In *G* the merged image of EB1 (*E*) and EB3 (*F*) staining is shown, in which EB1 is in *red* and EB3 is in *green*. Clear comet-like labeling is visible with both antibodies in the neuron and in the two glial cells. In *H* (neuronal growth cone) and *I* (cell periphery of a glial cell) deconvolution of confocal images is used to demonstrate clearly the EB3 localization to MT distal ends. The *large arrows* in *H* and *I* indicate clear examples of such EB3 localization. The *small arrow* in *I* points toward a MT end, which is not labeled by EB3. Given that the other end of this small MT is stained, we presume that this end represents a MT minus end. The cell periphery of the glial cell in *I* is particular in that it contains several of such "free" MTs. In *J* and *K* nocodazole was added to the culture medium before fixation of the cells. Note that the typical comet-like staining of EB1 and EB3 has vanished after this brief treatment. *L–Q*, Hippocampal neurons, transfected with EB3-GFP, were fixed 3–4 d after plating and stained with cytoskeletal markers. Costaining of EB3-GFP (*L*) in a growth cone with antibodies against tyrosinated α-tubulin (*M*) reveals that the GFP signals are located at the tip of MTs (the *arrow* indicates an example of such a tip in the merged image in *N*). Costaining of EB3-GFP (*O*) in a transfected neuron with antibodies against actin, followed by Alexa 594-conjugated secondary antibody incubation (*P*), reveals that EB3-GFP-positive MT plus ends are present in the growth cone and sometimes are detected in actin-rich filopodial extensions (see merged image in *Q*).

Characterization of GFP+TIP behavior in transfected COS-1 cells

Because endogenous +TIP localization (and, by implication, function) is conserved in non-neuronal and neuronal cultures, we next set out to compare GFP+TIP behavior, focusing again on CLIPs and EB1-related proteins. On the basis of published results we inserted the GFP tag at the N terminus of the CLIPs and at the C terminus of the EB1-related proteins (Fig. 3). In the case of GFP-CLIP-170, its dynamic behavior has been described in several reports (Perez et al., 1999; Akhmanova et al., 2001; Komarova et al., 2002a), whereas in the case of EB1-GFP, experiments in live *Xenopus* A6 cells and human neuroblastoma N2A cells have documented its dynamic behavior (Mimori-Kiyosue et al., 2000b; Morrison et al., 2002). However, neither for GFP-CLIP-115 nor for EB2-GFP and EB3-GFP have live imaging studies yet been reported. We therefore first compared the behavior of all of these proteins in transfected COS-1 cells, which were analyzed under a confocal microscope 20–48 hr after transfection (Fig. 3).

For live cell imaging we studied only cells with low expression levels of the GFP fusions, but even under these conditions EB2-GFP binds all along MTs and has no preference for MT distal ends (data not shown). The other GFP+TIPs, however, all move in comet-like dashes, mainly from the presumptive MTOC to the cell periphery, consistent with their preferential association with the growing ends of MTs [see movies 1 (www.eur.nl/fgg/ch1/galjart/jon.html) and 2 (available at www.jneurosci.org) for GFP-CLIP-115 and EB3-GFP behavior, respectively; the behavior of the other fusion proteins has been published previously and is not

Protein structure	GFP-fusions	Velocities in non-neuronal cells (μm/sec) *published*	*present study*
GFP 1 1046	*GFP-CLIP 115*	——	0.48 +/- 0.07 (n=84)
GFP 1 1320	*GFP-CLIP 170*	0.21 +/- 0.05 (n=59)[1)] 0.24 +/- 0.04 (n=41)[2)] 0.27 +/- 0.1 (n=110)[3)]	0.48 +/- 0.08 (n=74)
GFP 1 268	*EB1-GFP*	0.23 +/-0.05 (n=89)[4)] 0.2 +/- 0.02 (n=22)[5)]	0.50 +/- 0.05 (n=58)
GFP 1 326	*EB2-GFP*	——	No plus end labelling
GFP 1 281	*EB3-GFP*	——	0.49 +/- 0.03 (n=49)

Figure 3. Velocities of GFP+TIP fusion proteins in non-neuronal cells. COS-1 cells, expressing the indicated GFP+TIP fusion proteins, were monitored at 37°C on a Zeiss LSM510 confocal microscope and analyzed for GFP+TIP velocities. Only cells expressing low levels of the fusion proteins were investigated. For comparison, previously published values are indicated [[1]Perez et al. (1999); [2]Akhmanova et al. (2001); [3]Komarova et al. (2002a); [4]Mimori-Kiyosue et al. (2000); [5]Morrison et al. (2002)]. MT-binding domains (*black bars*) and coiled-coil regions (*gray bars*) are indicated in the CLIPs. The microtubule-binding motif has not been identified clearly in EB1-related proteins.

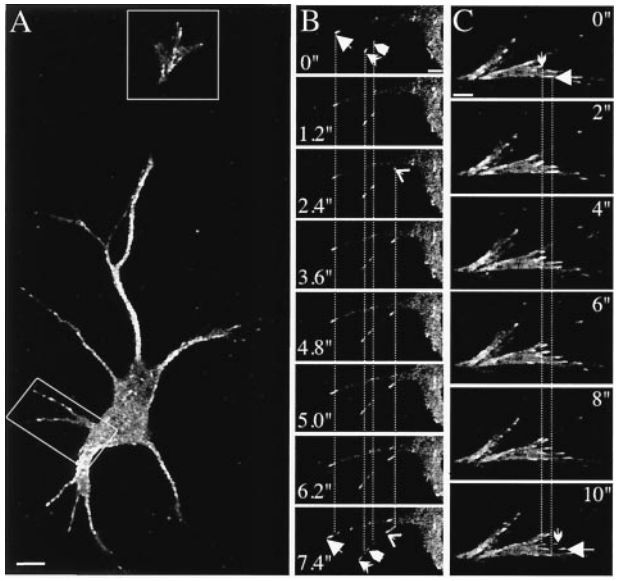

Figure 4. EB3-GFP localization in transfected hippocampal neurons. Hippocampal neurons were transfected with EB3-GFP, and live cells were analyzed 3–4 d later by confocal microscopy in a 37°C chamber. EB3-GFP comets are seen to move in all neuronal compartments. This figure contains images of movie 3 (available at www.jneurosci.org). The *rectangles* in *A* represent the areas magnified in *B* (cell body and dendrites) and *C* (growth cone). The images in *B* were acquired every 1.2 sec and every 2 sec in *C*. *Arrows* and *arrowheads* in these panels indicate the beginning and end positions of a selected number of EB3-GFP dashes. *Dotted lines* help to distinguish the movements of these dashes. The life time of the individual dashes differs, but each moves with an average velocity of ~0.2 μm/sec. Scale bars: *A*, 10 μm; *B*, 5 μm; *C*, 2 μm.

shown here]. Costaining with tubulin antibodies in fixed cells reveals that these comets represent MT distal ends, and low doses of nocodazole or taxol abolish GFP+TIPs staining at MT ends in transfected COS-1 cells (data not shown). We conclude that, of the five GFP markers that were analyzed, four (GFP-CLIP-115, GFP-CLIP-170, EB1-GFP, and EB3-GFP) faithfully label the ends of growing MTs in COS-1 cells.

The rates of GFP+TIP movement reported here (Fig. 3) are higher than values published previously (Perez et al., 1999; Mimori-Kiyosue et al., 2000b; Akhmanova et al., 2001; Komarova et al., 2002a; Morrison et al., 2002; Vaughan et al., 2002). This might be attributable to the different cell types used in some of the studies. In addition, we found that slight differences in temperature and/or in culture medium conditions affect these speeds [Fig. 3; compare GFP-CLIP-170 value in Akhmanova et al. (2001) with current value]. A similar result has been obtained by using GFP-p150^{Glued} as a plus end marker (Vaughan et al., 2002). Interestingly, the measured velocities of the different GFP fusion proteins are quite similar in transfected COS-1 cells in the current experiments (Fig. 3) despite the reportedly different functions of CLIPs and EB1-related proteins (Komarova et al., 2002b; Rogers et al., 2002; Tirnauer et al., 2002). These results indicate that at low levels of overexpression these GFP fusion proteins do not affect MT growth dynamics to a great extent.

GFP+TIP expression in mouse hippocampal neurons

Transfection of hippocampal neurons with GFP-CLIP-115, -CLIP-170, -EB1, and -EB3 yields comet-like GFP dashes in cells expressing low amounts of these proteins (Fig. 2*L,O*; data not shown). These dashes are present in all neuronal compartments, indicating that growing MTs are located throughout neurons. Importantly, the distribution of the different GFP+TIP fusion proteins is similar to that observed with the antibodies. Consistent with these data, we found that the MT plus end signal, as detected with EB3-GFP, is brighter than that detected with the other +TIP fusion proteins (data not shown).

EB1-GFP and GFP-CLIP-115 distribute along MTs at higher expression levels (data not shown). At these levels GFP-CLIP-170 aggregates in patches (data not shown), similar to its behavior in transfected non-neuronal cells (Pierre et al., 1994). We therefore concentrated on EB3-GFP for our further analysis, because this fusion protein remains associated with MT distal ends unless expressed at very high levels. Double-labeling studies in the growth cone with antibodies against tyrosinated (unmodified) α-tubulin reveal that EB3-GFP is located at distal segments of a subset of MTs (Fig. 2*L–N*; one example of MT plus end labeling by EB3-GFP is indicated with an *arrow*). We also visualized EB3-GFP dashes and actin simultaneously, using anti-actin antibodies. Both EB3-GFP-positive dashes (Fig. 2*O*) and actin-rich extensions (Fig. 2*P*) are detected clearly. Most, but not all, of the filopodial extensions in growth cones are devoid of EB3-GFP-positive comet-like dashes (Fig. 2*Q*). These data indicate not only that EB3-GFP is a faithful marker of MT plus ends but that low-level expression of the fusion protein does not influence neuronal growth cone formation to a great extent. Comparison of movements of EB3-GFP dashes in transfected COS-1 cells reveals no aberrant effect of the expressed fusion protein on MT growth rates with respect to other established MT plus end markers (Fig. 3). These data together suggest that EB3-GFP is the best suitable fusion protein for live studies of MT dynamics in transfected neurons.

To investigate growing neuronal MTs, we electroporated hippocampal neurons with EB3-GFP and examined live neurons with the confocal microscope 2–6 d later. Many moving fluorescent dashes are observed in these cells in all neuronal compartments, i.e., cell bodies, neurites, and growth cones (movie 3; available at www.jneurosci.org). Still images of EB3-GFP movements from movie 3 are depicted in Figure 4. Application of nocodazole and taxol abolishes the EB3-GFP dashes in live neurons (data not shown), again suggesting that EB3-GFP specifically associates with the ends of growing MTs.

Many of the EB3-GFP-positive fluorescent stretches in the neuronal cell body appear to move randomly (movie 3; available at www.jneurosci.org), consistent with results that use fixed neurons

Table 1. Forward and backward movement of EB3-GFP in neurons

Compartment	Dashes			EB3-GFP displacements			Displacements per dash[d]	
	n[a]	% f[b]	% b[c]	*n*	% f	% b	f	b
	Hippocampal cultures							
Proximal neurite	26	65	35	119	71	29	4.9	3.9
Distal neurite	15	87	13	55	87	12	3.7	3.5
Distal axon	9	100	0	37	100	0	4.1	
Distal axon[e]	47	83	17	137	83	17	2.9	2.9
Growth cone	7	100	0	28	100	0	4	
	PC cultures							
Proximal dendrites	54	65	35	145	64	36	2.6	2.7
Distal dendrites	51	75	25	151	74	26	2.9	3
Axon 1	20	100	0	65	100	0	3.25	
Axon 2	13	85	15	40	83	17	3	3.5

[a]Number (*n*) of dashes observed.

[b]Percentage (%) of forward (f) moving dashes.

[c]Percentage (%) of backward (b) moving dashes.

[d]EB3-GFP displacements per dash were calculated by dividing the number of displacements by the number of dashes. With an average acquisition time of 2.5 sec/frame and average velocity of 0.22 μm/sec, the average displacement per dash is ~1.65 μm.

[e]Distal axon near growth cone.

(Fig. 2). After entry into neurites the MT growth becomes restricted to the long axis and is therefore directional. Within neurites some comets touch the plasma membrane and then disappear, whereas other dashes move alongside the membrane for a number of frames. Most of the dashes move from the cell body toward the distal neurites (forward or anterograde growth); however, backward or retrograde movement (i.e., back to the cell body) is observed also. Retrograde MT growth constitutes ~35% of the total moving dashes or frames in proximal neurites of transfected hippocampal neurons (Table 1). Retrograde movements generally decline in more distal parts of the neurons (Table 1).

Behavior of EB3-GFP in differentiated Purkinje cell neurons

As an alternative to the hippocampal system we studied cerebellar PCs, because these neurons have a morphologically distinct dendritic compartment as compared with hippocampal neurons. Using immunostaining against calbindin-D28K, a marker specific for PCs in cerebellar cultures, we confirmed that healthy, viable cells with good dendritic arborizations and distinguishable axons are detectable as early as after 10 DIV (data not shown). Staining with a mixture of the three anti-CLIP antibodies indicates that these proteins are present in the cell bodies and dendrites of PCs (Fig. 5*A*,*B*). In peripheral dendrites the labeling pattern resembles the decoration of MT ends that we observed in other cell cultures (Fig. 5*B*; see *arrowheads*). MT plus end staining also is detected with EB antibodies (data not shown).

We used the SFV vehicle (Lundstrom et al., 2001b) to deliver EB3-GFP to highly differentiated PC neurons in culture. With this infection system live imaging studies of EB3-GFP movements are optimal ~5–8 hr after infection, because at later time points expression of the fusion protein becomes too high and MTs are bundled completely. At 5–8 hr after infection we observed bidirectional EB3-GFP movements in PC dendrites [Fig. 5*D*, Table 1; see also movies 4 (www.eur.nl/fgg/ch1/galjart/jon.html) and 5 (available at www.jneurosci.org)], whereas in axons most, but not all, movements are unidirectional (Fig. 5*C*; Table 1). A similar movement is detected in axons of infected hippocampal neurons of 10 DIV (movie 6; available at www.jneurosci.org). These results indicate that the directionality of EB3-GFP movements actually reflects the organization of the MT cytoskeleton in the different neuronal compartments (Baas et al., 1988, 1989).

Atypical behavior of EB3-GFP in neurons

Although most of the EB3-GFP comets move either anterogradely or retrogradely and in growth cones some dashes appear to extend into filopodia-like extensions, on rare occasions we observed pausing and/or oscillating GFP-positive dashes (see, for example, some of the EB3-GFP dashes in the growth cone in movie 3; available at www.jneurosci.org). In these cases we cannot determine whether EB3-GFP is on a pausing, shrinking, or growing MT end (which is pulled backward) because both anterograde and retrograde movements of MTs have been observed in growth cones (Dent et al., 1999).

Studies with SFV-mediated EB3-GFP delivery revealed movement of the fusion protein in highly dynamic hippocampal axons (movie 7; available at www.jneurosci.org), with a morphology strikingly similar to that of the recently described retracting axon (He et al., 2002). Some of the EB3-GFP dashes at the end of the axonal shaft of these typical axons move on curved tracks, which might represent curved and bent MTs. In addition, rapid EB3-GFP excursions into filopodia-like protrusions can be observed. In most instances the EB3-GFP signal disappears with collapse of the filopodium. We conclude that even under conditions that resemble axonal retraction EB3-GFP dashes (and, by implication, MT growth) persist.

Analysis of EB3-GFP movements

EB3-GFP dashes in neurons are observed on average for two to five frames or displacements (see average number of displacements per EB3-GFP dash in Table 1). The average number of displacements per dash is similar for forward and backward movements. For quantitation of the speed of EB3-GFP movements (and thus MT growth rates), we included only dashes that could be followed clearly for three frames or more. In electroporated hippocampal neurons the distance that these EB3-GFP dashes travel is comparable, irrespective of the compartment analyzed (Fig. 6*A*). In these neurons ~30–50% of the dashes can be followed for 2 μm (Fig. 6*A*). Taken together, the data in Table 1 and Figure 6*A* indicate that under normal culture conditions EB3-GFP movements are similar in the different neuronal compartments.

Velocities of EB3-GFP movements were calculated in electroporated hippocampal neurons and glial cells of 2–6 DIV, in in-

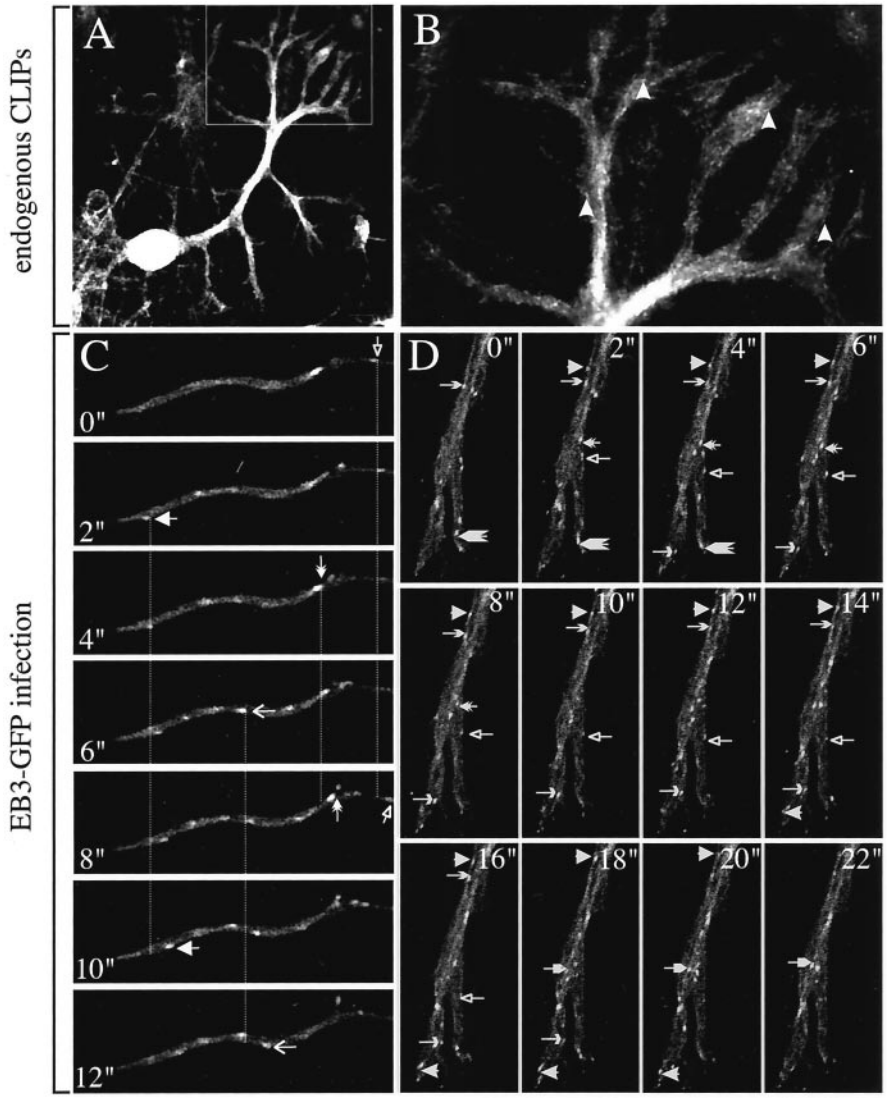

Figure 5. CLIP and EB3-GFP localizations in Purkinje cells. *A*, *B*, PC neurons of 10–17 d in culture were fixed and incubated with a mixture of antibodies recognizing both CLIP-115 and CLIP-170. *A*, The distinct initial dendritic arborization of the PCs is highly visible, indicating CLIP accumulation in this region of PCs. *B*, A comet-like labeling is visible in the more peripheral parts of the dendrite (examples of comet-like dashes are indicated by *arrowheads*). *C*, *D*, PC neurons of 10–17 DIV were infected with SFV-EB3-GFP, and the cells were analyzed 5–8 hr after infection by confocal microscopy in a 37°C chamber. *C*, Movements of EB3-GFP dashes in an axon are shown (each dash is indicated by a distinct *arrow*). Images were acquired every 2 sec. Anterograde movement of EB3-GFP dashes toward the growth cone is toward the *right*. *D*, Images (derived from movie 4; available at www.eur.nl/fgg/ch1/galjart/jon.html) demonstrate bidirectional movement of EB3-GFP dashes in dendrites (each dash is indicated by a distinct *arrow*).

fected differentiated PCs and neighboring glial cells of >10 DIV, and in the three examples of retracting hippocampal axons (10 DIV) that we observed (Table 2). As a control for the values of MT growth dynamics in neurons, obtained with EB3-GFP, we electroporated neurons with yellow fluorescent protein-tubulin but could not get transfected neurons with a recognizable fluorescent MT array (data not shown). We therefore electroporated neurons with EB1-GFP (movie 8; www.eur.nl/fgg/ch1/galjart/jon.html) and compared its behavior to that of EB3-GFP. Because EB1 and EB3 are highly similar proteins and might have similar effects on the MT network, we also wanted to transfect neurons with a reliable plus end marker that is structurally unrelated to EB3. For this we chose a mutant form of GFP-CLIP-170 (GFP-CLIP-170ΔHind), which lacks the C-terminal metal-binding motif, because studies in non-neuronal cells have shown that this domain is responsible for the formation of patches of overexpressed protein at the cell periphery (Pierre et al., 1994). When expressed in neurons, GFP-CLIP-170ΔHind does not aggregate in patches as does full-length GFP-CLIP-170 but, instead, moves in comet-like dashes (movie 9; www.eur.nl/fgg/ch1/galjart/jon.html).

The measurements show that the average velocity of EB3-GFP movement is very similar in electroporated hippocampal neurons, infected PCs, and in the single Golgi neuron taken along for evaluation (Table 2). In addition, the velocities of EB1-GFP (0.22 ± 0.07 μm/sec; 39 dashes measured) and GFP-CLIP-170ΔHind (0.25 ± 0.05 μm/sec; 35 dashes measured) in electroporated hippocampal neurons are also comparable. EB3-GFP speeds do not vary remarkably within different neuronal compartments, and there is no significant difference in average speed between comets moving in opposite directions (Table 2). The velocities measured in neurons are approximately one-half the speed of movement of EB3-GFP-labeled plus ends in COS-1 cells (compare Fig. 3, Table 1). One concern is that slight differences in the system set up and/or culture conditions might cause variations in EB3-GFP velocities in different cell types. We therefore measured velocities in neurons and glia cultured in the same chamber. EB3-GFP speeds in glia are comparable to the values derived from COS-1 cells (Table 1). These data indicate that MT growth rates are generally lower in neurons as compared with glia and COS-1 cells. However, in the three retracting axons the average velocity of EB3-GFP dashes is increased significantly as compared with normal values (Table 1; $p < 0.001$), yet it is still significantly lower than the values measured in glia (Table 1; $p < 0.001$).

In the original studies on GFP-CLIP-170 (Perez et al., 1999) and EB1-GFP (Mimori-Kiyosue et al., 2000b), the authors plotted the length of an individual comet versus the speed of movement of that particular dash. A stochastic association and dissociation behavior was detected for both GFP fusion proteins, leading to variation in the length of the individual dashes over time. Still, an increased speed of the dash generally was associated with an increased length of the comet tail. We measured average lengths and corresponding speeds of a large number of the dashes used for the calculations in Table 1 (Fig. 6*B–D*). These data suggest that an increased speed of movement, as observed in the population of EB3-GFP dashes derived from COS-1 cells and glia, correlates with an increased length of EB3-GFP staining of a MT. The average speed of the selected population of COS-1 and glial dashes is 0.49 ± 0.09 μm/sec, which corresponds to an average length of 1.14 ± 0.16 μm. For the neuronal dashes these values are 0.23 ± 0.06 μm/sec and 0.70 ± 0.11 μm, respectively.

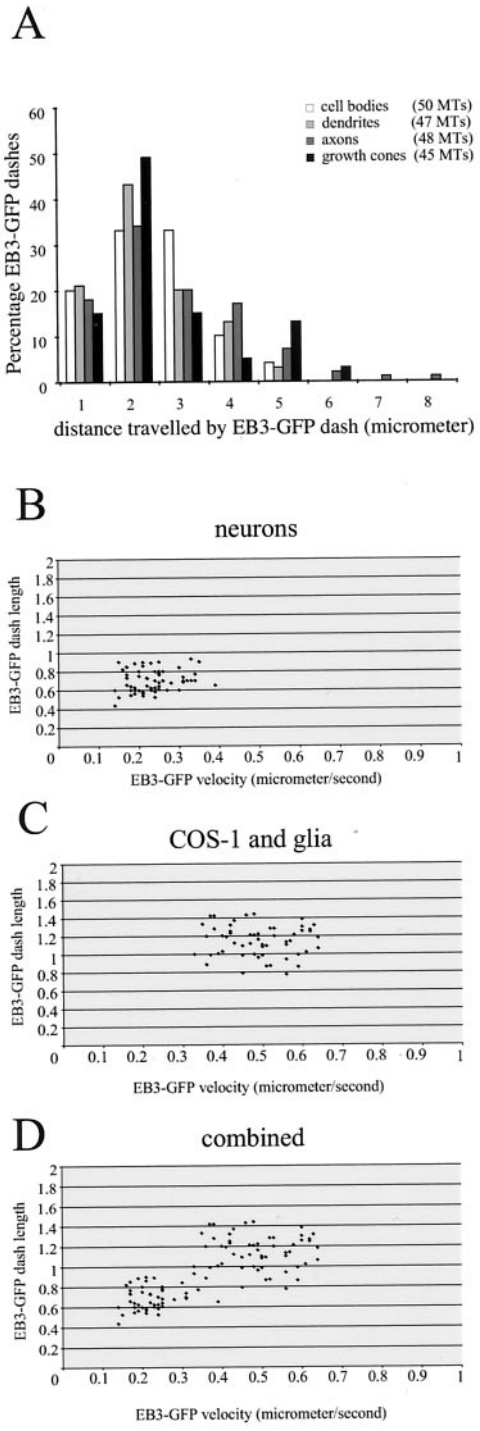

Figure 6. Distances traveled by EB3-GFP dashes in transfected neurons. *A*, Hippocampal neurons were transfected with EB3-GFP, and the cells were analyzed 3–4 d later by confocal microscopy in a 37°C chamber. The distance that individual EB3-GFP dashes could be followed was measured in different neuronal compartments (cell bodies, dendrites, axons, and growth cones). The total number of individual MTs that were counted is indicated. In all compartments the distance traveled by EB3-GFP dashes is comparable. *B–D*, The average speed and length of a selected number of EB3-GFP dashes derived from different measurements in neurons (*B*), COS-1 cells and glia (*C*), and the combined data (*D*) are plotted.

Table 2. Velocity of EB3-GFP dashes in neurons and glia

Neuronal compartment	Average velocity[a] (number of dashes measured)
Hippocampal cultures	
Cell body	0.22 ± 0.06 (64)
Neurites	0.22 ± 0.04 (52)
Neurite forward	0.22 ± 0.06 (91)
Neurite backward	0.21 ± 0.08 (20)
Growth cone	0.20 ± 0.07 (35)
Glia	0.43 ± 0.11 (63)
Retracting axons[b]	0.35 ± 0.06 (37)
PC cultures	
Dendrite forward	0.24 ± 0.07 (60)
Dendrite backward	0.26 ± 0.07 (21)
Axon forward	0.21 ± 0.04 (75)
Axon backward	0.24 ± 0.04 (8)
Cell body	0.22 ± 0.05 (20)
Golgi cell	0.28 ± 0.05 (12)
Glia	0.44 ± 0.11 (42)

[a] μm/sec ± SD.

[b] EB3-GFP velocity derived from infected hippocampal cultures.

Discussion

Here we have investigated the behavior of the distal ends of growing MTs in cultured hippocampal and Purkinje cell neurons mainly by following the movement of GFP-tagged EB3. Our conclusions are based on the assumption that EB3-GFP reliably marks the tips of growing MTs without changing MT growth parameters. Several observations support these statements. First, we show that endogenous EB3 colocalizes with the verified plus end marker EB1 at MT distal ends in cultured hippocampal neurons and glia. The MT plus end association of EB3 is confirmed further by using anti-tubulin antibodies. In contrast to the other +TIPs that have been analyzed, EB3 accumulates preferentially at neuronal plus ends with respect to glial cells, and no other intracellular structure is detected in neurons by the novel anti-EB3 antibodies. The MT plus end association of EB3 is sensitive to nocodazole and taxol, drugs that perturb MT dynamics and that have been shown to abolish MT plus end localization of several +TIPs (Perez et al., 1999; Mimori-Kiyosue et al., 2000b; Akhmanova et al., 2001). Costaining of EB3-GFP and tubulin in fixed neurons and COS-1 cells suggests that the comet-like GFP signals are located at the ends of MTs, in line with the endogenous EB3 localization. The addition of taxol and nocodazole abolishes EB3-GFP localization to MT distal ends, similar to the effect on endogenous EB3 and EB1. Furthermore, EB3-GFP, EB1-GFP, and mutant GFP-CLIP-170 show very similar behavior in transfected hippocampal neurons, suggesting that MT growth rates are not affected by low-level expression of these proteins. In a recent study MT growth rates were measured in the same cell (or cytoplast) that had been injected with fluorescent tubulin and that expressed GFP-CLIP-170 (Komarova et al., 2002a). MT growth rates (~0.30 μm/sec) were similar with the use of both fluorescent proteins, validating the use of +TIPS as markers for MT growth. Finally, a short report has appeared recently, describing the behavior of EB1-GFP in a neuroblastoma cell line (Morrison et al., 2002). Although this study is less detailed than our report, the properties and behavior of EB1-GFP in cells with neuronal features are consistent with our results in primary cultured hippocampal and PC neurons.

The average distance traveled by an EB3-GFP dash is not directly comparable to the average length of growth of an individual MT. For example, two consecutive and nearby EB3-GFP growth events that we record as separate in fact may represent a growth–pause (or slow growth)–growth event of one individual MT. Moreover, because we used a confocal imaging system for our analysis, in the neuronal cell body some of the plus ends may move in and out of focus because the thickness of the optical slice

is ~1 μm. Thus we may not capture a complete growth spurt of an individual MT in the cell body. Note that in both examples that have been mentioned the EB3-GFP-derived results underestimate the true value of the average length of an MT growth event. Thus it is likely that the latter are higher than the average distance traveled by EB3-GFP, which, on the basis of the data in Table 1 and Figure 6*A*, we estimate to be ~1–2 μm. The average length of MTs in young hippocampal neurons is ~4 μm both in minor processes and in an early axon (Yu and Baas, 1994). Although these studies were performed in rat embryonic neurons, they do correlate with our data and suggest that the movement of EB3-GFP reflects the growth of MTs in differentiating neurons.

Except in the case of retracting axons, we find that the speed of growing MTs and the average duration of growth events, as measured by the movement of EB3-GFP, are similar in all neuronal compartments, i.e., cell bodies, dendrites, axons, and growth cones. The graphs in Figure 6*B–D* indicate a correlation between length of distal MT end staining and speed of EB3-GFP movement and do not suggest the existence of more than one type of EB3-GFP movement. For example, if a significant proportion of EB3-GFP would associate with shrinking MTs, one would expect two populations of dashes to come forward in the graph in Figure 6*B*, because MT shrinking rates are higher than MT polymerization rates (Komarova et al., 2002a). Similarly, if a significant population of EB3-GFP molecules was transported by molecular motors, we also would expect to see this as a separate population in the graph, but we do not. We therefore propose that similar mechanisms underlie the dynamic association of EB3-GFP with MTs in neurons and non-neuronal cells.

Both in hippocampal neurons of 2–6 DIV and differentiated Purkinje cells we observed anterograde and retrograde movements of EB3-GFP. Most bidirectional EB3-GFP movements were detected in proximal dendrites, whereas in axons the vast majority of dashes moved toward the growth cone (with the noted exceptions). The directionality of EB3-GFP dash movement agrees with observations in rodent hippocampal neurons, in which the differentiation of the axonal and dendritic compartments is accompanied by changes in the polarity of MTs such that in (proximal) dendrites MT polarity is mixed, with approximately one-half of the plus ends distal to the cell body, whereas in axons all MTs have a plus end distal orientation (Baas et al., 1988, 1989). This is further evidence for a preferential association of EB3-GFP with the ends of growing MTs. Taken together, our data suggest that local MT polymerization occurs throughout neurons, irrespective of MT organization. These polymerization events may contribute to the formation of the MT network. However, because EB3-GFP is only a marker for growing MT plus ends, our analysis does not address the issue of movement of MT polymer in axons and dendrites or what percentage it constitutes of the MT assembly process (Baas, 1997; Chang et al., 1999; Terada et al., 2000).

In young hippocampal axons there is a shift toward shorter and longer MTs, and the total content of MTs in the early axon increases ~10-fold as compared with minor processes (Yu and Baas, 1994). As the axon grows further, MT mass increases even more. We do not find an obvious increase in the amount of EB3-GFP dashes in axons as compared with minor processes in electroporated hippocampal neurons of 2–6 DIV. This suggests that preferential MT stabilization in axons as compared with dendrites, and not increased MT polymerization frequencies, accounts for the increase in total MT polymer. Indeed it has been found that the proportion of stable, nocodazole-resistant MTs in axons is more than twice as high as that in dendrites (Baas et al., 1991) and that preferential stabilization of MTs occurs in the proximal part of axons (Baas et al., 1993). In addition, the labile MT proportion in axons is found as distinct domains at the plus ends of stable MTs (Baas and Black, 1990), and it has been shown that the plus ends of stable MTs serve as the sole nucleating structures for MTs in the axon (Baas and Ahmad, 1992). These data suggest that MT polymerization can occur on existing MTs in axons.

Using SFV-mediated EB3-GFP expression, we were able to document MT growth events in highly differentiated PC (and hippocampal) neurons, and we also recorded EB3-GFP movements in three retracting hippocampal axons. Consistent with the result that MT polymer mass does not diminish significantly in these axons (He et al., 2002), we detected EB3-GFP excursions into the growth cones of these axons, one of which was in the process of collapsing during the recording session (movie 7; available at www.jneurosci.org). Interestingly, MT growth rates are significantly higher in the three retracting axons that we observed as compared with MT growth rates under more static conditions. These increased MT growth rates must be balanced to maintain MT mass. We therefore hypothesize that MT dynamics are affected under conditions of axonal retraction, which may contribute to the curving and bending of MTs observed in these axons.

MT growth rates are determined in part by the concentration of free tubulin present in the cytoplasm of a cell. In neurons the balance of MTs versus free tubulin may be tilted in favor of the MTs such that less cytoplasmic tubulin is present than in non-neuronal cells. This may explain the lower neuronal MT growth rates we have observed. Another remarkable feat is the altered distribution of +TIPs at MT distal ends in cultured neurons versus non-neuronal cells. We have shown recently that a reduction in the levels of one of these +TIPS (i.e., CLIP-115) leads to neuronal dysfunction (Hoogenraad et al., 2002). The development of EB3-GFP as a tool for measuring MT growth rates will allow us to determine in more detail the consequences of a deletion of CLIP-115, as well as that of other +TIPs, on MT growth dynamics in mammalian neurons. This will be particularly interesting in view of the recent report that low-dose application of taxol and nocodazole abolishes the sensitivity to extracellular guidance cues of growth cones from embryonic *Xenopus* spinal neurons, whereas focal applications of these drugs cause growth cone turning without addition of the cues (Buck and Zheng, 2002).

References

Akhmanova A, Hoogenraad CC, Drabek K, Stepanova T, Dortland B, Verkerk T, Vermeulen W, Burgering BM, De Zeeuw CI, Grosveld F, Galjart N (2001) CLASPs are CLIP-115 and -170 associating proteins involved in the regional regulation of microtubule dynamics in motile fibroblasts. Cell 104:923–935.

Baas PW (1997) Microtubules and axonal growth. Curr Opin Cell Biol 9:29–36.

Baas PW, Ahmad FJ (1992) The plus ends of stable microtubules are the exclusive nucleating structures for microtubules in the axon. J Cell Biol 116:1231–1241.

Baas PW, Black MM (1990) Individual microtubules in the axon consist of domains that differ in both composition and stability. J Cell Biol 111:495–509.

Baas PW, Deitch JS, Black MM, Banker GA (1988) Polarity orientation of microtubules in hippocampal neurons: uniformity in the axon and nonuniformity in the dendrite. Proc Natl Acad Sci USA 85:8335–8339.

Baas PW, Black MM, Banker GA (1989) Changes in microtubule polarity orientation during the development of hippocampal neurons in culture. J Cell Biol 109:3085–3094.

Baas PW, Slaughter T, Brown A, Black MM (1991) Microtubule dynamics in axons and dendrites. J Neurosci Res 30:134–153.

Baas PW, Ahmad FJ, Pienkowski TP, Brown A, Black MM (1993) Sites of microtubule stabilization for the axon. J Neurosci 13:2177–2185.

Buck KB, Zheng JQ (2002) Growth cone turning induced by direct local modification of microtubule dynamics. J Neurosci 22:9358–9367.

Chang S, Svitkina TM, Borisy GG, Popov SV (1999) Speckle microscopic evaluation of microtubule transport in growing nerve processes. Nat Cell Biol 1:399–403.

Coquelle FM, Caspi M, Cordelieres FP, Dompierre JP, Dujardin DL, Koifman C, Martin P, Hoogenraad CC, Akhmanova A, Galjart N, De Mey JR, Reiner O (2002) LIS1, CLIP-170's key to the dynein/dynactin pathway. Mol Cell Biol 22:3089–3102.

de Hoop MJ, Meyn L, Dotti CG (1998) Culturing hippocampal neurons and astrocytes from fetal rat brain. In: Cell biology: a laboratory handbook, 2nd Ed (Celis JE, ed), pp 154–163. San Diego: Academic.

Dent EW, Callaway JL, Szebenyi G, Baas PW, Kalil K (1999) Reorganization and movement of microtubules in axonal growth cones and developing interstitial branches. J Neurosci 19:8894–8908.

De Zeeuw CI, Hoogenraad CC, Goedknegt E, Hertzberg E, Neubauer A, Grosveld F, Galjart N (1997) CLIP-115, a novel brain-specific cytoplasmic linker protein, mediates the localization of dendritic lamellar bodies. Neuron 19:1187–1199.

Dotti CG, Sullivan CA, Banker GA (1988) The establishment of polarity by hippocampal neurons in culture. J Neurosci 8:1454–1468.

Downing KH (2000) Structural basis for the interaction of tubulin with proteins and drugs that affect microtubule dynamics. Annu Rev Cell Dev Biol 16:89–111.

Ehrengruber MU, Lundstrom K, Schweitzer C, Heuss C, Schlesinger S, Gahwiler BH (1999) Recombinant Semliki Forest virus and Sindbis virus efficiently infect neurons in hippocampal slice cultures. Proc Natl Acad Sci USA 96:7041–7046.

Han G, Liu B, Zhang J, Zuo W, Morris NR, Xiang X (2001) The *Aspergillus* cytoplasmic dynein heavy chain and NUDF localize to microtubule ends and affect microtubule dynamics. Curr Biol 11:719–724.

He Y, Yu W, Baas PW (2002) Microtubule reconfiguration during axonal retraction induced by nitric oxide. J Neurosci 22:5982–5991.

Hoogenraad CC, Akhmanova A, Grosveld F, De Zeeuw CI, Galjart N (2000) Functional analysis of CLIP-115 and its binding to microtubules. J Cell Sci 113:2285–2297.

Hoogenraad CC, Koekkoek B, Akhmanova A, Krugers H, Dortland B, Miedema M, van Alphen A, Kistler WM, Jaegle M, Koutsourakis M, Van Camp N, Verhoye M, van der Linden A, Kaverina I, Grosveld F, De Zeeuw CI, Galjart N (2002) Targeted mutation of Cyln2 in the Williams syndrome critical region links CLIP-115 haploinsufficiency to neurodevelopmental abnormalities in mice. Nat Genet 32:116–127.

Komarova YA, Vorobjev IA, Borisy GG (2002a) Life cycle of MTs: persistent growth in the cell interior, asymmetric transition frequencies and effects of the cell boundary. J Cell Sci 115:3527–3539.

Komarova YA, Akhmanova AS, Kojima S, Galjart N, Borisy GG (2002b) Cytoplasmic linker proteins promote microtubule rescue *in vivo*. J Cell Biol 159:589–599.

Lundstrom K, Rotmann D, Hermann D, Schneider EM, Ehrengruber MU (2001a) Novel mutant Semliki Forest virus vectors: gene expression and localization studies in neuronal cells. Histochem Cell Biol 115:83–91.

Lundstrom K, Schweitzer C, Rotmann D, Hermann D, Schneider EM, Ehrengruber MU (2001b) Semliki Forest virus vectors: efficient vehicles for *in vitro* and *in vivo* gene delivery. FEBS Lett 504:99–103.

Mimori-Kiyosue Y, Shiina N, Tsukita S (2000a) Adenomatous polyposis coli (APC) protein moves along microtubules and concentrates at their growing ends in epithelial cells. J Cell Biol 148:505–518.

Mimori-Kiyosue Y, Shiina N, Tsukita S (2000b) The dynamic behavior of the APC-binding protein EB1 on the distal ends of microtubules. Curr Biol 10:865–868.

Morrison EE, Moncur PM, Askham JM (2002) EB1 identifies sites of microtubule polymerisation during neurite development. Brain Res Mol Brain Res 98:145–152.

Nakagawa H, Koyama K, Murata Y, Morito M, Akiyama T, Nakamura Y (2000) EB3, a novel member of the EB1 family preferentially expressed in the central nervous system, binds to a CNS-specific APC homologue. Oncogene 19:210–216.

Perez F, Diamantopoulos GS, Stalder R, Kreis TE (1999) CLIP-170 highlights growing microtubule ends *in vivo*. Cell 96:517–527.

Pierre P, Pepperkok R, Kreis TE (1994) Molecular characterization of two functional domains of CLIP-170 *in vivo*. J Cell Sci 107:1909–1920.

Rickard JE, Kreis TE (1991) Binding of pp170 to microtubules is regulated by phosphorylation. J Biol Chem 266:17597–17605.

Rogers SL, Rogers GC, Sharp DJ, Vale RD (2002) *Drosophila* EB1 is important for proper assembly, dynamics, and positioning of the mitotic spindle. J Cell Biol 158:873–884.

Schuyler SC, Pellman D (2001) Microtubule "plus-end-tracking proteins": the end is just the beginning. Cell 105:421–424.

Su LK, Qi Y (2001) Characterization of human MAPRE genes and their proteins. Genomics 71:142–149.

Terada S, Kinjo M, Hirokawa N (2000) Oligomeric tubulin in large transporting complex is transported via kinesin in squid giant axons. Cell 103:141–155.

Tirnauer JS, Grego S, Salmon ED, Mitchison TJ (2002) EB1–microtubule interactions in *Xenopus* egg extracts: role of EB1 in microtubule stabilization and mechanisms of targeting to microtubules. Mol Biol Cell 13:3614–3626.

Valetti C, Wetzel DM, Schrader M, Hasbani MJ, Gill SR, Kreis TE, Schroer TA (1999) Role of dynactin in endocytic traffic: effects of dynamitin overexpression and colocalization with CLIP-170. Mol Biol Cell 10:4107–4120.

Vaughan KT, Tynan SH, Faulkner NE, Echeverri CJ, Vallee RB (1999) Colocalization of cytoplasmic dynein with dynactin and CLIP-170 at microtubule distal ends. J Cell Sci 112:1437–1447.

Vaughan PS, Miura P, Henderson M, Byrne B, Vaughan KT (2002) A role for regulated binding of p150^{Glued} to microtubule plus ends in organelle transport. J Cell Biol 158:305–319.

Yu W, Baas PW (1994) Changes in microtubule number and length during axon differentiation. J Neurosci 14:2818–2829.

Chapter 6

Increased MT growth velocities in cultured neurons from CLIP-115 and CLIP-170 deficient mice

Tatiana Stepanova, Marja Miedema, Anna Akhmanova, Frank Grosveld and Niels Galjart

Summary

CLIP-115 and CLIP-170 are two related, microtubule binding proteins that involved in the regulation of microtubule dynamics and the action of the dynein-dynactin motor complex. In human, the gene encoding CLIP-115 is located within a region that is hemizygously deleted in patients with the neurodevelopmental disorder called Williams Syndrome. In mice haploinsufficiency for the CLIP-115 gene mimics features of Williams Syndrome, including a mild growth deficiency, brain abnormalities, hippocampal dysfunction and particular deficits in motor coordination. CLIP-170 deficient mice also show behavioural problems, indicating that CLIP-115 and -170 play important and unique roles in neuronal functioning. However, recent studies in CHO cells have shown that these proteins have redundant roles as rescue factors, acting in the cytoplasm to prevent microtubules from shrinking all the way back to the centrosome. Here, we show that MT dynamics is affected in neurons, but not in glia, derived from single CLIP-115 or CLIP-170 knock out mice. MT growth rates are increased in ~1.5 fold and the length of MT growth events is greater in neurons from CLIP knock out mice. We propose that this is due to an altered MT-tubulin balance in these cells, with a higher free tubulin concentration leading to increased MT growth rates. Thus, CLIP-115 and CLIP-170 have non-redundant roles in the regulation of MT dynamics in cultured neurons, implicating MT defects in the pathogenesis of Williams Syndrome (WS).

Introduction

The cytoskeleton is a network of intracellular protein filaments, which construct and maintain cellular architecture. The cytoskeleton can be extremely dynamic and is constantly remodelled [1]. Microtubules (MTs) are one of the three types of the cytoskeleton, together with actin and intermediate filaments. MTs are essential for cell division, cell migration, vesicle transport and cell polarity [2]. MTs are constructed from heterodimeric α- and β-tubulin subunits, which form protofilaments in a head-to-tail arrangement. The 13 protofilaments composed a polar tubular structure. Each MT has a fast growing "plus" end and slow growing "minus" end. In fibroblast-like cells, MTs are nucleated at the MT-organising centre (MTOC), which contains γ-tubulin and associated proteins. In most cases, minus ends remain embedded to the MTOC, while plus end grow into cytoplasmic space. In essence, with MT minus ends bound to the MTOC, MT dynamics is determined mostly at plus ends, which can undergo rapid bouts of subunit addition, followed by depolymerization. For example, in CHO cells it has been determined that MTs grow persistently all the way to the membrane [3]. Once the MTs reach the membrane, they significantly slow their growth velocity, because they encounter a physiscal barrier [4]. This highly increases their chances of undergoing a catastrophe, i.e. the switching from growth to shrinkage.

Neurons represent an enigmatic type of cells with respect to MT dynamics. Of all MTs, which are present throughout the whole cell, including axons, dendrites and growth cones, only few are attached to the centrosome, which is present in the cell body. The majority of MTs are either released from the MTOC and tightly packed in the axons and dendrites, or locally synthesized. In dendrites MTs are orientated in a "bipolar" manner, with about 50% of the MT plus ends directed towards the cell body and about 50% to the proximal part of the neuron [5]. In contrast, axonal MTs are uniformly polarized, with virtually all plus ends pointing towards the growth cone [5]. The questions of how the MT network reorganizes itself within neurons and how MT minus ends are stabilized has intrigued scientists for a long time [6, 7].

Depending on certain signals (e.g. the cell membrane), MTs undergo phases of growth, pause and shrinkage [8]. The switching between these states, which is referred to as

dynamic instability is one of the most important characteristics of MTs. This rearrangement of the MT network allows it to explore the three-dimensional cytoplasmic space. Proteins that regulate MT dynamics, have been identified and fall into two main classes [9], [10], [11], [12]. Stabilizing factors, such as the classical MAPs and XMAPs promote MT growth by reducing the catastrophe frequency and destabilizing factors, such as OP18/Stathmin family proteins and Kin 1 kinesins destabilize MTs by increasing the catastrophe rate. Proteins that are mentioned above localize along the MTs and are not limited to the MT ends.

Recent data have revealed a heterogeneous population of microtubule-binding proteins that accumulates mainly at the distal ends of polymerizing MTs [13]. Such localization is ideally suited for the regulation MT dynamics. MT plus end binding proteins, also called plus end-tracking proteins (+TIPs), are able to "surf" the dynamic ends of MTs [14]. EB1 [15], EB3 [16], APC [17], CLASP2 [18], LIS1 [19, 20], CLIP-170 [3, 21], CLIP 115 [3, 22] and the dynactin complex [23], have recently emerged as MT binding proteins that have been observed to be present on the MT plus ends. It has been shown that, tip1p, the CLIP-170 homologue from yeast, is involved in regulation of MT dynamics. In wild-type fission yeast MTs that touch the cell cortex near the middle of the cell, do not undergo catastrophe but continue growth and curve along the cortex toward the cell tip, when tip1p is present, but they do undergo catastrophe when tip1p is absent [24]. Thus, in tip1p-deficient cells, shorter MTs are present. The fact that in absence of Tip1p the catastrophe frequency specifically increases in certain cell regions, suggests that Tip1p could be an anti-catastrophe factor, which delays MT catastrophe until MTs have grown into cortical regions of cellular poles [24]. There are several possibilities to explain how this protein affects MT catastrophe. For instance Tip1p can keep the MT tip in an open sheet conformation, which is thought to prevent catastrophe [25], or it can inhibit the binding of catastrophe-inducing factors, or recruit catastrophe inhibiting factors [24]. Recently, a direct interaction was shown to exist between mal3p (the fission yeast homologue of the +TIP EB1) and tip1p and it was shown that mal3p suppresses catastrophes [26]. It is possible that this interaction prevents the premature catastrophes of MTs in central regions of the cell in wild type fission yeast. Interestingly, a deletion mutant of tip1p, which lacks the metal-binding motif at the C-terminus, is able to rescue the premature catastrophe phenotype in tip1p-deficient cells [24].

Since Tip1p is the fission yeast homolog of CLIP-170 (notably, the tip1p deletion mutant that is able to rescue MTs in central regions of the fission yeast cell resembles CLIP-115), it was interesting to find out whether CLIPs can have a similar influence on MT dynamics i.e. be anti-catastrophe factors, in mammalian cells. As mentioned above, it was shown that in CHO cells MTs grow almost continuously from the centrosome to the cell periphery. Once in the periphery MTs become especially dynamic and frequent rescues prevent them from complete shrinkage to the centrosome [27]. In order to keep MT growth persistent, CHO cells have low catastrophe frequency in the cytoplasm and high rescue frequency and rapid growth velocity. Studies of MT dynamics in mammalian cells suggest that CLIP-170 and CLIP-115 may play a similar role as tip1p in fission yeast [27]. By removing both CLIPs from MT ends, using a dominant negative CLIP-170Δ head mutant, it was shown that MT rescue frequency decreased seven fold, resulting in MTs shortening all the way back to the centrosome. The other parameters of dynamic instability such as velocities of MT growth or shortening and catastrophe frequency were not changed. These studies suggest that CLIPs act as rescue factors, or that they recruit a factor, which provokes MT rescue [27]. Interestingly, rescue in the cytoplasm is restored by expression of the head domain of the CLIPs, which contains a conserved MT binding motif. Since both CLIPs contain such motifs, they are in principle redundant factors with respect to promoting MT rescue. In fission yeast it was shown that a region including this motif (the CAP-GLY domain) is sufficient for interaction of tip1p with mal3p [26]. Could it be that overexpresion

of the MT binding motif of the CLIPs in CHO cells recruits EB1 to shrinking MTs and induces rescue?

Williams Syndrome (WS) is a neurodevelopmental disorder, which is caused by the hemizygous deletion of a region (the WS Critical Region, or WSCR) of approximately 1.6 Mb on chromosome band 7q11.23 [28]. In man the CYLN2 gene, which encodes CLIP-115, is located in the WSCR [29, 30] . Besides CYLN2, the WSCR contains at least 17 other genes, including those encoding syntaxin 1A, elastin and LIM kinase 1. In mice, Cyln2 is located at the telomeric end of chromosome 5 [31] in an area orthologous to human chromosome 7q11.23 [32]. Recently, we published that targeting of the Cyln2 gene in mice leads to neuronal dysfunction [33]. We documented defects including mild growth deficiency, brain abnormalities, hippocampal dysfunction and particular deficits in motor coordination [33]. It is remarkable that these features partially mimic those of WS patients. Importantly, they were observed in heterozygous CYLN2-knock out mice, indicating that haploinsufficiency for CYLN2 is linked to neurodevelopmental features of WS [33]. Studies on primary fibroblasts from CLIP-115 knock out mice revealed that absence of CLIP-115 did not significantly change MT dynamics. This corresponds with results, performed on CHO cells, where CLIP-115 and –170 have redundant functions with respect to MT dynamics.

CLIP-170 has been shown to exist as different isoforms [34], among which is a form called restin [35, 36]. The gene encoding CLIP-170 is therefore mostly called RESTIN (RSN), instead of CYLN1. Interestingly, whereas in man CYLN1 is located on chromosome 12, in mice the gene is located quite near to Cyln2 on chromosome 5. Current ENSEMBL predictions show a distance of approximately 10 megabases between Cyln1 and -2. Cyln1 is outside of the region, which is syntenic to the WSCR in human. Recently, we have made CLIP-170 deficient mice, which show no obvious phenotype, but for a severely decreased fertility in male mice (Akhmanova et al, manuscript in preparation) and mild behavioural abnormalities.

In order to understand how the reduced levels of CLIP-115 might contribute to the neurological phenotype of WS, we were interested in studying MT dynamics in cultured hippocampal neurons from CLIP-115 and CLIP-170 deficient mice. A priori, we were not expecting differences compared to wild type neurons, due to the redundant roles of the CLIPs in fibroblast-like cells. Here, however, we document a significant increase in MT growth rates in neurons from both of the single deficient CLIP knock out mice. We suggest that lack of either one of the CLIPs results in an altered MT balance in neurons. A higher free tubulin concentration in combination with lower amounts of MTs might explain the observed increase in MT growth rates.

Materials and methods

Neuronal cultures

The generation of CLIP-115 knock out mice was described earlier [33]. The generation of CLIP-170 knock out mice will be described elsewhere in detail (Akhmanova et al, manuscript in preparation). For the current study, we obtained embryos of E17.5 from timed matings of homozygous male and female CLIP-115, or CLIP-170 knock out mice. Genotypes were determined by Southern-blot or PCR analysis. Mouse hippocampal neurons and Purkinje cells were established from the knock out embryos, or from wild type C57/bl6 or fvb mice, as described earlier [16].

Antibodies and immunocytochemistry

The cultured neurons were fixed with methanol/paraformaldehyde and stained with different antibodies (the CLIP-115 and -170 specific antisera (2221; 2238 and 2360); EB3 rabbit

polyclonal antibodies (02-1005-07); monoclonal antibodies against EB1 (Transduction Laboratories), actin (Chemicon), acetylated alpha-tubulin, tyrosine alpha-tubulin and beta-tubulin (Sigma)) as described previously [16]. FITC-conjugated goat-anti-rabbit (Nordic Laboratories) and Alexa 594-conjugated goat anti-mouse (Molecular Probes) were used as secondary antibodies. Signals were captured as described previously [16]. Images were acquired using either a Leica DMRBE microscope, with a 100x oil immersion lens (NA 1.3) and a Hamamatsu C4880 camera, or a Zeiss LSM510 confocal microscope with a 63x oil immersion lens (NA 1.4).

Live cell imaging

To visualize MT growth rates in neurons, we expressed EB3-GFP as a marker. This fusion protein was not only chosen because of its excellent marking of the tips of growing MTs, but also because its presence in a neuron at low expression levels does not appear to disturb neuronal growth and differentiation in culture [16]. To introduce EB3-GFP into hippocampal neurons of 6-8 days DIV and into Purkinje cells of 14 days DIV, we used Semliki Forest Virus (SFV) particle-mediated infection, as described earlier [16]. Infected neurons were analyzed at 37 ^{0}C on a Zeiss LSM510 confocal laser-scanning microscope as described previously [16]. Images of GFP-TIP movements in transfected cells were acquired every 1-3 sec. Images were recorded and movies were assembled using LSM 510 software.

Calculation of MT growth parameters

After recording a time-lapse movie, we visually inspected the EB3-GFP dashes that could be followed for at least three consecutive frames. All measurements were performed on different areas of cultured neurons. The velocities of the EB3-GFP dashes were calculated by dividing the distance travelled by a dash, by the time spent travelling. The average duration of MT growth events in neurons from both knockouts and control mice was estimated.

Results

Immunocytochemistry on fixed preparations of CLIP deficient neurons

In a previous paper we demonstrated for the first time that several +TIPs localise not only to the distal ends of MTs in fixed neuronal preparations, but that they also are observed as fluorescent dashes in living neurons [16]. The latter are likely to represent the ends of growing MTs. A recent report completely supports our data, demonstrating movement of MT plus ends in the axonal shaft by expressing GFP-EB1 in Xenopus embryo neurons in culture [37]. Immunostaining of cultured neurons from single CLIP-115 and -170 knock out mice with specific polyclonal antibodies against either CLIP shows that in each knock out disappearance is observed of the particular MT end staining (data not shown). In contrast, co-staining with anti-tubulin and anti-EB antibodies reveals that MT plus ends are present throughout all neuronal compartments of each knock out genotype (data not shown). Removal of either of the respective CLIPs does not cause any obvious morphological alteration in cultured neurons, in terms of tubulin or actin staining.

Interestingly, enhanced accumulation of CLIP-170 and dynactin, was seen at MT ends of primary fibroblasts from CLIP-115 deficient mice [33], suggesting that CLIP-115 and –170 normally compete for binding to MT plus ends. It was suggested that in normal fibroblast-like cells the cytoplasmic concentration each of the CLIPs is in large excess of the total amount of available plus-end binding sites, so that when one of the CLIPs is absent, the other one can occupy more binding sites. We were interested whether a competition occurs between +TIPs for plus end binding in neurons. Data obtained from the immunocytochemical experiments,

however, did not demonstrate any accumulation of CLIPs, dynactin or EBs on the distal ends of neuronal MTs in primary cultures from knockouts (data not shown).

MT growth rates in CLIP deficient neuron

The hypothesis that CLIPs compete for binding to MT growing ends [33] and play redundant roles as rescue factors in MT dynamics in CHO cells [27], raised our interest in studying MT dynamics in neurons and glia of CLIP-115 and CLIP-170 knock out animals. The main question was whether the absence of either one of those proteins affects MT dynamics in terms of growth velocity. We therefore expressed the EB3-GFP fusion protein as a marker for growing MT ends, in cultured hippocampal neurons. Strikingly, we found a remarkable and statistically highly significant increase ($P<0.0001$) of ~1.5 fold in MT growth velocities in neurons derived from either the CLIP-115 or the CLIP-170 knock out mice, as compared to wild type mice (see Table I). Three observations strongly suggest that this increase reflects a physiological change in MT dynamics in the CLIP-deficient neurons. First, the increase is measured in knock out neurons only, whereas in knock out glia from the same culture dish (**Play movie 1)** the MT growth rates are comparable to those in glia of wild type mice. Second, we tested whether differences in the genetic background of different mouse strains influenced MT growth rates, but found that wild type neurons and glia from FVB mice had virtually identical values as c57/bl6 mice (Table I). Third, MT growth rates in glia and wild type neurons are identical to our previous report [16]. Interestingly, when Purkinje cells of CLIP-115 deficient mice were tested, we found the same increase as in hippocampal neurons, suggesting a pan-neuronal effect of the lack of CLIPs.

	hippocampal neurons	Purkinje Cells	glia
wild type (FVB)	0.22+/-0.05 (n=88, 14 cells)	0.23+/- 0.05 (n=58, 9 cells)	0.43+/-0.11 (n=63, 10 cells)
wild type (c57/bl6)	0,23+/-0,03 (n=54, 9 cells)	n.d.	0.41+/- 0.02 (n=26, 5 cells)
CLIP-115 knock out	0.32+/-0.04 (n=81, 15 cells)	0.31+/- 0.03 (n= 15, 5 cells)	0.41+/-0.05 (n=44, 8 cells)
CLIP-170 knock out	0.33+/-0.05 (n=88, 11 cells)	n.d.	0.42+/-0.07 (n=64, 13 cells)

Table I. MT growth rates in cultured neurons and glia.
Average velocities (micrometer/sec.) of EB3-GFP fusion protein in neurons and glial cells from wild type and both knock outs of CLIP mice. Cells, expressing EB3-GFP, were monitored at 37C on Zeiss LSM 510 confocal microscope and velocities were analyzed (n- total number of MTs, n.d. - not determined). Standard deviations are indicated.

Average growth velocities are calculated by dividing the distance that one EB3-GFP dash travels, by the time one can follow this dash and taking the average of multiple dashes in a number of cells (Table I). When these two parameters are plotted against each other (Fig. 1A), two features stand out. First, in the knock out neurons many of the fluorescent dashes can be followed for longer periods of time than in wild type neurons, indicating that a substantial fraction of MT growth events in knock out cells last longer. Second, irrespective of the genotype of neurons, there is a good correlation between distance of movement (plotted as length, y-axis) and the duration of movement (plotted as time, x-axis), indicating that all dashes move with a similar speed, even the ones that can be followed for a longer time.

A

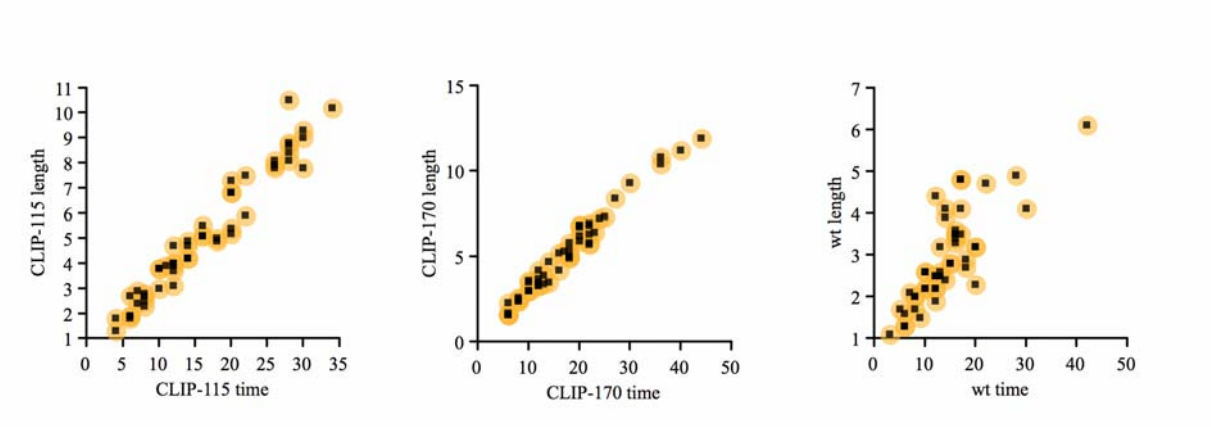

B

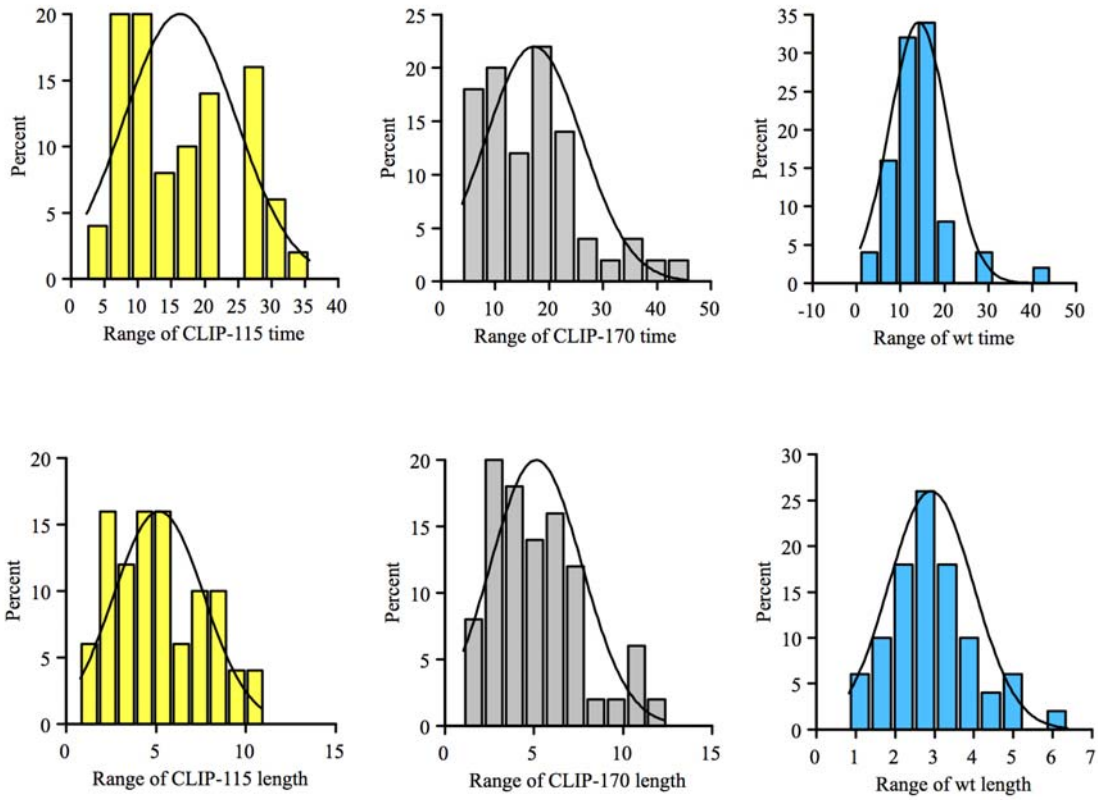

Fig.1 Comparison of MT growth events in neurons of different genotypes.
Hippocampal neurons expressing EB3-GFPwere analyzed by confocal microscopy in a 37C chamber. The distances that individual EB3-GFP dashes could be followed, were measured, independently of compartments, in neurons from wild type and knock out mice. (**A)** The correlation between distance of movement (plotted as length (micrometers), y-axis) and the duration of movement (plotted as time (sec), x-axis). (**B**) The duration of growth events (plotted as "range of time") and their distance (plotted as "range of length") are represented in a histogram of distribution versus probability.

When duration (plotted as "range of time") and distance (plotted as "range of length") of EB3-GFP dashes are represented in a histogram of distribution versus probability (Fig. 1B), the difference between the narrow range in wild type neurons and the much wider range in

knock out cells is clear. This is reflected by the "normal distributions" of time (see curves in upper panel of Fig. 1B), which have a similar midpoint peak in the three genotypes, but are much broader in CLIP-deficient cells. Interestingly, in CLIP-115 neurons two peaks appear to be present with a midpoint at ~9 seconds and at ~25 seconds. Taken together the data strongly suggest that many parameters of MT dynamics are altered in single CLIP-deficient knock out neurons.

Discussion

Here we have described the cellular phenotype in cultured neurons from single CLIP-115 and CLIP-170 knock out mice, which were generated in our laboratory. Cultured hippocampal neurons and Purkinje cells from CLIP knock out animals were developing and differentiating properly, showing no obvious morphological differences compared to control neurons. Since it was proposed that both CLIPs play an important, yet redundant, role in MT dynamics and CLIP-115 knock out mice have an interesting neurological phenotype, which might be related to WS [33], we were interested in studying MT dynamics in neurons from both single CLIP knock out animals.

It was shown previously that velocities of MT growth in normal neurons (~0.20 micron/sec) do not vary in different compartments of the cell [16]. The MT growth behaviour in retracting axons, during growth cone collapse represents a notable exception to normal MT dynamics in neurons [16]. We observed intensive MT growth in retracting axons and, surprisingly, we found that the MT growth rates were significantly higher compared to parameters from "static" axons. During axonal retraction, MTs undergo both reconfiguration and depolymerization, in addition to growth. Since the growth rate of MTs is dependent on the concentration of free tubulin molecules in the cytoplasm, the balance between free cytoplasmic tubulin and the polymeric form is one of the important parameters for MT growth rate and persistence. If in a retracting growth cone, there is more MT depolymerisation than elsewhere in the neuron, there is a local increase of cytoplasmic tubulin concentration, which might lead to enhanced MT polymerization velocities in retracting axons. We propose that an altered MT-tubulin balance also underlies the change in MT growth rates in neurons from CLIP-deficient mice.

Studies in CHO cells have shown that CLIPs play a role as rescue factors in the cytoplasm, where they mediate the transition from shrinkage to growth [27]. Consequently, in normal CHO cells, only a short part of the MT will depolymerise, before being rescued by CLIP (and interacting factors). In CHO cells the removal of both CLIPs from MT tips leads to the complete depolymerization of MTs to the MTOC [27]. It is possible that in CLIP knock out neurons an increased, persistent MT depolymerization occurs, caused by the absence of one of the CLIPs, which enlarges the cytoplasmic pool of free tubulin and results in the increase of polymerization speed of MTs. Because the chance of a catastrophe is inversely correlated to MT growth velocity [4], an increased MT growth velocity should be accompanied by increased time and length of MT growth events, that is, if no barriers, such as membranes, are encountered in the growth spurt. This is exactly what we find: increased MT growth rates are accompanied by longer growth spurts in neurons from the CLIP-deficient mice.

MT growth velocities in glial cells of knock out animals were not changed compared to wild type. These data correspond to our results involving MT growth rate studies on fibroblasts, where lack of CLIP-115 did not affect MT growth velocities [33]. We do not detect different growth rates either in primary fibroblasts from CLIP-170 knock out mice (data not shown). Thus, fibroblasts and glial cells act alike when single CLIPs are removed.

CLIP-115 and –170 are redundant MT rescue factors in CHO cells [27], so why does the removal of one of the CLIPs influence MT growth velocities specifically in neuronal cells, but not in fibroblasts-like cells? Several explanations could account for this fact, which are not mutually exclusive. First, there is variation in types and amounts of +TIPs in glia, fibroblasts and hippocampal neurons. CLIPs appear to be more abundant in glia than in neurons, while for EB3 the reverse is the case [16]. EB1 is equally expressed in glia and hippocampal neurons. Interestingly, differentiated Purkinje cells contain absolutely no EB1, but express EB3 instead (data not shown). A higher level of CLIPs in glia and fibroblasts indicates that absence one of the CLIP can be compensated for by the other. In neurons, the levels of each CLIP might be too low to allow compensation. We suggest that in neurons, MTs are not rescued frequently enough and undergo depolymerization from their plus ends. This leads to an increased level of free tubulin in cytoplasm.

The second explanation has to do with the way MTs are organized in different cell types. In dividing cells, interphase MTs are anchored at the centrosome by minus ends and their plus ends are directed to the cell periphery. Thus, MT dynamics is regulated at the plus end, by dynamic instability (one could also state that the MTOC is a major regulator of MT dynamics by eliminating the minus end pathway). However, in many terminally differentiated cells, like neurons [5] or epithelial cells [38] MTs are not bound to the centrosome and are distributed in the cytoplasm, including axons and dendrites**.** It is not clear yet how MTs elongate in the latter compartments and how neurons maintain total MT mass, which increases tremendously during development. In our previous work we observed events of MT growth in all neuronal compartments and at different stages of development with velocities and number of MT growth events being similar and not depending on stage of differentiation [16]. We proposed that local MT polymerization takes place throughout neuronal cells. During development stabilization of MTs in particular compartments might cause the accumulation in total MT polymer [39]. It has been shown that MT nucleation in neurites occurs exclusively on already existing, stable MTs [40]. If shrinking MTs are rescued in lesser frequency in CLIP-deficient neurons, they shrink further back and eventually eliminate part of the pool of MT nucleation sites in axons and dendrites. This leads to a decreased amount of MTs and, consequently, increased tubulin levels. This, in turn, results in higher MT growth rates and increased growth duration times. Finally, it could be that in neurons the minus end pathway also plays a role in sustaining normal MT-tubulin ratios, by providing free tubulin through depolymerization from selective minus ends. If this pathway is altered in CLIP-deficient neurons, it might also contribute to increased tubulin levels.

If the compensation theory is correct, than removal of both CLIPs in fibroblasts is expected lead to increased MT growth rates. However, in CHO cells where both of CLIPs were removed from MT plus ends, no differences in MT growth velocity were documented [27]. We hypothesize that in this type of cells, more frequent formation of new MTs occurs at the centrosome, so that the MT balance is maintained. In neurons, such compensation can not occur, because the most MT synthesis does not originate at the MTOC.

References

1. Bloom, K., *Microtubule cytoskeleton: navigating the intracellular landscape.* Curr Biol, 2003. **13**(11): p. R430-2.
2. Gundersen, G.G., *Evolutionary conservation of microtubule-capture mechanisms.* Nat Rev Mol Cell Biol, 2002. **3**(4): p. 296-304.

3. Komarova, Y.A., I.A. Vorobjev, and G.G. Borisy, *Life cycle of MTs: persistent growth in the cell interior, asymmetric transition frequencies and effects of the cell boundary.* J Cell Sci, 2002. **115**(Pt 17): p. 3527-39.
4. Dogterom, M. and B. Yurke, *Measurement of the force-velocity relation for growing microtubules.* Science, 1997. **278**(5339): p. 856-60.
5. Baas, P.W., et al., *Polarity orientation of microtubules in hippocampal neurons: uniformity in the axon and nonuniformity in the dendrite.* Proc Natl Acad Sci U S A, 1988. **85**(21): p. 8335-9.
6. Hirokawa, N., Terada, S., Funakoshi, T., and Takeda, S., *Slow axonal transport: the subunit transport model.* Trends Cell Biol., 1997. **7**: p. 384-388.
7. Baas, P.W.a.B., A. Trends Cell Biol. 7, 380-384. [Medline], *Slow axonal transport: the polymer transport model.* Trends Cell Biol., 1997. **7**: p. 380-384.
8. Desai, A. and T.J. Mitchison, *Microtubule polymerization dynamics.* Annu Rev Cell Dev Biol, 1997. **13**: p. 83-117.
9. Cassimeris, L., *Accessory protein regulation of microtubule dynamics throughout the cell cycle.* Curr Opin Cell Biol, 1999. **11**(1): p. 134-41.
10. Andersen, S.S., *Spindle assembly and the art of regulating microtubule dynamics by MAPs and Stathmin/Op18.* Trends Cell Biol, 2000. **10**(7): p. 261-7.
11. McNally, F.J., *Microtubule dynamics: Controlling split ends.* Curr Biol, 1999. **9**(8): p. R274-6.
12. Walczak, C.E., *Microtubule dynamics and tubulin interacting proteins.* Curr Opin Cell Biol, 2000. **12**(1): p. 52-6.
13. Galjart, N. and F. Perez, *A plus-end raft to control microtubule dynamics and function.* Curr Opin Cell Biol, 2003. **15**(1): p. 48-53.
14. Carvalho, P., J.S. Tirnauer, and D. Pellman, *Surfing on microtubule ends.* Trends Cell Biol, 2003. **13**(5): p. 229-37.
15. Mimori-Kiyosue, Y., N. Shiina, and S. Tsukita, *The dynamic behavior of the APC-binding protein EB1 on the distal ends of microtubules.* Curr Biol, 2000. **10**(14): p. 865-8.
16. Stepanova, T., et al., *Visualization of microtubule growth in cultured neurons via the use of EB3-GFP (end-binding protein 3-green fluorescent protein).* J Neurosci, 2003. **23**(7): p. 2655-64.
17. Mimori-Kiyosue, Y., N. Shiina, and S. Tsukita, *Adenomatous polyposis coli (APC) protein moves along microtubules and concentrates at their growing ends in epithelial cells.* J Cell Biol, 2000. **148**(3): p. 505-18.
18. Akhmanova, A., et al., *Clasps are CLIP-115 and -170 associating proteins involved in the regional regulation of microtubule dynamics in motile fibroblasts.* Cell, 2001. **104**(6): p. 923-35.
19. Coquelle, F.M., et al., *LIS1, CLIP-170's key to the dynein/dynactin pathway.* Mol Cell Biol, 2002. **22**(9): p. 3089-102.
20. Sapir, T., M. Elbaum, and O. Reiner, *Reduction of microtubule catastrophe events by LIS1, platelet-activating factor acetylhydrolase subunit.* Embo J, 1997. **16**(23): p. 6977-84.
21. Perez, F., et al., *CLIP-170 highlights growing microtubule ends in vivo.* Cell, 1999. **96**(4): p. 517-27.
22. Hoogenraad, C.C., et al., *Functional analysis of CLIP-115 and its binding to microtubules.* J Cell Sci, 2000. **113**(Pt 12): p. 2285-97.
23. Vaughan, K.T., et al., *Colocalization of cytoplasmic dynein with dynactin and CLIP-170 at microtubule distal ends.* J Cell Sci, 1999. **112**(Pt 10): p. 1437-47.
24. Brunner, D. and P. Nurse, *CLIP170-like tip1p spatially organizes microtubular dynamics in fission yeast.* Cell, 2000. **102**(5): p. 695-704.
25. Chretien, D., S.D. Fuller, and E. Karsenti, *Structure of growing microtubule ends: two-dimensional sheets close into tubes at variable rates.* J Cell Biol, 1995. **129**(5): p. 1311-28.
26. Busch, K.E. and D. Brunner, *The microtubule plus end-tracking proteins mal3p and tip1p cooperate for cell-end targeting of interphase microtubules.* Curr Biol, 2004. **14**(7): p. 548-59.
27. Komarova, Y.A., et al., *Cytoplasmic linker proteins promote microtubule rescue in vivo.* J Cell Biol, 2002. **159**(4): p. 589-99.
28. Francke, U., *Williams-Beuren syndrome: genes and mechanisms.* Hum Mol Genet, 1999. **8**(10): p. 1947-54.
29. Hoogenraad, C.C., et al., *The murine CYLN2 gene: genomic organization, chromosome localization, and comparison to the human gene that is located within the 7q11.23 Williams syndrome critical region.* Genomics, 1998. **53**(3): p. 348-58.
30. Osborne, L.R., et al., *Identification of genes from a 500-kb region at 7q11.23 that is commonly deleted in Williams syndrome patients.* Genomics, 1996. **36**(2): p. 328-36.
31. Tassabehji, M., et al., *Williams syndrome: use of chromosomal microdeletions as a tool to dissect cognitive and physical phenotypes.* Am J Hum Genet, 1999. **64**(1): p. 118-25.

32. Valero, M.C., et al., *Fine-scale comparative mapping of the human 7q11.23 region and the orthologous region on mouse chromosome 5G: the low-copy repeats that flank the Williams-Beuren syndrome deletion arose at breakpoint sites of an evolutionary inversion(s).* Genomics, 2000. **69**(1): p. 1-13.
33. Hoogenraad, C.C., et al., *Targeted mutation of Cyln2 in the Williams syndrome critical region links CLIP-115 haploinsufficiency to neurodevelopmental abnormalities in mice.* Nat Genet, 2002. **32**(1): p. 116-27.
34. Griparic, L. and T.C. Keller, 3rd, *Differential usage of two 5' splice sites in a complex exon generates additional protein sequence complexity in chicken CLIP-170 isoforms.* Biochim Biophys Acta, 1999. **8**(2): p. 119-24.
35. Griparic, L., J.M. Volosky, and T.C. Keller, 3rd, *Cloning and expression of chicken CLIP-170 and restin isoforms.* Gene, 1998. **206**(2): p. 195-208.
36. Griparic, L. and T.C. Keller, *Identification and expression of two novel CLIP-170/Restin isoforms expressed predominantly in muscle.* Biochim Biophys Acta, 1998. **21**: p. 1-3.
37. Ma, Y., et al., *Quantitative analysis of microtubule transport in growing nerve processes.* Curr Biol, 2004. **14**(8): p. 725-30.
38. Mays, R.W., K.A. Beck, and W.J. Nelson, *Organization and function of the cytoskeleton in polarized epithelial cells: a component of the protein sorting machinery.* Curr Opin Cell Biol, 1994. **6**(1): p. 16-24.
39. Baas, P.W., et al., *Sites of microtubule stabilization for the axon.* J Neurosci, 1993. **13**(5): p. 2177-85.
40. Baas, P.W. and F.J. Ahmad, *The plus ends of stable microtubules are the exclusive nucleating structures for microtubules in the axon.* J Cell Biol, 1992. **116**(5): p. 1231-41.

Chapter 7

Analysis of tetracyclin-inducible GFP-CLIP170 and GFP-CLASP2 expressing 3T3 cell lines

Tatiana Stepanova, Gert van Cappellen, Anna Akhmanova, Adriaan Houtsmuller, Frank Grosveld and Niels Galjart

Summary

CLIP-170 and CLASP2 are interacting proteins, each of them is involved in a unique aspect of the regulation of microtubule dynamics. In CHO cells, CLIP-170 acts as a rescue factor, which participates in the oscillatory behaviour of microtubules near the cell membrane. CLASP2 is able to stabilize microtubules in highly specific cell locations upon reception of signalling cues. When fused to GFP, both proteins show the typical "microtubule plus end tracking" behaviour, which characterizes so-called +TIPs, an ever enlarging group of proteins that specifically associate with the ends of growing microtubules. Several mechanisms have been proposed to account for microtubule tip association, among which are treadmilling and motor protein delivery. Here, we have generated stably transfected 3T3 cells, using the tetracycline inducible promoter system, to express GFP-CLIP170 and –CLASP2. We demonstrate that, when expressed at low levels, both fusion proteins behave as their endogenous counterparts in terms of intracellular distribution. The dynamic behaviour of GFP-CLIP170 clearly differs from that of GFP-CLASP2 in that the first only marks the ends of growing MTs, while the latter also accumulates at sites where the ends of stabilized MTs are concentrated, such as focal adhesions and leading edges. Using fluorescence recovery after photobleaching (FRAP), we show that GFP-CLIP170 is a mobile protein in cells. The behaviour of GFP-CLASP2 is variable. At focal adhesions areas, we found both mobile and relatively immobile pools of GFP-CLASP2, while at the leading edge of 3T3 cells GFP-CLASP2 is mobile but less than within the cytoplasm of cells. Thus, the dynamic behaviour of the protein changes upon accumulation of CLASP to particular sites within the cell. This change, in turn, may render microtubules more stable.

Introduction

Microtubules (MTs) play an important role in many cellular processes. They are essential for correct segregation of chromosomes during mitosis, organelle transport, cell polarity and cell migration. A remarkable feature of the MT cytoskeleton that is critically involved in all of these processes is called dynamic instability, i.e. the switching of MT ends from one behaviour (growth, pause or shrinkage) to another. This highly important aspect of MT dynamics is regulated by a large group of structurally different MT- or tubulin-associated proteins [1-4]. The +TIPs (MT plus-end tracking proteins) are proteins that localise specifically at the distal ends of growing MTs and that help to regulate MT dynamics [5, 6]. CLIPs (cytoplasmic linker proteins) [7-9] and CLASPs (CLIP-associating proteins) [10] represent two classes of +TIPs that differently influence MT dynamics. In CHO cells CLIPs have been suggested to act as rescue factors, or to be able to recruit such factors to the distal ends of MTs, reverting a shrinking MT to a growing one [11]. In the absence of CLIPs, a shrinking MT is not rescued and complete depolymerization of the MT to the MT organizing centre (MTOC) ensues. Thus in CHO cells where CLIPs are present, MTs are capable of undergoing oscillatory motions near the cell membrane. Similar to the action of CLIPs, the fission yeast homologue of CLIP-170, called tip1p, acts as a MT anti-catastrophe factor [12]. CLASPs play a stabilising role in MT dynamics and are involved in the local regulation of MT dynamics [10]. It was demonstrated that after serum induction in migrating fibroblasts, CLASPs relocalise to the distal ends of stabilised MTs at the leading edge of the cell and that this redistribution depends on GSK3-beta [10]. Interestingly, a similar behaviour was later shown for APC [13-15], suggesting that APC and CLASPs regulate MT dynamics in a cell signalling dependent manner.

Considering the importance of CLIPs and CLASPs in the regulation of MT dynamics, we were interested in analyzing the mechanism of their accumulation on the distal MT ends. In addition, we were interested in determining whether this accumulation changes in different cell regions and/or under different conditions. It was demonstrated earlier, using fluorescent time lapse imaging in combination with fluorescence speckle microscopy (FSM), that the plus-end tracking of CLIP-170 and EB1 is mediated by a "treadmilling" mechanism [16, 17] . This mechanism involves the specific association of these proteins with a freshly synthesized MT tip, followed by dissociation with first-order kinetics. Such a behaviour generates the now well know "comet-like" association of GFP-TIPs with growing MT ends. However, delivery of +TIPs to the MT end may also occur via motor proteins [18, 19]**.** A combination of these two mechanisms, or alternative mechanisms, could also be envisaged. We reasoned that we could distinguish between different mechanisms, using the technique of fluorescence recovery after photobleaching (FRAP), in which an area of the cell were the GFP-TIP is expressed, is bleached and the recovery of fluorescent signals is measured. This recovery is measured both at MT tips as well as in cytoplasmic cellular areas.

The tetracycline-controlled transcription system (Tet-system) [20] of eukaryotic cells was used for generation of GFP-CLIP170 and GFP-CLASP2 stable cell lines. Using this system we reasoned that we should be able to manipulate the expression levels of GFP-CLIP170 and –CLASP2 at will, as it is know that abundant overexpression of these proteins can have severe consequences for the MT network and lead to artefactual situations [21-24] . Here, we characterize stably expressing 3T3 cell lines and use them for live cell imaging, migration assay and FRAP experiments. We demonstrate that GFP fusions of CLASP2 and CLIP170 in cell lines, stably transfected with GFP-CLASP2 and GFP-CLIP170 DNAs, faithfully represent the endogenous proteins in 3T3 cells. We conclude that GFP-CLASP2 and GFP-CLIP170 stable cell lines are suitable and very useful for study of these proteins behaviour in living cells.

Materials and methods

Plasmid construction

For generation of GFP-CLIP170 a rat brain cDNA (accession number AJ237670), encoding a CLIP-170 isoform with a 115 amino acid deletion in the C-terminal portion of the coild-coil region [22], was used. pTRE-GFP-CLIP170 was generated by inserting a GFP-CLIP170 insert as AgeI/ApaI fragment into a synthetically generated linker site in the EcoRI site of pTRE. The pTRE-GFP-CLASP2 was generated using a short isoform of CLASP2 (CLASP2gamma, accession number AJ276961), by a similar strategy as pTRE-GFP-CLIP170. In this case, to enhance splicing, we added a beta-globin intron just after GFP-CLASP2 in the pTRE vector. The rtTA2-M2 (pUHrT 62-1) regulator plasmid DNA was a kind gift of H. Bujard. The neomycin resistance plasmid (pHA178neo, vector pSP72), is a derivative of pMC1-NeopolyA, in the puromycin resistance plasmid (also pSP72 based), the selection gene is under control of the PGK promoter.

Cell culture and transfection

Swiss 3T3 fibroblasts were cultured in (1:1) DMEM/F10 medium with 8 % fetal calf serum. Cell lines, stably expressing GFP fusion proteins under doxicyclin control, were generated according to the instructions of the supplier (Clontech). Briefly, 3T3 cells were grown to 80% confluence and subsequently transfected with two linearized DNA plasmids (rtTA2-M2 and pHA178neo), using lipofectamine 2000 (Invitrogen). Selected, neomycin-positive clones were transfected with linearized pTRE GFP-CLIP170 DNA or pTRE GFP-

CLASP2 DNA, together with a PGK-puromycin DNA, using lipofectamine 2000. Positive clones after neomycin and puromycin selection represent stable cell lines containing GFP-CLIP170 or GFP-CLASP2 fusions under control of rtTA. Different amounts of doxicyclin were added to induce variable expression levels of GFP-fusion proteins.

Immunocytochemistry

3T3 cells stably expressing GFP-CLIP170 or GFP-CLASP2 were induced by addition of doxicyclin (Dox) for 6-15 hours. Cells were fixed and immunocytochemistry was performed as described earlier [21, 22]. Cells were stained with different primary antibodies. Monoclonal antisera against acetylated alpha-tubulin (Sigma), polyclonal antisera against detyrosinated alpha-tubulin (a kind gift of C. Bulinski), monoclonal antibodies against vincullin, paxillin (Sigma) and GM130 (Transduction Laboratories) were used in a 1:100 dilution. Polyclonal rabbit antisera against CLASP2 (2358), CLIP-170 (2260) and CLIP-115 (2238) have been described [21, 22] and were used in a dilution of 1:300. Alexa 594-conjugated goat anti-mouse or anti-rabbit (Molecular Probes,1:500) and Alexa 350 sheep anti-mouse (Molecular Probes,1:300) were used as secondary antibodies. Images were acquired using either a Leica DMRBE microscope, with a 100x oil immersion lens (NA 1.3) and equipped with a Hamamatsu C4880 camera or with a Zeiss LSM510 confocal microscope.

Western blot analysis

For western blotting 3T3 cell cultures were harvested 24 hours after Dox induction, and total protein extracts were prepared. Western blotting was performed as described earlier [22]. Proteins were detected the aforementioned rabbit polyclonal antibodies against CLIPs and CLASP2 in a 1:2000 dilution, or anti-GFP (Clontech) in a 1:2500 dilution. Secondary goat anti-rabbit antibodies, coupled to alkaline phosphatase (Sigma) were used at 1:7000.

Live imaging

For cell migration experiments, we used a wound healing model as described previously [21, 22]. Briefly, 3T3 cells were grown to confluence, after which serum was removed for 24-48 hours. Subsequently, a stripe of cells was scratched off, creating a "wound" in the monolayer and serum was added to the culture medium again [25]. The migration of cells into the wound was analyzed at 37 ^{0}C on a Zeiss LSM510 confocal laser-scanning microscope (wavelength 633, laser 1%). Cells were analyzed for 9-15 hours. Phase contrast images were acquired every 15-30 minutes, acquisition was started immediately after wounding.

The time-lapse imaging of GFP-CLIP170 fluorescence, to record growth speeds of MTs was performed as described previously[21, 23]. For both the time-lapse imaging and bleaching studies a Zeiss LSM510 system was used (488 nm laser set at 2%, image acquisition every 2-3 seconds (approximately 200 images per experiment). Bleaching was performed during the time-lapse assay, after 50 images (50 iterations with 488 nm laser set at 100%). The time-lapse imaging was continued for 150-200 seconds after bleaching. The movies were assembled and different parameters (velocities of MT growth and cell migration, the fluorescent intensities in FRAP assay) estimated using LSM 510 software.

Results

Generation of GFP-CLIP170 and GFP-CLASP2 3T3 cell lines

Since it has been demonstrated that the abundant overexpression of CLIP-170 and CLASP2 causes MT aggregation and bundling [21-24], we used the regulatable tetracyclin controlled transcription system (tet-on system) for the generation of stable cell lines,

containing GFP-CLIP170 or –CLASP2. The tet-on system has several advantages compared to other regulated gene expression systems that function in mammalian cells [20]. The successful establishment of a cell line, which expresses a gene with potentially counter-selective properties, requires that the gene be transcriptionally silent prior to its induction. In principle, the tet-on system provides this possibility. Studies on the dynamic behaviour of GFP-CLIP170 and GFP-CLASP2, by live cell imaging, requires a protein expression level that is comparable to that of the endogenous protein. The expression level of the gene of interest in the tet-on system can be regulated by addition of different amounts of doxicyclin (a tetracyclin analogue).

We chose to establish stably expressing 3T3 cells because of their large, spread out cytoplasm, in which MT dynamics can be inspected relatively easily with a fluorescence microscope. Moreover, MT dynamics in relationship to cell motility has been extensively studied in this type of cells [26-29]. Cotransfection of 3T3 cells with the rtTA2-M2 regulator plasmid DNA (pUHrT 62-1) and a neomycin resistance plasmid DNA (pHA178neo) gave 33 rtTA-positive clones from 100 resistant ones. One of these positive tet–on clones was cotransfected with pTRE-GFP-CLIP170 and a puromycin resistance plasmid, which yielded 12 GFP-CLIP170-positive clones out of 300 resistant ones. The same rtTA-positive clone was also transfected with pTRE-GFP-CLASP2 plasmid DNA and the puromycin resistance plasmid, which yielded 9 GFP-CLASP2-positive clones out of 100 puromycin resistant clones. Clone selection for GFP fusion protein was done by fluorescent microscopy, i.e. clones that contained fluorescent cells after doxicyclin induction were considered as positive (data not shown).

To select tet-inducible clones with the lowest background GFP signal, we analyzed protein extracts of GFP-CLIP170 and GFP-CLASP2 expressing cell lines, either treated with doxicyclin, or not treated. This western blot analysis (Figs. 1 and 2 and data not shown) revealed that in both types of stable cell lines GFP fusion protein signal is present, even in the absence of doxicyclin, indicating that, at least in our hands, the tet-on system is somewhat leaky. Perhaps this leakiness of the system resulted in low numbers of clones and the constant loss of cells containing the introduced gene of interest during the maintenance of cells in culture. We selected three GFP-CLASP2 expressing clones (from 9 positive) and three GFP-CLIP170 expressing clones (from 12 positive) for further analysis. As shown in Figs 1 and 2, some of these clones are inducible by doxicyclin, but they all contain low GFP fusion protein signal in the absence of the inducer. However, the western blot data also demonstrate a correct size of GFP-CLIP170 (Fig. 1) and GFP-CLASP2 (Fig. 2) and, importantly, no other GFP-fusion products are detected, suggesting that only one fusion protein is synthesized in each stable cell line. Interestingly, induction of GFP-CLASP2 in 3T3 clone 86 appears to lead to a reduction in the level of endogenous CLASP2 (Fig. 2), suggesting a feedback mechanism for the regulation of CLASP2 levels in a cell.

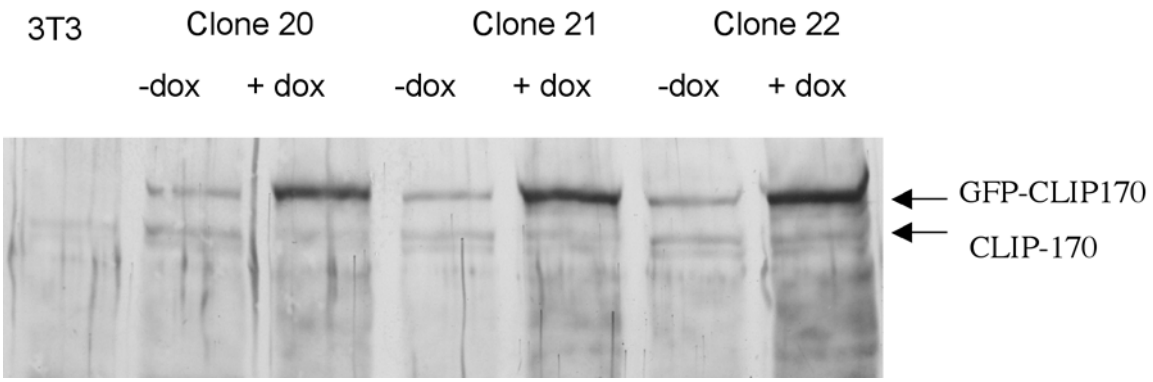

Fig 1. Western blot of 3T3 cell lines, stably expressing GFP-CLIP170. Western blot (with anti-CLIP antiserum) of protein extracts of three different, GFP-CLIP170 expressing cell lines, (with or without Dox) demonstrates correct size of GFP-CLIP170. Clones are inducible, but the system is leaky.

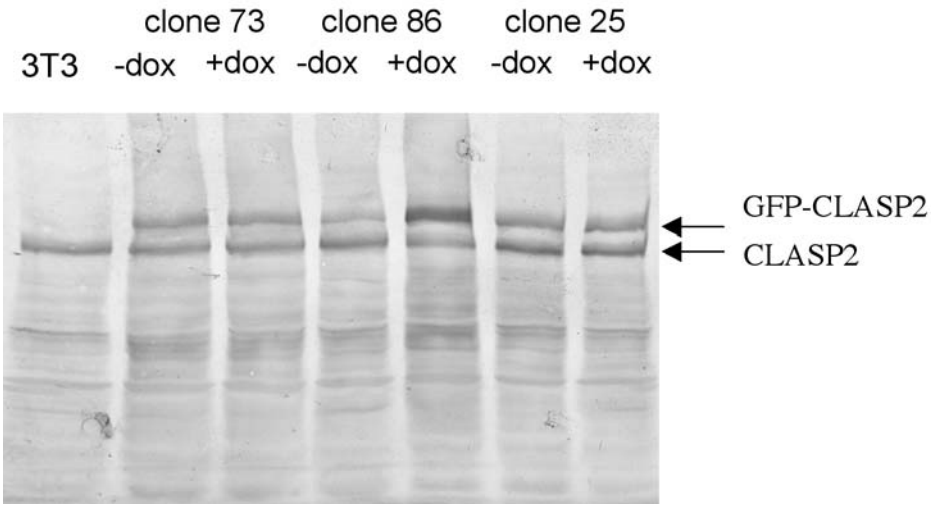

Fig 2. Western blot of 3T3 cell lines, stably expressing GFP-CLASP2. Western blot (with anti-CLASP antiserum) of protein extracts of three different, GFP-CLASP2 expressing cell lines, (treated with Dox, or not treated) demonstrates correct size of GFP-CLASP2. Clone 86 is inducible, but the system is leaky.

Analysis of GFP-CLIP170 and GFP-CLASP2 positive 3T3 cells

We performed a detailed cell microscopic analysis on the fluorescent localization of GFP-CLIP170 and GFP-CLASP2 in all positive clones 20 and 86, respectively (see movies 1 and 2, supplemental information). Both time-lapse as well as fixed cell investigations (data not shown) demonstrated the presence of comet-like dashes on the distal ends of MTs. Moreover, accumulation of GFP-CLASP2 was observed near the Golgi apparatus in non-migratory cells (Fig. 3a). We performed an in vitro wound healing assay on GFP-CLASP2 cells to investigate the relocalisation of this +TIP after serum induction. 3T3 cells stably transfected with GFP-CLASP2 DNA were grown to confluence, then serum was removed from the medium. After 24-48 hr of serum starvation, a stripe of cells was scratched off, creating a "wound" in the monolayer and subsequently serum was added to the culture medium again. Cells at the wound edge became polarized and accumulation of GFP-CLASP2 was observed at their leading edges.

A

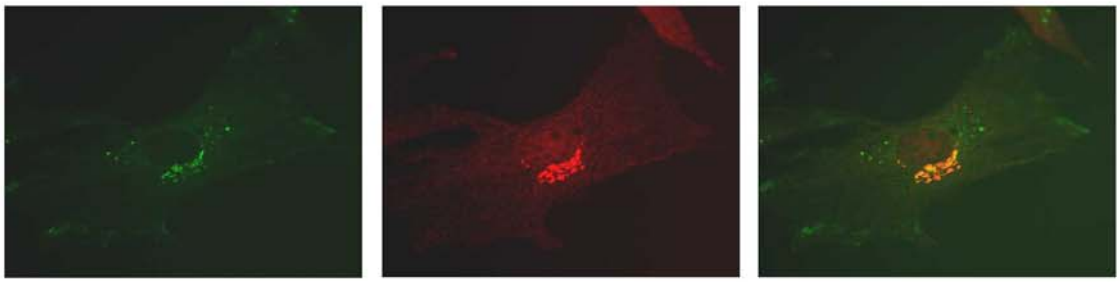

GFP-CLASP2 | Golgi marker GM130 | Merge

B

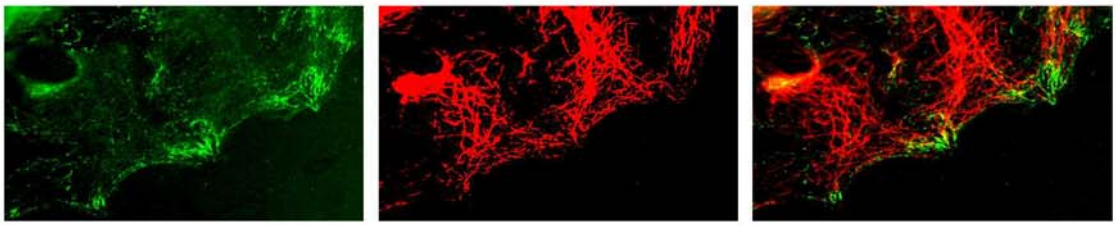

GFP-CLASP2 | Acetylated.tub | Merge

C

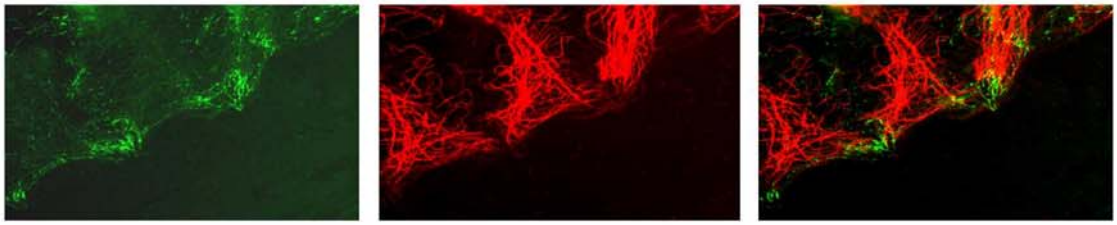

GFP- CLASP2 | Glu.tub | Merge

D

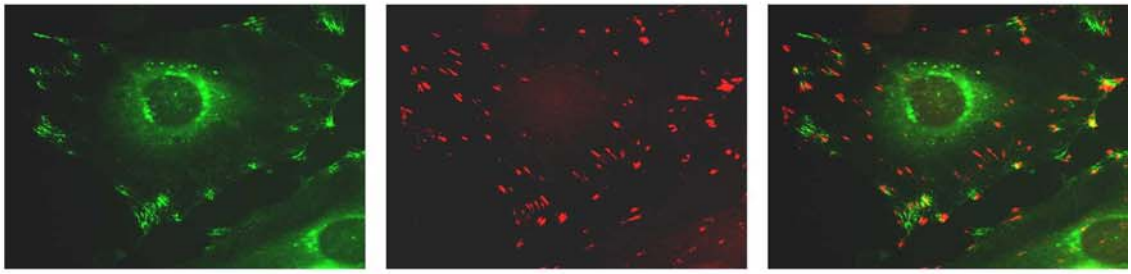

GFP-CLASP2 | Paxillin(Abs) | Merge

E

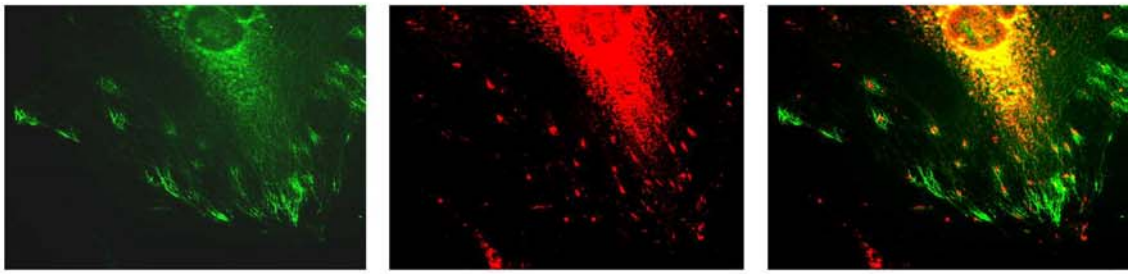

GFP-CLASP2 | Vincullin (Abs) | Merge

Fig 3. Localisation GFP-CLASP2 in stably transfected 3T3 cells.
3T3 cells stably transfected with GFP-CLASP2 were fixed and stained with **(A)** anti-GM130, **(B)** anti-acetylated tubulin (wound healing assay), or **(C)** anti-detyrosinated tubulin (wound healing assay), **(D)** anti-paxillin or **(E)** anti-vincullin antisera (red signals).

Immunocytochemistry with Abs against stabilised forms of tubulin (acetylated (Ac) tubulin (Fig. 3b) and detyrosinated (Glu) tubulin (Fig. 3c) demonstrated that many stabilized MT bundles display a high accumulation of GFP-CLASP2 at their distal ends. These data reveal a similar behaviour of GFP-CLASP2 and endogenous CLASP protein in the wound healing assay of 3T3 cells. In addition, GFP-CLASP2 was detected at focal adhesions, as visualized by co-staining with anti-vincullin and anti-paxillin antibodies (Fig. 3d and e, respectively). It is noteworthy that an exact colocalization GFP-CLASP2 with vincullin or paxillin was not observed very often. Moreover, some focal adhesions were completely GFP-CLASP2 free and some GFP-CLASP2 accumulations were not surrounded by vincullin or paxillin.

The application of lithium chloride, an inhibitor of GSK-3beta (glycogen synthase kinase), on starved 3T3 cells, stably expressing GFP-CLASP2, caused a significant increase of GFP-CLASP2 at distal ends of MTs (data not shown), which corresponds to previous results obtained with endogenous protein [21]. Under serum stimulation in the wound healing assay, treatment with lithium chloride leads to complete removal of GFP-CLASP2 from the leading edge of migrating cells and to accumulation on MT distal ends all over the cytoplasm (data not shown)**.**

Similar immunochemistry experiments on 3T3 cells, expressing GFP-CLIP170 showed that, similar to endogenous protein, GFP-CLIP 170 localises on the distal ends of MTs were it also colocalises with CLIP-115 (data not shown). In contrast to GFP-CLASP2, GFP-CLIP170 does not accumulate to leading edge MTs and does not respond to LiCl. In conclusion, the localization and behaviour of both GFP-CLIP170 and GFP-CLASP2 completely corresponds to the endogenous distribution of these +TIPs in fixed mammalian cells [10, 22, 30].

Dynamic behaviour of GFP-CLIP170 and GFP-CLASP2

Since GFP fusions of CLASP2 and CLIP170 in stably transfected, 3T3 cell lines faithfully recapitulate the behaviour of endogenous proteins these cell lines appeared suitable for study of the dynamic behaviour of the fusion proteins. We first compared the speed of movement of "comet-like" GFP-CLIP170 dashes in 3T3 cells to the movement in transiently transfected cells [31]. Fluorescent dashes of 3T3-derived GFP-CLIP 170 **(Play movie 2)** move from the MTOC area towards the cell periphery with an average velocity of 0,47+/-0,06 micron/sec (6 cells, 33 MTs, see movie 1 for visualization of this movement). This is identical to our previously published data obtained on transiently transfected cells [10]. Taken together, the data suggest that GFP-CLIP170 in stable 3T3 cell lines recapitulates the behaviour of endogenous CLIP-170. Since CLIP-170 is a very well-characterised protein, which was shown to treadmill on MT ends in mammalian cells in culture, we used the GFP-CLIP170 cell line as control in different experiments to study the mechanism of CLASP accumulation at MT plus ends.

At low expression levels GFP-CLASP2 localizes to MT distal ends, whereas at higher levels, the fusion protein accumulates along the whole MT length, causing MT rearrangement and bundling when highly overexpressed (data not shown). In motile 3T3 cells, accumulation of GFP-CLASP2 is detected at MT distal ends in the leading edge area and at focal adhesions

(Fig. 3). We were interested in the dynamics of the protein at these different sites. It was published before that at low expression levels in transiently transfected COS-1 cells, GFP-CLASP2 behaves very similar to GFP-CLIP170, accumulating on the growing MT ends and moving with the same velocity [10]. In the cytoplasm of 3T3 cells, away from cell edges, GFP-CLASP2 fluorescent dashes **(Play movie 3)** move with an average velocity 0,48 +/-0,09 micron/sec (11 cells, 63 MTs), similar to transiently transfected COS-1 cells. In a wound-healing assay, before 3T3 cells received serum, we observed just a few GFP-CLASP2 dashes in the cytoplasm (data not shown). We visualised the beginning of GFP-CLASP2 redistribution to the leading edges of 3T3 cells within 3-5 minutes after serum addition, and about 15-20 min later observed a complete accumulation of polarized GFP-CLASP2 at the wound edge of cellular monolayer **(Play movie 4)**.

We questioned whether cell migration into a wound influences MT growth velocities. We therefore performed wound healing assays using both GFP-CLIP170 and GFP-CLASP2 cells with low expression levels of GFP fusion proteins. After the addition of serum, which induced migration and caused polarization of GFP-CLASP2, we were able to measure the velocities of fluorescent dashes in cells containing GFP-CLIP170 and GFP-CLASP2. We focussed only on MTs in cytoplasmic areas and not on GFP-CLASP2 accumulations at focal adhesions, or near cell membranes, because in the latter case we could not be certain that GFP-CLASP2 was at the end of an MT. In GFP-CLIP170 expressing 3T3 cells we determined an average velocity of 0,45+/-0,03 micron/sec (12 cells, 67 dashes, 6 independent experiments)**,** and could show no variation in speed in different regions of the cell **(Play movie 5)**. These results suggest that cell migration does not affect MT growth velocity. The average speed of fluorescent dashes in migrating GFP-CLASP2 expressing cells **(Play movie 6)** was very similar to that in GFP-CLIP170 expressing cells, i.e. 0,44+/-0,05 micron/sec (9 cells, 57 dashes, 5 independent experiments). During cell movement, we did not find any significant cell-region dependent differences in the velocities of GFP-CLASP2 or GFP-CLIP170 positive fluorescent dashes within one cell. These observations correspond with data, published earlier, that during cell migration, the MTs in different cell regions grow with similar velocity that does not depend on the direction of MT growth [32]. While behaviour of CLIP-170 is similar in migrating non-motile cells, CLASP2 relocalizes to the leading edge of moving fibroblast. However, such specific relocalization of CLASP2, during cell migration, does not influence the MT growth velocities, which are similar in different cell regions and comparable to these parameters in steady cells.

Influences of GFP-CLIP170 and GFP-CLASP2 on cell migration

The accumulation of GFP-CLASP2 at the leading edge and at focal adhesions of motile 3T3 cells raised our interest as to a role of this protein in the process of cell migration itself. We therefore performed cell migration assays using the GFP-CLASP2 stable cell line **(Play movie 7)**, with or without doxicyclin induction, to regulate the expression level of the GFP fusion protein. In each experiment, we measured the speed with which cells were able to migrate into a wound for 9-12 hours. These experiments demonstrated no difference in cell migration speeds between the GFP-CLASP2 cells compared to control 3T3 cells (Table I). Treatment with doxicyclin does not make a difference, indicating that mild overexpression of GFP-CLASP2 does not influence cell migration.

When we performed a wound healing assay of stably transfected GFP-CLIP170 3T3 cells, we noted that the overexpression of GFP-CLIP170 does cause a decrease in cell movement velocity (Table I). This correlates with the removal of CLASP2 from the leading edge of cells, as was shown by immunostaining cells with Abs against CLASP2 and a reduction in the levels of acetylated (stable) MTs (Fig. 6). Thus, in contrast to GFP-CLASP2,

overexpressed GFP-CLIP170 affects cell movement, as well as CLASP2 polarization, removing it from the leading edge.

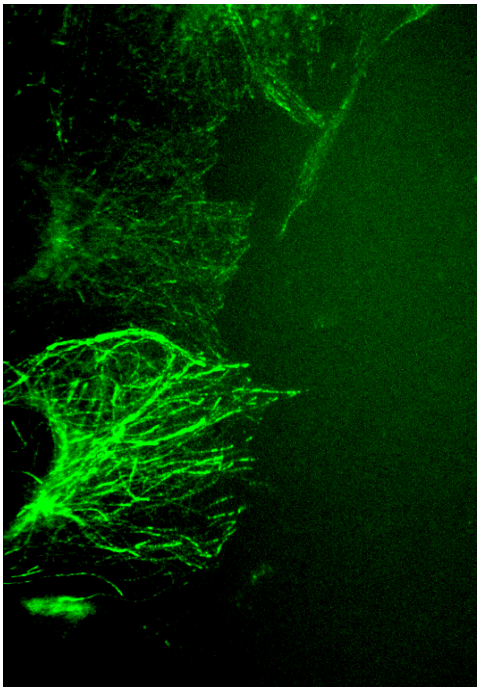

GFP-CLIP 170

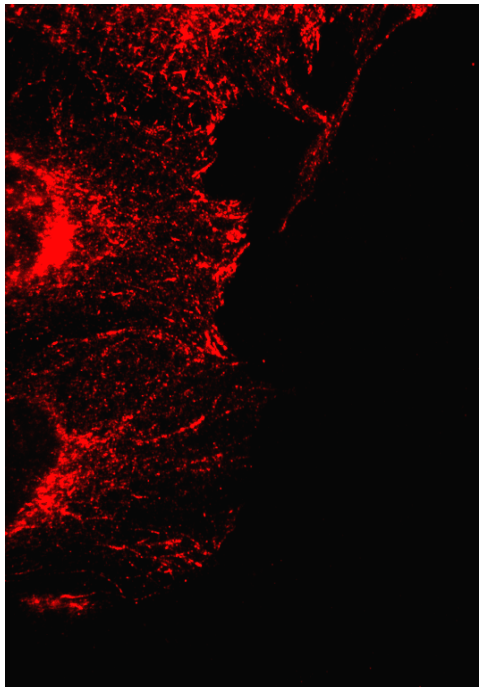

CLASP Abs

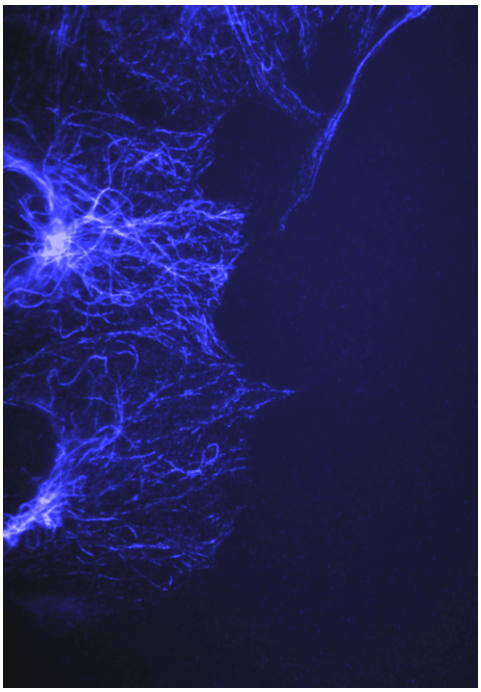

Acetylated tub.

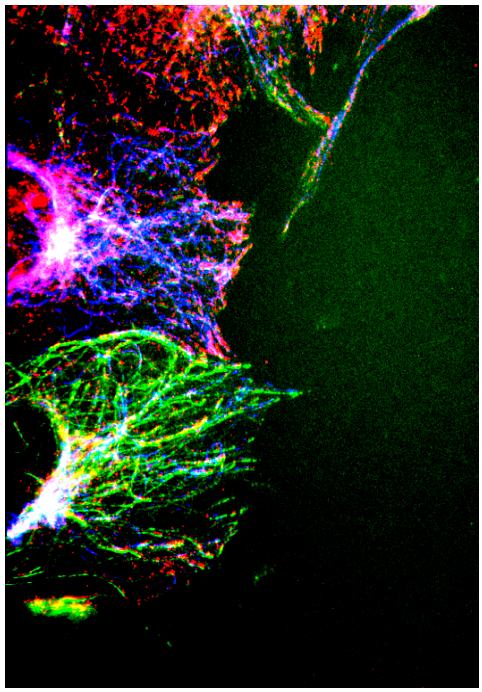

Merge

Fig 6. Overexpression of GFP-CLIP170 effects CLASP2 polarization at the leading edge of 3T3 cells. Migrating 3T3 cells, stably transfected with GFP-CLIP170, were fixed and stained with anti-CLASP (red) and anti-acetylated tubulin (blue) sera.

That the number of stabilised MTs is diminished in cells with reduced CLASP2 at the leading edge, is in line with its role in induction of local MT stabilization [10]. However, that this is caused by overexpression of GFP-CLIP 170 in motile cells is highly surprising, since overexpressed CLIP-170 is able to aggregate MTs and render them stable.

3T3 cell line	concentration of Dox (µg/ml)	migration velocities of 3T3 cells (µm/min)
control 3T3 cells	no Dox	0,21+/- 0,05 (n=65, e=3)
control 3T3 cells	1µg/ml	0,20+/- 0,04 (n=35, e=1)
GFP-CLIP170	no Dox	0,20+/- 0,03 (n=56, e=2)
GFP-CLIP170	0.1 µg/ml	0,17+/- 0,04 (n=29, e=2)
GFP-CLIP170	0.5 µg/ml	0,15+/- 0,05 (n=12, e=1)
GFP-CLIP170	1µg/ml	0,09+/- 0,04 (n=55, e=3)
GFP-CLASP2	no dox	0,21+/- 0,03 (n=35, e=2)
GFP-CLASP2	1µg/ml	0,20+/- 0,04 (n=27,e=2)

Table I. Cell migration velocities of different 3T3 cell lines (µm/min) at various Dox concentrations (n- number of measurements, e- independent experiments). The overexpression of GFP-CLIP170 causes a decrease in cell movement velocity.

FRAP analysis of GFP-CLIP170 and GFP-CLASP2 in 3T3 cells

Several mechanisms have been proposed to explain the accumulation of +TIPs on the distal ends of growing MTs. Among those, treadmilling at plus ends of growing MTs, shown for CLIP-170 [8, 9] and EB1[33] and protein translocation along MTs to the plus ends by kinesin protein motors, demonstrated for adenomatous polyposis coli (APC) [34, 35] and Tea1p [36], are best known. We used fluorescent recovery after photobleaching (FRAP) to analyze movement of GFP-CLIP170 and GFP-CLASP2 in motile 3T3 cells. It has been established for mammalian CLIP-170 that it accumulates on the MT distal ends by treadmilling [8, 9]. We used the movies obtained from GFP-CLIP170 cells therefore as control for our experiments with GFP-CLASP2 cells.

Qualitative analysis of FRAP experiments with GFP-CLIP170 expressing cells (7 cells with 21 selected cell areas analyzed, see Fig.4 **(Play movie 8)** for an example) revealed that recovery of fluorescence within bleached regions (see ROI 4 in Fig. 4) is achieved within approximately 50 seconds after bleaching. Note that we often bleached large areas of the cell. Thus, recovery of fluorescent signal can not be complete. In addition, in Fig. 4 the rectangle that marks the bleached region also covers areas outside the cell, hence recovery of that region can not reach levels of intracellular other regions. As shown in Fig. 4, when equivalent ROIs are taken, fluorescent intensities in non-bleached and bleached regions reach the same level ~50 seconds after bleaching, indicating that GFP-CLIP170 is present in the cytoplasm only as a mobile fraction.

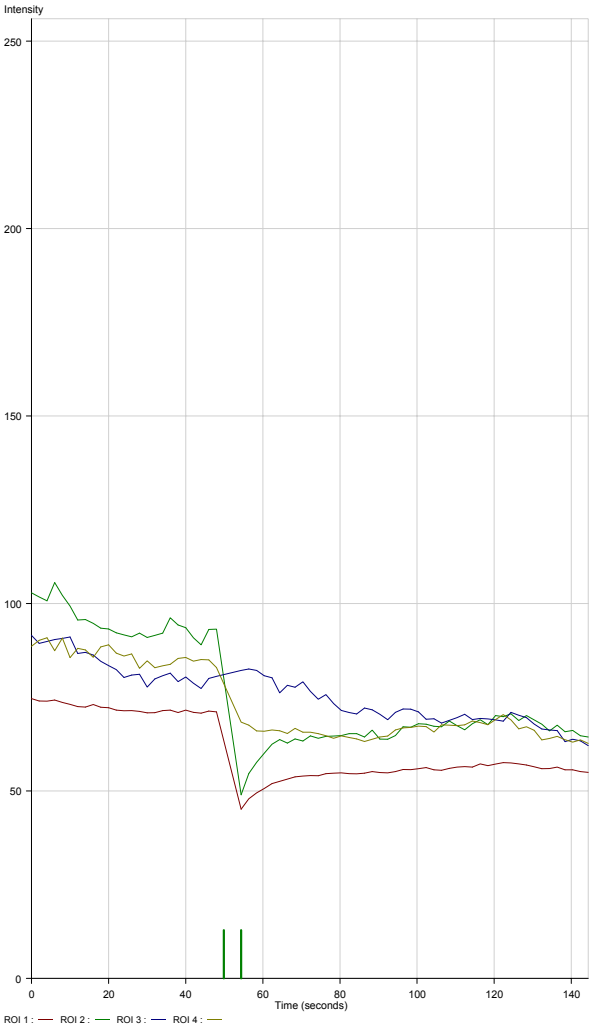

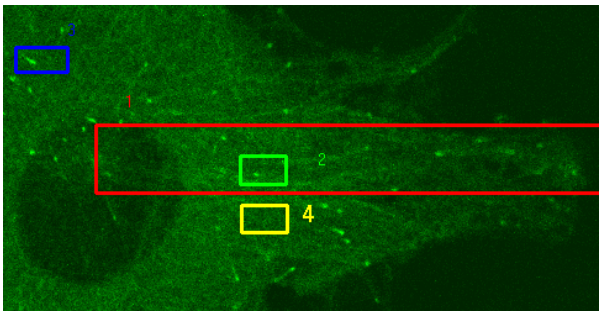

Figure 4. FRAP analysis of GFP-CLIP170 expressing 3T3 cell line.
Right panel: a still image of GFP-CLIP170 expressing cell. Note the comet-like dashes throughout the cytoplasm. The image was taken just before bleaching, which was done during 5 seconds in the large red square. The smaller squares represent the regions of interest (ROI) taken to measure fluorescent intensity before and after bleaching. The same colours are used in the left panel, which shows average fluorescent intensities of the different areas during the experiment.

Imaging of motile 3T3 cells, stably transfected with GFP-CLASP2 DNA demonstrated a novel behaviour of this fusion protein. Besides the GFP-CLASP2 fluorescent dashes representing growing MT tips, we observed accumulations of GFP-CLASP2 in areas near the cell edge and next to focal adhesions, which appeared more static than the "comet-like" dashes. Each accumulation had its distinct dynamic pattern of behaviour. Interestingly, fluorescent dashes of GFP-CLASP2, which represent growing MTs, continuously entered and exited areas of "static" GFP-CLASP2 accumulation. Still, the latter were able to change size within several seconds, becoming larger or smaller **(Play movie 9)**. They could also disappear completely**.** Some of the GFP-CLASP2 positive areas appeared more stable than others. However, none of them was permanent within the period of the movie.

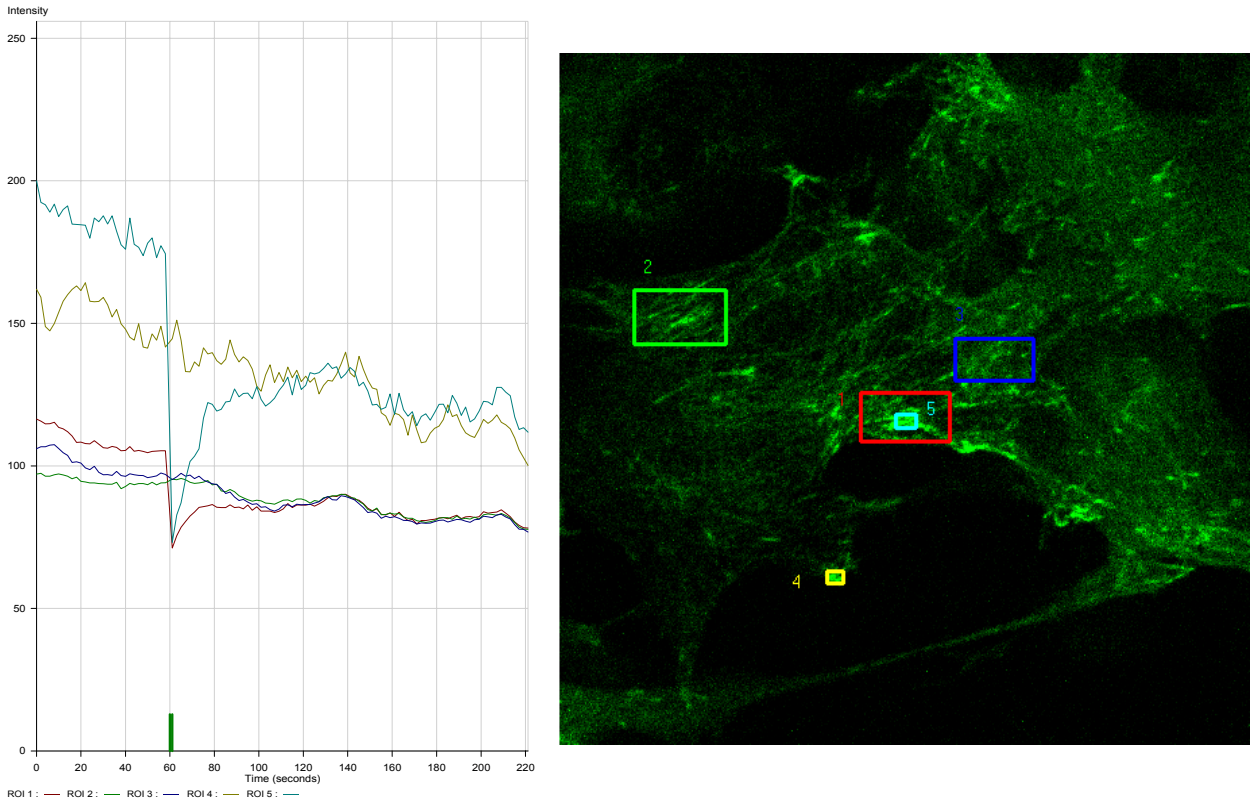

Figure 5. FRAP analysis of GFP-CLASP2 cell line.
Right panel: a still image of GFP-CLASP2 expressing cell. Note the comet-like dashes throughout the cytoplasm, in addition to accumulations at focal adhesion areas. The image was taken prior to bleaching, which was done during 1 second in the red square. The smaller squares represent the areas taken to measure fluorescent intensity. The same colours are used in the left panel, which shows average fluorescent intensities of the different areas during the experiment.

To analyze the process of GFP-CLASP2 accumulation at specific cell areas, we bleached different areas of the cell, including sites with focal adhesions (Figs. 5-7) and the leading edges (Fig. 8). We then selected different areas inside and outside of the bleached regions to compare fluorescent recovery in focal adhesions, leading edges and cytoplasmic areas. As shown in Figs. 5-7, initial fluorescent intensities in the small, selected focal adhesion areas are higher than in cytoplasmic areas, indicating significant accumulation of GFP-CLASP2 at focal adhesions. The same observation was made for the leading edge (Fig. 8). Strikingly, GFP-CLASP2 in focal adhesion areas appears to consist of a mobile fraction (judged to be ~70%, see Fig. 5 **(Play movie 10)**, ROI 5 in light blue), which recovers after ~60 seconds, and a relatively immobile fraction (~30%, see Fig. 5, ROI 5 in light blue). In Figs. 6 **(Play movie 11)** and 7 **(Play movie 12)** the behaviour of GFP-CLASP2 at focal adhesion areas is validated, although the percentages of mobile and immobile fractions differ somewhat. In Fig. 6, ROI 4 (yellow) marks an area of the cytoplasm next to, but not within, a focal adhesion site, which is marked by ROI 2 (green). In both rectangles, fluorescence recovery occurs after bleaching. However, fluorescence recovery in ROI 4 is complete within ~60 seconds after bleaching, whereas in the focal adhesion area marked by ROI 2, fluorescence recovery is ~50 % of the initial value. Thus, in cytoplasmic regions GFP-CLASP2 is mobile, even when these are next to focal adhesion areas.

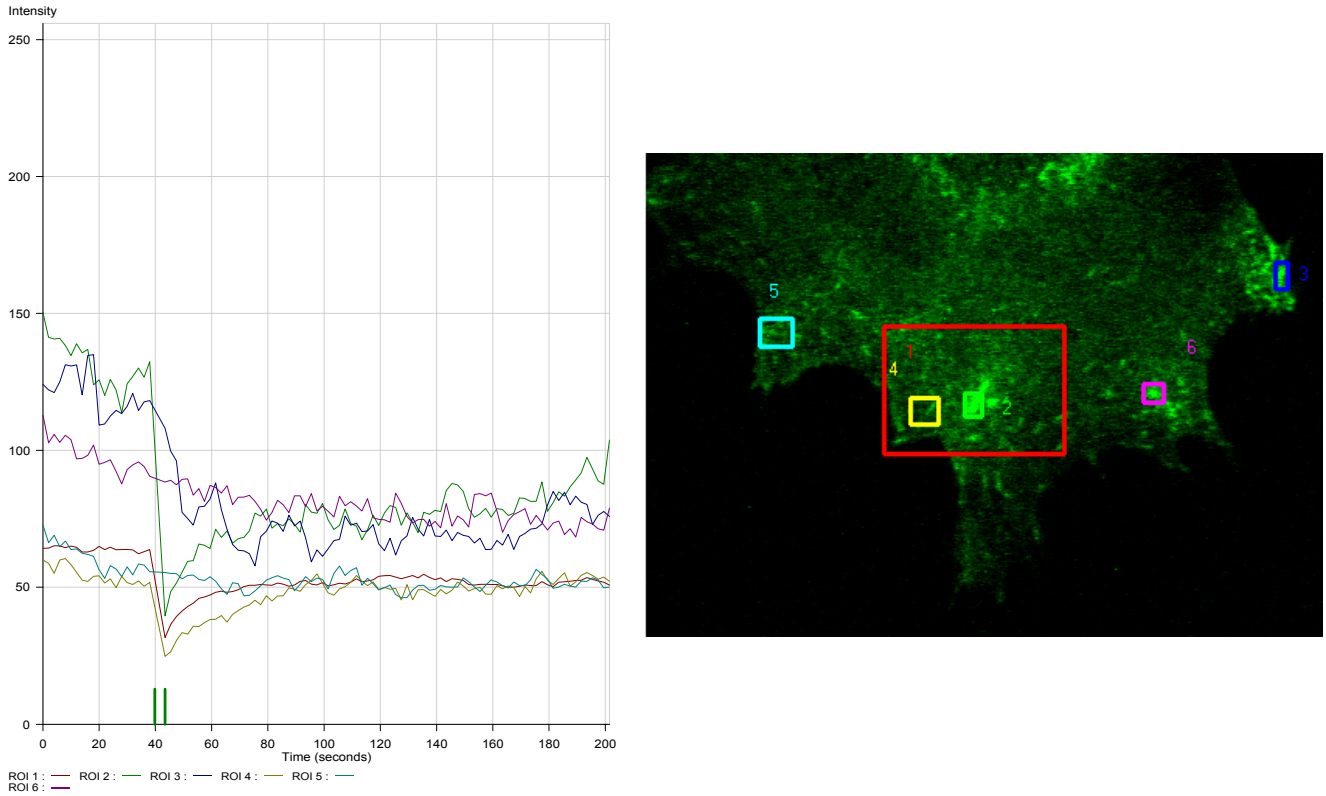

Figure 6. FRAP analysis of GFP-CLASP2 cell line.
Right panel: still image of GFP-CLASP2 expressing cell. The image was taken prior to bleaching, which was done during 5 seconds (red square). The smaller squares represent the areas taken to measure fluorescent intensity. The same colours are used in the left panel, which shows average fluorescent intensities of the different areas during the experiment.

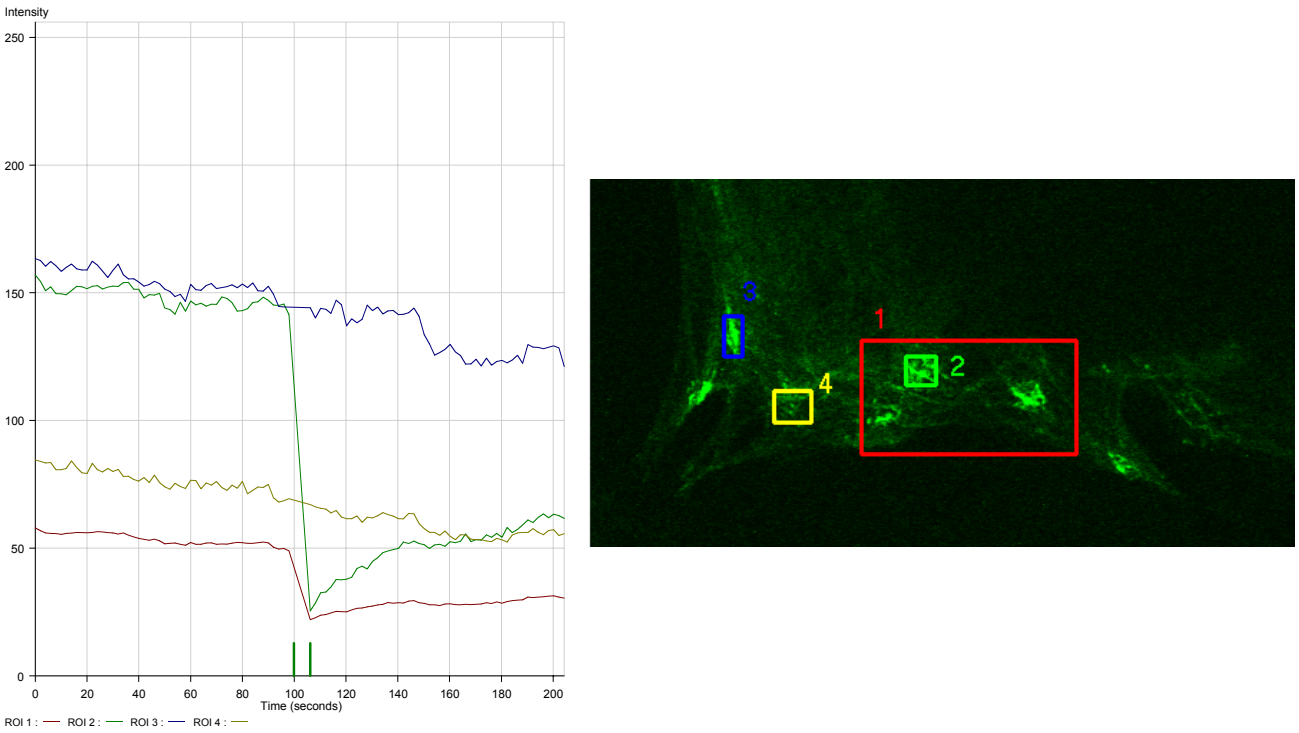

Figure 7. FRAP analysis of GFP-CLASP2 cell line.
Right panel: still image of GFP-CLASP2 expressing cell. The image was taken just before bleaching, which was done during ~5 sec (red square). The smaller squares represent areas taken to measure fluorescent intensity. The same colours are used in the left panel, which shows average fluorescent intensities of the different areas during the experiment.

In Fig. 7 a region was bleached (marked in red) which contains three focal adhesion areas. One of these areas was followed throughout the experiment, as were two other sites outside of the bleached area. Clearly, bleaching has little influence on the fluorescence in the latter two areas (note the decrease in signal in ROI 3 (blue) approximately 30 seconds after bleaching, we believe this represents bleaching-independent adjustment of the focal adhesion). In ROI 2 (green) which is within the bleach zone, fluorescence recovery occurs, but reaches only ~35 % of the initial value within 250 seconds.
Interestingly, FRAP experiments (in total 5 cells with 17 selected cell areas measured) with GFP-CLASP2 expressing cells in the wound healing model, which stimulates formation of a leading edge, revealed recovery of fluorescence within 220 seconds imaging (Fig. 8) **(Play movie 13)**. This recovery is approximately three times slower compared with the recovery time of cytoplasmic GFP-CLASP2 or of the mobile fraction of GFP-CLASP2 in focal adhesion areas. These data suggest that GFP-CLASP2 at the leading edge is more static (immobile) compared to the free cytoplasmic fraction, yet it is not immobile.

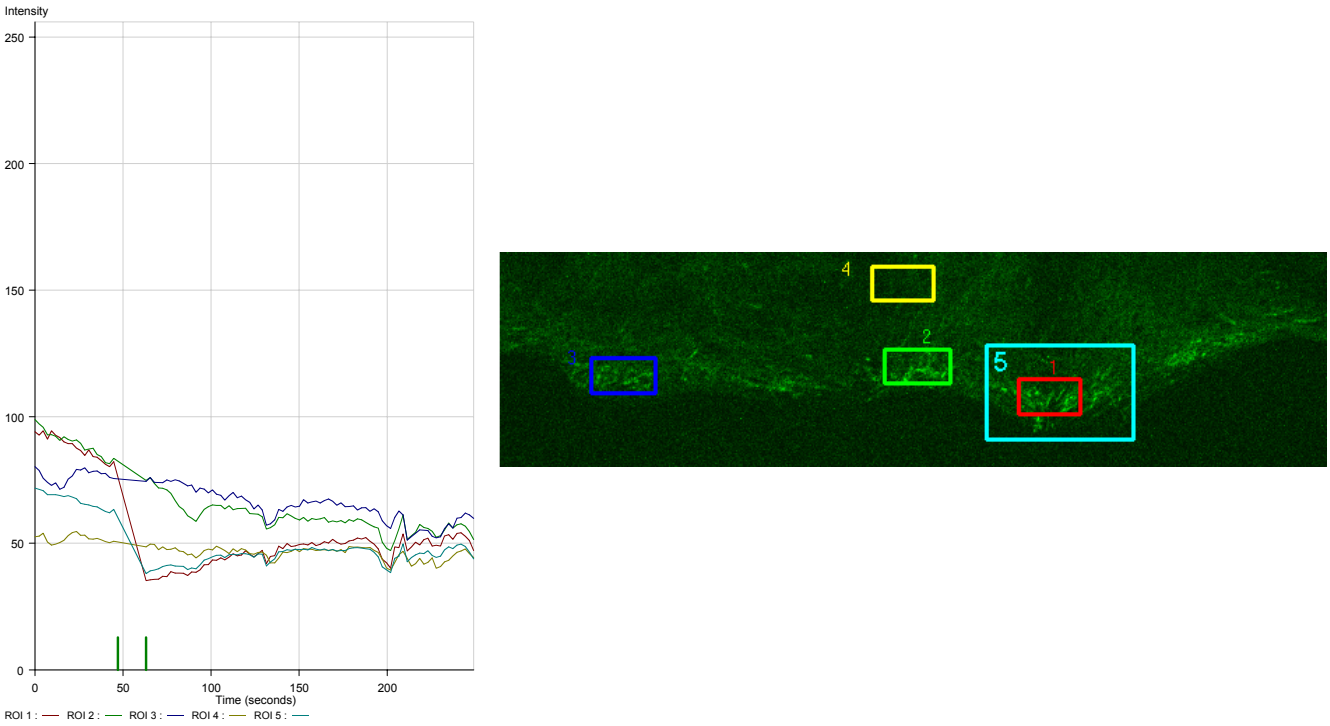

Figure 8. FRAP analysis of GFP-CLASP2 cell line.
Right panel: still image of GFP-CLASP2 expressing cell. The image was taken before bleaching, which was done during ~16 sec in the red square. The smaller squares represent the areas taken to measure fluorescent intensity. The same colours are used in the left panel, which shows average fluorescent intensities of the different areas during the experiment.

Discussion

Stable lines of GFP-CLASP2 and GFP-CLIP170 expressing 3T3 cells were generated to study how these two proteins behave dynamically, particularly during cell migration. For development of stable cell lines, we used the inducible Tet-on system, where gene expression can be regulated by addition of different concentrations of doxicyclin. We found, however, that in most clones a low level of GFP fusion protein expression was present in the absence of doxicyclin. Irrespective of this, we isolated a number of cell lines in which we could regulate GFP fusion protein expression to some extent. It should be noted that within a cell line, after addition of doxicyclin, individual cells still differed in expression level. Thus, where the population of cells, as measured by western blot, showed roughly equal expression of GFP fusion as compared to the endogenous protein, individual cells varied in expression levels.

The CLASP polarization at the leading edge of motile fibroblasts was described earlier [10]. GFP-CLASP2 accumulation at focal adhesions is a novel observation, which is corroborated by immunocytochemical staining with antibodies against CLASP2 (data not shown). Focal adhesions are places of attachment of actin filaments to the extracellular matrix, mediated by transmembrane linker glycoproteins (integrins) in the plasma membrane. In motile cells, there are several different types of focal adhesions depending on extracellular matrix components. Focal adhesions are very dynamic structures that constantly undergo assembly and disassembly during cell migration. It was proposed that although the actin drives cell movement, the MT cytoskeleton influences polarization by modulating substrate

adhesion via specific targeting interactions with adhesion complexes [37]. The spatial interaction between MTs and substrate adhesions was first described using conventional microscopy [38] and recently confirmed by dual colour TIRF (total internal reflection fluorescence) microscopy [37]. Moreover, by cotransfecting cells with DsRed-zyxin and GFP-CLIP170, Krylyshkina and co-workers have clearly demonstrated that the MT targeting into adhesion complexes involves the polymerization, but not sliding of MTs [37]. In line with these results, we visualised by confocal laser-scanning microscope MTs with GFP-CLASP2 at their plus ends to grow over and into immobile GFP-CLASP2 accumulations, which we presume to be adhesions complexes. Interestingly, we observed, that the GFP-CLASP2 dashes entering focal adhesions were always following the same tracks. This observation corresponds to and can be explained by an earlier suggestion, that MTs polymerise along another cytoskeletal element (most likely, actin) that terminates in adhesion complexes [37, 39]. Alternatively, it is tempting to speculate that the interaction between CLASP2 and actin (or an actin-binding protein) actually causes MTs to follow the same track. We visualised size changes and, sometimes, the complete disassembly of particular GFP-CLASP2 accumulations after the entering of growing MTs, decorated with GFP-CLASP2. Our observations are consistent with previous findings that focal adhesion targeting by MTs correlates with adhesion complex turnover or adhesion release [37, 38, 40] and are supported by recent TIRF data that MTs are able to target very precisely into single adhesion foci, modulating specifically their turnover [37]. Evidence indicates that kinesin may deliver a regulatory factor that promotes focal adhesion disassembly [41].

We suggest that CLASP polarization on the leading edge of migrating 3T3 cells is important for cell migration. The experiments where CLASP2 was removed from the leading edge by GFP-CLIP-170 overexpression clearly demonstrated a decrease of cell migration velocity. The number of stable MTs was also reduced in cells by overexpression of GFP-CLIP170. Although this is consistent with previous data on the role of CLASPs in the induction of local MT stabilization [10], overexpression of GFP-CLIP170 has been shown to lead to stable, bundled MTs.

We speculate that accumulation of CLIP-170 along MTs attracts CLASP2 to these bundles, because CLIP-170 and CLASP2 interact. This reduces the pool of CLASP2 available to the leading edge of a cell. Along MTs CLASP2 is not activated by local cues. It is possible that the reduction in cell migration speed in GFP-CLIP170 overexpressing 3T3 cells is the direct result of mislocalization of CLASP2, however, it is also possible that the generation of rigid MTs, due to the overexpression of GFP-CLIP170, is the cause and the mislocalization simply another consequence.

It was hypothesised that stable MTs are more important for providing the direction of locomotion, contributing to the persistence of lamella at the leading edge [42] than for motility itself [32]. Experiments with low drug concentration showed that the suppression of MT dynamic turnover by nocodazole and vinblastine restrains fibroblast migration [43]. Correspondingly, our direct measurements of MT growth in 3T3 GFP-CLIP 170 and GFP-CLASP2 cells demonstrated high MTs dynamics in different cell regions including the leading edge.

Analysis of MT behaviour during cell migration has shown that at the leading edge MTs spent more time in growth phase, less in shortening and pausing, and the catastrophe frequency is reduced compare the other cell regions, however, no significant differences in rates of MT growth were found [32]. In the current study, measuring the MT growth velocity in different regions of GFP-CLIP170 and GFP-CLASP2 cells during migration we did not find any significant differences in this parameter of MT dynamics. No evidence about the regional MT regulation by stabilizing factors or catastrophe-promoting factors in migrating cells has been found so far. However, it was proposed that plus end binding proteins such as

APC and CLASPs might regionally regulate MT dynamics and promote MT growth into advancing lamellipodia [44]. Indeed, while CLIP-170 does not seem to have any preference for certain areas of the cell, CLASPs bind to ends of acetylated MT orientated toward the leading edge in migrating cells [10]. It was shown that APC is transported along the MTs to the plus ends where it accumulates specifically on the tips of MTs growing in actively protruding areas [34, 45]. Moreover, APC stabilises MTs in vitro and in vivo [46].

We reasoned that we could study the behaviour of CLIP-170 and CLASP2 in cells, using FRAP. Our qualitative FRAP analysis does not allow any conclusion about the conformation of GFP-CLASP2 and GFP-CLIP170 in "free cytoplasm". However, the most interesting finding in these studies was that GFP-CLASP2 seems to be present in a cell in different fractions, depending on its distribution. The focal adhesion areas contain a mobile and immobile fraction of CLASP2, while at the leading edge CLASP2 seems to be mobile, but less so than CLASP2 in "free cytoplasm". These data suggest that the fractions of CLASP2 in focal adhesion complexes and at leading edges are modulated differently. The novel cell lines allow us to study the distinct regulatory mechanisms that enable CLASP2 accumulation at different sites in a cell.

The mechanism proposed for microtubule tip association of CLIP-170 and EB1 ("treadmilling"), involves the specific association of these proteins with a freshly synthesized MT tip, followed by dissociation with first-order kinetics from the MT lattice. Treadmilling may also explain CLASP2 association with MT plus ends in the cytoplasm but the moment CLASP2 enters focal adhesion sites or leading edges of cells, the mechanism must change because CLASP2 changes mobility.

Although the MT cytoskeleton is essential for directed migration of many cell types [44], the regulation of MT dynamics during cell motility and the structural/regulatory interactions between cytoskeletal components remain not well understood at molecular level. Therefore, the further elucidation of the role of CLASP2 in regulation of MT dynamics, particularly during cell migration, and the mechanism of accumulation of CLASP2 on MTs, represents a special interest for future investigations.

References

1. Walczak, C.E., *Microtubule dynamics and tubulin interacting proteins*, in *Curr Opin Cell Biol*. 2000. p. 52-6.
2. McNally, F.J., *Microtubule dynamics: Controlling split ends*, in *Curr Biol*. 1999. p. R274-6.
3. Andersen, S.S., *Spindle assembly and the art of regulating microtubule dynamics by MAPs and Stathmin/Op18*, in *Trends Cell Biol*. 2000. p. 261-7.
4. Cassimeris, L., *Accessory protein regulation of microtubule dynamics throughout the cell cycle*, in *Curr Opin Cell Biol*. 1999. p. 134-41.
5. Carvalho, P., J.S. Tirnauer, and D. Pellman, *Surfing on microtubule ends*, in *Trends Cell Biol*. 2003. p. 229-37.
6. Galjart, N. and F. Perez, *A plus-end raft to control microtubule dynamics and function*, in *Curr Opin Cell Biol*. 2003. p. 48-53.
7. Hoogenraad, C.C., et al., *Functional analysis of CLIP-115 and its binding to microtubules*, in *J Cell Sci*. 2000. p. 2285-97.
8. Perez, F., et al., *CLIP-170 highlights growing microtubule ends in vivo*, in *Cell*. 1999. p. 517-27.
9. Komarova, Y.A., I.A. Vorobjev, and G.G. Borisy, *Life cycle of MTs: persistent growth in the cell interior, asymmetric transition frequencies and effects of the cell boundary*, in *J Cell Sci*. 2002. p. 3527-39.
10. Akhmanova, A., et al., *Clasps are CLIP-115 and -170 associating proteins involved in the regional regulation of microtubule dynamics in motile fibroblasts*. Cell. Vol. 104. 2001. 923-35.
11. Komarova, Y.A., et al. *Cytoplasmic linker proteins promote microtubule rescue in vivo*. in *J Cell Biol*. 2002.

12. Komarova, Y.A., et al., *Cytoplasmic linker proteins promote microtubule rescue in vivo.* J Cell Biol, 2002. **159**(4): p. 589-99.
13. Zumbrunn, J., et al., *Binding of the adenomatous polyposis coli protein to microtubules increases microtubule stability and is regulated by GSK3 beta phosphorylation.* Curr Biol, 2001. **11**(1): p. 44-9.
14. Mogensen, M.M., et al., *The adenomatous polyposis coli protein unambiguously localizes to microtubule plus ends and is involved in establishing parallel arrays of microtubule bundles in highly polarized epithelial cells.* J Cell Biol, 2002. **157**(6): p. 1041-8.
15. Barth, A.I., K.A. Siemers, and W.J. Nelson, *Dissecting interactions between EB1, microtubules and APC in cortical clusters at the plasma membrane.* J Cell Sci, 2002. **115**(Pt 8): p. 1583-90.
16. Diamantopoulos, G.S., et al., *Dynamic localization of CLIP-170 to microtubule plus ends is coupled to microtubule assembly*, in *J Cell Biol*. 1999. p. 99-112.
17. Tirnauer, J.S., et al., *EB1-microtubule interactions in Xenopus egg extracts: role of EB1 in microtubule stabilization and mechanisms of targeting to microtubules.* Mol Biol Cell, 2002. **13**(10): p. 3614-26.
18. Jimbo, T., et al., *Identification of a link between the tumour suppressor APC and the kinesin superfamily.* Nat Cell Biol, 2002. **4**(4): p. 323-7.
19. Browning, H., D.D. Hackney, and P. Nurse, *Targeted movement of cell end factors in fission yeast.* Nat Cell Biol, 2003. **5**(9): p. 812-8.
20. Gossen, M., et al., *Inducible gene expression systems for higher eukaryotic cells*, in *Curr Opin Biotechnol*. 1994. p. 516-20.
21. Akhmanova, A., et al., *Clasps are CLIP-115 and -170 associating proteins involved in the regional regulation of microtubule dynamics in motile fibroblasts.* Cell, 2001. **104**(6): p. 923-35.
22. Hoogenraad, C.C., et al., *Functional analysis of CLIP-115 and its binding to microtubules.* J Cell Sci, 2000. **113**(Pt 12): p. 2285-97.
23. Stepanova, T., et al., *Visualization of microtubule growth in cultured neurons via the use of EB3-GFP (end-binding protein 3-green fluorescent protein).* J Neurosci, 2003. **23**(7): p. 2655-64.
24. Pierre, P., R. Pepperkok, and T.E. Kreis, *Molecular characterization of two functional domains of CLIP-170 in vivo.* J Cell Sci, 1994. **107**(Pt 7): p. 1909-20.
25. Gundersen, G.G., I. Kim, and C.J. Chapin, *Induction of stable microtubules in 3T3 fibroblasts by TGF-beta and serum.* J Cell Sci, 1994. **107**(Pt 3): p. 645-59.
26. Sammak, P.J. and G.G. Borisy, *Direct observation of microtubule dynamics in living cells.* Nature, 1988. **332**(6166): p. 724-6.
27. Schulze, E. and M. Kirschner, *New features of microtubule behaviour observed in vivo.* Nature, 1988. **334**(6180): p. 356-9.
28. Shelden, E. and P. Wadsworth, *Observation and quantification of individual microtubule behavior in vivo: microtubule dynamics are cell-type specific.* J Cell Biol, 1993. **120**(4): p. 935-45.
29. Lieuvin, A., et al., *Intrinsic microtubule stability in interphase cells.* J Cell Biol, 1994. **124**(6): p. 985-96.
30. Rickard, J.E. and T.E. Kreis, *Identification of a novel nucleotide-sensitive microtubule-binding protein in HeLa cells.* J Cell Biol, 1990. **110**(5): p. 1623-33.
31. Stepanova, T., et al., *Visualization of microtubule growth in cultured neurons via the use of EB3-GFP (end-binding protein 3-green fluorescent protein)*, in *J Neurosci*. 2003. p. 2655-64.
32. Wadsworth, P., *Regional regulation of microtubule dynamics in polarized, motile cells*, in *Cell Motil Cytoskeleton*. 1999. p. 48-59.
33. Tirnauer, J.S., et al., *EB1-microtubule interactions in Xenopus egg extracts: role of EB1 in microtubule stabilization and mechanisms of targeting to microtubules*, in *Mol Biol Cell*. 2002. p. 3614-26.
34. Mimori-Kiyosue, Y., N. Shiina, and S. Tsukita, eds. *Adenomatous polyposis coli (APC) protein moves along microtubules and concentrates at their growing ends in epithelial cells*. J Cell Biol. Vol. 148. 2000. 505-18.
35. Jimbo, T., et al., *Identification of a link between the tumour suppressor APC and the kinesin superfamily*, in *Nat Cell Biol*. 2002. p. 323-7.
36. Browning, H., D.D. Hackney, and P. Nurse, *Targeted movement of cell end factors in fission yeast*, in *Nat Cell Biol*. 2003. p. 812-8.
37. Krylyshkina, O., et al., *Nanometer targeting of microtubules to focal adhesions*, in *J Cell Biol*. 2003. p. 853-9.
38. Kaverina, I., O. Krylyshkina, and J.V. Small, *Microtubule targeting of substrate contacts promotes their relaxation and dissociation*, in *J Cell Biol*. 1999. p. 1033-44.
39. Salmon, W.C., M.C. Adams, and C.M. Waterman-Storer, *Dual-wavelength fluorescent speckle microscopy reveals coupling of microtubule and actin movements in migrating cells*, in *J Cell Biol*. 2002. p. 31-7.

40. Kaverina, I., K. Rottner, and J.V. Small, *Targeting, capture, and stabilization of microtubules at early focal adhesions*, in *J Cell Biol*. 1998. p. 181-90.
41. Krylyshkina, O., et al., *Modulation of substrate adhesion dynamics via microtubule targeting requires kinesin-1*, in *J Cell Biol*. 2002. p. 349-59.
42. Gundersen, G.G. and J.C. Bulinski, *Selective stabilization of microtubules oriented toward the direction of cell migration*, in *Proc Natl Acad Sci U S A*. 1988. p. 5946-50.
43. Liao, G., T. Nagasaki, and G.G. Gundersen, *Low concentrations of nocodazole interfere with fibroblast locomotion without significantly affecting microtubule level: implications for the role of dynamic microtubules in cell locomotion*, in *J Cell Sci*. 1995. p. 3473-83.
44. Wittmann, T. and C.M. Waterman-Storer, *Cell motility: can Rho GTPases and microtubules point the way?*, in *J Cell Sci*. 2001. p. 3795-803.
45. Nathke, I.S., et al., *The adenomatous polyposis coli tumor suppressor protein localizes to plasma membrane sites involved in active cell migration*, in *J Cell Biol*. 1996. p. 165-79.
46. Zumbrunn, J., et al., *Binding of the adenomatous polyposis coli protein to microtubules increases microtubule stability and is regulated by GSK3 beta phosphorylation*, in *Curr Biol*. 2001. p. 44-9.

General discussion and future directions

Microtubules (MTs) are one of three types of filaments that make up the cytoskeleton. MTs are essential for cell division, cell migration, vesicle transport and cell polarity [1]. Depending on certain signals, MTs undergo phases of growth, pause and shrinkage [2]. The switching between growing and shortening states and vice versa, which is referred to as dynamic instability, is one of the most important characteristics of MTs. This rearrangement of the MT network allows it to explore the three-dimensional cytoplasmic space. MT dynamic instability [3, 4] is regulated by MT-associated proteins, such as the +TIPs, a new class of plus end-tracking proteins that bind specifically to the growing ends of MTs [5].

Earlier, we demonstrated for the first time that several +TIPs localise to the plus ends of growing MTs in living neurons [6]. The study of MT dynamics in cultured neurons, using EB3-GFP fusion protein as a marker for growing MT ends, revealed events of MT growth in all neuronal compartments and at different stages of development. A remarkable observation was that velocities and number of MT growth events were very similar at different stage of differentiation [6]. The data suggest that local MT polymerization contributes to the formation of the MT network in all neuronal compartments [6].

A recent report completely supports our data, demonstrating movement of MT plus ends in the axonal shaft by expressing GFP-EB1 in Xenopus embryo neurons in culture [7]. In this manuscript the polymer transport model, which states that tubulin is transported as a polymer along the axon, is rejected. Quantitative analysis of MT assembly/disassembly demonstrated that none of the MTs in the axonal shaft was rapidly transported, suggesting that transport of axonal MTs is not required for delivery of newly synthesized tubulin to the growing nerve processes [7]. Thus, in Xenopus axons of this type, local MT polymerization is the sole contributor to MT synthesis. However, there is a striking difference in the average length of MTs in the Xenopus system, compared to hippocampal neurons (100 micron versus 4 micron). This leaves the possibility intact that the polymer transport model might contribute to MT synthesis in hippocampal neurons.

CLIPs (cytoplasmic linker proteins) and CLASPs (CLIP-associating proteins) are interacting proteins belonging to the +TIP family. It was suggested that they regulate MT dynamics of fibroblast-like cells differently [8-10]. While CLIPs have been suggested to act as rescue factors (or to be able to recruit such factors to the distal ends of MTs), reverting a shrinking MT to a growing one, CLASPs play a stabilising role in MT dynamics and are involved in the local regulation of MT dynamics [9, 10].

In man the CYLN2 gene, which encodes CLIP-115, is located in the WSCR (Williams Syndrome critical region) [11]. Williams Syndrome (WS) is a neurodevelopmental disorder, which is caused by the hemizygous deletion of a region of approximately 1.6 Mb WSCR of chromosome band 7q11.23 [11].

Recently, we published that targeting of the Cyln2 gene in mice leads to neuronal dysfunction [12]. We documented defects including mild growth deficiency, brain abnormalities, hippocampal dysfunction and particular deficits in motor coordination [12]. It is remarkable that these features partially mimic those of WS patients. CLIP-170 deficient mice, made in our laboratory, show no obvious phenotype, but for a severely decreased fertility in male mice (Akhmanova et al, manuscript in preparation) and behavioural abnormalities.

In order to understand how the reduced levels of CLIP-115 might contribute to the neurological phenotype of WS, we analyzed MT dynamics in cultured hippocampal neurons from CLIP-115 and CLIP-170 deficient mice. Surprisingly, we document a significant increase in MT growth rates in neurons from both single CLIP knock out mice, compare with wild type neurons. Growth of MTs is directly dependent on the concentration of free tubulin molecules in cytoplasm. Thus, the most likely explanation for the phenotype in CLIP-deficient neurons is that the free cytoplasmic tubulin is increased.

We suggest that in CLIP knock out neurons, the absence of one of the CLIP causes an increased, MT depolymerization, which in turn, enlarges the cytoplasmic pool of free tubulin and results in the increase of polymerization speed of growing MTs. Moreover, we found that increased MT growth rates are accompanied by longer growth spurts in neurons derived from CLIP-deficient mice. This is explained by the fact, that the chance of a catastrophe is inversely correlated to MT growth velocity. Interestingly, MT growth velocities in glial cells and fibroblasts of knock out animals were not changed compared to wild type. Thus, the major conclusion from this work is that the functions of CLIP-115 and -170 are not redundant in neurons, which is presumably due to the different way MTs are organized in this highly polarized cell type.

We have hypothesized that the deletion of CLIP-115 is likely to contribute to some of the neurological symptoms of WS patients. In particular, we proposed that lack of CLIP-115 might cause abnormalities in dynein-dependent transport, since CLIP-115 competes with CLIP-170 for MT plus ends and interacts with the regulator of dynein motility, called Bicaudal-D [12]. Here we demonstrate that the absence of CLIP-115 alters the dynamics of the MT network in neurons from knockout mice.

Future investigations still are necessary to elucidate the question whether aberrant microtubule dynamics and /or transport may affect neuronal outgrowth and growth cone motility, which in turn can lead to the abnormal brain morphogenesis and impair the synaptic plasticity in CLIP-deficient mice. The observations that CLIP deficiency leads to altered MT dynamics has implications for the interpretation of the molecular mechanisms underlying WS, which could be categorized as being a disorder of the MT cytoskeleton. A future direction of the work will be to better characterize how different types of neurons synthesize their MTs, for example testing whether the polymer transport model is absent in all neurons or not (i.e. whether the centrosome contributes significantly to MT synthesis in neurites or not). Once this work has been completed we need to address the contribution of the minus-end pathway to local tubulin concentrations.

In addition, we are going to investigate MT dynamics in neurons from CLIP double knockout mice, which are viable and have recently become available in our laboratory. Since our research has demonstrated that the differences in MT dynamics depend on MT organization and functional specification of particular cell types, we plan to perform MT growth analysis on neuronal and fibroblast-like cells. The deficiency of the particular +TIP, affects MT dynamics and can result in a redistribution of proteins on the MT tip. We believe that the mechanism of regulation of MT dynamics by plus end binding proteins is provided by a combinatory effect of all +TIPs.

It was speculated that CLIPs act as MT rescue factors, whereas CLASPs stabilize microtubules in specific cell locations upon reception of signalling cues [9, 10]. GFP fusions of both proteins demonstrate the typical “microtubule plus end tracking” behaviour, which characterizes group of proteins that specifically bind to the ends of growing microtubules [5, 13]. To analyze the dynamics of GFP fusions of both proteins and the mechanism of their accumulation on MT tips, we generated 3T3 cell lines stably expressing GFP-CLIP170 and GFP–CLASP2 that faithfully represent the endogenous proteins, and performed live cell imaging experiments, migration assays and FRAP analysis on stable cell lines.

Besides the CLASP polarization at the leading edge of motile fibroblasts, described earlier [14], we document here a novel observation of its behaviour, an accumulation at focal adhesions in 3T3 cells. It is noteworthy that an exact colocalization of GFP-CLASP2 with vincullin or paxillin was not observed very often. Moreover, some focal adhesions were completely devoid of GFP-CLASP2 and, conversely, some GFP-CLASP2 accumulations were not surrounded by vincullin or paxillin. We visualised by confocal laser-scanning microscopy MTs with GFP-CLASP2 at their plus ends.

These grow over and into immobile GFP-CLASP2 accumulations, which we presume to be adhesion complexes. Interestingly, we observed, that the GFP-CLASP2 dashes entering focal adhesions were always following the same tracks, indicating an interaction between MTs (and/or perhaps GFP-CLASP2) and actin (or an actin-binding protein), which guides MTs to adhesion complexes. We visualised size changes and, sometimes, the complete disassembly of particular GFP-CLASP2 accumulations after the entering of growing MTs, decorated with GFP-CLASP2. These observations raised our interest in further investigations of the role of CLASP2 in focal adhesion turnover/release, the mechanism of assembly of GFP-CLASP2 at focal adhesions and the dynamic behaviour of this protein in cell migration processes. Future studies will address these issues.

When CLIP-170 is overexpressed, CLASP2 is removed from the leading edge, lending further evidence to the hypothesis that these two interacting proteins can influence the function of each other. In this context, cells derived from knockout mice, represent a good model for future investigations that address the question how a CLIP deficiency alters CLASP behaviour and redistribution. Moreover, we observed a reduction of cell migration velocity when GFP-CLIP-170 was overexpressed and CLASP2 was removed from the leading edge. It is not clear whether the reduction in cell migration speed in GFP-CLIP170 overexpressing 3T3 cells is the direct result of CLASP2 mislocalization, or an "indirect" consequence of CLIP-170 overexpression. It is possible that, due to the overexpression of GFP-CLIP170, MTs become rigid and cell migration slows down. Additional experiments are required to elucidate whether CLASP polarization itself is important for cell migration or not. It was proposed that plus end binding proteins such as APC and CLASPs might regionally regulate MT dynamics and promote MT growth into advancing lamellipodia [15]. It was shown that APC is transported along the MTs to the plus ends where it accumulates specifically on the tips of MTs growing in actively protruding areas [16, 17].

Using fluorescence recovery after photobleaching (FRAP), for study the behaviour of CLIP-170 and CLASP2 in cells we showed that GFP-CLIP170 is a mobile protein in cells. The behaviour of GFP-CLASP2 is variable. At focal adhesions areas, we found both mobile and relatively immobile pools of GFP-CLASP2, while at the leading edge of 3T3 cells GFP-CLASP2 is mobile, but less than within the cytoplasm of cells. Thus, the dynamic behaviour of the protein changes upon accumulation of CLASP to particular sites within the cell.

The mechanism proposed for microtubule tip association of CLIP-170 and EB1 ("treadmilling"), involves the specific association of these proteins with a freshly synthesized MT tip, followed by dissociation with first-order kinetics from the MT lattice. Treadmilling may also explain CLASP2 association with MT plus ends in the cytoplasm but the moment CLASP2 enters focal adhesion sites or leading edges of cells, the mechanism must change because CLASP2 changes mobility.

The plus ends of MTs are complex, very dynamic structures, which contain many different proteins. The functions of these proteins, their interaction with each other and their mechanism of targeting to the MT ends will help us to understand the molecular mechanisms of regulation of MT dynamics. We speculate that, the mechanism of MT dynamics regulation is provided by the combinatory effect of all +TIPs and is related to the MT organization and functional specification of particular cell types.

References

1. Gundersen, G.G., *Evolutionary conservation of microtubule-capture mechanisms.* Nat Rev Mol Cell Biol, 2002. **3**(4): p. 296-304.
2. Desai, A. and T.J. Mitchison, *Microtubule polymerization dynamics.* Annu Rev Cell Dev Biol, 1997. **13**: p. 83-117.

3. Mitchison, T. and M. Kirschner, *Dynamic instability of microtubule growth.* Nature, 1984. **312**(5991): p. 237-42.
4. Gelfand, V.I. and A.D. Bershadsky, *Microtubule dynamics: mechanism, regulation, and function.* Annu Rev Cell Biol, 1991. **7**: p. 93-116.
5. Galjart, N. and F. Perez, *A plus-end raft to control microtubule dynamics and function.* Curr Opin Cell Biol, 2003. **15**(1): p. 48-53.
6. Stepanova, T., et al., *Visualization of microtubule growth in cultured neurons via the use of EB3-GFP (end-binding protein 3-green fluorescent protein).* J Neurosci, 2003. **23**(7): p. 2655-64.
7. Ma, Y., et al., *Quantitative analysis of microtubule transport in growing nerve processes.* Curr Biol, 2004. **14**(8): p. 725-30.
8. Perez, F., et al., *CLIP-170 highlights growing microtubule ends in vivo.* Cell, 1999. **96**(4): p. 517-27.
9. Akhmanova, A., et al., *Clasps are CLIP-115 and -170 associating proteins involved in the regional regulation of microtubule dynamics in motile fibroblasts.* Cell, 2001. **104**(6): p. 923-35.
10. Komarova, Y.A., et al., *Cytoplasmic linker proteins promote microtubule rescue in vivo.* J Cell Biol, 2002. **159**(4): p. 589-99.
11. Francke, U., *Williams-Beuren syndrome: genes and mechanisms.* Hum Mol Genet, 1999. **8**(10): p. 1947-54.
12. Hoogenraad, C.C., et al., *Targeted mutation of Cyln2 in the Williams syndrome critical region links CLIP-115 haploinsufficiency to neurodevelopmental abnormalities in mice.* Nat Genet, 2002. **32**(1): p. 116-27.
13. Carvalho, P., J.S. Tirnauer, and D. Pellman, *Surfing on microtubule ends.* Trends Cell Biol, 2003. **13**(5): p. 229-37.
14. Akhmanova, A., et al., *Clasps are CLIP-115 and -170 associating proteins involved in the regional regulation of microtubule dynamics in motile fibroblasts*. Cell. Vol. 104. 2001. 923-35.
15. Wittmann, T. and C.M. Waterman-Storer, *Cell motility: can Rho GTPases and microtubules point the way?*, in *J Cell Sci*. 2001. p. 3795-803.
16. Mimori-Kiyosue, Y., N. Shiina, and S. Tsukita, eds. *Adenomatous polyposis coli (APC) protein moves along microtubules and concentrates at their growing ends in epithelial cells*. J Cell Biol. Vol. 148. 2000. 505-18.
17. Nathke, I.S., et al., *The adenomatous polyposis coli tumor suppressor protein localizes to plasma membrane sites involved in active cell migration*, in *J Cell Biol*. 1996. p. 165-79.

List of abbreviations

Ab	antibody
Ac-tubulin	acetylated tubulin
ALS	amyothropic lateral sclerosis
APC	adenomatous polyposis coli protein
MTs	microtubules
NF	neurofilament
ATP	adenosine triphosphate
ADP	adenosine diphosphate
GTP	guanosine triphosphate
MTOC	microtubule-organizing centre
HGF	hepatocyte growth factor
FRAP	fluorescent recovery after photobleaching
MAPs	microtubule-associated proteins
HMW	proteins high-molecular-weight protein
FRET	fluorescence resonance energy transfer
+TIPs	plus end-tracking proteins
LIS	lissencephaly
EBs	end-binding proteins
GFP	green fluorescent protein
CLASPs	CLIP-associating proteins
GSK-3β	glycogen synthase kinase-3β
CLIPs	cytoplasmic linker proteins
BIM1p	binding to microtubules 1 protein
CNS	central nervous systems
XMAP	Xenopus microtubule associated protein
XKCM1	Xenopus kinesin catastrophe modulator-1
FSM	fluorescent speckle microscopy
Tet-system	tetracycline-controlled transcription system
pTRE	tetracycline responsive plasmid
rtTA	reverse tetracycline transactivator
Dox	doxicyclin
LSM	laser-scanning microscope
DsRed	red fluorescent protein
WS	Williams Syndrome
SFV	Semliki Forest Virus
WSCR	Williams Syndrome critical region
FCS	Fluorescence Correlation Spectroscopy
C-terminus	carboxy- terminus
N-terminus	amino- terminus
CAP-Gly	cytoskeletal associated protein glycine conserved domain
CYLN2	cytoplasmic linker protein 2 gene
DNA	deoxyribonucleic acid
Glu-tubulin	glutamylated (detyrosinated) tubulin
γ-TuRC	γ-tubulin ring complex

Movie legends

Movie 1, *knockout of CLIP170, axon of hippocampal neuron and glia*
Embryonic hippocamlpal neurons (7 DIV) derived from knockout of CLIP170 mouse were infected with SFV particles, containing EB3-GFP encoding RNA. Cells were maintained at 37 ^{0}C in conditioned culture medium. Neurons and glia from the same culture dish expressing low levels of the fusion protein were examined 3-4 hours post-infection, by confocal microscopy. Notice movement of fluorescent dashes (EB3-GFP that binds to the MT growing ends) in both knockout glia and neuronal axon. A total of 100 images were acquired every 2 seconds laser 488 nm, 2%.

Movie 2, *GFP-CLIP170 stable line*
3T3 cells, stably expressing GFP-CLIP170 DNA, were maintained at 37 ^{0}C in normal culture medium and analyzed by confocal microscopy. Notice movement of fluorescent dashes GFP-CLIP170 that bind to the plus ends of MTs. A total of 100 images were acquired every 2 seconds laser 488 nm, 2%.

Movie 3, *GFP-CLASP2 stable line*
3T3 cells, stably expressing GFP-CLASP2 DNA, were maintained at 37 ^{0}C in normal culture medium and analyzed by confocal microscopy. Notice movement of fluorescent dashes GFP-CLASP2 that bind to the plus ends of MTs and specific accumulation of CLASP2 in the focal adhesion areas. A total of 100 images were acquired every 2 seconds laser 488 nm, 2%.

Movie 4, *GFP-CLASP2 stable line, relocalization on the leading edge*
3T3 cells, stably expressing GFP-CLASP2 DNA, were maintained at 37 ^{0}C in serum free culture medium (wound healing assay). After addition of serum, cells were analyzed by confocal microscopy. Notice GFP-CLASP2 redistribution to the leading edges of 3T3 cells within 3-5 minutes after serum addition. A complete accumulation of polarized GFP-CLASP2 at the wound edge of cellular monolayer was visualized after 15-20 minutes. A total of 100 images were acquired every 20 seconds laser 488 nm, 6 %.

Movie 5, *GFP-CLIP170 stable line, wound healing assay*
3T3 cells, stably expressing GFP-CLIP170 DNA, were maintained at 37 ^{0}C in serum free culture medium (wound healing assay). After addition of serum, cells were analyzed by confocal microscopy. Notice movement of fluorescent dashes GFP-CLIP170 that bind to the plus ends of MTs. A total of 100 images were acquired every 2 seconds laser 488 nm, 2%.

Movie 6, *GFP- CLASP2 stable line, wound healing assay*
3T3 cells, stably expressing GFP-CLASP2 DNA, were maintained at 37 ^{0}C in serum free culture medium (wound healing assay). After addition of serum, cells were analyzed by confocal microscopy. Notice movement of fluorescent dashes GFP-CLASP2 that bind to the plus ends of MTs. GFP-CLASP2 redistribution to the wound edge of cellular monolayer. A total of 100 images were acquired every 2 seconds laser 488 nm. 2%.

Movie 7, *GFP-CLASP2 stable line, cell migration assay*
3T3 cells, stably expressing GFP-CLASP2 DNA, were maintained at 37 ^{0}C in serum free culture medium (wound healing assay). After addition of serum, cells were analyzed by

confocal microscopy. Notice the cell migration to the wound. A total of 24 images, 60 stacks were acquired every 30 minutes, laser 633 nm. 1%.

Movie 8, *bleaching GFP-CLIP170 stable line*
3T3 cells, stably expressing GFP-CLIP170 DNA, were maintained at 37 ^{0}C in culture medium and analyzed by confocal microscopy. Notice movement of fluorescent dashes GFP-CLIP170 that bind to the plus ends of MTs. The bleaching during 5 seconds (50 iterations, 100% 488nm laser) was performed after 50 seconds of time-lapse imaging. A total of 70 images were acquired every 2 seconds laser 488 nm. 4%.

Movie 9, *GFP-CLASP2 stable line, focal adhesion*
3T3 cells, stably expressing GFP-CLASP2 DNA, were maintained at 37 ^{0}C in culture medium and analyzed by confocal microscopy. The fluorescent dashes of GFP-CLASP2 represent growing MTs. The accumulation of GFP-CLASP2 in the focal adhesion area changes its size within several seconds, becoming larger or smaller. A total of 100 images were acquired every 2 seconds laser 488 nm. 4%.

Movie 10, *bleaching GFP-CLASP2 stable line*
3T3 cells, stably expressing GFP-CLASP2 DNA, were maintained at 37 ^{0}C in culture medium and analyzed by confocal microscopy. Notice movement of fluorescent dashes GFP-CLASP2 that bind to the plus ends of MTs and enter/exit areas of "static" GFP-CLASP2 accumulation. The bleaching during 1 second (50 iterations, 100% 488nm laser) was performed after 60 seconds of time-lapse imaging. A total of 110 images were acquired every 2 seconds laser 488 nm. 5%.

Movie 11, *bleaching GFP-CLASP2 stable line*
3T3 cells, stably expressing GFP-CLASP2 DNA, were maintained at 37 ^{0}C in culture medium and analyzed by confocal microscopy. Notice movement of fluorescent dashes GFP-CLASP2 that bind to the plus ends of MTs and enter/exit areas of "static" GFP-CLASP2 accumulation. The bleaching during 5 seconds (50 iterations, 100% 488nm laser) was performed after 40 seconds of time-lapse imaging. A total of 100 images were acquired every 2 seconds laser 488 nm. 4%.

Movie 12, *bleaching GFP-CLASP2 stable line, focal adhesion*
3T3 cells, stably expressing GFP-CLASP2 DNA, were maintained at 37 ^{0}C in culture medium and analyzed by confocal microscopy. Notice GFP-CLASP2 accumulation in the focal adhesion areas. The bleaching during 6 seconds (50 iterations, 100% 488nm laser) was performed after 100 seconds of time-lapse imaging. A total of 100 images were acquired every 2 seconds laser 488 nm. 3%.

Movie 13, *bleaching GFP-CLASP2 stable line, leading edge*
3T3 cells, stably expressing GFP-CLASP2 DNA, were maintained at 37 ^{0}C in serum free culture medium (wound healing assay). After addition of serum, cells were analyzed by confocal microscopy. Notice movement of fluorescent dashes GFP-CLASP2 that bind to the plus ends of MTs. GFP-CLASP2 redistribution to the wound edge of cellular monolayer.
The bleaching during 16 seconds (50 iterations, 100% 488nm laser) was performed after 48 seconds of time-lapse imaging. A total of 100 images were acquired every 2,4 seconds laser 488 nm. 2%.

Summary

The cytoskeleton is a network of intracellular protein filaments that constructs and maintains a cellular architecture. Microtubules (MT) are one of the three types of the cytoskeleton, and are essential for cell division, cell migration, vesicle transport and cell polarity [1]. MTs are the polymers of globular α/β tubulin subunits, which are arranged in a cylindrical tube measuring 24 nm in diameter. MTs are polar structures with a slow growing minus end and fast growing plus end. They are also responsible for various others cell processes, including the beating of cilia and flagella, the transport of membrane vesicles in the cytoplasm, the promotion of extension of the neuronal growth cone. These movements result from the special feature of MTs called dynamic instability [2, 3], or the actions of microtubule motor proteins.

The heterogeneous population of microtubule-binding proteins that accumulates mainly at the distal ends of polymerizing MTs can regulate their dynamics [4]. MT plus end binding proteins, also called plus end-tracking proteins (+Tips), are able to "surf "the dynamic ends of MTs [5]. EB1 [6], EB3 [7], APC [8], CLASP2 [9], LIS1 [10, 11], CLIP-170 [12, 13], CLIP 115 [13, 14] and the dynactin complex [15], have recently emerged as MT binding proteins that have been observed on the MT plus ends.

Recently, we demonstrated for the first time that several +TIPs localise on the plus ends of growing MTs in living neurons [7]. The study of MT dynamics in cultured neurons, using EB3-GFP fusion protein as a marker for growing MT ends, showed events of MT growth in all neuronal compartments and at the different stage of development. Remarkably, the velocities and the number of MT growth events were very similar and did not depend on the stage of differentiation [7]. The data suggest that local MT polymerization contributes to the formation of the MT network in all neuronal compartments [7].

A recent report completely supports our data by expressing GFP-EB1 in Xenopus embryo neurons in culture [16]. Two members of the +TIPs family, the CLIPs (cytoplasmic linker proteins) and CLASPs (CLIP-associating proteins), were suggested, to regulate MT dynamics differently in fibroblast-like cells [9, 17]. While CLIPs act as MT rescue factors, CLASP2 stabilizes microtubules in specific cell locations upon reception of signalling cues [9, 17].

We speculate that CLIP-115 and -170 might play important and unique roles in neuronal functioning. It has been documented earlier that CLIP-115 knock out mice mimic features of the neurodevelopmental disorder called Williams Syndrome, including a mild growth deficiency, brain abnormalities, hippocampal dysfunction and particular deficits in motor coordination [18]. CLIP-170 deficient mice also showed behavioural problems. Interestingly, we found that MT dynamics was altered (increase of growth velocities and the length of MT growth events) in neurons, but not in glia, derived from single CLIP-115 or CLIP-170 knock out mice. It was proposed that growth of MTs is directly depended on the concentration of free tubulin molecules in the cytoplasm. The balance between free cytoplasmic tubulin and its polymerized form is one of the important parameters for the velocity of MT polymerization.

We suggest that in CLIP knock out neurons, the absence of one of the CLIPs causes an increased, persistent MT depolymerization. This in turn, enlarges the cytoplasmic pool of free tubulin and results in an increase of polymerization speed of growing MTs. Probably, CLIPs play non-redundant roles as rescue factors in the regulation of MT dynamics in cultured neurons. In contrast, they do compensate the absence of each other in fibroblast-like cells, as MT dynamics is not affected in the absence of either CLIP-170 or CLIP115.

To study the behaviour of CLIP-170 and CLASP2 in living cells and the mechanism of their accumulation on MT tips, we generated stably expressing GFP-CLIP170 and GFP–CLASP2 cell lines that faithfully represent the endogenous proteins in 3T3 cells.

We documented that when CLIP-170 is overexpressed, CLASP2 is removed from the leading edge, suggesting that these two proteins can influence each other functions. In this context, cells derived from knockout mice, represent a good model for future investigation of how CLIP deficiencies may alter CLASP behaviour and redistribution.

In addition CLASP polarization at the leading edge of motile fibroblasts, described earlier [19], we document here a novel observation of its behaviour; namely, an accumulation at focal adhesions in motile 3T3 cells. This observation raised our interest in further investigations the role of CLASP in cell migration. In particular, we are interested in the mechanism of assembly of CLASP accumulations in focal adhesions and at the leading edge, and in role of CLASP in focal adhesion turnover/release.

Our qualitative FRAP analysis does not allow any conclusion about the conformation of GFP-CLASP2 and GFP-CLIP170 in "free cytoplasm". However, the most interesting finding in these studies was that GFP-CLASP2 seems to be present in a cell in different fractions, depending on its distribution. The focal adhesion areas contain a mobile and immobile fraction of CLASP2, while at the leading edge CLASP2 seems to be mobile, but less so than CLASP2 in "free cytoplasm". These data suggest that the fractions of CLASP2 in focal adhesion complexes and at leading edges are modulated differently. The novel cell lines allow us to study the distinct regulatory mechanisms that enable CLASP2 accumulation at different sites in a cell.

The complete understanding of molecular mechanisms of MT dynamics regulation requires further investigation of the functions of tip complex proteins, i.e. their interaction with MTs and with each other, and the mechanisms of targeting to the MT growing ends.

References

1. Gundersen, G.G., *Evolutionary conservation of microtubule-capture mechanisms.* Nat Rev Mol Cell Biol, 2002. **3**(4): p. 296-304.
2. Gelfand, V.I. and A.D. Bershadsky, *Microtubule dynamics: mechanism, regulation, and function.* Annu Rev Cell Biol, 1991. **7**: p. 93-116.
3. Mitchison, T. and M. Kirschner, *Dynamic instability of microtubule growth.* Nature, 1984. **312**(5991): p. 237-42.
4. Galjart, N. and F. Perez, *A plus-end raft to control microtubule dynamics and function.* Curr Opin Cell Biol, 2003. **15**(1): p. 48-53.
5. Carvalho, P., J.S. Tirnauer, and D. Pellman, *Surfing on microtubule ends.* Trends Cell Biol, 2003. **13**(5): p. 229-37.
6. Mimori-Kiyosue, Y., N. Shiina, and S. Tsukita, *The dynamic behavior of the APC-binding protein EB1 on the distal ends of microtubules.* Curr Biol, 2000. **10**(14): p. 865-8.
7. Stepanova, T., et al., *Visualization of microtubule growth in cultured neurons via the use of EB3-GFP (end-binding protein 3-green fluorescent protein).* J Neurosci, 2003. **23**(7): p. 2655-64.
8. Mimori-Kiyosue, Y., N. Shiina, and S. Tsukita, *Adenomatous polyposis coli (APC) protein moves along microtubules and concentrates at their growing ends in epithelial cells.* J Cell Biol, 2000. **148**(3): p. 505-18.
9. Akhmanova, A., et al., *Clasps are CLIP-115 and -170 associating proteins involved in the regional regulation of microtubule dynamics in motile fibroblasts.* Cell, 2001. **104**(6): p. 923-35.
10. Coquelle, F.M., et al., *LIS1, CLIP-170's key to the dynein/dynactin pathway.* Mol Cell Biol, 2002. **22**(9): p. 3089-102.
11. Sapir, T., M. Elbaum, and O. Reiner, *Reduction of microtubule catastrophe events by LIS1, platelet-activating factor acetylhydrolase subunit.* Embo J, 1997. **16**(23): p. 6977-84.

12. Perez, F., et al., *CLIP-170 highlights growing microtubule ends in vivo.* Cell, 1999. **96**(4): p. 517-27.
13. Komarova, Y.A., I.A. Vorobjev, and G.G. Borisy, *Life cycle of MTs: persistent growth in the cell interior, asymmetric transition frequencies and effects of the cell boundary.* J Cell Sci, 2002. **115**(Pt 17): p. 3527-39.
14. Hoogenraad, C.C., et al., *Functional analysis of CLIP-115 and its binding to microtubules.* J Cell Sci, 2000. **113**(Pt 12): p. 2285-97.
15. Vaughan, K.T., et al., *Colocalization of cytoplasmic dynein with dynactin and CLIP-170 at microtubule distal ends.* J Cell Sci, 1999. **112**(Pt 10): p. 1437-47.
16. Ma, Y., et al., *Quantitative analysis of microtubule transport in growing nerve processes.* Curr Biol, 2004. **14**(8): p. 725-30.
17. Komarova, Y.A., et al., *Cytoplasmic linker proteins promote microtubule rescue in vivo.* J Cell Biol, 2002. **159**(4): p. 589-99.
18. Hoogenraad, C.C., et al., *Targeted mutation of Cyln2 in the Williams syndrome critical region links CLIP-115 haploinsufficiency to neurodevelopmental abnormalities in mice.* Nat Genet, 2002. **32**(1): p. 116-27.
19. Akhmanova, A., et al., *Clasps are CLIP-115 and -170 associating proteins involved in the regional regulation of microtubule dynamics in motile fibroblasts*. Cell. Vol. 104. 2001. 923-35.

Samenvatting

Het celskelet bestaat uit een netwerk van eiwit filamenten, die een cellulaire architectuur opbouwen en onderhouden. Microtubuli behoren tot een van de drie typen van het celskelet, de andere twee zijn actine en intermediaire filamenten. Microtubuli zijn essentieel voor celdeling, celmigratie, celpolariteit, en vervullen een belangrijke rol bij het transport van celorganellen of eiwitmoleculen over langere afstanden binnen de cel. Microtubuli zijn buisvormige structuren met een doorsnede van 24 nm. Zij zijn opgebouwd uit twee typen eiwitten, alpha- en beta-tubuline genaamd, die een dimeer vormen en die gezamenlijk op een hele speciale manier worden ingebouwd in de buis. Microtubuli zijn polaire structuren met aan een kant een langzaam groeiend eind (het zogenaamde minus-einde) en aan de andere kant een eind dat heel dynamisch kan zijn en snel kan groeien, of depolymeriseren (het plus einde).

De kabelstructuur van microtubuli maakt ze uitermate geschikt voor een rol bij het bewegen van cilia en flagella, evenals voor het fungeren als een soort transportrails, waarlangs motor eiwitten diverse cytoplasmatische materialen vervoeren. Terwijl deze twee functies meer door stabiele microtubuli worden vervuld, is de dynamische instabiliteit van microtubuli, dus hun voortdurende groeien en afbreken, vooral aan het plus einde, belangrijk voor het doorvoeren van veranderingen in celstructuren. Een voorbeeld hiervan is het uitgroeien van neurieten in zenuwcellen. Er is een heterogene populatie van eiwitten ontdekt, die specifiek binden aan het uiterste einde van groeiende microtubuli, en die zowel dienen om de dynamiek van microtubuli te reguleren als om transport processen te controleren. Tot deze klasse van “microtubuli plus einde bindende eiwitten”, in het Engels “plus end-tracking proteins” (afgekort “+TIPs”) genaamd, behoren EB1, EB3, APC, CLASP2, LIS1, CLIP-170, CLIP-115 en het dynactine complex. Onze onderzoeksgroep is geïnteresseerd in deze eiwitten. In het kader van mijn promotie onderzoek heb ik het gedrag van deze +TIPs bestudeerd, met als hoofddoel te kijken naar zenuwcellen, omdat die een andere manier van organisatie hebben van hun microtubuli cytoskelet dan andere cellen en omdat mutatie van een van de +TIPs (CLIP-115) een rol zou kunnen spelen bij het ontstaan van de ontwikkelingsstoornis Williams Syndroom.

Ik heb “green fluorescent protein” (GFP) aan verschillende +TIPs gefuseerd en het gedrag van de fusie-eiwitten bestudeerd in levende cellen, met behulp van fluorescentie microscopie. Door elke paar seconden een opname te maken van een levende cel, kon ik het dynamische gedrag bestuderen van de GFP-TIPs en daarmee ook conclusies trekken over de dynamiek van de groeiende microtubuli zelf. In deze studies bleek van alle +TIPs het EB3-GFP fusie-eiwit als marker het beste te zijn voor de analyse van groeiende einden van de microtubuli. Wij lieten voor het eerst zien dat +TIPs zich aan het plus einde van de groeiende microtubuli in levende neuronen bevinden. De studie van de microtubuli dynamiek in gekweekte neuronen heeft de gebeurtenissen van microtubuli groei in alle neuronale compartimenten, tijdens de verschillende stadia van ontwikkeling aangetoond. Opmerkelijk is dat de snelheden en hoeveelheid van microtubuli groei gebeurtenissen gelijkwaardig en onafhankelijk van het stadium van zenuwcel ontwikkeling waren. Deze resultaten suggereren dat lokale microtubuli polymerisatie aan de formatie van het netwerk van microtubuli bijdraagt in alle neuronale compartimenten. Een recente publicatie van een andere groep ondersteunt onze resultaten geheel en demonstreert de beweging van groeiende microtubuli door middel van EB1-GFP in axonen van gekweekte kikker neuronen.

Een ander stuk van mijn promotie onderzoek heb ik gewijd aan twee leden van de +TIP familie, de CLIPs (cytoplasmic linker proteins) en de CLASPs (CLIP-associating proteins), die, zoals de naam al suggereert, een interactie met elkaar aan kunnen gaan. CLIPs en CLASPs reguleren desondanks ieder op verschillende wijze de microtubuli dynamiek in

fibroblasten. Terwijl CLIPs zich gedragen als factoren die krimpende microtubuli omzetten tot groei, zijn CLASPs juist stabiliserende factoren van microtubuli, maar alleen in specifieke locaties binnen een cel. Cellen, afkomstig van "knock out" muizen, vertegenwoordigen een goed model voor onderzoek naar hoe het gebrek aan CLIPs het gedrag én de herverdeling van CLASPs kan beïnvloeden. Ik heb de rol van CLIPs in gekweekte neuronen bestudeerd, weer met behulp van EB3-GFP, om te kijken naar de dynamiek van microtubuli in neuronen waarin hetzij CLIP-115, hetzij CLIP-170 afwezig is. Uit mijn proeven blijkt dat CLIP-115 en -170 ieder een belangrijke rol hebben bij het reguleren van deze dynamiek, aangezien we vonden dat de groeisnelheden van microtubuli en de lengte van de individuele groei-spurten toegenomen waren in neuronen, maar niet in glia, verkregen uit CLIP-115 of CLIP-170 "knock out" muizen. Aangezien groei van microtubuli direct afhankelijk is van de concentratie van vrije tubuline moleculen in het cytoplasma suggereren onze resultaten dat de concentratie van vrije tubuline is toegenomen in "knock out" neuronen. Wij suggereren dat in CLIP "knock out" neuronen door de afwezigheid van een van de CLIPs minder vaak microtubuli krimp in groei omgezet wordt, dat er daardoor een verhoogde microtubuli depolymerisatie is, wat op zich weer de cytoplasmische massa van vrije tubulin vergroot. Dit resulteert in een verhoging van de polymerisatiesnelheid van de groeiende microtubuli.

Mijn bevindingen hebben gevolgen voor hoe wij de pathogenese van Williams Syndroom interpreteren, aangezien wij nu denken dat een mild defect in microtubuli dynamiek een klein stukje van het ontstaan van deze ziekte zou kunnen verklaren. Wij hadden al eerder beschreven dat CLIP-115 "knock-out" muizen eigenschappen hebben, die een beetje lijken op afwijkingen die men ziet in patiënten met Williams Syndroom, zoals bijvoorbeeld milde afwijkingen in groei en de opbouw van de hersenen, en lichte defecten in gedrag en motoriek.

Om het gedrag van CLIP-170 en CLASP2 in 3T3 fibroblasten te bestuderen hebben wij stabiele GFP-CLIP170 en GFP-CLASP2 cellijnen gegenereerd. In mijn promotie onderzoek heb ik aangetoond dat, in lage hoeveelheden, de fusie-eiwitten zich in de stabiele cellijnen op dezelfde wijze gedragen als de endogene eiwitten. Dus kunnen deze lijnen voor verder onderzoek gebruikt worden. Ik heb een aantal inleidende proeven gedaan waarin ik de concentratie en dynamiek van fusie eiwitten trachtte te meten met behulp van zogenaamde "bleaching" experimenten. Deze proeven moeten verder uitgewerkt worden. Verder heb ik gevonden dat wanneer GFP-CLIP170 tot overexpressie gebracht wordt, CLASP2 verwijderd wordt van het plus eindjes van microtubuli aan de rand van de cel, omdat het aan GFP-CLIP170 gaat binden dat zich elders in de cel bevindt. Dit ondersteunt ons resultaat dat deze twee eiwitten met elkaar een interactie kunnen aangaan en elkaars functie kunnen beïnvloeden. Naast de ophoping van GFP-CLASP aan het uiteinde van kruipende fibroblasten, zoals eerder was beschreven, heb ik een nieuwe plek van ophoping van GFP-CLASP bestudeerd, namelijk ophoping bij intracellulaire plekken ("focal adhesions", of FA) waar cel-matrix contacten plaatsvinden. Deze observaties voedde onze interesse om verder onderzoek te doen naar de rol van CLASP in cel hechting en migratie processen. Wij zijn in het bijzonder geïnteresseerd in het mechanisme van het assembleren van CLASP in FA plekken en in de rol van dit eiwit aan het uiteinde van de cel en in de dynamiek van FA plekken.

Om een beter beeld te krijgen van moleculaire mechanismen die ten grondslag liggen aan de regulatie van microtubuli dynamiek is in mijn optiek verder onderzoek nodig naar de functies van +TIPs, hun interacties met microtubuli en met elkaar en naar de mechanisme(n) van hun accumulatie aan het einde van groeiende microtubuli.

List of publications

Okon E., Pouliquen D., Okon P., Kovaleva Z., **Stepanova T**., et al. Biodegradation of magnetite dextran nanoparticles in the rat. A histologic and biophisical study.
Laboratory Investigation 1994 Dec; 71 (6): 895-903

StepanovaT. et al. Different effects of laminin and collagen III type on the cytoskeleton and myofibrillar assembly of cultured cardiomyocytes.
Acta Histochemica et Cytochemica 1996, vol 29: 860-861, supplement

Akhmanova A., Hoogenraad CC., Drabek K., **Stepanova T**., et al. Clasps are CLIP-115 and –170 associating proteins involved in the regional regulation of microtubule dynamics in motile fibroblasts.
Cell 2001 Mar 23; 104 (6): 923-35

Matanis T., Akhmanova A., Wulf P., Weide T., **Stepanova T**. et al. The RAB 6 binding proteins Bicaudal-D regulates COPI- independent Golgy-ER transport by recruiting the dynein-dynactin motor complex**.**
Nat Cell Biol 2002 Dec; 4 (12): 986-992

Stepanova T., Slemmer J., Hoogenraad CC. et al. Visualization of microtubule growth in cultured neurons via the use of EB3-GFP (end-binding protein 3-green fluorescent protein)
J. Neuroscience 2003 Apr 1; 23 (7): 2655-64

Hoogenraad CC, Wulf P, Schiefermeier N, **Stepanova T**, et al. Bicaudal D induces selective dynein-madiated microtubule minus end-directed transport.
EMBO J. 2003 Nov 17; 22 (22): 6004-6015

Tatiana Stepanova, Gert van Cappellen, Anna Akhmanova, Adriaan Houtsmuller and Niels Galjart.
Fluorescence recovery after photobleaching (FRAP) analysis of GFP-CLIP170 and GFP-CLASP2 using tetracyclin-inducible 3T3 cell lines
(Manuscript in preparation)

Tatiana Stepanova, Marja Miedema, Anna Akhmanova and Niels Galjart
Increased MT growth velocities in cultured neurons from CLIP-115 and CLIP-170 deficient mice
(Manuscript in preparation)

Curriculum Vitae

Name: Tatiana Stepanova
Born: 15 August 1969, Leningrad (St-Petersburg), Russia

1986 - 1991:	MSc, St-Petersburg State University, Faculty of Biology, Department of Embryology.
1992 - 1994:	Junior Researcher Laboratory of Cell Pathology, Institute of Cytology, Russian Academy of Science, St. Petersburg.
1995 - 1997:	Ph D student, Department of Cell Culture, Institute of Cytology, Russian Academy of Science, St. Petersburg.
1999 - 2000:	Technician, Department of Biochemistry, Medical faculty, Erasmus University, Rotterdam.
2000 - 2004:	PhD. student, Department of Cell Biology and Genetics, Medical faculty, Erasmus University, Rotterdam.

Dankwoord

Om te beginnen wil ik graag iedereen bedanken die heeft meegeholpen met het verwezenlijken van dit proefschrift.

Ik wil Frank, als mijn promotor, speciaal bedanken voor alle hulp en advies met het proefschrift en de stellingen. Niels, ondanks dat je vaak druk met andere dingen bezig was, of gauw wegvluchtte als ik kwam, wil ik je erg bedanken voor alle discussies en bijdragen in dit project. Je hebt destijds een nieuwe confocale microscoop gekocht. Niemand wist toen nog hoe deze werkte. Dit hebben we samen uitgezocht met grote hulp van Gert van Capellen, ook voor zijn hulp ben ik erg dankbaar. Het was echt spannend om de eerste filmpjes te maken. Nu zijn wij professionals, klaar voor Hollywood. Bedankt voor je flexibiliteit en je positieve instelling voor dit project, zelfs toen ik die niet had.

Ook wil ik de leden van de kleine commissie: Dies Meijer, Chris de Zeeuw en Wim Vermeulen, bedanken voor de hulp bij het afmaken van het proefschrift en vooral voor jullie nuttige commentaar.

Anna en Casper bedankt voor het inwerken, samenwerken en de ondersteuning. Björn hartelijk bedankt voor al het werk dat je hebt gedaan voor mij met de muizen. Ik wil Helen en Filipe bedanken voor het meenemen van goede muziek om in het lab naar te luisteren.

Xenia en Filipe, bedankt voor jullie fijne vriendschap en dat jullie mijn paranimfen willen zijn. Samen hebben we onder andere heerlijk gegeten in Praag en zijn daar fijn een paar dagen ziek van geweest. Verder wil ik de alle labmaatjes Marja, Gideon, Marco, TV ster "Oh ja, joh?" Frank, Michiel, Nanda en Anne-Laure bedanken voor de gezellige tijd (en het veel te koud zetten van de airco). Ik wil ook nog Arjan bedanken voor zijn hulp met de celsortering en Michael voor zijn "virussen" (SFV-EB3-GFP).

Ook wil ik Marieke speciaal bedanken voor al haar ondersteunend werk. Verder wil ik Arthur, Melle, Sjozef, de medewerkers van de keuken, de EDC'ers en de fotografen bedanken van het regelen van veel verschillende dingen. Alle mensen van de 7^{e}, 10^{e} en 12^{e}, die ik niet genoemd heb: bedankt voor alle hulp en de goede sfeer.

Als laatste wil ik nog familie en vrienden bedanken. Mijn ouders en broer voor al hun steun en liefde, ook al zijn zij zo ver weg. Yolanda, Jan, Kees, tante Will en tante Ans voor hen getoonde interesse en aandacht. Mijn vriendinnen Svetlana, Natasja en Angelica wil ik ook graag bedanken voor de gezelligheid, advies en leuke tijden die we samen hebben.

Ook wil ik mijn lieve dochtertje Katja bedanken voor haar positieve en hartelijke warmte en liefde. En "last but not least" wil ik mijn man Frans bedanken voor alle morele steun, geduld en hulp de hele tijd.

Tot slot voor iedereen die dit proefschrift heeft gelezen of dit heeft geprobeerd of net gedaan heeft alsof, dit was het dan eindelijk.